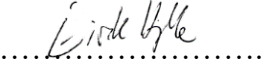




Universitetet
i Stavanger

FACULTY OF SCIENCE AND TECHNOLOGY

MASTER'S THESIS

Study programme/specialisation: Marine & offshore technology/ Marine operations	Spring semester, 2018 Open/ Confidential
Author: Eirik Inge Hjelle	 (signature of author)
Programme coordinator:	Professor Muk Chen Ong
Supervisor(s):	Professor II Jan Inge Dalane
Title of master's thesis: Evaluation of the Pendulous Installation Method in Ultradeep water Evaluering av pendelinstallasjon-metoden i ultradypt vann	
Credits: 30	
Keywords: -Subsea installation -Marine operations -Ultradeep water -Pendulous installation method	Number of pages: 130 + supplemental material/other: 28 Stavanger, 14/06/2018 date/year

Summary

The purpose of this thesis was to evaluate the use of the Pendulous Installation Method (PIM) for subsea equipment in water depths down to 4,000 meters. The basic concept of the PIM is to lower the payload in a pendulum trajectory rather than vertically. The idea behind the topic was to study what it would take for the oil & gas industry to start production in deeper water than what is possible today. The installation of necessary equipment was identified as an issue. The scope of the thesis was to describe the challenges of operations in ultradeep water and evaluate the PIM to see if it can be an alternative to conventional installation in 4,000 meters. This was accomplished by a literature study and use of numerical simulations in the SIMO software. A standard risk analysis was also carried out.

The PIM was developed by Petrobras in the 2000's. Their motivation for the development was the prospect of being able to install heavy equipment to ultradeep water without using specialized heavy lift vessels. This necessitated use of fibre rope rather than steel wires. Petrobras did not have access to field proven Fibre Rope Deployment Systems (FRDS), which are necessary to safely use fibre ropes for vertical installation. In the PIM the operation starts with the rope already paid out to full length, solving issues related to handling of the rope. It can thus deploy equipment without special rigging.

The SIMO software allows for design of models that can be used for numerical simulation of marine operations. The models used in this thesis included the installation vessel and four different payload types. The equipment was coupled to the vessel by a lifting line. The models were limited to obtaining global results. In this thesis the lift line tension, lowering times and vertical and horizontal motions during the landing were studied. The characteristics of the results compared favourably to the results obtained by Petrobras during their numerical simulations and their full-scale model test.

The results obtained in this thesis indicate that the PIM is not very sensitive to water depth. This is due to the use of a fibre rope that is weight neutral in water. The system also has a constant natural period through the lowering, meaning that there is less chance of resonance compared to conventional installation. None of the conditions studied in this thesis led to resonant behaviour, and the total tension in the lifting line never exceeded the minimum breaking load of the line. The lowering time was also significantly lower than the reference used for vertical installation. The landing process is not changed from conventional installation when applying the PIM, but the motions of the payload did only exceed the accept criteria in harsh wave conditions.

The PIM is faster than conventional installation, and the highest tension in the simulations occurred after the pendulum trajectory was finished. When measures are implemented the risk in the operation is acceptable. The PIM allows for use of less technologically advanced vessels to lower heavy equipment to the seabed, which can reduce the installation cost. The conclusion of the thesis is that the method can be a good alternative to conventional installation in ultradeep water.

Preface

This master thesis was written in the spring of 2018, at the University of Stavanger. It is submitted to the Department of Mechanical and Structural Engineering and Materials Science, as part of the master's program in Marine and Offshore Technology.

I would like to thank my supervisor, Professor Jan Inge Dalane, for proposing the topic. Working with this thesis has been educational, but also very interesting. A reason for this is the fascinating subject. I would also like to thank him for guidance and the valuable feedback I have been given in our regular meetings. It has been encouraging to work when he has shown genuine interest in the project, and very helpful when he has provided necessary information for writing the thesis.

I would also like to thank Lin Li for taking the time to answer questions about the SIMO software, and providing tutorials and general assistance. The simulations were an important part of the thesis, and her help has been greatly appreciated.

Stavanger, 14th of June 2018

Eirik Inge Hjelle

A handwritten signature in black ink, reading "Eirik Inge Hjelle". The signature is written in a cursive style with a large initial 'E'.

Table of Contents

- Summary i
- Preface..... ii
- Table of Contents iii
- List of Figures v
- List Tables vii
- Nomenclature viii
- 1. Introduction 1
 - 1.1 Background for the topic 2
 - 1.2 Concept of the Pendulous Installation Method 3
 - 1.3 Development of the Pendulous Installation Method 4
 - 1.4 Approach of this thesis 6
 - 1.5 Literature study..... 7
- 2. Installation in ultradeep water 11
 - 2.1 Subsea lifting operations 12
 - 2.2 Challenges in ultradeep water 20
 - 2.3 Subsea equipment..... 30
 - 2.4 Risk management in marine operations 31
 - 2.5 Economics of installation in ultradeep water 38
- 3. Theory 41
 - 3.1 Marine Environment..... 42
 - 3.2 Dynamics of marine operations..... 46
 - 3.3 Vessel Motions 50
 - 3.4 Lifting operations in deep water..... 52
 - 3.5 Marine Operations 56
- 4. Pendulous Installation Method..... 61
 - 4.1 General description..... 61
 - 4.2 Requirements..... 62
 - 4.3 Procedures 63
 - 4.4 Advantages and challenges 66
 - 4.5 Risk Analysis..... 68
- 5. SIMO modelling and inputs 77
 - 5.1 General 77
 - 5.2 Environment 78
 - 5.3 Equipment 79
 - 5.4 Rigging 80
 - 5.5 Vessel 82

5.6	Verification of models.....	82
5.7	Simulations.....	86
5.8	Sources of errors.....	87
6.	Results and discussions	89
6.1	Lifting capacity.....	90
6.2	Resonance.....	102
6.3	Time consumption.....	104
6.4	Horizontal offset.....	108
6.5	Landing and accuracy.....	113
6.6	Risk.....	121
6.7	Economics	122
7.	Conclusion.....	123
7.1	Conclusion.....	123
7.2	Future work	125
	References	127
Appendix A)	Specification sheets	a
Appendix B)	Simulation inputs.....	e
B.1	Simulation cases	e
B.2	Vessel RAO	h
B.3	Payload properties	m

List of Figures

Figure 1-1: ROV in ultradeep water (The Sea Musketeers, 2016).....	1
Figure 1-2: Shallow water and deepwater Subsea CAPEX, excerpt from Subsea Technology Handbook (Bai & Bai, 2012).	2
Figure 1-3: Pendulous Installation Method (Cerqueira, Roveri, Peclat, & Labanca, 2006).....	4
Figure 1-4: Left: Dummy manifold being lowered into the water. Right: The Installation vessel, an AHTS	5
Figure 2-1: Installing subsea production systems (Aker Solutions, n.a.)	11
Figure 2-2: Normand Maximus (Maritim Magasin, 2016)	14
Figure 2-3: Typical phases in a subsea lifting operation	15
Figure 2-4: Using vessel to shield a lifting operation.....	17
Figure 2-5: Sheave Installation Method (Wang, et al., 2012).	19
Figure 2-6: Reduced effective crane capacity due to self-weight of steel.....	21
Figure 2-7: Rolls-Royce FRDS handling system (Subsea World News, 2014).....	23
Figure 2-8: Increase of natural period for waterdepths	25
Figure 2-9: Lowering times for different hoisting speeds	27
Figure 2-10: Relocation of suspended payload	28
Figure 2-11: Vertical excursions and resettling times (Lian & Sortland, 1996)	28
Figure 2-12: Risk Analysis Process (Aven, 2015).	34
Figure 2-13: HAZOP flowchart (Aven, 2015).	36
Figure 2-14: Bow-tie diagram	36
Figure 2-15: Risk matrix, adapted from DNV-RP-H101 (Det Norske Veritas, 2003, p. 36).....	37
Figure 2-16: Deepwater subsea CAPEX	39
Figure 3-1: Marine environment (Vladtime, 2015).....	41
Figure 3-2: Combination of wave components. (National Instruments, 2012).	44
Figure 3-3: JONSWAP and Pierson-Moskowitz spectrum	45
Figure 3-4: Dynamic amplification factor for different relative frequencies.	48
Figure 3-5: Simple pendulum.....	49
Figure 3-6: Vessel degrees of freedom (Prasanna, 2014).....	51
Figure 3-7: Roll-induced heave	51
Figure 3-8: Horizontal offset of cable and payload (Det Norske Veritas, 2009).	56
Figure 3-9: α -factor tables, excerpt from DNV-OS-H101 (Det Norske Veritas, 2011).....	57
Figure 3-10: Required weather window (Det Norske Veritas, 2011).....	58
Figure 3-11: Classification of restricted or unrestricted operations (Det Norske Veritas, 2011).	59
Figure 4-1: Pendulous Installation Method divided into phases	61
Figure 4-2: Work breakdown structure of the PIM.	62
Figure 4-3: Pendulous Installation Method as described by Petrobras (Costa & de Lima, 2017).	64
Figure 4-4: Pendulous installation method as described by Wang et al. (Wang, et al., 2013).	65
Figure 4-5: Fault tree for event “Wire ruptures”	72
Figure 4-6: Fault tree for event “Payload is not released”	72
Figure 4-7: Risk matrix for PIM.....	75
Figure 5-1: Modelling in SIMA	77
Figure 5-2: Coordinates of interest.....	78
Figure 5-3: Current profiles.....	79
Figure 5-4: Equipment models from geniE.....	80
Figure 5-5: Deployment line and vessel.....	82
Figure 5-6: Tension obtained from numerical analysis and measurements by Petrobras (Roveri & Vardaro, 2006).	83
Figure 5-7: Tension obtained in SIMO simulations for this thesis.....	84

Figure 5-8: Velocity obtained from numerical analysis and measurements by Petrobras (Roveri & Vardaro, 2006)	85
Figure 5-9: Velocity from SIMO simulations for this thesis.....	85
Figure 5-10: Spike in tension due to simple wire coupling.....	87
Figure 5-11: “Wave” on deployment line	88
Figure 6-1: Screenshot from SIMO, landing of 280T	89
Figure 6-2: Lift line tension and vertical velocity of payload for 280T-manifold.	91
Figure 6-3: Gradual increase in tension for all equipment types.....	92
Figure 6-4: Gradual increase of tensions in Phase 2 in different water depths	92
Figure 6-5: Tension in different water depths	93
Figure 6-6: Tension for different wave peak periods	94
Figure 6-7: Maximum tension for different Tp (280T-manifold)	95
Figure 6-8: Maximum tension for different Tp (XT)	96
Figure 6-9: Wave directions	97
Figure 6-10: Max lift line tensions in different wave directions.	97
Figure 6-11: Lift line tension in Tp=8s for 280T-manifold	98
Figure 6-12: Maximum and minimum tensions for different wave conditions (280T-manifold).....	99
Figure 6-13: Maximum and minimum tensions for different wave conditions (XT).....	100
Figure 6-14: Natural periods for different systems	103
Figure 6-15: Tension variation with Hs and Tp	104
Figure 6-16: Lowering times for the PIM at increasing water depth.	105
Figure 6-17: Vertical velocity of 280T-manifold.....	105
Figure 6-18: Vertical position of payload as a function of time.....	106
Figure 6-19: Lowering time sensitivity to current direction.....	107
Figure 6-20: Slow drift of vessel.....	108
Figure 6-21: Correcting for slow drift.....	109
Figure 6-22: Horizontal motion during phase 2	109
Figure 6-23: Horizontal offset for different current conditions.....	110
Figure 6-24: Horizontal offset of 280T-manifold for different Tp.....	111
Figure 6-25: Horizontal offset of 280T-manifold for different Hs.....	112
Figure 6-26: Adjusting for mean horizontal offset.....	114
Figure 6-27: Horizontal oscillations of suspended 280T-manifold.....	115
Figure 6-28: Horizontal velocity of suspended 280T-manifold	115
Figure 6-29: Largest horizontal-motion amplitudes.....	116
Figure 6-30:Horizontal oscillations for different Hs (280T-manifold)	117
Figure 6-31: Horizontal velocity of 280T-manifold for different Hs.....	117
Figure 6-32: Vertical oscillations of 280T-manifold in Hs=1m.....	118
Figure 6-33: Locating the biggest peak-to-peak difference.....	119
Figure 6-34: Vertical oscillations for different Tp (280T-manifold)	119
Figure A-1: Dyneema fibre rope specification excerpt (EuroFibres, n.a.)	a
Figure A-2: Rolls Royce subsea crane specification excerpt (Roll Royce, n.a.).....	b
Figure A-3: Rexroth AHC specs excerpt (Rexroth, n.a)	c
Figure A-4: Sonardyne acoustic tracking (Sonardyne Inc, 2016).	d
Figure B-1: Heave 0.0 degrees	h
Figure B-2: Heave 45 degrees	h
Figure B-3: Heave 90 degrees	i
Figure B-4: Heave 135 degrees	i
Figure B-5: Heave 180 degrees	j
Figure B-6: Pitch 0 degrees	j
Figure B-7: Pitch 45 degrees	k
Figure B-8: Pitch 90 degrees	k
Figure B-9: Pitch 135 degrees	l
Figure B-10: Pitch 180 degrees	l

List Tables

Table 2-1: Weight and dimension of different rope materials for an MBL of 1,000 tons (Wang, et al., 2013).....	21
Table 2-2: Risk assessment parameters (Det Norske Veritas, 2003).	33
Table 2-3: Suggested HAZID work sheet	35
Table 2-4: Average day rates for different vessel types (Bai & Bai, 2012).	39
Table 4-1: EPH for phase 1.	68
Table 4-2: HAZID work sheet for undesired events in phase 1	69
Table 4-3: EPH for phase 2.	70
Table 4-4: HAZID work sheet for undesired events in phase 2	70
Table 4-5: EPH for phase 3.	71
Table 4-6: HAZID work sheet for undesired events in phase 3	71
Table 4-7: Cause study	73
Table 4-8: Consequence study	73
Table 5-1:Payload dimensions	80
Table 5-2: Lift line coupling properties.....	81
Table 5-3: Theoretical and numerical tension in deployment line.	86
Table 6-1: Lift line tension for different water depths ($H_s = 2m$, $T_p = 8s$).....	93
Table 6-2: Highest and lowest maximum tensions for different wave conditions (Phase 2, 280T-manifold).	95
Table 6-3: Highest and lowest maximum tensions for different wave conditions (Phase 2, XT).	95
Table 6-4: Max tensions for different wave directions (Phase 2, 280T-manifold).	98
Table 6-5: Maximum and minimum tensions for different wave conditions (280T-manifold).	100
Table 6-6: Dynamic amplification factors for 280T-manifold in different conditions.	100
Table 6-7: Maximum and minimum tensions for different wave conditions (XT)	101
Table 6-8: Lowering time of PIM in different water depths	106
Table 6-9: Offsets due to current.....	110
Table 6-10: Largest horizontal-motion amplitudes	116
Table 6-11:Horizontal velocity of 280T-manifold in different sea states.	118
Table 6-12: Vertical oscillations for 280T-manifold in all conditions.....	120
Table 6-13: Maximum vertical velocity and acceleration of 280T-manifold.....	120
Table B-1: Simulation current cases phase 3	e
Table B-2: Simulation equipment types phase 2.....	e
Table B-3: Simulation current direction phase 2.....	e
Table B-4: Simulation wave cases phase 2	f
Table B-5: Simulation wave cases phase 3	g
Table B-6: 280T-payload element properties.....	m
Table B-7: 150T-manifold element properties	n
Table B-8: XT element properties.....	o
Table B-9: THS element properties.....	p

Nomenclature

Abbreviations	Definition
A&R	Abandon & Recovery
AHC	Active Heave Compensation
AHTS	Anchor Handling Tug Supply
ALARP	As Low As Reasonably Practicable
CAPEX	CAPital EXpenditure
DAF	Dynamic Amplification Factor
DNV	Det Norske Veritas
DP	Dynamic Positioning
DSV	Diving Support Vessel
FRDS	Fibre Rope Deployment System
HLV	Heavy Lift Vessel
HMPE	High Modulus Polyethylene
Hs	Significant Wave Height
MBL	Minimum Breaking Load
MODU	Mobile Offshore Drilling Unit
OCV	Offshore Construction Vessel
OS	Offshore Standard
OSCV	Offshore Subsea Construction Vessel
OTC	Offshore Technology Conference
PHC	Passive Heave Compensation
PIM	Pendulous Installation Method
PLEM	Pipeline End Manifold
RAO	Response Amplitude Operator
ROT	Remotely Operated Tool
ROV	Remotely Operated Vehicle
RP	Recommended Practice
RSV	ROV Support Vessel
SWL	Safe Working Load
Tp	Wave peak period
UBL	Ultra-short Base Line
WD	Water depth
XT	(subsea) Xmas tree

Blank

Chapter 1

Introduction

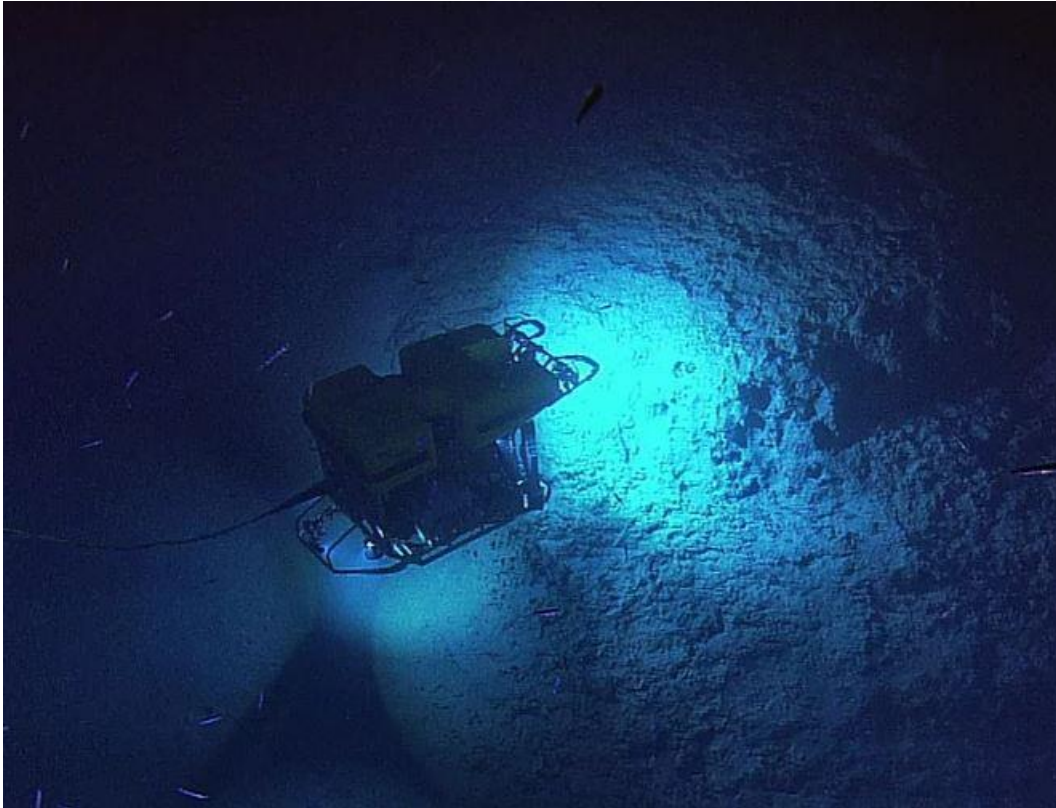


Figure 1-1: ROV in ultradeep water (The Sea Musketeers, 2016)

In 2015, offshore oil accounted for almost a third of the total global oil production (EIA, 2016). Offshore production allows the industry to continue conventional methods, drilling into fluid reservoirs, rather than turning to unconventional methods such as fracking and shale oil. Most of today's offshore production is done in shallow water (<500m), but in the first decade of this millennium the oil & gas industry began production in what is considered ultradeep water. Water depths greater than 1,500 meters are considered ultradeep. It has thus come a long way since the beginning. The first submerged oil wells in salt water were drilled in the late 1800's, in the United States. These were hardly anything like what is thought of today as offshore field developments. The first wells were drilled from piers that were built from shore and into the ocean, and the first freestanding drilling platform was built in 1938. The rapid expansion into increasingly deeper water has continued since then. Today the world record for deepest production is at the Stones Field, where subsea production equipment has been installed lower than 2,900 meters. The current trend is that production in deeper water is increasing. As the industry is trying to reduce the cost of production, attempts are made to move away from topside facilities, and instead focus subsea production and processing. This is especially beneficial when the production is moved into ultradeep waters.

However, it requires installation of more types of equipment, sometimes very heavy, to extreme water depths. This is where improvements in installation methods comes in.

1.1 Background for the topic

“It’s not rocket science. Oh, no, it is much, much more complicated”. The quote is from Matthew Franchek from the University of Houston and was made while talking about drilling into very deep hydrocarbon reservoirs in ultradeep waters. And there *are* several challenges to overcome if the oil & gas industry is to start production in deeper water than today. Currently technologies are qualified down to 3,000 meters, but what does it take to go below this? There are economic issues, but also technological ones. The major technology gaps going from 3,000 meters to 4,000 meters are related to subsea production equipment and the installation of such. For the moment ignoring the limitations of the equipment itself, there are still a number of uncertainties related to the installation of subsea equipment in ultradeep water. From a technological point of view, water depth, weight and dimensions are challenges. But from an economic point of view, availability of suitable vessels and the cost of operating these are also concerns. These operations may require advanced offshore construction vessels equipped with fibre rope deployment systems just to have the ability to lower subsea equipment to the desired depth. This is because in deeper water, steel wires will rapidly consume the effective lifting capacity of the cranes. In theory these fibre rope systems can lower equipment to unlimited water depths, as some fibre ropes are completely buoyant in water. There are still some issues with these fibre rope systems though, that are also discussed in this thesis. Other challenges facing the industry in ultradeep water is positioning of the equipment, tracking and monitoring as well as ROV support.

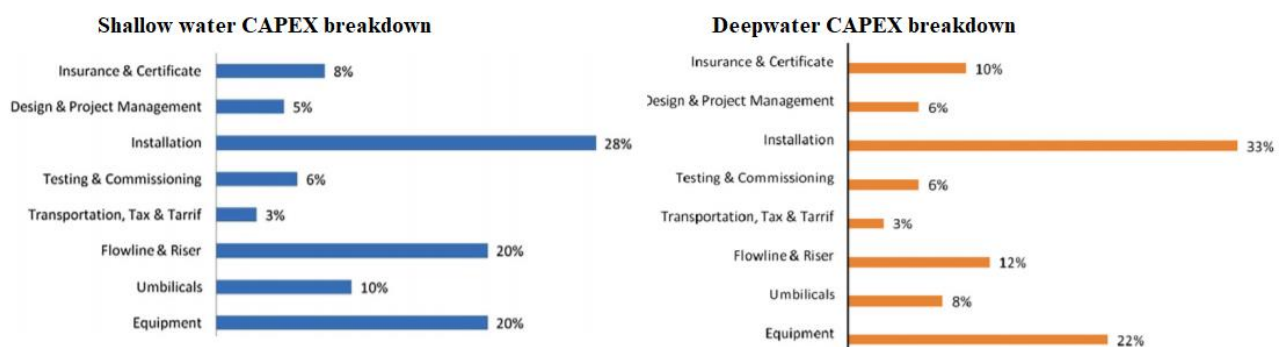


Figure 1-2: Shallow water and deepwater Subsea CAPEX, excerpt from *Subsea Technology Handbook* (Bai & Bai, 2012).

Making installation more cost-efficient has become a priority, especially with a volatile oil price. According to an article published by Offshore Magazine, deepwater developments must be considered mega-projects as the capital expenditure routinely exceeds five billion dollars (D'Souza, 2015). With cost-efficiency in mind, many boxes can be ticked by improving the installation process itself. Figure 1-2 is retrieved from chapter 6.2 in *Subsea Technology Handbook* by Qiang Bai and Yong Bai,

illustrating that the installation is the costliest part of the subsea CAPEX. It is also seen that this becomes even more significant in deep water. Reducing the cost of the installation will again reduce the risk involved, as the consequence of an undesired event becomes smaller. Failures are of course unacceptable: more importantly with regards to risk is that good technical solutions will reduce the probability of undesired events. Two main cost-drivers for installations are the time spent on the operation, and the cost of the vessels available in the region. This makes it desirable to use vessels with low day-rates for as short a time as possible, and to deploy vessel with a low mobilisation cost.

In ultradeep water though, special or high capacity vessels may be necessary. Smaller vessels may be unsuitable to lower heavy equipment to large water depths. It is also desirable to improve the robustness of the operational limits. For operations in ultradeep water the required weather windows are already long, and there is a significant probability of long periods of waiting on weather. With more robust operational limits, the time spent waiting on weather will be reduced.

Some companies have tried to develop unconventional installation methods that addresses these issues. When successful, this could be what sparks the interest of the oil & gas industry to attempt starting production in even deeper water. Early in the 2000's Petrobras developed one such unconventional installation method and used it to deploy a subsea manifold to water depths of almost 2000 meters. This was the pendulous installation method. The focus of this thesis was to evaluate the effect of applying this method in water depths beyond 3,000 meters.

1.2 Concept of the Pendulous Installation Method

The Pendulous Installation Method (PIM) as a concept, as described by Petrobras, is to lower payload to the seafloor in a pendulum trajectory. This is achieved by using two vessels. One vessel remains directly above the target site (Installation Vessel), while the other transports the payload away (Launch vessel). During the transportation, the payload is connected to the Installation Vessel by a fibre rope (deployment line). The payload is transported to a distance from the Installation Vessel that corresponds to about 90% of the water depth. The final elongation of the fibre rope must be considered so that the payload does not hit the seabed during or at the end of the pendulum trajectory. The payload is then lifted over board and through the splash zone from the launch vessel. At a suitable water depth, where it is not affected by the effects of the wave zone, it is released. It will then follow a pendulum trajectory rotating around the Installation Vessel. Due to the drag force on the payload and the deployment line, the system will act as a damped pendulum. This means that the payload will reach a suspended equilibrium position below its connection to the Installation Vessel without overshooting. Then it can be lowered vertically the remaining distance to the target site. By connecting a length of steel wire to the topside end of the rope, active heave compensation can also be applied without any special considerations or mechanisms regarding the fibre rope. The concept of the PIM is illustrated in Figure 1-3, retrieved from *The Need for the Pendulous Installation Method*.

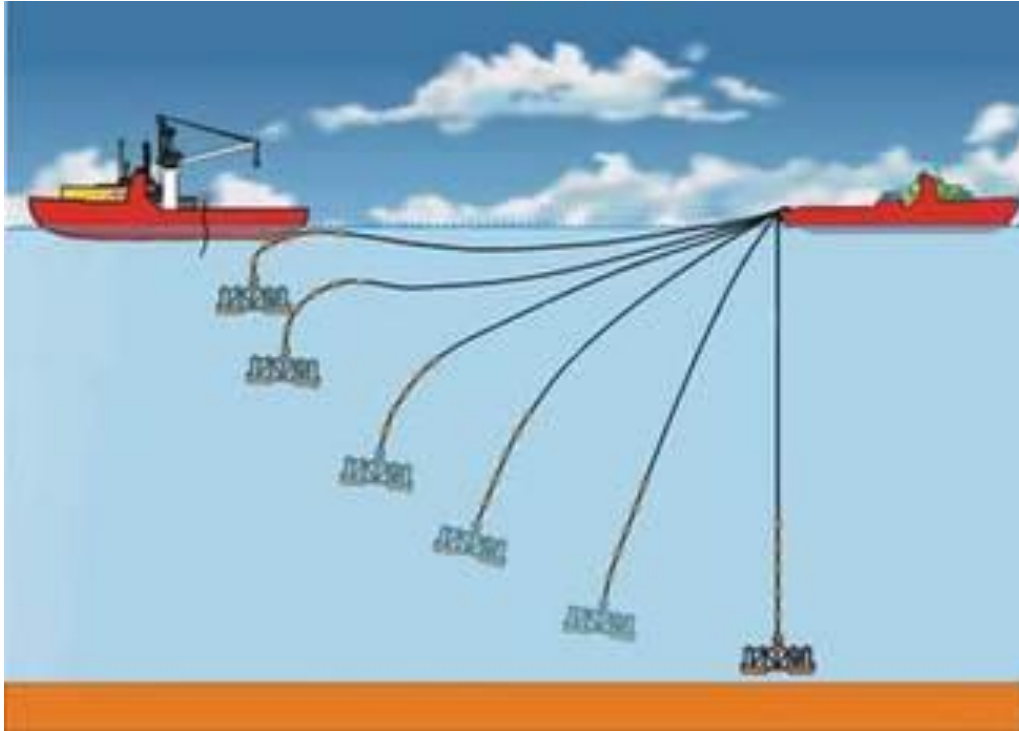


Figure 1-3: Pendulous Installation Method (Cerqueira, Roveri, Peclat, & Labanca, 2006)

1.3 Development of the Pendulous Installation Method

The PIM was put into development by Petrobras in the early 2000's to install heavy equipment to large water depths without the use of specialized vessels. At the time fields were being developed offshore in depths between 1000 and 2000 meters. They did not have access to field proven Fibre Rope Deployment Systems (FRDS) that fulfilled the requirements, and so their alternatives were therefore to utilize special construction vessels, or lower equipment using the drill-string from their own Mobile Offshore Drilling Units (MODU). The former alternative is very expensive, as the required heavy lift vessels are expensive to deploy, and often occupied with other tasks.

One such example is the installation of Shell's Perdido spar platform in the Gulf of Mexico, which was supposed to be installed by Heerema's DCV Balder. However, to fit Balder's schedule the delivery of the platform was accelerated six months, reducing the time for the FEED study and contract negotiations (Lohr & Smith, 2010). Furthermore, utilizing their own MODUs would also be expensive, and inefficient as these would then not be available for their drilling, workover or completion tasks. Thus, the study began to see how they could use smaller vessels to install heavy equipment in deep water. This need led to the conception of the PIM.

The main constraints to overcome was the self-weight of the steel wire rope without access to a proven FRDS and the axial resonance in the system. Lowering equipment in a pendulum trajectory had several benefits, in theory. When not requiring high capacity subsea cranes, they could use conventional vessels with no special riggings and mechanisms. Figure 1-4 shows excerpts from slide

17 in *Pendulous Installation Method Report of the Full Scale Offshore Test* (Stock, Ferreira, da Silva, & Machado, 2006). The payload is being lowered into the sea from a crane barge, while it is being installed by an anchor handling vessel.

The PIM also reduced the chance for axial resonance due to the long initial length of the wire, and the fibre rope was not subjected to repeated bending, friction or compressive forces in heave compensation systems. It was also cost effective when compared to using specialized vessels (Cerqueira, Roveri, Peclat, & Labanca, 2006). The Petrobras specialists did extensive testing, both using numerical simulations and model testing, to qualify the method. The final qualification was done in a full-scale test, using a dummy model of the manifold that was to be installed. This was done in 2005 without damage to vessels, personnel or equipment, and the conclusion was that the operation was easy and safe, with a good comparison between the numerical analysis and the model test. This qualified the technology for use to Petrobras (Kuppens, da Silva, Contarini, & Pinto, 2006). The method was then used to install two manifolds on the Roncador field.



Figure 1-4: Left: Dummy manifold being lowered into the water. Right: The Installation vessel, an AHTS

It should be noted that since the PIM was invented, new FRDSs and Fibre Rope Cranes (FRC) has become available to the market, delivered by companies such as Huisman, MacGregor and Rolls Royce. In the same way as the PIM, these allow smaller vessels to perform operations in very deep water. It is marketed as 4,000 meters and beyond by Huisman, as reported by Offshore Support Journal (Offshore Support Journal, 2018). These cranes are at the time of writing relatively recent additions to the market, either made available in 2017 or will become available in 2018. The ultradeep waters are thus becoming more available using conventional approaches as well, and the development is interesting to follow. Even with recent developments in crane technology, the PIM is a relevant study as it does not require this new specialized equipment. It is therefore interesting to see the effect of performing it in still untried water depths, to evaluate how it compares to the conventional installation methods.

1.4 Approach of this thesis

Offshore marine operations in deep water are complicated. The environmental conditions like wind, waves and currents, and the forces these exert, must be studied closely. Often these can be difficult to predict precisely, especially for longer operations. Many forces must be considered, and it is not always easy to predict the loads and responses of object, vessel or lifting wire. Still, through the years the industry has gained valuable experience in conventional marine operations. An example is lifting objects through the splash zone. In many cases this part of the operation is the most difficult to analyse. This is where the largest forces on the payload are experienced, and these are not constant during the lift. In proximity of the free surface, the hydrodynamic properties of the object will also be variable, and dependent on the vertical position. According to Marintek, the most accurate way of predicting the forces is through model testing (Marintek, 2003).

However, multiple studies have been done on the subject of crossing the splash zone. DNV GLs recommended practice DNV-RP-H103 (Det Norske Veritas, 2009) provides a section on how to improve modelling of this phase. An extensive discussion of the Recommended Practice (RP) has also been carried out by Gudmestad and Sarkar, with an emphasis on hydrodynamic coefficients and analysis methodology, in *Splash zone lifting analysis of subsea structures* (Gudmestad & Sarkar, OMAE2010-20489, 2010). With this in mind, the main focus of this thesis will be the unconventional phase of the PIM, namely the pendulum trajectory.

The purpose of this thesis was to evaluate the effect of applying the PIM when installing subsea equipment in water depths between 3,000 and 4,000 meters. This was done partly by studying available information about the subject and marine operations, including risk assessment and the current state of offshore technology. It was also done by establishing a model of the scenario using the DNV GL simulation platform SIMA. The platform allows for simulations in the software SIMO, which is a computer program for simulation of complex, general multi-body marine operations. It has a complete environment model and includes models for mooring systems and dynamic positioning with thrusters (Marintek, 2003).

Scope of work

The thesis was planned to cover the following:

- Create an overview of the current technological capacities of the industry, related to installation in ultradeep waters.
- Give an operational overview of the pendulum installation method. Also suggest why it can be beneficial to apply it for installation in ultradeep waters.
- Perform a standard risk analysis of the pendulous installation method.
- Model simulation of the PIM using the SIMO software.

- Sensitivity analysis of the PIM in a water depth of 4,000 meters, using different equipment and different environmental conditions.
- Discussion of the PIM based on simulation results and other findings from the thesis.
- Conclusion

1.5 Literature study

The thesis involves studies of marine operations and related technology in general, as well as achieving an understanding of the challenges related to installations in ultradeep water. While much information is available about conventional installation methods, publications about the PIM are limited. Apart from documents, presentations and papers published by Petrobras during and shortly after the two successful installations, not much information is available.

The different offshore standards and recommended practices published by DNV GL provide comprehensive, general information about marine operations. The Recommended Practice DNV-RP-H103 (Det Norske Veritas, 2009) provides methods for analysing several aspects of subsea installation, like lifting through the wave zone, deepwater lowering and landing. This includes estimation of the forces acting on the system and also approximation of hydrodynamic coefficients. It also provides information about weather criteria and availability analyses. Weather criteria, operational limits and how to define these are elaborated more in the DNV GL Offshore Standard (OS) DNV-OS-H101 (Det Norske Veritas, 2011), while DNV-RP-C205 gives extensive information on how to estimate environmental loads (Det Norske Veritas, 2014). The most relevant for this thesis is the estimation of current and wave conditions. There is also information on the slender element approximation, which allows for necessary simplifications of the modelling.

Risk management and analysis is an important element when considering marine operations. DNV-RP-H101 is a document where risk management in marine operations is discussed. It is the recommended practice of DNV. Its purpose is to establish guidelines and recommendations for the process required to reach an acceptable and controlled exposure to risk during marine operations, for personnel, environment, assets and reputation (Det Norske Veritas, 2003). Another source of information about risk analysis that was studied was *Risk Analysis* by Terje Aven. This book presents an accessible and concise guide to performing risk analysis in a wide variety of fields (Aven, 2015).

For general information about subsea engineering, the *Subsea Engineering Handbook* by Yong Bai and Qiang Bai (Bai & Bai, 2012) was a useful tool. It provides an overview of most aspects of subsea development, ranging from necessary equipment and installations methods to vessel utilization and economics. Several of the other sources mentioned in this sub-chapter are also referenced in the book, amongst others the RPs and OS' from DNV.

When it comes to the current technology levels for deepwater installation, papers published by the Offshore Technology Conference (OTC) and International Society of Offshore and Petroleum Engineers (ISOPE) were very relevant. Also, different industry sources are useful to get an overview of the current capacities of ROVs, FRDSs and acoustic positioning. Alan Wang et al. published a paper titled *Latest Progress in Deepwater Installation Technologies*, where a lucid overview of both conventional and unconventional methods is given (Wang, et al., 2012). The paper describes installation vessels and their capacities, and the need to swap steel for fibre rope in deep water. It also introduces the sheave installation method, pendulous installation method and pencil buoy method, and why these were developed. Both the sheave and pendulous methods are presented as examples for how to apply smaller vessels for deepwater installations. The purpose of the pencil buoy method is to submerge the payload in benign conditions (inshore) and transport it to the installation site where the conditions are typically harsher.

As part of the OTC in Brazil, 2017, Petrobras published a paper titled *Installation of Manifolds- A Success Story* (Costa & de Lima, 2017). The paper presents challenges faced by Petrobras when installing heavy equipment in deep waters, and the evolution of their installation techniques. It describes how Petrobras has developed several unconventional installation methods to overcome their limitations when it came to technology and availability of vessels. The PIM is described as “an excellent option to make feasible the installation of the Submarine Production Manifold”. In the paper, it is compared to other unconventional methods, and pros and cons are listed. Advantages that are listed are the short operating window for the launch vessel, being immune to resonance for great depths and not requiring heave compensation systems during lowering. The main disadvantage is the necessity of comprehensive planning prior to the operation.

A special workshop about the PIM was held in Hamburg in 2006, as part of the 25th International Conference on Offshore Mechanics and Arctic Engineering. Here Petrobras gave several presentations about different aspects of the method, and these are now available. The following are those considered most relevant for this thesis.

Maxwell Cequeira et al. described why the method was developed in a presentation called *The Need for the Pendulous Installation Method* (Cerqueira, Roveri, Peclat, & Labanca, 2006). The basis of the presentation was that Petrobras was studying development of fields in depths down to 3,000 meters. The problems to overcome were the self-weight of steel lifting wires, axial resonance, unavailability of FRDSs, and high cost of the necessary vessels. Fibre rope solved the self-weight issue, and lowering the payload in a pendulum trajectory omits the necessity of an FRDS. The presentation concludes that the PIM allows for use of conventional vessels with no special rigging, it prevents axial resonance and that it is cost effective compared to use of special vessels.

In *Numerical Analyses and Sensitivity Studies for Development of the Pendulous Method* (Roveri & Vardaro, 2006), Roveri and Vardaro explains the process used to develop and qualify the method. The first step was numerical analyses using the simulation tool Orcaflex to demonstrate the feasibility of the method. In their presentation they included the results for wire tension and the velocity of the payload from their time domain simulation, and so it can be used for comparison. Next, they did model testing in a laboratory with increasingly large models, from 1:130 to 1:35. The qualification process ended with a full-scale test in 2005 in a water depth of 1850 meters. Measured values from the last test agreed with the numerical analyses, for example wire tension and load characteristics. This makes it relevant for comparison.

The report from the full-scale test was also presented, in *Pendulous Installation Method Report of the Full Scale Offshore Test* (Stock, Ferreira, da Silva, & Machado, 2006). The presentation shows illustrations of how the method is performed, and the roles and requirements of the vessels involved. It was concluded that the PIM is an easy and safe operation, and that the good comparison between numerical analyses, the scaled model tests and the full-scale test qualified the technology.

In *Subsea Manifold Design For Pendulous Installation Method in Ultra Deep Water* (Ribeiro, Segura, & Ferreira, 2006), the design of subsea manifolds is discussed. There is a particular emphasis on whether it is beneficial to adapt the design of a manifold to remove issues like rotation and oscillations. The closing remark is that a more hydrodynamically optimal structure can be designed for the next manifold project.

Alan M. Wang et al. published a paper about the PIM that is one of few not published by Petrobras. *Pendulous Installation Method and its Installation Analysis for a Deepwater Manifold in South China Sea* (Wang, et al., 2013) was published as part of the conference of the International Offshore and Polar Engineering in Anchorage, USA in 2013. It explains the process of the PIM in exquisite detail, and it uses many of the same Petrobras sources that are mentioned above. Simulation results from SIMO are also displayed, as well as benefits of the method and technical information about fibre ropes. It should be noted that the method described is different from the Petrobras method, as Wang et al. suggests that the payload remains connected to the launch vessel and is lowered by this vessel reversing towards the installation vessel. Such an approach is slower, but it also grants more control of the payload.

De Boer, Braadbaard and Nieuwenkamp published a paper titled *Deep Sea Installation with Fibre Rope Technology – a New Concept in Winches for the best performance and durability of Rope* in context with a 2013 conference with the Society of Petroleum Engineers. Here the necessity of using fibre rope in ultradeep water is explained with regards to lifting capacity and winch requirements. The paper elaborates on the issues with using fibre rope as well, making it an ideal supplement to the marketed information provided by the industry. These issues necessitated the design of special fibre

rope deployment systems (de Boer, Braadbaart, & Nieuwenkamp, 2013). An earlier paper published by Sverre Torben et al. titled *Fibre Rope Deployment System for Ultradeepwater installations* addresses the same issues (Torben S. R., Ingeberg, Bunes, Bull, & Paterson, 2007). The papers on FRDSs are generally describing how FRDS systems allow for use of fibre ropes in deep water without risking damage to the rope or it having its properties deteriorate during the operation.

Chapter 2

Installation in ultradeep water



Figure 2-1: Installing subsea production systems (Aker Solutions, n.a.)

“Marine operations” is defined by Det Norske Veritas as follows: “Non-routine operations of a limited defined duration carried out for overall handling of an object at sea (offshore, inshore and at shore). Marine operations are normally related to handling of objects during temporary phases from or to the quay side or construction sites to its final destination or installation site. Marine operations include activities such as load transfer operations, transport, installation, sub sea operations, decommissioning and deconstruction, rig moves and pipe laying” (Det Norske Veritas, 2003). In other words, marine operations shall bring an object from one safe condition to another safe condition. In *Marine Technology and Operations*, Ove Tobias Gudmestad (Gudmestad, Marine Technology and Operations Theory and Practice, 2015) also includes the sensitivity to the weather in his definition. Gudmestad classifies the operations based on the tasks being performed:

- Pipeline installation
- Pipeline towing
- Umbilical installation
- Drilling
- Well interventions
- Equipment installation subsea; through moonpool; over the side.

This thesis was focused on the latter of the categories mentioned above. The process of installation of equipment will be different from case to case. The different operations usually require different types

of vessels and have different operational limits. The requirements with regards to equipment and planning also depend on the environment in which the operation is to be carried out. The offshore industry has gained much experience with activities in shallow water, and also in relatively deep water. The ultradeep operation sites can however present significant challenges, as large water depths cause issues with capacity, landing accuracy, duration and more.

The purpose of this chapter is to provide an overview of the current technology status of the oil & gas industry when it comes to installation of subsea hardware in ultradeep water. This is to elaborate on what is currently considered possible when it comes to such operations and what different methods are applied to different scenarios. The chapter includes information on what vessels are used for installations, the issues that must be considered when operating in ultradeep water, and the risks and economics involved. In chapter 4 these issues are addressed in context with the PIM.

2.1 Subsea lifting operations

Conventional installation of subsea hardware is considered a subsea lifting operation. Unlike topside installation or cargo transfer, the payload must now be lifted through the water surface. The purpose of the operation is to move the payload from the deck of a transport vessel and down to the seabed. The whole installation operation can be divided into sub-operations like mobilization, transportation, submerging, lowering and landing. The operation or sub-operations cannot be considered completed until the payload is in a safe position, i.e. does not require constant supervision. Such an operation can be handled using several different methods. The most practical solution will be determined by the size and weight of the payload, as well as the capabilities of the vessel or vessels involved, water depth and environmental conditions.

2.1.1 Installation vessels

Many types of vessels can be used for installation of subsea hardware, both for conventional and non-conventional installation methods. In *Subsea Engineering Handbook* by Yong Bai and Qiang Bai (Bai & Bai, 2012) classifies the typical vessels that can be used in a conventional installation into five:

- 1) Tugboats and transportation barges (Transportation)
- 2) Drilling vessels (Lifting)
- 3) Heavy lifting vessels (Lifting)
- 4) Offshore Support Vessels (ROV and/or diver support)
- 5) Pipelaying Vessels (Pipeline Installation)

This is a simplification, as some specialized vessels can perform several different types of tasks, and some vessels are suitable for tasks they were not originally intended for. For example, a dedicated pipelaying vessel can have deck space enough for transportation, and crane capacity for installation. A large, advanced Offshore Subsea Construction Vessel (OSCV) can be able to perform all necessary

sub-operations in an installation operation, including supporting both divers and ROVs. A short description of vessels typically used for installations is given below:

- **Barge**

Barges outfitted with a crane can be used both for transportation and installation. They are relatively simple and therefore cheap to operate (Bai & Bai, 2012). Due to the large waterline area they have a short natural period and are therefore more likely to come into resonance with local wind waves. This makes them very sensitive to environmental conditions. They are typically dependent on one or more tug boats to move from location to location.

- **Anchor Handling Tug Supply (AHTS)**

AHTSs are designed to support anchoring operations, but when fitted with high capacity Abandon & Recovery (A&R) winches they can also be used in installation operations. They are relatively cheap in day-rates and mobilization and have high availability. They are fuel efficient compared to large vessels and can in some cases also be used for transport. According to de Lima and Costa (Costa & de Lima, 2017), Petrobras use them frequently for unconventional installation methods. They can also be used to manoeuvre submerged payloads that are suspended from other vessels.

- **ROV Support Vessel**

ROV Support Vessels launches remotely operated vehicles to support subsea operations. Depending on the operation, ROVs can provide surveillance or measurements, or perform light to heavy intervention tasks like assisting in the positioning of equipment or connecting or releasing components (Bai & Bai, 2012).

- **Diving Support Vessel**

Diving Support Vessels are specially equipped to support diver operations in shallow water (<500 meters). They have submersible hyperbaric chambers, compression chambers and other equipment that allows divers to operate. Divers can perform certain tasks that ROVs cannot, or perform them faster, and thus they are sometimes required. Today, diving operations are restricted for HSE reasons, but previously divers would operate at almost 500 meters water depth.

- **Pipe-Laying Vessel**

PLVs are vessels specially equipped to lay pipes. Depending on the laying method, they are classified as J-lay, S-lay or reel-ray. Which type is used depends on the water depth and pipes, as they have different installation characteristics. For example, J-lay is suitable for deep water, and for umbilicals reel-lay is the only option as there is no need for welding on site. Some PLVs are also equipped with subsea cranes.

- **Drilling Vessel**

Mainly intended for drilling operations, they can however be used for installations as they will have good positioning abilities and high capacity lifting capabilities. These can be drill ships, semi-submersibles or jack-up rigs, and are Mobile Offshore Drilling Units (MODU). The jack-up can only be used in very shallow water, while the two formers are well suited for deepwater installation. Using semi-submersible vessels for installation is expensive and is keeping them from their main tasks. Accurate day-rates will vary, but in *Subsea Engineering Handbook* it is suggested that HLV semi-submersibles used for installation can cost more than 400,000 dollars per day when operating in more than 1,500 meters water depth (Bai & Bai, 2012).

- **Offshore Construction Vessel (OCV)**

OCVs, sometimes called Offshore Subsea Construction Vessel (OSCV) are ships designed to perform or support construction and installation of subsea structures. According to Bai & Bai (Bai & Bai, 2012) they are typically equipped with cranes with a capacity of around 250 tons, though this varies significantly. Many modern OCVs combine multiple capabilities to provide a complete installation platform with lifting, ROV/Diver support, large deck-space for transport, pipelaying facilities and high capacity winch systems.



Figure 2-2: Normand Maximus (Maritimt Magasin, 2016)

As mentioned some OCVs can combine all these capabilities. One such example is Solstad Farstad's OSCV Normand Maximus, illustrated in Figure 2-2. According to the shipowner's website, the vessel has cargo deck area of 2,400 square meters, a crane capacity of 900 metric tons, pipe laying capabilities, dynamic positioning and ROV support (Solstad Farstad ASA, 2017). It is thus capable of performing comprehensive marine operations on its own, from transport to installation. These vessels are, however, expensive to deploy.

- **Heavy Lift Vessel (HLV)**

HLVs are special lifting vessels with high lifting capacities. According to Bai & Bai, most have between 500-1000 tons. However, some semi-submersible construction vessels (SSCV) like Heerema's Deepwater Construction Vessel (DCV) Thialf have a lifting capacity of 14,200 tons according to their website. These can lower heavy subsea equipment to large water depths without using fibre rope. (Heerema, n.a.)

2.1.2 Conventional subsea lifting

An operation is considered a subsea lifting operation when the payload is lowered into the water. Conventional subsea lifting can generally be divided into five phases, which are illustrated in Figure 2-3. Depending on the approach to the installation, other phases may be included. For example, if the crane's lifting wire capacity is insufficient an A&R winch can be applied. The crane will then lower the payload through the splash zone, and then the load will be transferred to the winch. There are different challenges to the different phases of a subsea lift, and these are addressed accordingly. The lift-off, off-boarding and submerging are complex, and the strongest and most variable forces are acting on the object when it crosses the splash zone.

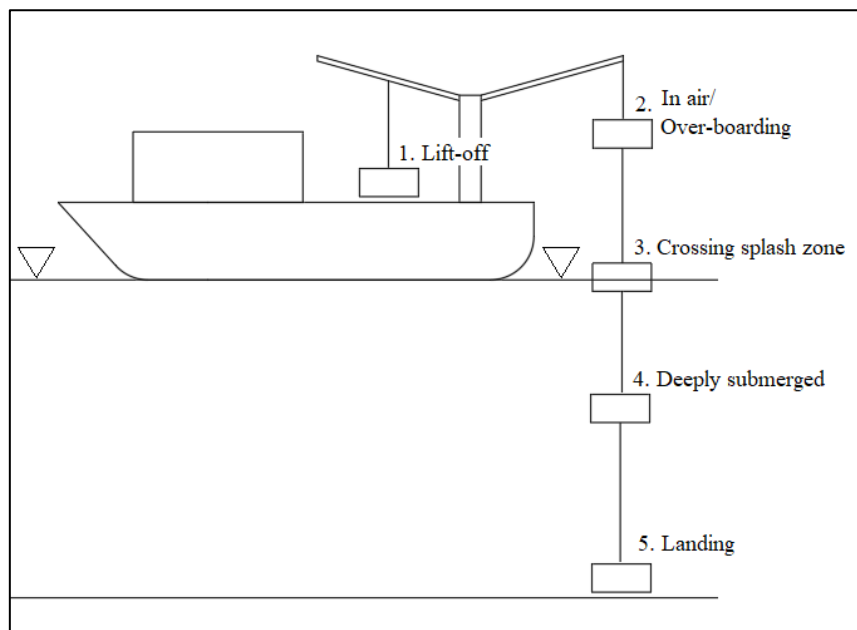


Figure 2-3: Typical phases in a subsea lifting operation

However, the industry has much experience with these phases. In deep water, the most challenging phases are therefore when the payload is deeply submerged, as well as the landing. The characteristics of each phase are described below. The following description is based on lectures given by post doc Lin Li (Li, 2017) and DNV-RP-H103 (Det Norske Veritas, 2009)

2.1.2.1 *Lift-off from deck*

The initial phase of a subsea lift presents a challenge as one wishes to increase the tension in the lifting wire gradually, while at the same time lift the object fast enough to avoid the object re-hitting the deck

due to dynamic responses in the liftwire. This can cause both damage to the deck as well as snap loads in the wire. In addition, the friction of the object is gradually reduced, which can cause sliding if excessive rotational vessel motions are present (Li, 2017).

There are two different scenarios when it comes to lifting the payload off the deck, lifting from the crane vessel's own deck or lifting from another vessel such as a transportation barge. The consequences of an undesired event are the same, and the types of undesired events are also the same. The difference is the relative motion between the two vessels. They may have different responses to the waves, which increases the risk of impacts.

2.1.2.2 In air/over-boarding

While in the air, the lifted object is subject to gravity. The static tension in the wire is at its highest, and the motions of the vessel causes dynamic loading as well. These variations in the loading causes parametric excitation, which can lead to large pendulum motions of the object. This can be reinforced if there is roll or pitch motions of the vessel (Li, 2017).

The main challenge when the object is in mid-air is to avoid collisions due to the pendulum motions, as this can cause injury to personnel or damage to the lifted object, deck equipment or the vessel. If necessary, the excessive horizontal motion can be controlled by using tugger lines (deck winches) (Li, 2017).

Lin Li proposes the following criteria for a safe lift in air (Li, 2017):

- Avoid excessive pendulum motion
- Avoid slack wire (Second lift-off after re-hit).
- Avoid overload (Stuck object, peak tension at lift-off).
- Avoid too hard landing (Limit velocity, insert soft contact elements).
- Hit target within defined tolerances (Design for manageable tolerances with respect to weather).
- Have ability to handle unexpected changes (Robust design, safe job analysis).
- Ensure acceptable stability (Accurate centre of gravity position).

2.1.2.3 Crossing the splash zone

The crossing of the splash zone is complex due to the many forces involved. The significant variation of the forces due to gradual submersion and changes in added mass is a challenge. The tension is reduced as the object becomes immersed in water, though snap loads can occur if a wave through causes the object to lose buoyancy. The capacity of the lifting equipment must be checked, and the DAF must be calculated. The stability of the lifted object can also be reduced for non-symmetric objects, and impact forces on the object can also damage the structure. A way of reducing the impact

of the waves is to use the vessel to shield the lowering, as shown in Figure 2-4. The object can also be lowered through a moonpool to avoid the impact of the waves.

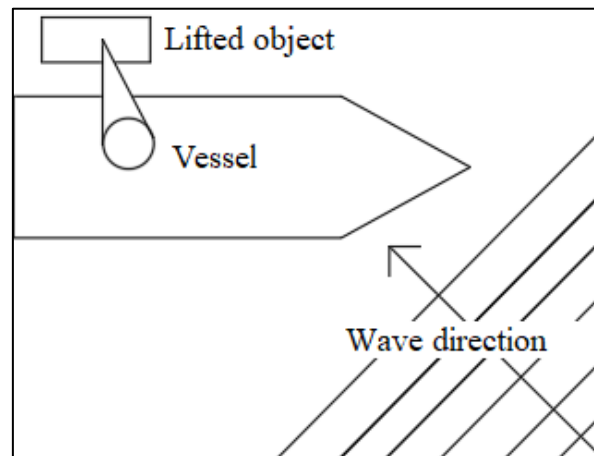


Figure 2-4: Using vessel to shield a lifting operation

DNV-RP-H103 provides comprehensive information on how to most accurately model the forces in the splash zone, however a numerical analysis is usually preferred. Numerical analyses are also challenging due to the unpredictable setting and many variables involved. Lin Li proposes two methods: Slow lowering in small, regular waves or repeated lowering in irregular waves (Li, 2017). The loads can then be considered stochastic variables: statistical analyses of the and study of the time series then allows for estimation of the extreme forces.

2.1.2.4 *Deeply submerged*

When the object is deeply submerged, wave kinematics are less important. The force of the current, however, becomes increasingly important as it creates a drag force on the lifting wire and the payload. In deep water a significant length of wire is affected by the current, and so the drag force becomes large. This in turn can push the object away from the target area, causing a horizontal offset. Light cables and loads are more susceptible to horizontal offset due to currents. This necessitates topside manoeuvring to reposition the payload, which for deeper water will cause delays. This is elaborated in chapter 2.2.5.

Because of the large damping force of the water, the pendulum motion of the system is typically damped out. However, the system can become subject to vertical oscillations due to the wave induced motions of the vessel. The natural period of the system becomes longer for a longer lifting wire, and as the object is lowered it is likely to come into resonance with the ocean waves. This can cause excessive vertical oscillating motions. As explained by de Vries et. al from Heerema MC, these oscillations can cause high dynamic loads. If the object is heavy the dynamic loading can approach the maximum capacity of the rigging. An example used by Bai & Bai in *Subsea Engineering Handbook* is that a 44-ton suction anchor can cause a wire tension of 460 tons due to added mass and dynamic

loading. If the object is light, on the other hand, the dynamics may cause a slack wire (de Vries, van Drunen, van Dijk, & Zoontjes, 2011). This motion can be reduced by applying heave compensation.

Heave compensation systems can be active (AHC) or passive (PHC). PHC is a system that does not consume external power but can use a soft spring to alter the phase between the motion of the vessel and the response in the payload. AHC is a system that applies external power to reduce or remove the response of the payload by retracting or feeding out the liftwire. There are several designs for how to do this, but the intended result is that the payload shall not move vertically due to wave conditions. Heave compensation systems can be integrated in cranes or they can be mobile. The capabilities of heave compensation systems vary, MacGregor advertises that their AHC cranes has a lift capacity of up to 600 tonnes (MacGregor, 2017).

2.1.2.5 Landing and positioning

The landing and positioning phase of the subsea lift is critical as there is a possibility of damaging the equipment as well as the landing site. Landing velocity cannot be too high, and care must be taken to achieve the required accuracy. This can be a challenge due to the mentioned horizontal offset, as well as the vertical oscillations. If ROVs are deployed to assist with the landing, such oscillations can damage the ROV. During landings, if excessive vertical motions are expected, heave compensation can be applied to reduce or negate these.

For positioning, acoustic signals are used to pinpoint the location of the payload. This is done with either Long Base-Line (LBL), Short Base-Line (SBL) or Ultrashort Base-Line (UBL), which are different transponder arrangements for acoustic positioning systems. For shallow water, guidelines are sometimes used for precise installation, but in ultradeep water this is not practical. For landing equipment on pre-installed anchors or similar operations, docking cones and rods of different heights are used. This allows the landing to be handled by connecting to the tallest rod, then using the connection to rotate about it, lowering the next cone to another rod. With two points docked, the object can be landed in the correct position. The rotation prior to the second docking is typically done using an ROV, though pre-installed clump weights and winch arrangements can also be used to position the equipment.

Requirements for landing accuracy depend on the type of equipment. A spool, jumper or pipeline end manifold (PLEM) might require very accurate positioning, while larger structures that are to be connected can be placed within a larger margin. Typically, an envelope with a certain margin is determined prior to the installation and then the equipment is landed within these limits.

2.1.3 Non-conventional installation methods

Installations that do not follow the procedure from chapter 2.1.2 are considered non-conventional. These have been developed to overcome different challenges, like vessel availability or depth

restrictions. For example, Petrobras have developed and executed several such methods, like the PIM described in the introduction, to reduce their dependency on renting expensive HLVs or using their own drilling vessels for installation tasks. The innovative solutions often include using AHTS vessels due to their high availability and relatively low day-rates. The purpose of this sub-chapter is to highlight other attempts to omit challenges related to installation in ultradeep water. Other than the PIM, examples of non-conventional methods are:

- **Subsea Load Transfer**

Not unlike conventional installation and might even be considered as such. Similar concept as mentioned in the introduction of the subchapter: The load is transferred from the crane used for submerging the equipment, but to another vessel rather than an onboard winch. A crane vessel can be used to lower the equipment into the water, and then the load can be transferred to an AHTS that continues the lowering. The added benefit is that the crane does not need a long range. Requires at least two vessels, and capacities for ROV support, A&R winch and a subsea crane. A special case of this was done by Petrobras when it was found that the weather window could be significantly widened by adding a section of nylon rope to the lifting system. This was done by having a crane vessel lowering the equipment to a target depth, and then transferring the load to an AHTS winch fitted with a length of nylon rope. The transfer was done topside and required the vessels to be in close proximity. A vessel fitted with a subsea crane and an AHTS were required (Costa & de Lima, 2017).

- **Sheave Installation Method**

Similar to conventional installation. It was developed by Petrobras to allow for installation in deeper water than one of their MODUs were able to perform. The main difference is that the lowering into deep water is done by using an AHTS and a sheave to lower the equipment as shown in Figure 2-5. The MODU is used to submerge the equipment and then the AHTS uses its winch, which has a longer range than the MODU, to land it. Another AHTS is used to maintain the orientation of the equipment. Requires one MODU and two AHTSs, as well as ROV support (Wang, et al., 2012). Figure 2-5 is an excerpt from *Latest Progress in Deepwater Installation Technologies* (Wang, et al., 2012).

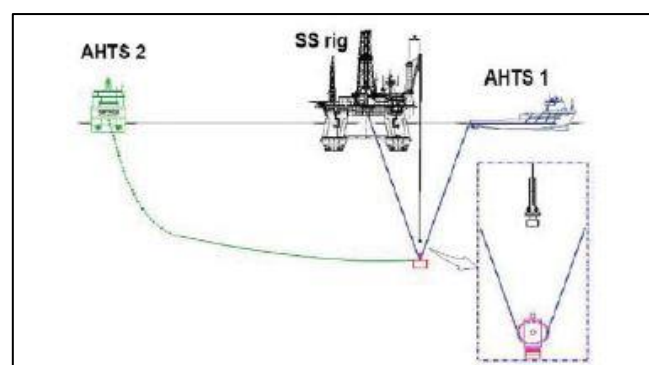


Figure 2-5: Sheave Installation Method (Wang, et al., 2012).

- **Pencil Buoy Method**

The pencil buoy method is a wet tow solution developed by Aker Solutions. The concept is that the payload is submerged at a sheltered, inshore location and then suspended from a custom-made pencil buoy. Then the equipment can be towed to the installation site by an AHTS and installed when convenient. This method is designed for unrestricted operations, as the suspended object can be considered in a safe position. Both the suspended equipment and the buoy might be subjected to complex hydrodynamic loads due to waves and currents. Requires a subsea crane inshore, ROV support and an AHTS. (Wang, et al., 2012). The benefit is that the operational limits become larger, as the payload can be lowered in harsher conditions than usual, since it is not lowered through the splash zone during the installation.

2.2 Challenges in ultradeep water

Most offshore hydrocarbon production is as of 2018 done in shallow water. Shallow water is a relative expression, and in the oil & gas industry water depths smaller than 500 meters are considered shallow. Between 500 meters and 1,500 meters is considered deep water, and more and more fields are developed in these depths. Past 1,500 meters is considered ultradeep water. Production facilities have been installed on such water depths, and the record is close to 3,000 meters. But installation of equipment in these depths represent significant challenges for multiple reasons, like lifting capacity, manoeuvring of the payload and landing accuracy. This section elaborates on some of the issues and how they are, or can be, overcome.

2.2.1 Issue with lifting capacity

Self-weight of steel wire ropes

Steel lifting wire rope is the most commonly used lifting wires for subsea lifting operations. Steel has a well understood dynamic behaviour and good material characteristics. However, it has a high material density. When the water depth increases the self-weight of the steel becomes a problem. For illustration purposes, a wire rope of diameter 127 millimetres is considered, as is done by Wang et. al. (Wang, et al., 2013) and using the same numbers. It can have a submerged weight of about 45 kilograms per meter. Given these numbers, the wire will have a self-weight of more than 157 tons at 3,500 meters, which is more than the weight of much of the equipment that is to be installed. For smaller OCVs this is unacceptable, and so expensive drilling vessels or HLVs must be deployed. Compared to smaller vessels this leads to higher cost. Figure 2-6 shows the effective capacity of an OCV with a 200-ton crane for the mentioned scenario, and as seen the capacity is reduced to such a degree that heavy equipment can no longer be installed.

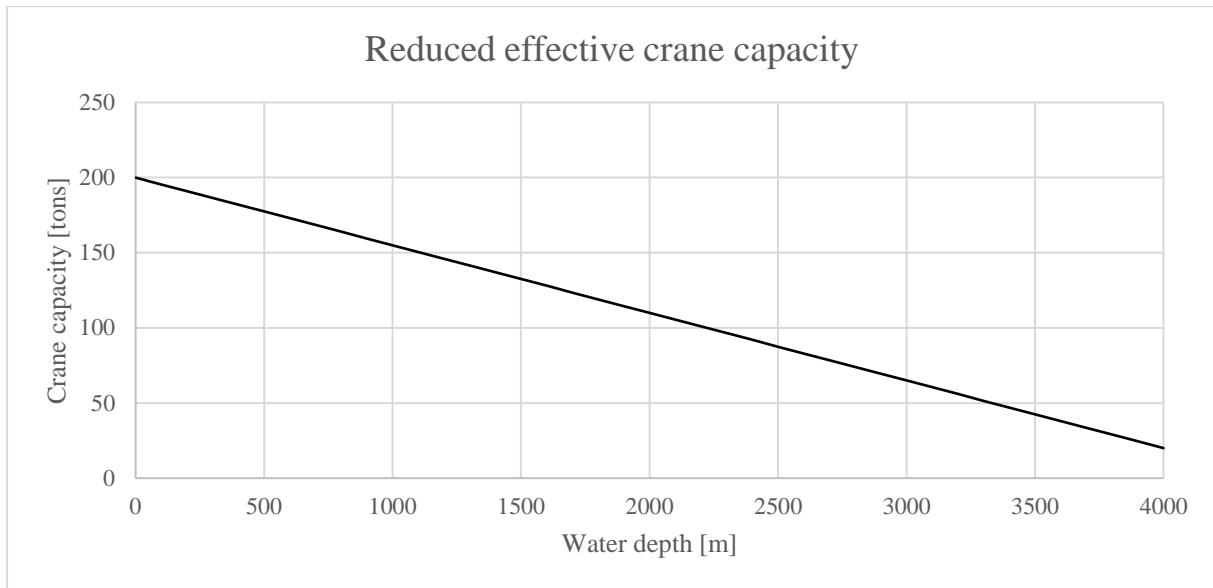


Figure 2-6: Reduced effective crane capacity due to self-weight of steel.

Synthetic fibre ropes

The solution has been to switch from steel wire ropes to synthetic fibre ropes. Many types of fibre ropes are in use for different purposes and using these can eliminate the impact of self-weight. This is because they are either very light or even naturally buoyant in water. Wang et. al. describes different types of fibre ropes like polyester, aramid nylon and high modulus polyethylene (HMPE) in *Latest Progress in Deepwater Installation Technologies*, and Table 2-1 is adapted from that paper to show the difference in in properties. These numbers are based on ropes with 1,000 MBL. HMPE is described as the most promising candidate given high strength, low density, short elongation at break, long fatigue life and resistant to chemicals and sea water. As seen in Table 2-1 a relatively small diameter HMPE-rope that is buoyant in water can hold as much as a slightly smaller steel wire, making it practical with regards to winch storage and logistics (Wang, et al., 2012). By also noting the weight in air, 3,000 meters of the HMPE rope weighs around 25 tons while 3,000 meters of steel is 174 tons. This is an advantage when it comes to logistics and handling during mobilisation.

Table 2-1: Weight and dimension of different rope materials for an MBL of 1,000 tons (Wang, et al., 2013).

Parameter	Unit	HMPE	Aramid	Polyester	Nylon	Steel
Weight in air	[kg/m]	8.4	12.0	23.0	25.0	58.0
Weight in water	[kg/m]	Neutral	3.3	5.9	2.5	4.9
Overall diameter	[mm]	125	120	175	200	110

Issues with fibre rope

While using fibre rope instead of steel solves the self-weight problem, there are also issues with fibre ropes. In *Deep Sea Installation with Fibre Rope Technology- a New Concept in Winches for the Best Performance and Durability of Rope*, de Boer, Braadbaard and Nieuwenkamp elaborated on these issues and how the industry tried to solve them. They listed the following differences between steel and fibre rope (de Boer, Braadbaart, & Nieuwenkamp, 2013):

- Fibre rope is more sensitive to temperature and has a lower heat-transfer coefficient.
- Fibre rope has a lower axial stiffness.
- Fibre rope is more sensitive to wear, both internal and external.
- Fibre rope is less sensitive to wire fatigue. It is however still an issue for heave compensated systems due to constant cyclic bending (Torben S. R., Ingeberg, Bunes, Bull, & Paterson, 2007).
- Fibre rope shows viscoelastic and viscoplastic behaviour.

Alan Wang et al. (Wang, et al., 2013) adds the following issues in *Pendulous Installation Method and its Installation Analysis for Deepwater Manifold in South China Sea*:

- Fibre rope is more susceptible to creep during prolonged static loads.
- Fibre rope is more susceptible to rope crushing due to compressive forces in the spool.

De Boer et al. lists two main mechanisms that cause dissipation of energy in the rope and thus generating heat:

- 1) **Bending of the rope:** Internal dissipation of energy caused by bending of an axially loaded rope. Caused by friction between different strands in the rope. A simulation showed that the frictional energy dissipated only in the area where the rope was bent (de Boer, Braadbaart, & Nieuwenkamp, 2013).
- 2) **Interaction between rope and reeling system:** Different forces on at both ends of the reel causes slipping, resulting in dissipation of surface energy and abrasion on the surface of the rope (de Boer, Braadbaart, & Nieuwenkamp, 2013).

Because an AHC constantly subjects the rope to bending, the total effect of fewer bends in the FRDS itself was small. The focus was therefore put on reducing the energy dissipation due to slip (de Boer, Braadbaart, & Nieuwenkamp, 2013). This led to the development of special traction winches, Cable Traction Control Unit (CTCU) used in FRDSs. Torben et al. describes these in *Fibre Rope Deployment System for Ultradeepwater Installations*. These are winch systems where the speed and torque on each sheave is controlled individually to avoid accumulation of slip, and the load is actively shared between the sheaves within the load limits of the individual sheaves (Torben S. R., Ingeberg,

Bunes, Bull, & Paterson, 2007). One such FRDS is displayed in Figure 2-7, retrieved from an article in Subsea World News from 2014.



Figure 2-7: Rollis-Royce FRDS handling system (Subsea World News, 2014)

Accurate constant tension functions, active heave compensation and brake handling according to requirements for offshore cranes allows the FRDS to be integrated with cranes (Torben S. R., Ingeberg, Bunes, Bull, & Paterson, 2007). These advanced fibre rope cranes are as of spring 2018 recent additions to the market according to Offshore Support Journal (Offshore Support Journal, 2018), but will open deeper water to subsea developments by conventional lifting operations.

2.2.2 ROV support

An ultradeep development is far beyond the reach of divers, and so it is necessary to deploy Remotely Operated Vehicles (ROV) to support installations and run interference. Divers are usually restricted to around 250 meters by regulations due to health & safety issues, though the record in the North Sea is 500 meters. This means that all tasks in ultradeep water must be handled by ROVs or AUVs (Autonomous Underwater Vehicles). As defined by Bai & Bai, ROVs are free-swimming submersible craft used to perform subsea tasks such as valve operations, hydraulic functions and other general tasks (Bai & Bai, 2012). Depending on the type, they typically perform tasks like monitoring and aiding in orientation of suspended equipment during installations. They are required for observation and verification and releasing hooks and wires.

In a paper titled *Guidelines for Installing ROV Systems on Vessels or Platforms*, the International Marine Contractors Organisation (IMCA) classified ROVs into five classes:

Class I) Observation ROV

Small compact vehicles which can be fitted with cameras/lights and sonar only. They are primarily intended for pure observation, although they may be able to handle one additional sensor (International Marine Contractors Association, 2013).

Class II) Observation ROV with Payload

These systems are fitted with two simultaneously viewable cameras and a sonar as standard and are capable of handling additional sensors as payload. They can also have basic manipulator capacities. They should be able to operate without loss of original function while carrying two additional sensors (International Marine Contractors Association, 2013)

Class III) Work class ROV

This class can also be divided Work Class and Heavy Work Class. It is vehicles large enough to carry extra sensors and manipulators as a matter of course without loss of functionality. Class III vehicles commonly have a multiplexing capability that allows additional sensors and tools to operate without being hardwired through the umbilical. These vehicles are generally larger and more powerful than smaller classes. They usually depend on more topside support (International Marine Contractors Association, 2013).

These vehicles are necessary when considering installation in ultradeep water to do manual tasks like connecting or orienting equipment. ROVs or AUVs will be necessary as traditional methods used in shallow water becomes impractical in such depths. One such issue is positioning during landing, as mentioned in chapter 2.1.2.5.

Class IV) Towed and Bottom Crawling

Typically, these are large and heavy vehicles that use tracks or wheels to manoeuvre instead of thrusters. They are often designed for specific tasks like trenching and burial of flowlines. Require significant topside support (International Marine Contractors Association, 2013).

Class V) Prototype or Development Vehicles

Vehicles in this class includes those still being developed or those regarded as prototypes. Special purpose vessels that does not fit into other classes are also assigned to class V (International Marine Contractors Association, 2013)

Status of work class ROVs

ROVs used for surveys or observation can reach far beyond 4,000 meters, and recently advances have been done for other classes as well. Work class and heavy work class ROVs can also reach 4,000 meters now, and this is of importance as they are necessary for installation operations. Oceaneering advertises several class III ROVs capable of diving to water depths of 4,000 meters, like the

Maximum ROV. This is listed as an optional capacity, unlike the standard version where the depth rating is 3,000 meters. This vehicle has dual manipulators and thrust capacities of 1,000 kg forward, 950 laterally and 1,300 vertically. Others Oceaneering heavy work class ROVs able to reach 4,000 meters are the Nexxus and the Millennium Plus (Oceaneering, n.a.). The ability of class III ROVs to operate in 4,000 meters means that it has become possible to use ROVs to support installations.

2.2.3 Issue of resonance

Resonance is dynamic behaviour where periodic loading is applied to a system in the same frequency as the system's own natural frequency. This causes significant dynamic responses in the system, which can lead to unacceptable loads or motions. In this case, the periodic loading is applied by the waves to the vessel which transfers the response to the crane tip. The local wave frequency must be considered in order to determine the risk of resonance. Sea states are typically described using the peak period of the waves. This means that the natural period of the system, rather than natural frequency, can be compared with the peak period to determine if there is a possibility for resonant behaviour.

Theory about resonance is covered in chapter 3.2 about dynamics, where it is explained that the natural frequency is dependent on the mass and stiffness of the system. The stiffness of the system depends both on the mechanical properties of the wire and its length. The latter means that the stiffness, and thus the natural period, changes during the lowering. Figure 2-8 shows the natural period, i.e. the inverse of the frequency, of lifting systems using wire rope or HMPE rope. The example assumes a payload of 150 tons. As seen in Figure 2-8, the period of both systems increases, and they are therefore more likely to come in resonance with more high-energy sea waves, which typically have peak periods between for example 5 and 12 seconds. Measurements in *Floatover Feasibility in Brazilian Sea Water* by Zhang, Jeong and Sprecken shows that these values are typical in several regions with deep waters, such as offshore Brazil and the Gulf of Mexico (Jeong, Zhang, & Sprecken, 2013, p. 2).

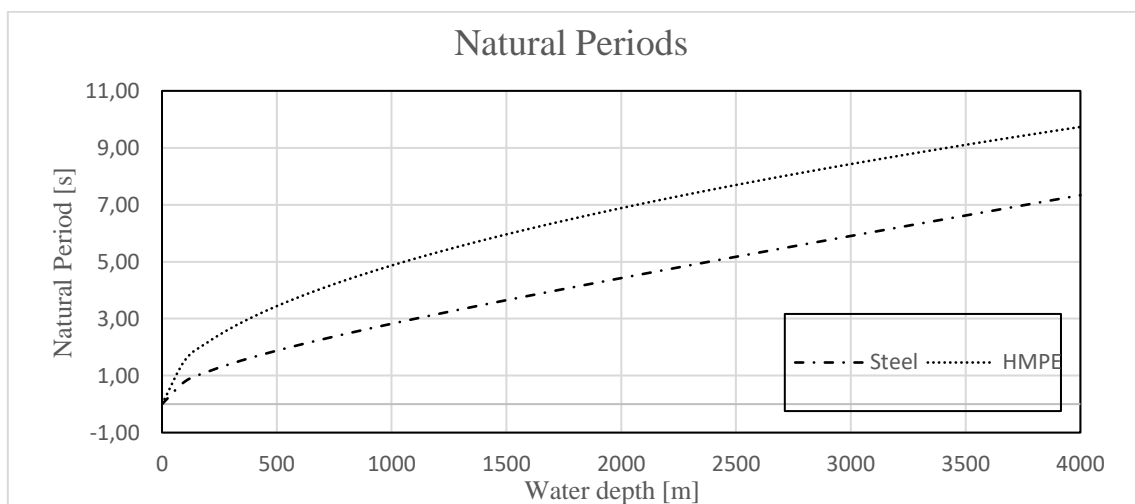


Figure 2-8: Increase of natural period for water depths

The increase in the period comes from the lifting system becoming longer as more rope is spooled out. This means that during the lowering the system is likely to travel through water depths where it comes into resonance with waves. For extreme water depths there will therefore be a higher likelihood of coming into resonance with a higher number of waves. These “resonance depths” should be calculated beforehand, to allow for implementation of measures. These measures can be increasing the lowering speed to quickly pass through the region or applying active heave compensation. Note that heave compensation, as mentioned in chapter 2.2.1, can have a negative effect on fibre ropes.

In the case of resonance, or damped resonant behaviour, the system will be subjected to significant responses. These are in the form of axial oscillations, meaning that the lifting wire is tensed and released repeatedly. The main concern in such a scenario is that the dynamic loads can cause the wire tension to approach the safe working load of the lifting system. This is unacceptable, and would require a higher safety factor, reducing the allowed capacity of the system. Another option is to use a stronger rope. However, that may also be impractical or expensive. In the opposite case of high loads, if the dynamic component of the load is higher than the static load, the wire will become slack. This leads to a snap load, which can be twice as high as the static load.

The responses in the system are also a problem when the payload is being landed on the seabed or approached by ROVs. The oscillations will make it difficult to connect to the payload and might also damage an ROV already connected to it. If uncontrolled, the payload might also hit an observing ROV should it be in close proximity to it. During a landing operation the payload can be damaged if the velocity is too high, and there is also a possibility of damaging the integrity of the landing site.

2.2.4 Issue with time consumption

An obvious effect of the increased water depth is longer lowering times. The lowering time is in effect unproductive time and is an issue both for lowering equipment and deploying ROVs. Depending on the hoisting speed the lowering times for increasing water depth can vary as illustrated in Figure 2-9. These graphs are based on a constant lowering velocity. In reality, this may be impractical as the operation might require manoeuvring or reduced or increased speeds at some points during the lowering. For example, in *Field Pilot of Subsea Equipment Installation in Deep Water using Fibre Rope in Two-fall Arrangement* Torben and Ingeberg describes a lowering operation using an FRDS to lower a 100-ton payload. Here the peak capacity of the FRDS is 90 meters per minute, however the speeds they operate with are between 24 m/min and 36 m/min, in different stages of the lowering (Torben & Ingeberg, 2011). The lowering speed can also depend on the shape, size and mass of the payload. Issues with stability might require a lower velocity, as can a heavy load. For this thesis a reference value of 40m/min was considered a suitable reference, though it is understood that a real scenario might see higher or lower speeds.

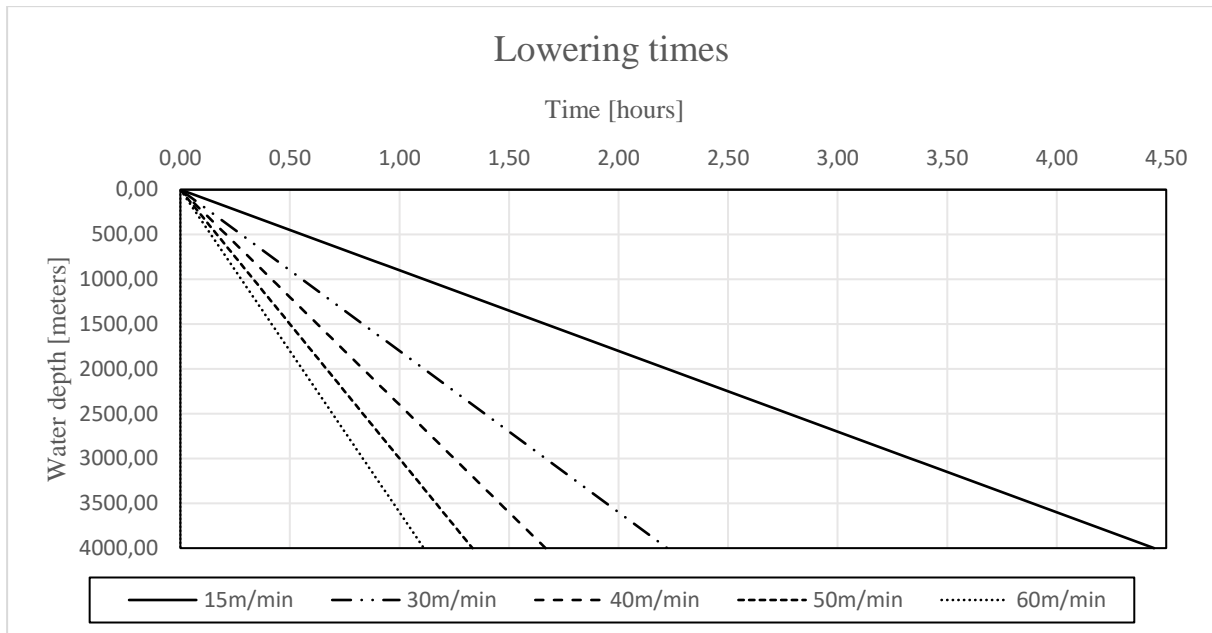


Figure 2-9: Lowering times for different hoisting speeds

Another consideration is whether the winch must be lowered, retrieved and lowered multiple times. For developments where it is necessary to lower several payloads, the accumulating time spent on lowering can become significant. With reference to Figure 2-9, 2-3 hours may well be acceptable for one round, but for four pieces the time will more than quadruple when also considering the time spent on landing and retrieving the hook. Time consumption for lowering is different for different operations. The very obvious conclusion to this sub-chapter is that for increasing water depths the time spent on the lowering can become significant, and any way of reducing it will be interesting to study.

2.2.5 Issue of horizontal offset and manoeuvring of suspended payloads.

The drag force generated by the current is likely to create a horizontal offset when lowering a payload. So even if the vessel, equipped with DP, remains in its position, the payload will drift. This is true for equipment, and also for Remotely Operated Tools (ROT) or ROVs with limited manoeuvring capabilities. Repositioning of the suspended equipment will then become necessary, and this is done by moving the vessel topside. However, there will be a delay between the topside motion and the response of the payload. The payload will have a vertical response due to the drag force causing a curving of the lifting line to reduce the effective length, and it will take time for it to settle back. The situation is illustrated in Figure 2-10. For light equipment the settling time may be very long, but also heavier objects can take time. This is unproductive time that should be reduced when possible.

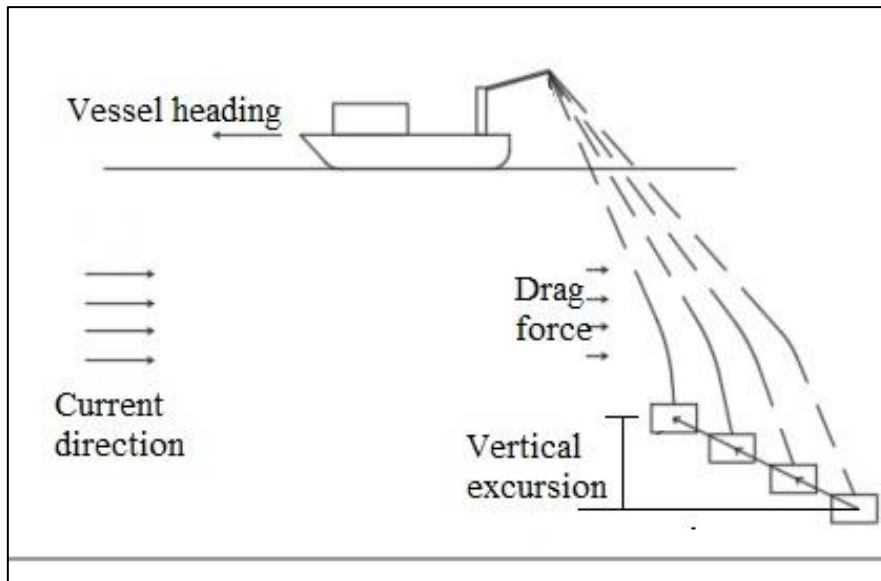


Figure 2-10: Relocation of suspended payload

In *Manoeuvring of Bodies Suspended at Extreme Water Depth* Walter Lian and Bjørn Sortland discuss the issue of repositioning suspended objects by use of topside motions (Lian & Sortland, 1996). They also did numerical simulations. The scenario they studied involved a 10-ton ROT suspended at 1,500 meters, as well as a case involving a 250 kg ROT. The vessel was repositioned by 300 meters in three minutes, and it is noted that reducing on increasing the speed with 50 percent did not affect the response of the suspended object.

Their simulations show that both the light and the heavy systems have vertical excursions and require time to settle. Figure 2-11 is an excerpt from their paper, and it shows the results. As seen, even the heavy system can have a vertical excursion of more than 100 meters, with a settling time of over 40 minutes. The resettling time is a function of the current speed, the weight of the payload and the cable and the direction of the vessel motion versus the current (Lian & Sortland, 1996).

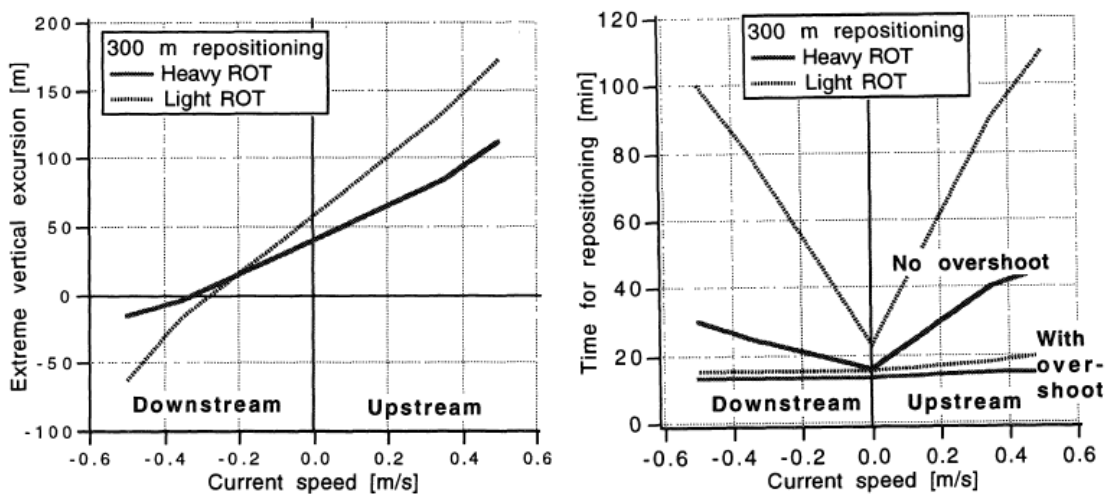


Figure 2-11: Vertical excursions and resettling times (Lian & Sortland, 1996)

Their suggestion for reducing the resettling time is to use an “overshoot method”, where the vessel sails past its intended position during repositioning, and then returns to the target site. As seen in Figure 2-11, this reduces the resettling time considerably, especially for the light payload. For heavy payloads the resettling time may be short compared to the duration of the operation, but it should still be studied.

It is noted that the simulations carried out by Lian and Sortland were done for a water depth of 1,500 meters. Installation in 4,000 meters, as is the focus of this thesis, will mean more than twice the length of the lift line. This will subject a much longer section of the line to the drag force. That said, the velocity of the current is typically lower in deeper water. Detailed studies of the topic should be done prior to any operation in deeper water.

2.2.6 Issue with landing accuracy and positioning

Landing equipment in ultradeep water is a challenge for several reasons. While guidelines are useful for precision installation in shallow waters, it becomes increasingly impractical to apply this method when entering deeper waters. Instead the equipment must be landed as accurately as possible without being connected to the seabed. Concerns with the accuracy of landing operations can be tracking the payload, but also excessive horizontal motions or horizontal offset as mentioned.

Earlier, tracking of deeply submerged equipment have been an issue. However, recent acoustic positioning systems such as the Sonardyne Ranger 2 Ultrashort Baseline are able to track equipment with high precision far beyond water depths where installation of subsea equipment is contemplated. According to its data sheet (see Figure A-4 in the appendix), it can track unlimited number of target to water depths beyond 7,000 meters. When optimised it has more than 0.1 percent system accuracy and updates the position maximum every second. It is also able to interface with dynamic positioning systems (Sonardyne Inc, 2016).

Horizontal motion is another issue for landing accuracy. Manoeuvring the payload to compensate for a constant offset as mentioned in the previous chapter does not remove the issue with horizontal oscillations. These oscillations are results of the topside motions, as waves excite the system. Accurately manoeuvring the payload by use of crane is also difficult because of the delay between the manoeuvre and the payload’s response, and crane tip motions will cause even more oscillations than a winch mounted on the deck of the vessel. While 3D-motion compensating cranes are on the market, at the time of submission of this thesis none have capacities higher than 20 tons. For excessive motions, one solution can be installing clump weights and winch systems and connect these to the payload.

The required precision and the weather conditions are the determining factor for successful landing operations with respect to accuracy. If high precision is required, the operational limits will become lower which again will reduce the weather windows of the operations.

2.3 Subsea equipment

The subsea production system (SPS) is a collective name for the subsea equipment installed on a field that contributes to the production of oil and gas. They can range in complexity from single production wells to large field developments with subsea processing equipment like separators or compressors. Particularly in deep water it is beneficial to locate more equipment on the seabed. The size and weight of the different equipment types vary, and the installation operation of these might therefore be different. Some typical types of subsea equipment are listed below.

- **Subsea Xmas tree**

Assembly of piping and valves and associated controls and instrumentations that is landed and locked on top of the subsea wellhead for controlling the fluid from the well (Bai & Bai, 2012). Can be produced in a vertical or horizontal configuration, where the direction refers to the production valves. Size and mass varies, but typical dimensions can be 5 x 5 x 4 meters and 50 tons.

- **Subsea wellhead**

A structure for supporting the casing strings in the well. It usually includes a guide base; thus, the wellhead is also used for guiding while installing the tree (Bai & Bai, 2012).

- **Subsea manifold**

Manifolds are structures in which produced fluid from multiple wells are collected into single flowlines, as a way to reduce the number of connections to the production unit. Manifolds are sometimes combined in templates, so that Xmas trees can be placed into slots in the manifold. Manifolds vary in size as the requirements depend on the number of production wells connected to it. Typically, they can be between 100 and 300 tons if the structure is combined with a template, and around 10 x 10 x 5 meters in dimensions. The dummy-manifold used by Petrobras in the full-scale model test was 280 tons and around 16x8x5 meters (Stock, Ferreira, da Silva, & Machado, 2006).

- **Subsea processing equipment**

In the future there may be a wish to install different types of equipment. To increase efficiency and reduce the requirements of topside facilities, more equipment is designed to process the produced fluids subsea. This can simplify transportation or maintain and increase production. Processing can be separation of oil, gas and seawater, to avoid transporting water and thus allowing a larger volume of valuable fluids. It can also be compression of gas, heating or cooling, drying of gas and or cleaning of produced water. Concepts are being considered where all production, processing and transportation or storage is done in facilities installed on the seabed, to reduce the dependency on topside installations. The size of these types of equipment depends on its purpose and concept. A vertical gravity separator can for example be 25 meters tall.

2.4 Risk management in marine operations

This chapter is based on the content of *DNV-RP-H101* for risk management in marine operations, and *Risk Analysis* by Terje Aven for general risk analysis approaches. Risk can be considered as the two-dimensional combination of consequences and the uncertainties associated with these. The uncertainty is related to the probability of an initiating event happening and the outcome of such an event. In marine operations there is always an element of risk involved, and this risk should be studied in order to manage it properly. The main objective of a risk analysis is to describe risk by presenting an informative risk picture. Aven suggests creating a risk picture based on the *initiating event*, *consequences*, *probabilities* and *knowledge* (Aven, 2015). When thought of as negative, the initiating event can be considered an *undesired event*.

Important terms related to risk management are, as defined by DNV (Det Norske Veritas, 2003):

- **Hazard:** Potential source of risk
- **Accident:** Event that which cause injury, illness and/or damage/loss to assets, environment or third parties.
- **Incident:** Event or chain of events which could have caused injury, illness and/or damage/loss to assets, environment or third parties.
- **Risk analysis:** Use of available information to identify hazards and to estimate risk.
- **Risk assessment:** Overall process of risk analysis and evaluation.
- **ALARP:** As Low As Reasonably Practicable. The risk should be as low as *reasonably practicable* rather than as low as *possible*, as there are usually measures that *can* reduce the risk but that are impractical or too expensive to implement.

A risk analysis can be qualitative, quantitative or a combination. A quantitative description of the risk may be very useful but is dependent on sufficient background knowledge. It can be unsafe to provide a quantitative representation of the risk picture if the numbers are based on weak knowledge. A qualitative or semi-quantitative analysis may be just as useful because it highlights potential hazards, and so those responsible can consider if measures are necessary.

Aven separates between simplified, standard and model-based risk analysis (Aven, 2015). Model-based risk analysis is primarily quantitative, whereas a standard risk analysis can be qualitative and quantitative. This thesis contains a limited standard risk analysis of the pendulous installation method, with an emphasis on hazard identification. The analysis can be found in chapter 4.5.

2.4.1 Parameters for risk assessment of marine operations

DNV recommends that risk within marine operations is assessed against criteria for the following:

- Personnel

- Environment
- Assets
- Reputation

Risk analyses can be qualitative or quantitative. Because marine operations have an element of uniqueness, it might be difficult to do a quantitative analysis. It is however recommended to always perform qualitative risk assessments. The assessment parameters and related keywords proposed by DNV are listed in Table 2-2, from DNV-RP-H101 (Det Norske Veritas, 2003). These parameters should be used to create a risk picture for the marine operation as a whole.

Personnel exposure

Personnel safety may be considered the most important consideration during marine operations. The focus is reducing the exposure of personnel to risk. This is done mainly by reducing the probability of undesired events. The personnel involved in the operation should have the required skills and skill level to be able to perform their tasks in a safe and efficient manner. Experience with similar operations is a factor that reduces the probability of an undesired event. It is necessary that the personnel are aware of both their own and other tasks in the operation, to avoid misunderstandings or disagreements. If all involved are aware of what to do at all times the probability of an undesired event is reduced. The minimum number of personnel necessary for safe operations should be present, to expose as few as possible to the hazards of the work site. This reduces both the probability and the consequence of an undesired event.

Overall project particulars

The risk of delays is related to the probability of it happening and the potential consequences. Probability can be increased by poor planning, and the consequence can be increased cost. Replacement time/cost and repair possibilities should also be considered. Involvement of external resources might change the ability to manage the operation properly (not necessarily negatively), depending on the communication between those involved.

Existing field infrastructure

Existing infrastructure can affect the risk picture by providing more options if it is support infrastructure. However, it also represents exposed assets that must be considered when for example handling heavy objects.

Handled objects

The value, structural strength and robustness of an object should be included in the risk picture. Valuable objects with low structural strength, such as control modules, will represent a high risk. A steel frame will have high structural strength and the risk is therefore lower.

Table 2-2: Risk assessment parameters (Det Norske Veritas, 2003).

Assessment Parameter	Keywords for assessment
Personnel exposure	-Qualification and experience of personnel -Organisation -Required presence -Shift arrangements -Deputy and backup arrangements
Overall project particulars	-Delay -Replacement time/cost -Repair possibilities -No. of interfaces and contractors/subcontractors. -Project development period
Existing field infrastructure	-Infrastructure – surface -Infrastructure – subsea
Handled object	-Value -Structural strength/robustness
Marine Operation method	-Novelty and feasibility -Robustness -Type of operations -Previous experience -Installability
Equipment use	-Margins/robustness -Condition/Maintenance -Previous experience -Suitability -Experience with operators or contractors
Operational aspects	-Cost of mobilised equipment -Language barriers -Season/environmental conditions -Local Marine traffic -Proximity to shore

Marine operation method

The method applied will impact the risk picture significantly. A new method, like the PIM, represents a higher risk as there is less relevant experience. Some methods and types of operations are more robust than others, for example with respect to the environmental conditions.

Equipment used

The risk picture is influenced by the operators' familiarity with the equipment, as well as its condition and suitability for the specific operation.

Operational aspects

The risk picture is influenced by the specific aspects of the marine operation. The cost and spread of mobilised equipment can increase the consequences, and possible language barriers can increase the probability of undesired events due to miscommunications. Local marine traffic and environmental conditions also affects the risk picture.

2.4.2 Risk management process

The risk analysis process is a description of all activities done to manage risk. This includes identifying risks and deciding how to manage them. Terje Aven suggests the process illustrated in Figure 2-12 for a general risk analysis. The steps can be divided into planning, assessment and treatment as shown in the figure. The procedure is general, and for marine operations it can be applied to multiple aspects of the operation.

The first step in Figure 2-12 is "Problem definition, information gathering and organisation of the work". For marine operations the problem is specified, and relevant data such as experience from similar events and weather data are usually available. As for selection of analysis method, marine operations should involve multiple. These are used for the risk assessment, and the product should be a complete risk picture. Possible measures are then identified, assessed and compared before a decision is made for which to implement.

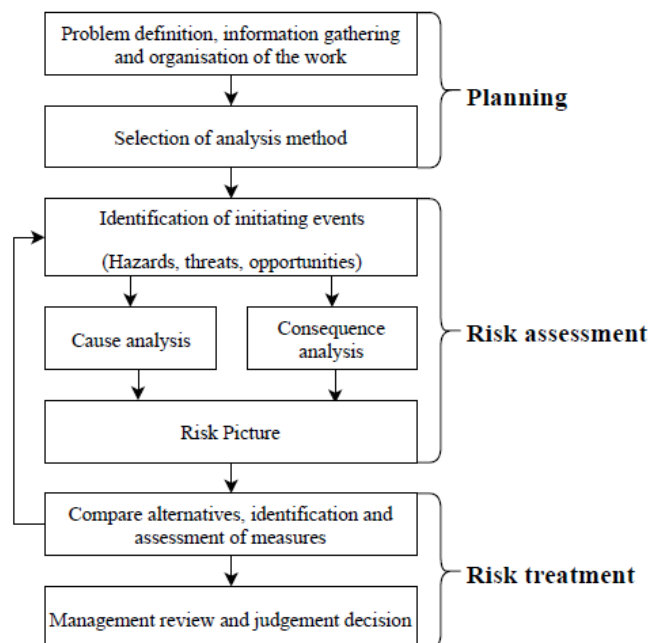


Figure 2-12: Risk Analysis Process (Aven, 2015).

2.4.3 Hazard identification

The purpose of hazard identification is to identify, list and describe hazards. Several methods are suggested in *RP-H101* in its appendix B, such as Hazard Identification Analysis (HAZID) or Hazard and Operability Analysis (HAZOP). “HAZID is used to identify and evaluate hazards when the operations and procedures have been developed and may be a useful technique to reveal weaknesses in the design and the marine operations detailed procedures. The technique is used to identify and evaluate hazards early in a project, being conducted at the conceptual and front-end engineering stages” (Det Norske Veritas, 2003). A HAZID is typically reported in sheets such as Table 2-3. For a semi-quantitative risk analyses, one can also include a risk value, which is a probability multiplied with a consequence value.

Table 2-3: Suggested HAZID work sheet

Operation: -						
Activity	Undesired event	Description of consequence	Existing risk reducing measures	Actions/reassures to reduce/eliminate risk	Responsible for implementations	Comments
-	-	-	-	-	-	-

As for HAZOP, DNV mentions three variants: Early Procedure HAZOP (EPH), System HAZOP and Procedure HAZOP, for early in the process, complex systems or for a finished procedure respectively. Aven defines it as such: “A HAZOP study is a systematic analysis of how deviation from the design specifications in a system can arise and an analysis of the risk potential of these deviations” (Aven, 2015). A HAZOP is based on guidewords that describe scenarios. In *DNV RP-H101* appendix B there are suggested guidewords for a HAZOP of marine operations. Applied guidewords in this thesis, and descriptions, for an EPH are (Det Norske Veritas, 2003):

- No/Not/Don’t (The intended activity does not occur, no direct substitute takes place).
- More (higher physical condition/higher activity than intended).
- Less (lower physical condition/lower activity than intended).
- As well as (An additional component/condition present).

A Procedure HAZOP is applied when a *detailed* procedure is available. The guidewords are therefore more specific. The purpose is to ask, “what if?” for the specific guidewords. Examples by DNV are:

- Weather: Unclear weather-restrictions or unexpected deterioration of weather.
- Impact: Impact between objects.
- Drop: Drop of objects from a higher level.
- Rupture: Rupture of critical equipment.

In a HAZOP, the guidewords are used to address deviations, and then causes and consequences of such deviations are determined and addressed. Figure 2-13 illustrates the general procedure.

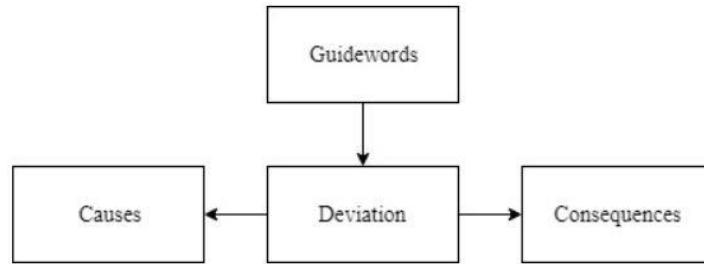


Figure 2-13: HAZOP flowchart (Aven, 2015).

2.4.4 Cause & Consequence analyses

For each initiating event, or deviation, identified, Aven writes that cause and consequence analyses should be carried out. The outcome of cause and consequence analyses can be presented in a bow-tie diagram as illustrated in Figure 2-14.

The purpose of a cause study is to determine what conditions or environments are needed for the initiating event to occur. This is done by considering what creates possible causes for specific initiating events, and there might be more than one. Typically, a cause analysis can be carried out as a brainstorming or more sophisticated techniques, but experts on the activities with in-depth understanding should be involved. In many cases the analysis will require dividing it into sub-analyses as illustrated to the left in Figure 2-14. If one has access to failure data, these can be used as a basis for a semi-quantitative analysis (Aven, 2015).

The purpose of a consequence analysis is to address the possible consequences. One initiating event might have different consequences of varying degrees of severity. When the causes and consequences are identified, one can also determine which, if any, barriers to implement. These barriers can either be designed to prevent the initiating event from occurring or to limit the effect of the consequences. (Aven, 2015).

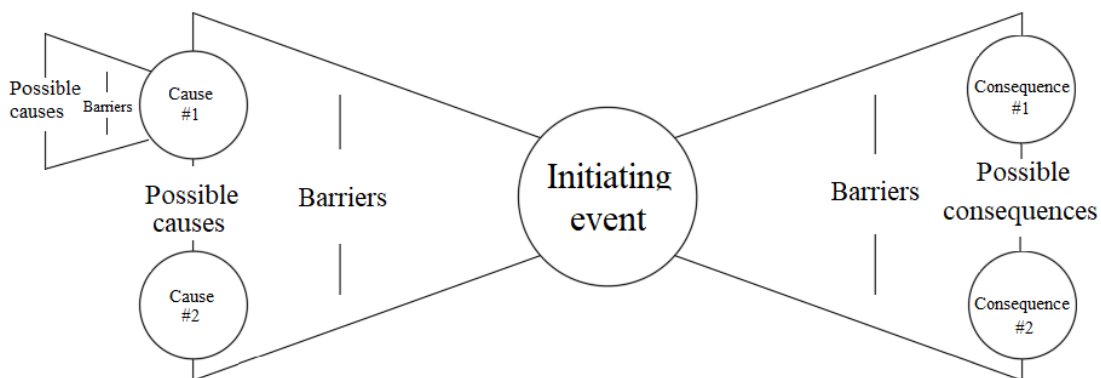


Figure 2-14: Bow-tie diagram

2.4.5 Risk description

To describe the risk, it can be divided into categories. DNV recommends in *DNV-RP-H101* that risk be divided into low, medium and high. Low risk is considered acceptable, while medium or high risk should lead to implementation of risk reducing measures. Probability and consequences should also be divided into categories. The categories for consequences should have specific criteria established in accordance with HSE policy and goals. Probability categories should be qualitatively described, guided by experiences from similar types of operations (Det Norske Veritas, 2003). Having divided the risk into categories, it can be presented by means of a risk matrix as shown in Figure 2-15 which is adapted from *DNV-RP-H101*.

Consequence					Probability			
Descriptive	Personnel	Environment	Assets	Reputation	Remote (A) Has occurred, not likely	Unlikely (B) Could occur	Likely (C) Easy to postulate	Frequent (D) Occur regularly
1. Extensive	Fatalities	Global or national effect. Restoration >10 years	Project/Product consequence cost >USD 10 mill	International impact/negative exposure	A1 = S	B1 = S	C1 = U	D1 = U
2. Severe	Major injury	Restoration >1 year. Cost >USD 1 mill.	Project/Product consequence cost >USD 1 mill	Extensive national impact	A2 = A	B2 = S	C2 = S	D2 = U
3. Moderate	Minor injury	Restoration >1 month. Cost >USD 1 K	Project/Product consequence cost >USD 100 K	Limited national impact	A3 = A	B3 = A	C3 = S	D3 = S
4. Minor	Illness or slight injury	Restoration <1 month. Cost <USD 1 K	Project/Product consequence cost < USD 100 K	Local impact	A4 = A	B4 = A	C4 = A	D4 = S
<i>Low Risk:</i> Acceptable risk (A) subject to application of the principle of ALARP and those activities specified in <i>DNV-RP-H101</i>								
<i>Medium Risk:</i> Operation can be executed after cost efficient measures are implemented and the analyses team has found the risk satisfactory (S).								
<i>High Risk:</i> If the undesired event after measures is evaluated to have <i>unacceptable risk (U)</i> the operation shall not be carried out. If the operation is still to be carried out, formal application for deviation shall be filed according to established procedures.								

Figure 2-15: Risk matrix, adapted from *DNV-RP-H101* (Det Norske Veritas, 2003, p. 36).

2.4.6 Risk treatment

Aven defines risk treatment as the process of selection and implementation of measures to modify risk, including measures to avoid, reduce, optimise and transfer risk (Aven, 2015). The following measures are recommended by DNV. Note that these are summaries from *DNV-RP-H101*.

- Operational Feasibility Assessments:

All marine operations shall be confirmed as feasible. It is important to do this at an early stage in order to avoid extra costs due to for example changing of vessels. Critical activities should also be identified as early as possible. The input to the assessment is a method description (Det Norske Veritas, 2003).

- Document Verification

Essential for quality assurance. This shall prevent design or planning errors. All documents shall be registered in a master document register and controlled (Det Norske Veritas, 2003).

- Familiarisation

Thorough familiarisation of personnel with their tasks. All involved personnel should have in-depth understanding of their tasks and who is responsible. Training videos, detailed drawings, operation manuals et cetera are inputs, as are experience reports. A procedure HAZOP should also be regarded as part of the familiarisation (Det Norske Veritas, 2003).

Further measures that are applicable to marine operations are:

- Personnel Safety Plans
- Emergency preparedness.
- Marine Readiness Verification
- Inspection and testing
- Survey of vessels
- Toolbox talk.

The measures described and mentioned are implemented to reduce the chance of an initiating event, or the consequences of such an event. For example, document verification and familiarisation are barriers to prevent an initiating event, while emergency preparedness and personnel safety plans are barriers to minimise the consequences.

2.5 Economics of installation in ultradeep water

This chapter considers briefly the economics of installation operations. However, it is noted that it is beyond the scope of this thesis to estimate accurately the cost of marine operations. The cost of installation operations can be a significant part of the CAPEX, though it obviously varies greatly from case to case. Bai & Bai suggests in the *Subsea Engineering Handbook* that the installation operation can represent as much as a third of the total CAPEX of the project, as shown in Figure 2-16.

Vessel availability, weight and size of equipment, installation method and potential special tools are considerations that must be made, and heavy equipment or specialized vessels can be very expensive.

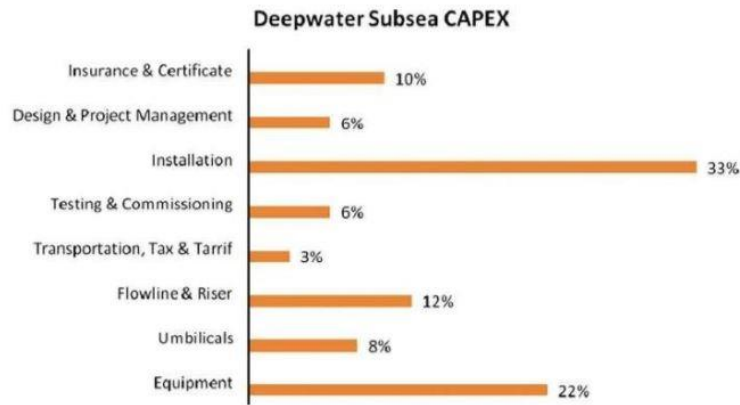


Figure 2-16: Deepwater subsea CAPEX

The Four main components of the cost of installation are according to Bai & Bai (Bai & Bai, 2012):

- 1) Vessel mobilization and demobilization
- 2) Vessel day-rate and installation spread
- 3) Special tooling rent cost
- 4) Cost associated with vessel downtime or standby waiting time.

All components depend on the type of operation. Mobilization and demobilization can range from a few hundred thousand to several millions depending on the vessel (Bai & Bai, 2012), and day-rates are extremely volatile. An example of this was the tenfold increase over two weeks for North Sea AHTSs, from 70,000 NOK to 700,000 NOK, as Westshore Shipbrokers told Norwegian internet newspaper E24 in April 2018 (Sundberg, 2018). Bai & Bai lists some average vessel day-rates in *Subsea engineering handbook* in its chapter 6.5, and these are here listed in Table 2-4.

Table 2-4: Average day rates for different vessel types (Bai & Bai, 2012).

Vessel types	Average day rates
Drill ship < 1,500 m WD	\$240,000
Semi-submersible < 500 m WD	\$250,000
Semi-submersible > 500 m WD	\$290,000
Semi-sub > 1,500 m WD	\$430,000
Jack-up 100 m WD	\$90,000
Jack-up > 100 m WD	\$140,000
AHTS	\$50,000
Pipe laying vessel < 200 m WD	\$300,000
Pipe laying vessel > 200 m WD	\$900,000

To include other sources, in lecture notes provided by Lin Li it is suggested that floating crane vessels can cost between NOK 2 million to NOK 3 million and ATHSs in the range of NOK 700K to NOK 1 million a day (Li, 2017). Either way it is clear that prolonged operations can accumulate to a significant cost. Cost of engineering and project management must also be included. Wages vary, however studying Figure 2-16 it can be seen that design and project management only makes up around six percent of the CAPEX, i.e. relatively little compared to the installation cost.

As the costs rise and margins become smaller, the industry is becoming increasingly interested in reducing the cost of subsea developments. In *OG21 TTA4 Report Subsea Cost Reduction*, an OG21 report from April 2015, several topics were addressed that would reduce cost. One of these is to “increase the efficiency of marine operations”. Cost saving, or advantageous features mentioned are increased use of simulations, both real-time and during preparation. This can help familiarise crew with their tasks, as well as providing fact-based decision support. Real-time simulations also contribute to situational awareness (OG21, 2015).

Enhanced training of personnel for challenging operational scenarios is another measure to reduce time and cost. The report suggests that these measures will increase the efficiency of the overall marine operations. The report concludes with a cost reduction of 4% by improving the efficiency of marine operations with 25% (OG21, 2015). For multi-billion projects this can potentially mean hundreds of millions saved.

Chapter 3

Theory

To study installation of subsea equipment, it is necessary to be familiar with the theory behind the many different aspects of marine operations. The physics in a marine operation comprises ocean wave theory, fluid mechanics, multibody dynamics and mechanics of solids. When it comes to offshore lifting as opposed to onshore lifting, the most notable difference is the wave induced motions of the system. Knowledge of vessel motions is therefore essential. The waves cause a response of the vessel which causes motion of the crane tip, exciting oscillations in the lifting system. It is necessary to understand the coupled motion of the topside vessel and the immersed object, coupled by the lifting wire. An understanding of the mechanics of the lifting wire itself is also important to be able to evaluate the forces acting on it. Knowledge of the marine environment itself is also required when considering the different forces acting on the system, be it forces from the current, waves, or hydrostatic forces.



Figure 3-1: Marine environment (Vladtime, 2015).

3.1 Marine Environment

Waves, winds and currents are parts of the marine environment that can exert forces on offshore structures or vessels. Waves apply dynamic loading, and waves can typically be measured and described by wave spectra. This chapter describes the basics about wave theory. Currents are more difficult to describe: typically, local measurements are required. The chapter contains information on how currents are treated during planning for marine operations. Wind is an important factor when the payload is in the air, however since the focus of this thesis is ultradeep water it is not elaborated on here.

3.1.1 Waves

3.1.1.1 *Linear Wave Theory*

Linear wave theory describes the core theory of ocean surface waves. This theory is based on linear relations and boundary conditions, and the resulting waves have a sinusoidal shape. This is called regular waves. This is not sufficient to describe the real surface conditions, because the real waves are a combination of different wave heights, wave lengths and periods. The latter is considered irregular waves. Irregular waves can be described by a Fourier transformation as a sum of regular waves, which is why linear waves can be used as the basis of description of ocean waves. The following is retrieved from *Marine Technology and Operations* by Professor Over Tobias Gudmestad (Gudmestad, Marine Technology and Operations Theory and Practice, 2015). Long crests perpendicular to the flow direction is assumed, i.e. the waves are considered two-dimensional.

The sine or cosine wave has the following surface profile:

$$\xi = \xi(x, t) = \xi_0 \sin(\omega t - kx) \quad (1)$$

Where:

- $\xi_0 = \text{Amplitude}$,
- $\omega = \frac{2\pi}{T} = \text{angular frequency}$, $T = \text{wave period}$
- $k = \frac{2\pi}{L} = \text{wave number}$, $L = \text{wave length}$
- $d = \text{water depth}$.

The surface profile for waves is derived from the fluid velocity potential function for flow Φ . For irrotational, incompressible flow, the two-dimensional Laplace equation for the function is:

$$\nabla^2 \phi = \frac{\partial^2 \phi}{\partial x^2} + \frac{\partial^2 \phi}{\partial z^2} = 0 \quad (2)$$

Given the dynamic boundary conditions:

$$\text{Bottom Boundary Condition: } \frac{\partial \phi}{\partial z} \Big|_{z=-d} = 0$$

Dynamic Free surface boundary condition: $\xi = -\frac{1}{g} \frac{\partial \phi}{\partial t} \Big|_{z=0}$

$$\Phi(x, z, t) = \frac{\xi_0 g \cosh k(z+d)}{\omega \cosh(kd)} \cos(\omega t - kx) \quad (3)$$

Equation (3) is the wave velocity potential function. The energy per unit area of a harmonic wave is proportional to the amplitude squared, i.e. $E \propto \xi^2$.

In very deep water, $d \gg z$ in equation (3). This simplifies the expression:

$$\frac{\cosh k(z+d)}{\cosh(kd)} = \frac{e^{k(z+d)}}{e^{kd}} = e^{kz}$$

To study the forces from the water, it is often useful to look at the water particle velocity. Water particle velocities are obtained by taking the derivative of the potential function. The horizontal velocity of the wave particle is then given by:

$$u = \frac{\partial \phi}{\partial x} = \frac{\xi_0 k g \cosh k(z+d)}{\omega \cosh(kd)} \sin(\omega t - kx) \quad (4)$$

Given the deepwater simplification, the horizontal water particle velocity is given by:

$$u = \frac{\xi_0 k g}{\omega} e^{kz} \sin(\omega t - kx) \quad (5)$$

From equation (5) it can be seen that the water particle velocity depends on k and z . Z is the vertical position of the water particle, and k is the wave number.

Often it is useful to look at both the wave length and the wave period. The relation between these is called the *dispersion relation*, and is presented by Gudmestad as:

$$\frac{\omega^2}{gk} = \tanh(kd) \quad (6)$$

For very deep water, $kd \gg 1$, which gives $\tanh(kd) \sim 1$. This gives the dispersion relation for deep water, and a relation between wave length and wave period:

$$\omega^2 = gk \rightarrow \left(\frac{2\pi}{T}\right)^2 = g \left(\frac{2\pi}{L}\right) \rightarrow L = \frac{g}{2\pi} T^2 \rightarrow$$

$$L = 1,56T^2 \quad (7)$$

3.1.1.2 Irregular waves

Regular waves are not usually a good description of the actual wave conditions, as the waves are typically made up of different waves. Irregular waves can be described as a sum of sinusoidal waves through a Fourier transformation, as shown in Figure 3-2

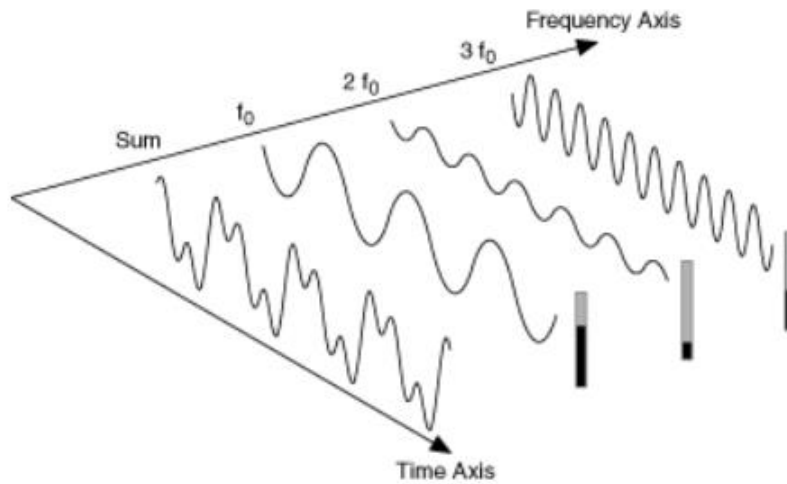


Figure 3-2: Combination of wave components. (National Instruments, 2012).

The surface function for n wave components can thus be written as:

$$\xi(t) = \sum_{n=1}^{\infty} \xi_n \cos(\omega_n t - \theta_n) \quad (8)$$

where:

- ξ_n = Amplitude of a wave component
- θ_n = phase of a wave component.

In the frequency domain, that is along the frequency axis instead of the time axis, the distance between these wave components is given by $\Delta\omega = \frac{2\pi}{T} = \text{Constant}$.

3.1.1.3 Wave Spectrum

Two different measurements of the sea surface elevation during a specific sea state will yield different results, as the surface does not repeat itself. To describe how the energy of the sea waves is distributed the function $S(\omega) = \frac{1}{2} \frac{\xi_n^2}{\Delta\omega}$ is introduced to plot a wave spectrum. The wave spectrum is used to describe the sea state because while the time series will be different, the distribution for frequencies is similar. For infinitely small spaces in the frequency domain, the spectrum becomes a continuous curve. Several spectra are described in *Marine Technology and Operations*. For a fully developed sea state, the Pierson-Moskowitz spectrum is often used. However, for this project the JONSWAP (Joint North Sea Wave Project) spectrum was used for the simulation. As seen from Figure 3-3, the JONSWAP spectrum is better for modelling the energy of the highest waves.

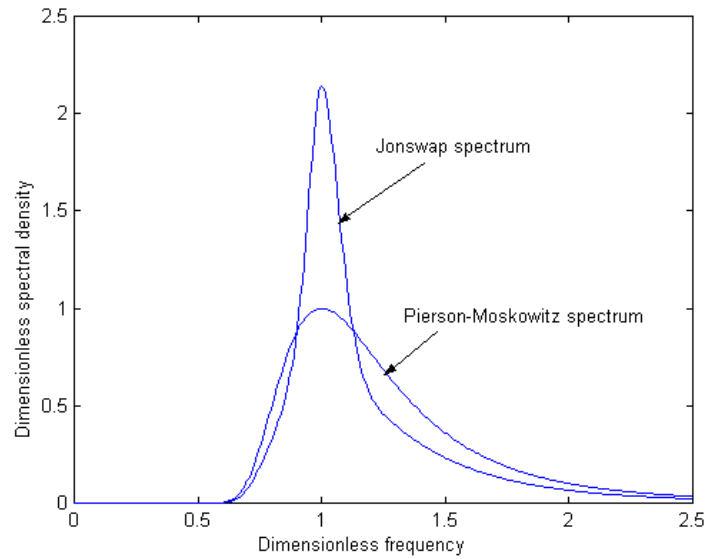


Figure 3-3: JONSWAP and Pierson-Moskowitz spectrum

The spectrum is defined as:

$$S(\omega) = \bar{\alpha} g^2 \omega^{-5} \exp\left(-1.25 \left(\frac{\omega}{\omega_p}\right)^{-4}\right) \gamma * \exp\left(-\frac{(\omega - \omega_p)^2}{2\sigma^2 \omega_p^2}\right) \quad (9)$$

Where:

- $\bar{\alpha}$ = modified Phillips constant = $5.058 \left[\frac{H_s}{T_p}\right]^2 (1 - 0.287 \ln \gamma)$
- ω_p = peak frequency
- γ = peakedness parameter.

The JONSWAP spectrum is usually determined from the following three parameters:

- H_s = Significant Wave Height. Defined as the average of the highest third of the waves in a period, usually 3 hours. Sometimes denoted $H_{s/3}$. This gives a more useful description of the sea conditions than the average of all waves, because the number of small waves is larger than the number of large waves.
- T_p = Peak period (or dominating harmonic period). Defined as $T_p = \frac{2\pi}{\omega_p}$, where the peak frequency is the frequency related to the maximum value of the spectrum.
- γ = peak parameter. This determines the shape of the spectrum given the H_s and T_p . In *Marine Technology and Operations*, it is given between 1 and 7, dependent on the location.

Significant wave height and Peak period are often used to describe sea states, as it describes the severity of the waves and the period of the waves with the highest energy. This is of interest for evaluating the response vessels utilized in marine operations.

3.1.2 Currents

The information in this sub-chapter is retrieved from *DNV-RP-C205 – Environmental Conditions and Environmental Loads* (Det Norske Veritas, 2014).

Currents can cause large, steady excursions of a suspended payload, as it exerts a drag force on lifting wires along their entire length. Quoting the RP, “Information on statistical distribution of currents and their velocity profile is generally scarce for most areas of the world. Current measurement campaigns are recommended during early phases of an offshore oil exploration development. Site specific measurements should extend over the water column and over the period that captures several storm events.” (Det Norske Veritas, 2014).

Current velocity and direction can vary with depth, typically smaller in deep water. Close to the water surface, the current velocity profile is stretched or compressed due to surface waves. In general, the current velocity vector varies in space and time. Local current velocity should be taken as the sum of each current component present. These components are also dependent on water depth. They can be for example wind generated currents, tidal currents, longshore currents or loop and eddy currents.

In this thesis the current models were adapted from location specific measurements from *Deepwater current profile data sources for riser engineering offshore Brazil* (Jeans, et al., 2012).

3.2 Dynamics of marine operations

The theory for this section is adapted from *Marine Technology and Operations* (Gudmestad, Marine Technology and Operations Theory and Practice, 2015). Marine operations are dynamic events. Neglecting the dynamics of a marine operation would cause one to neglect the maximum values for all responses, as the responses are the sum of static and dynamic loads.

3.2.1 Free damped oscillations

The governing equation for dynamics of a single degree of freedom system is the equation of motion:

$$m\ddot{u} + c\dot{u} + ku = F(t) \quad (10)$$

Where:

- m = the mass of the system
- \ddot{u} = acceleration, \dot{u} = velocity, u = position
- c = damping [kg/s]. For subsea lifts this is typically the drag force.
- k = stiffness [N/m] or [Nm/degree].

- $F(t) = \text{an external force.}$

The stiffness is the rigidity of the system. For example, in a steel bar, the axial stiffness is the force required for elongation. For a vessel in heave, it is the product of water density, gravity and surface area.

In the absence of external forces, $F(t)$ is equal to zero. The natural frequency of a system is defined as $\omega_0 = \sqrt{\frac{k}{m}}$. Equation (10) can now be written as:

$$\ddot{u} + \frac{c}{m} \dot{u} + \omega_0^2 u = 0 \quad (11)$$

The solution of the characteristic equation for equation (11) for an exponent s then:

$$s_{1,2} = \left(\frac{c}{2m}\right) \pm \sqrt{\left(\frac{c}{2m}\right)^2 - \omega_0^2} \quad (12)$$

The term relative damping $\lambda = \frac{c}{2m\omega_0}$ is used to determine this, giving a damped frequency:

$$\omega_d = \omega_0 * \sqrt{1 - \lambda^2} \quad (13)$$

And the response of a system can now be given by:

$$u = e^{-\lambda\omega_0 t} (A \sin \omega_d t + B \cos \omega_d t) \quad (14)$$

Depending on the damping, this equation may yield the following:

- **Underdamped system:** The expression under the root in equation 9 is negative, giving an imaginary number. This represents oscillatory motion. Because damping is present, the oscillations will decay, i.e. the amplitudes will be reduced for each cycle.
- **Critically damped system:** the expression under the root is equal to zero. The system will quickly return to its equilibrium state. The time to reach the equilibrium is determined by the initial conditions.
- **Overdamped system:** the expression under the root is positive. There is no oscillation, only a decaying motion towards the equilibrium. The time to reach the equilibrium is determined by the initial conditions.

3.2.2 Forced Oscillations

Harmonic loading is given as a sine function, and in the same way regular waves can be added together into irregular waves, loading terms can be added together through Fourier expansions. A harmonic load can be given as:

$$F(t) = F_0 \sin(\omega t) \quad (15)$$

When the oscillations are forced, the response is given by a sum of the homogeneous equation (14) and a particular solution: $u = u_h + u_p$, where the particular solution is given by:

$$u_p = u_0 \sin(\omega t - \theta) \quad (16)$$

Where:

- $u_0 = \text{amplitude} = \frac{F_0}{m\omega_0^2} D = \frac{F_0}{k} D$
- $\theta = \text{phase angle} = \tan^{-1} \left(\frac{2\lambda\beta}{1-\beta^2} \right)$

given $D = \text{Dynamic Amplification Factor (DAF)}$:

$$D = \left(\left(1 - \left(\frac{\omega}{\omega_0} \right)^2 \right)^2 + \left(2\lambda \left(\frac{\omega}{\omega_0} \right) \right)^2 \right)^{-0.5} \quad (17)$$

DAF describes the magnitude of the dynamic response compared to the response from the static loading. The phase angle is the angle between the loading and the response. A forced oscillation with the same frequency as the system's natural frequency, i.e. relative frequency $\left(\frac{\omega}{\omega_0} \right) = 1$ gives resonance, or uncontrolled oscillation. Real cases are typically damped to some extent, inhibiting the oscillation. Figure 3-4 shows the relation between the relative frequency and the DAF for different damping. As seen, for a relative frequency of 1 for no damping causes uncontrolled dynamic amplification. This is obviously undesirable.

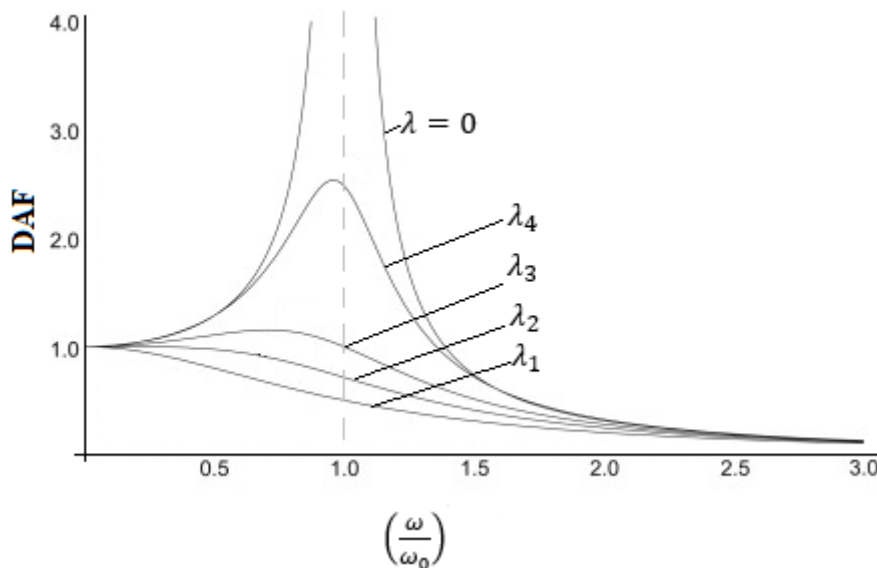


Figure 3-4: Dynamic amplification factor for different relative frequencies.

3.2.3 Pendulum Motion

The equation of motion is valid for rotational motion with response measured in degrees. For a simple pendulum the mass of the string is neglected. In the absence of damping, the pendulum is only affected by the gravity and the string tension T . With reference to Figure 3-5 the following equation can be derived for the pendulum motion:

$$F = m\ddot{u} \rightarrow -mg\sin(\theta) = m(l\ddot{\theta}). \text{ [For limited motion, } \sin(\theta) \approx \theta \text{]}$$

$$\rightarrow \ddot{\theta} + \frac{g}{l}\theta = 0 \quad (18)$$

Introducing the natural frequency $\omega_0 = \sqrt{\frac{g}{l}}$, it can be seen that the systems natural frequency is not mass-dependent. Including damping, the equation becomes:

$$\ddot{\theta} + c\dot{\theta} + \omega^2\theta = 0 \quad (19)$$

For a subsea lift, damping is provided by the drag force. The drag force is typically large enough to prevent pendulum motions.

Note that ω_0 is the angular natural frequency. The relationship between the angular and oscillation frequency f is given by $\omega_0 = 2\pi f$. The natural period of the system is then given by $T_0 = 2\pi/\omega_0$. Referencing section 2.1, if the system natural period coincides with the wave peak period the system will be in resonance, and excessive motions are expected.

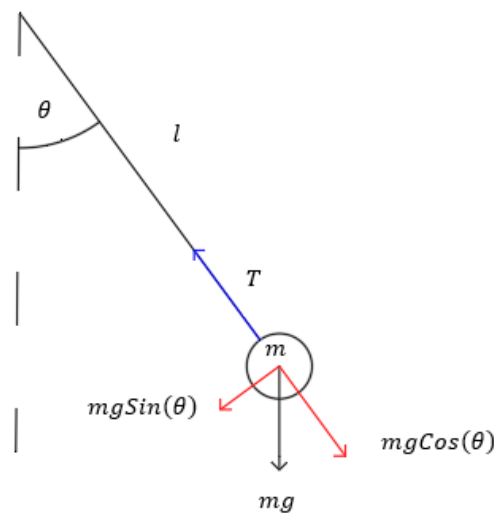


Figure 3-5: Simple pendulum

3.3 Vessel Motions

The theory in this section is adapted from *Marine technology and operations*. As described by professor Gudmestad (Gudmestad, Marine Technology and Operations Theory and Practice, 2015), when interacting with waves, the vessel response is determined by its Response Amplitude Operator (RAO). The RAO determines the response of a vessel to a wave with a given significant wave height and frequency. The direction of the wave relative to the vessel can also significantly impact the vessel response. For a moving vessel, the encounter frequency (how often a vessel interacts with a wave) will determine the response rather than the wave frequency. As described by Orcina (Orcina, u.d.), the RAO is determined for the frequency domain, and the different responses are given as a function of the frequency. The RAO for a specific response is given in meter per meter for translational motion, and degree per meter for rotational motion, as well as phase. The phase describes the delay of the response relative to the wave.

If the wave spectrum for a location and the frequency response characteristics of a vessel is known, the response spectrum for the vessel in that location is found from:

$$S_{\sigma\sigma}(\omega) = |G(\omega)|^2 * S(\omega) \quad (20)$$

Where:

- $S_{\sigma\sigma}(\omega)$ = Response spectrum for a specific response, for example heave.
- G = the transfer function of the response of the vessel. This can be defined as the RAO of the system.
- $S(\omega)$ = The wave spectrum.

Using this relation, the specific response for different conditions can be found. This is not necessarily motions, but any type of response that can be given as a function of the wave frequency. Gudmestad uses stress at a point as an example (Gudmestad, Marine Technology and Operations Theory and Practice, 2015). Note that the RAO is usually provided by the owner of the vessel or the shipyard.

A vessel at sea has six degrees of freedom, with reference to Figure 3-6:

- Surge – Translational motion along the x-axis
- Sway – Translational motion along the y-axis
- Heave – Translational motion along the z-axis
- Roll – Rotational motion about the x-axis
- Pitch – Rotational motion about the y-axis
- Yaw – Rotational motion about the z-axis.

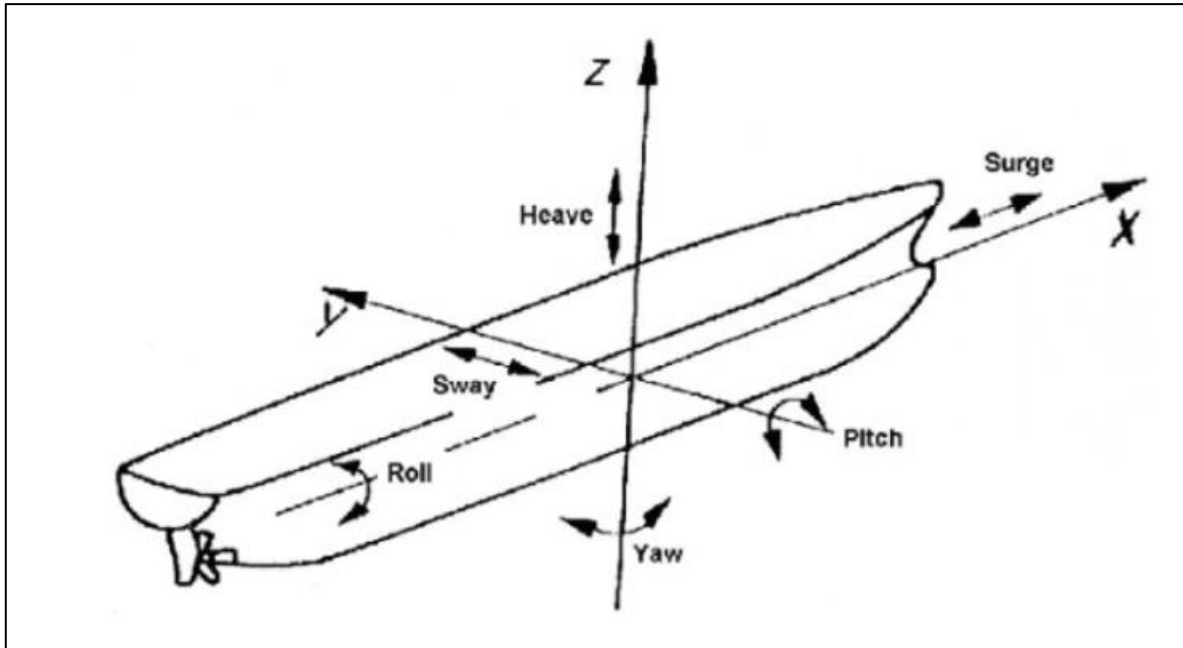


Figure 3-6: Vessel degrees of freedom (Prasanna, 2014)

Coupled motion

When multiple bodies are interacting in the same system the system changes properties. One must account for how one degree of freedom affects others. Because all degrees of freedom interact the new properties of the combined system are presented in matrices. Recalling that the natural frequency of a system is $\omega_0 = \sqrt{\frac{k}{m}}$, in a system consisting of multiple bodies both the stiffness k and the mass m would be matrices.

The Figure 3-7 shows a simple example of the coupled motion. Here the heave of the payload is a sum of the heave of the vessel and the roll-induced heave of the payload.

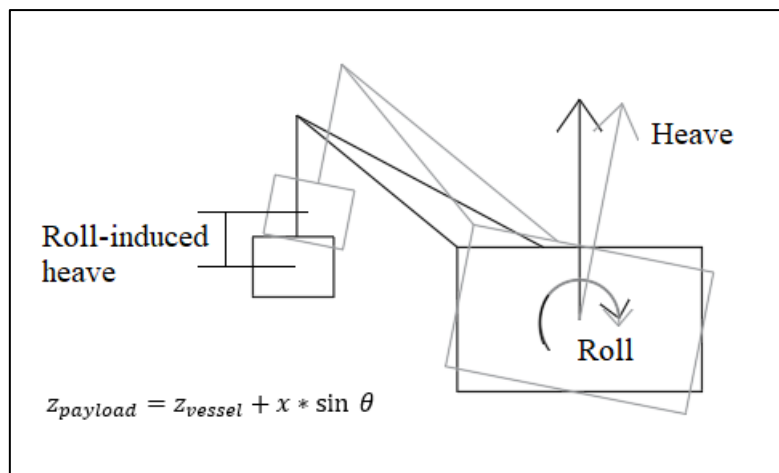


Figure 3-7: Roll-induced heave

3.4 Lifting operations in deep water

The theory in this section is retrieved from Det Norske Veritas (DNV)'s Recommended Practice (RP) H-103 on subsea lifting (Det Norske Veritas, 2009). This sub-chapter contains the aspects that are special when considering lifting operations in deep water. The information from the RP is used to determine what forces to consider, what simplifications can be made, and how these will affect the model.

3.4.1 Forces

Forces considered in lifting operations in deep water:

- $F_{Line} = \text{Liftwire force}$
- $W_0 = \text{Weight of payload in air}$
- $W_s = \text{Weight of payload in water}$
- $F_B = \text{Buoyancy force}$
- $F_I = \text{Inertia force}$
- $F_D = \text{Drag force}$

Drag and inertia forces are calculated using the coefficients of drag and added mass respectively. Added mass is the mass of the fluid that is accelerated by the acceleration of a submerged object in motion. These are experimental and dependent on the relative flow properties and object geometry.

- Drag coefficient = $C_D = C_D(Re, KC, \Delta)$
- Added mass coefficient $C_A = C_A(Re, KC, \Delta)$

For cylindrical objects, these are dependent on the Reynold's number Re , Keulegan-Carpenter number KC and relative roughness Δ . These are respectively defined as:

$$Re = \frac{uD}{\nu}, \quad KC = \frac{v_m T}{D}, \quad \Delta = \frac{k}{D}.$$

Where:

- $u = \text{total flow velocity}$
- $D = \text{diameter}$
- $k = \text{roughness height}$
- $T = \text{Wave period or oscillation period}$
- $v_m = \text{maximum orbital particle velocity}$
- $\nu = \text{fluid kinematic viscosity}$

The RP contains tabulated values for the drag and added mass coefficients for different shapes. Rough cylinders are often given a drag coefficient of 1.05, while the added mass coefficient of a circular cross section is given as 1.00 in the RP-H105 table A1.

3.5.1.1 Liftwire force

The liftwire force is the sum of a mean force and a time dependent dynamic force due to the vessel motions. The mean force is equal to the sum of all mean forces or given by the static elongation of the cable $F_{static} = k * \delta x$. The dynamic load is a sum of all dynamic forces, or a function of the dynamic liftwire elongation, $F_{dynamic}(t) = k * \delta x(t)$, where k is the axial stiffness of the liftwire and $\delta x(t)$ is the elongation of the cable. Hence for elongation of the cable, the tension is increased.

$$F_{Line} = F_0 + F_{dynamic}(t) \quad (21)$$

3.5.1.2 Submerged weight of payload

The submerged weight of the payload is equal to the mass of the object times the gravitational acceleration, minus the buoyancy force. The buoyancy force is equal to the mass of the displaced liquid. This is assuming the payload is not flooded during the lift or flooded in advance. For a lift through the water surface, the buoyancy force is time dependent as the volume is gradually submerged, but for a deeply submerged object it is constant. The submerged weight of the object is thus:

$$W_s = Mg - \rho_{water}Vg \quad (22)$$

Where:

- ρ_{water} = the density of water
- M = mass of object
- V = Submerged volume of object.

3.5.1.3 Drag force

The drag force of an object is given as a function of the relative velocity of the object, working against the motion. Hence it can be considered a damping force for oscillatory motion. The typical contributions to the drag force for a submerged object is its motion and the velocity of the current. The drag force is given by:

$$F_D = \frac{1}{2} \rho_{water} C_D A_p u(t)^2 \quad (23)$$

Where:

- $C_D = \text{drag coefficient}$
- $A_p = \text{projected area on flow direction}$
- $u = \text{relative velocity.}$

3.5.1.4 Inertia force

The inertia force due to a relative motion between the water and an object is given by:

$$F_I = -(M + m_{added})\ddot{u} \quad (24)$$

Where:

- $m_{added} = \text{added mass, for a circular cross section given as } m_{added} = \rho C_A A_{reference}$

3.5.2 Slender objects approximation

Many objects can be approximated by taking them as a combination of slender elements, that is elements with circular cross sections that have a small diameter compared to their length. The normal force on the object cross section is then neglectable compared to the force in the radial direction. The force per unit length on a moving slender object can be calculated by the Morison load formula:

$$f_N(t) = -\rho C_A A \ddot{r} - \frac{1}{2} \rho C_D D \dot{r} |\dot{r}| \quad (25)$$

Where:

- $A = \text{Cross sectional area}$
- $\ddot{r} = \text{relative radial acceleration of object}$
- $\dot{r} = \text{relative radial velocity of object}$

3.5.3 Stretched length of lifting wire

The stretched length of the lifting wire is given by the tension and the axial stiffness of the wire. As mentioned in the beginning of section 2.4, the tension is given as a sum of the static and dynamic force in the wire. The static elongation is calculated from the submerged weight of the payload and the self-weight of the wire:

$$L_{stretched,static} = L \left[1 + \frac{W_s + \frac{1}{2}wL}{EA} \right] \quad (26)$$

Where:

- $L_{stretched} = \text{the stretched length of the wire}$
- $L = \text{initial length of wire}$
- $w = \text{submerged weight of wire per unit length [kg/m]}$

- $E = \text{Young's modulus of the wire}$
- $A = \text{Wire cross sectional area}$

The maximum dynamic elongation is given by the amplitude of the dynamic load. The dynamic load is governed by the topside motion. For long oscillation periods or an infinitely stiff wire, and without viscous forces, the payload would follow the topside motion. However, in reality the ratio between the topside amplitude η for a given frequency and payload motion is given by:

$$H(\omega) = \frac{|\eta_L|}{\eta} \quad (27)$$

Where $|\eta_L|$ is the absolute value of the amplitude of the payload. $|\eta_L|$ is dependent on the inhibiting forces in vertical direction described in this chapter, as well as linear damping in the wire. It is also dependent on the position along the cable, making the dynamic force a function of z and time. The elongation at the payload is given for $z=L$, and is thus given as:

$$L_{stretched} = L \left[1 + \frac{W_s + \frac{1}{2}wL + F(t)}{EA} \right] \quad (28)$$

If the dynamic load exceeds the static load, the wire will become slack when the amplitude is negative.

3.5.4 Horizontal offset due to steady forces

For a deeply submerged object, the steady force on the liftwire and the object causes a horizontal offset. For an axially stiff wire with negligible bending stiffness and a heavy object at the end, the offset in a unidirectional current is given by:

$$x(z) = \int_z^0 \left[\frac{F_{D0} + \frac{1}{2}\rho \int_{-L}^{z_1} C_{Dn} D_c (U_c(z_2))^2 dz_2}{W + w(z_1 + L)} \right] dz_1 \quad (29)$$

Where:

- $F_{D0} = \text{The hydrodynamic drag force on the lifted object given current velocity at } z=L, \text{ as described in section 2.4. It follows that the horizontal offset of the object is given for } x(L).$
- $\frac{1}{2}\rho \int_{-L}^{z_1} C_{Dn} D_c (U_c(z_2))^2 dz_2 = \text{the total drag force on the cable.}$
- $C_{Dn} = \text{the drag coefficient of the cable. This may also be a function of } z.$
- $U_c(z) = \text{current velocity at depth } z.$

For a uniform current, the hydrodynamic drag on the cable per unit length is given by:

$$f_{Dc} = \frac{1}{2}\rho C_{Dn} D_c U_c^2 \quad (30)$$

Figure 3-8 is a reference to equations (29) and (30). Note that the figure is retrieved from the RP, and $\xi(z)$ is the horizontal offset. In equation (29) it is denoted $x(z)$ to separate it from the surface profile in chapter 3.1.1.

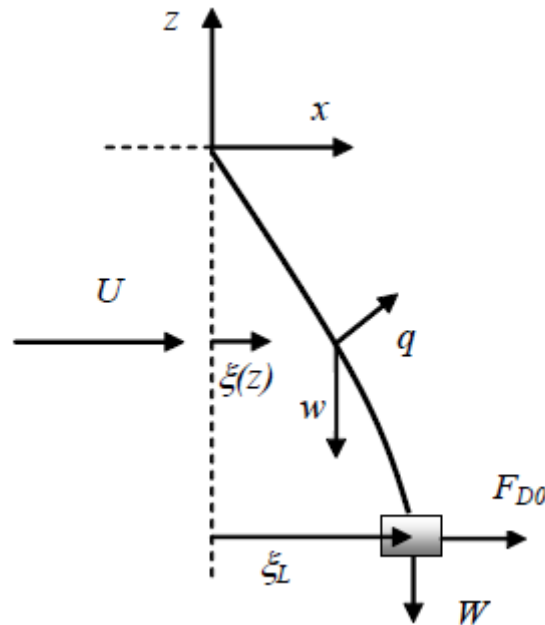


Figure 3-8: Horizontal offset of cable and payload (Det Norske Veritas, 2009).

Note that of horizontal displacement due to dynamic loads, it is written in the RP: “Such oscillations may be highly damped due to viscous drag on cable and lifted object”.

3.5 Marine Operations

3.5.1 Operational requirements

The following theory about operation criteria and weather restrictions is retrieved from DNV-OS-H101 (Det Norske Veritas, 2011). Limiting weather conditions must be established prior to the execution of a marine operations, i.e. operational limits (OP_{LIM}). This is typically at least, but not limited to, significant wave height H_s . Also, uncertainties with regards to the weather forecast should be considered. In DNV-OS-H101 this is done by use of an α -factor to reduce the operational limit to an acceptable level for weather forecasts:

$$OP_{WF} = \alpha * OP_{LIM} \quad (31)$$

Where:

OP_{WF} = Forecasted operational criteria (for example $H_{s,WF}$)

α = α -factor ($0.55 < \alpha < 1.0$)

OP_{LIM} = Limiting operational environmental criteria (for example $H_{s,LIM}$)

α should make sure that the probability of exceeding $1.5 * OP_{LIM}$ is less than 10^{-4} . For North Sea and Norwegian sea conditions α is normally selected from tables 4-1 through 4-5 in DNV-OS-H101 (Det Norske Veritas, 2011, pp. 32,33). For operations longer than 24 hours where the weather is monitored, one is referred to tables 4-1 and 4-2 as applicable. Figure 3-9 shows these tables excerpted from DNV-OS-H101 (Det Norske Veritas, 2011). With a meteorologist on site, table 4-3 can be used. As seen from the figures, higher level observations allow for higher α -factors. This gives a smaller reduction in the forecasted operational limits.

Table 4-1 α -factor for waves, base case							
Operational Period [h]	Design Wave Height [m]						
	$H_z = 1$	$1 < H_z < 2$	$H_z = 2 = 2$	$2 < H_z < 4$	$H_z = 4$	$4 < H_z < 6$	$H_z \geq 6$
$T_{POP} \leq 12$	0.65	Linear Interpolation	0.76	Linear Interpolation	0.79	Linear Interpolation	0.80
$T_{POP} \leq 24$	0.63		0.73		0.76		0.78
$T_{POP} \leq 36$	0.62		0.71		0.73		0.76
$T_{POP} \leq 48$	0.60		0.68		0.71		0.74
$T_{POP} \leq 72$	0.55		0.63		0.68		0.72

Table 4-2 α -factor for waves, Level B highest forecast							
Operational Period [h]	Design Wave Height [m]						
	$H_z = 1$	$1 < H_z < 2$	$H_z = 2$	$2 < H_z < 4$	$H_z = 4$	$4 < H_z < 6$	$H_z \geq 6$
$T_{POP} \leq 12$	0.68	Linear Interpolation	0.80	Linear Interpolation	0.83	Linear Interpolation	0.84
$T_{POP} \leq 24$	0.66		0.77		0.80		0.82
$T_{POP} \leq 36$	0.65		0.75		0.77		0.80
$T_{POP} \leq 48$	0.63		0.71		0.75		0.78
$T_{POP} \leq 72$	0.58		0.66		0.71		0.76

Table 4-3 α -factor for waves, Level A with meteorologist at site							
Operational Period [h]	Design Wave Height [m]						
	$H_z = 1$	$1 < H_z < 2$	$H_z = 2$	$2 < H_z < 4$	$H_z = 4$	$4 < H_z < 6$	$H_z \geq 6$
$T_{POP} \leq 12$	0.72	Linear Interpolation	0.84	Linear Interpolation	0.87	Linear Interpolation	0.88
$T_{POP} \leq 24$	0.69		0.80		0.84		0.86
$T_{POP} \leq 36$	0.68		0.78		0.80		0.84
$T_{POP} \leq 48$	0.66		0.75		0.78		0.81
$T_{POP} \leq 72$	0.61		0.69		0.75		0.79

Figure 3-9: α -factor tables, excerpt from DNV-OS-H101 (Det Norske Veritas, 2011)

3.5.2 Duration of marine operations

The duration of marine operations is defined by a reference period:

$$T_R = T_{POP} + T_C$$

Where:

T_R = Operation reference period

T_{POP} = Planned operation period

T_C = Estimated maximum contingency time

T_{POP} shall be based on a detailed schedule for the operation, and T_C shall be added to cover possible contingency situations and general uncertainty. If these are not assessed in detail, T_R should normally be taken as at least two times the planned operation period ($T_R \geq 2 * T_{POP}$). If there is extensive experience from similar operations, contingency time can normally be $0.5 * T_{POP}$. A T_C of less than 6 hours is normally not acceptable. Exceptions can be made for short, simple operations that are well documented.

3.5.3 Restricted and unrestricted operations

Marine operations may be classified as weather restricted or unrestricted operations based on their duration. The main difference in the classification of marine operations is how the environmental loads are selected. In DNV-OS-H101 they are defined as:

- Weather restricted:** Operations with defined restrictions to the characteristic environmental conditions, planned performed within the period for reliable weather forecasts. Marine operations with a reference period T_R less than 96 hours and a planned operation time T_{POP} less than 72 hours may normally be defined as weather restricted. These are not considered completed until the handled object is in a safe condition. Before initiation, a forecasted weather window with conditions $OP_{WF} = \alpha * OP_{LIM}$ must be forecasted. Start point of a restricted operation is normally defined from the issuance of the latest weather forecast. Figure 3-10, retrieved from DNV-OS-H101 illustrates the operation period (Det Norske Veritas, 2011).

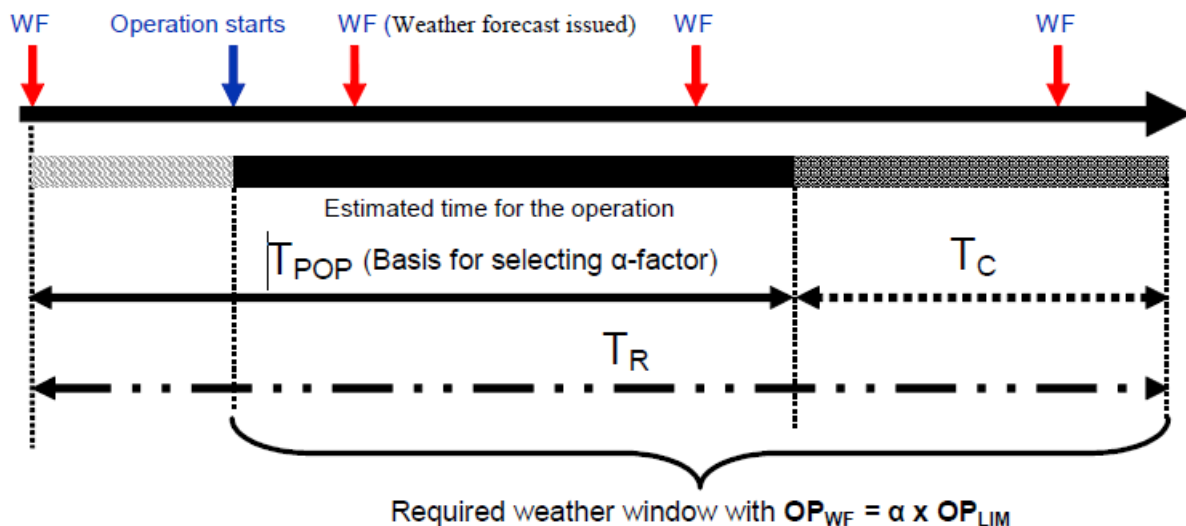


Figure 3-10: Required weather window (Det Norske Veritas, 2011)

- Unrestricted:** Operations with characteristic environmental conditions estimated according to long term statistics. Marine operations with longer duration than indicated for weather restricted operations ($T_{POP} > 72$ hours, $T_R > 96$ hours) are considered unrestricted. Environmental criteria for these operations should be based on extreme value statistics. Note

that operations with a longer duration can also be considered weather restricted if a continuous weather surveillance is implemented, and the object can be brought to a safe condition within the maximum allowable period for weather restricted operations (Det Norske Veritas, 2011).

Figure 3-11 illustrates the process of classifying a marine operation as restricted or unrestricted.

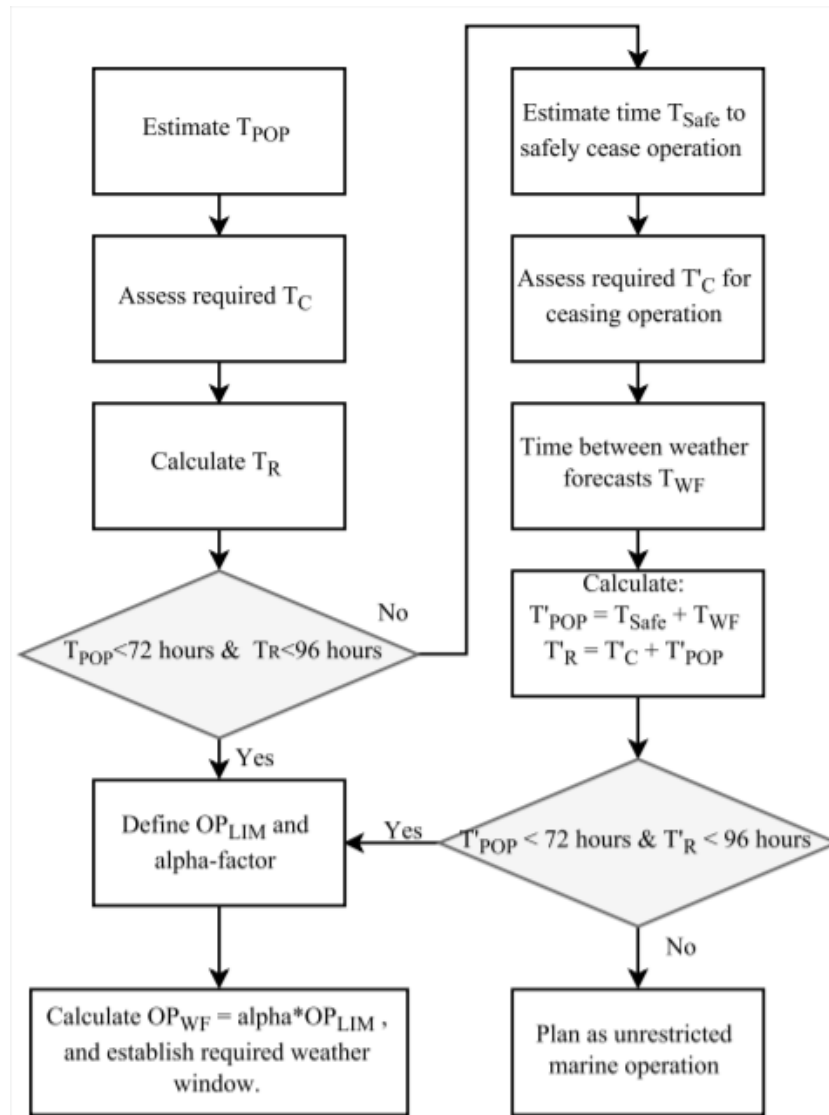


Figure 3-11: Classification of restricted or unrestricted operations (Det Norske Veritas, 2011).

Chapter 4

Pendulous Installation Method

The pendulous installation method is as mentioned in the introduction a non-conventional installation method developed by Petrobras. The purpose was to develop a method where they would overcome the challenges of ultradeep water without specialized HLVs, or their own drilling vessels. Qualified FRDSs were not available at the time. This chapter gives a thorough overview over the method, explaining the characteristics and the general procedure. In addition, the chapter contains a standard risk analysis of the method. In this thesis the Petrobras method was studied, however it is noted that Alan Wang et al. described an alternative approach in *Pendulous Installation Method and its Installation Analysis for a Deepwater manifold in South China Sea*. Both approaches are described in chapter 4.3.

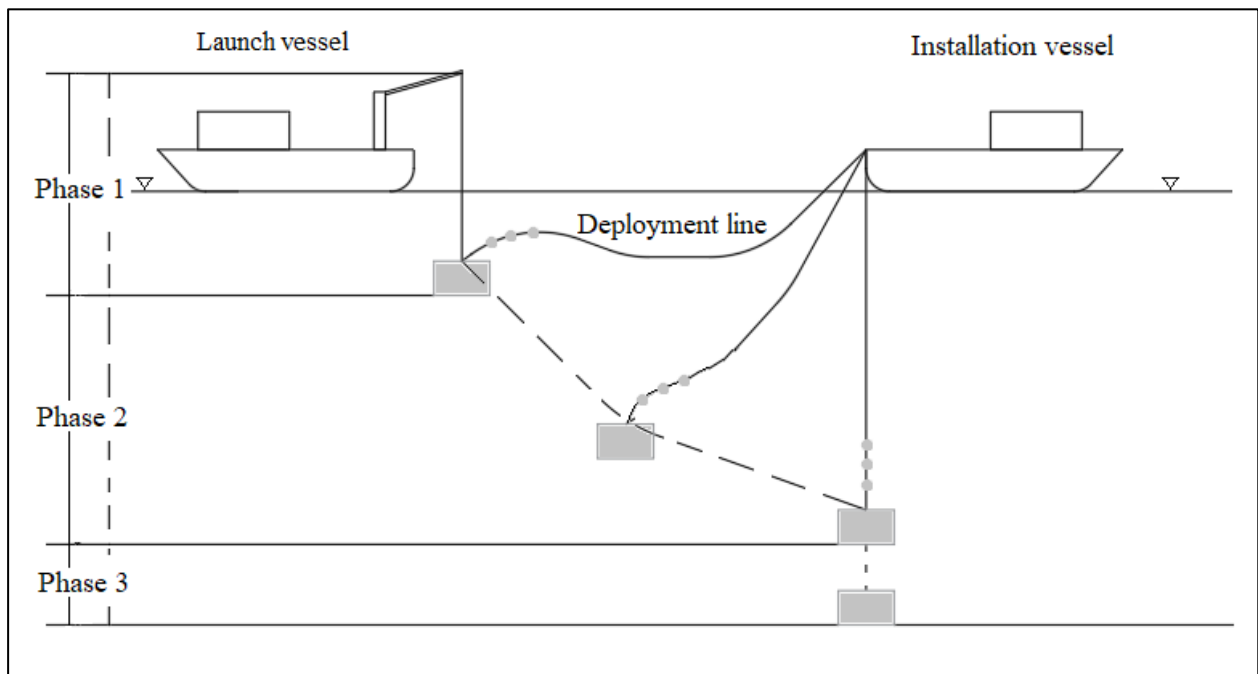


Figure 4-1: Pendulous Installation Method divided into phases

4.1 General description

Figure 4-1 illustrates the basic concept of the PIM. Two vessels are involved, the launch vessel and the installation vessel. The launch vessel is positioned at a distance of around 90 percent of the water depth away from the installation site. It submerges and releases the payload, which will then follow a pendulum trajectory towards the target site. It follows this trajectory until it is suspended from the installation vessel at a suitable distance from the seabed. The idea behind the method was to use fibre ropes without requiring an FRDS. Therefore, the deployment line (see Figure 4-1) is made out of fibre rope. It is attached to an A&R winch, and when suspended it can be lowered conventionally. The payload is then landed on the seabed, as for a conventional installation. Topside, a length of steel wire

can be connected to the fibre rope. This allows for use of AHC systems without special treatment for the fibre rope. This is an advantage over use of an FRDS.

The PIM can be divided into three main phases: Lift-off and submersion, free-fall and landing. The first and last phases are the same as for conventional installation methods. The difference and key characteristic of this method is phase two.

Phase 1 - Lift-off and submerging: Carried out by the launch vessel. Payload is lifted off deck and lowered through the splash zone. Challenges related to this phase are described in chapter 2.1.2.3. The phase ends when the payload is submerged and ready to be released.

Phase 2 - Free-fall: Payload is released from crane at launch vessel. It then follows a pendulum trajectory. Challenges related to this phase is discussed in this sub-chapter 4.4. The phase ends when the payload is suspended from the installation vessel.

Phase 3 - Landing: Payload is lowered to the seabed. Challenges related to this phase is described in chapter 2.1.2.5. The phase ends when the payload is landed on the seabed.

Figure 4-2 shows a simple work breakdown structure of the PIM. This is similar for many marine operations, however here there must be a high emphasis on the planning. This is because there is little experience with this method, and the hydrodynamic behaviour of the payload is less predictable than for conventional installation.

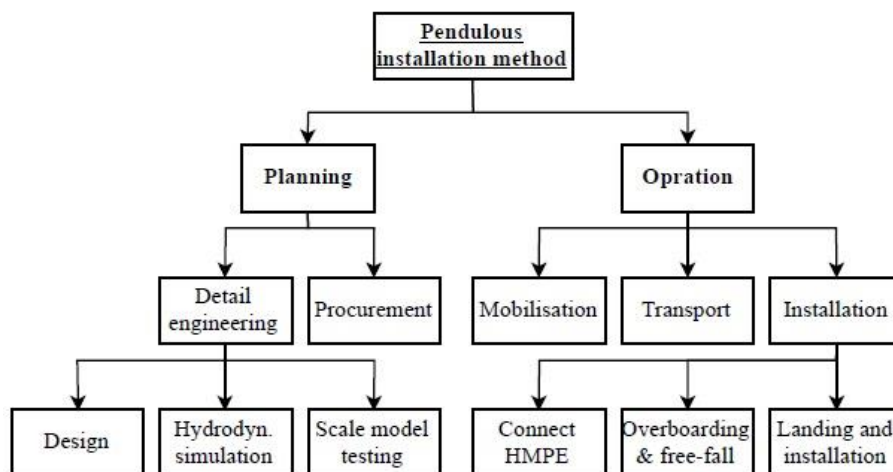


Figure 4-2: Work breakdown structure of the PIM.

4.2 Requirements

Which vessels are required for the method depends on the capabilities of the vessels that are involved. If some of the vessels can only perform single tasks, more might be required. The obvious example is

Petrobras' test "installation" of a dummy manifold. In addition to the installation vessel they used a crane barge, three AHTS's and an ROV support vessel (Stock, Ferreira, da Silva, & Machado, 2006).

In general, at a minimum the following capacities are required for executing the PIM:

- Deck space for transport
- Offshore crane for over-boarding the payload and lowering it below the wave zone (~50m).
- A&R winch and DP together on one vessel (installation vessel).
- Sufficient length of HMPE rope.
- At least one ROV support platform (two if one is not using divers or remotely operated release shackles for the launch). An ROV is required to assist with the landing.

To be able to perform the PIM with only two vessels, the following requirements must be met:

- Launch vessel must be equipped with a crane for shallow waters, with the capacity to submerge the payload down to around 50 meters.
- Launch vessel must have sufficient deck space for transportation of the payload.
- Installation vessel must be equipped with a winch with sufficient capacity for required length of HMPE fibre rope, capable of holding the payload.
- Installation vessel must have ROV support capabilities to assist with landing.
- Installation vessel must have DP capability.
- Installation vessel should have AHC as it may be necessary during phase 3.

4.3 Procedures

There are two published procedures for performing the PIM, presented by different sources. The Petrobras approach was the one studied in this thesis. However, it is also relevant to describe the method proposed by Alan Wang et al. The similarity is the pendulum trajectory. The difference is that in the latter the launch vessel stays connected to the payload throughout the lowering. This method allows the payload to be manoeuvred while suspended but is also significantly slower as the lowering requires synchronisation of the launch vessel reversing and the paying out of more cable.

Petrobras approach

The Petrobras approach to the PIM is shown in Figure 4-3 b). This method is performed by launching the payload into a free-fall pendulum trajectory. Figure 4-3 illustrates different aspects of it.

- 1) Initially the installation vessel (Vessel 1) and the launch vessel (Vessel 2) are both positioned above the target site. The payload is located on the deck of vessel 2. Vessel 1 deploys an ROV to assist the landing. This is done early to avoid unproductive time.

- 2) The payload is connected in a fibre rope (deployment line) to an A&R winch on vessel 1, using a tri-plate rigging arrangement as shown in Figure 4-3 c).
- 3) Vessel 2 transports the payload away from the target site, as shown in Figure 4-3 a), to a distance that corresponds to about 90 percent of the water depth at the target site. The deployment line is fed out freely and will thus have a final length corresponding to about 90 percent of the water depth.

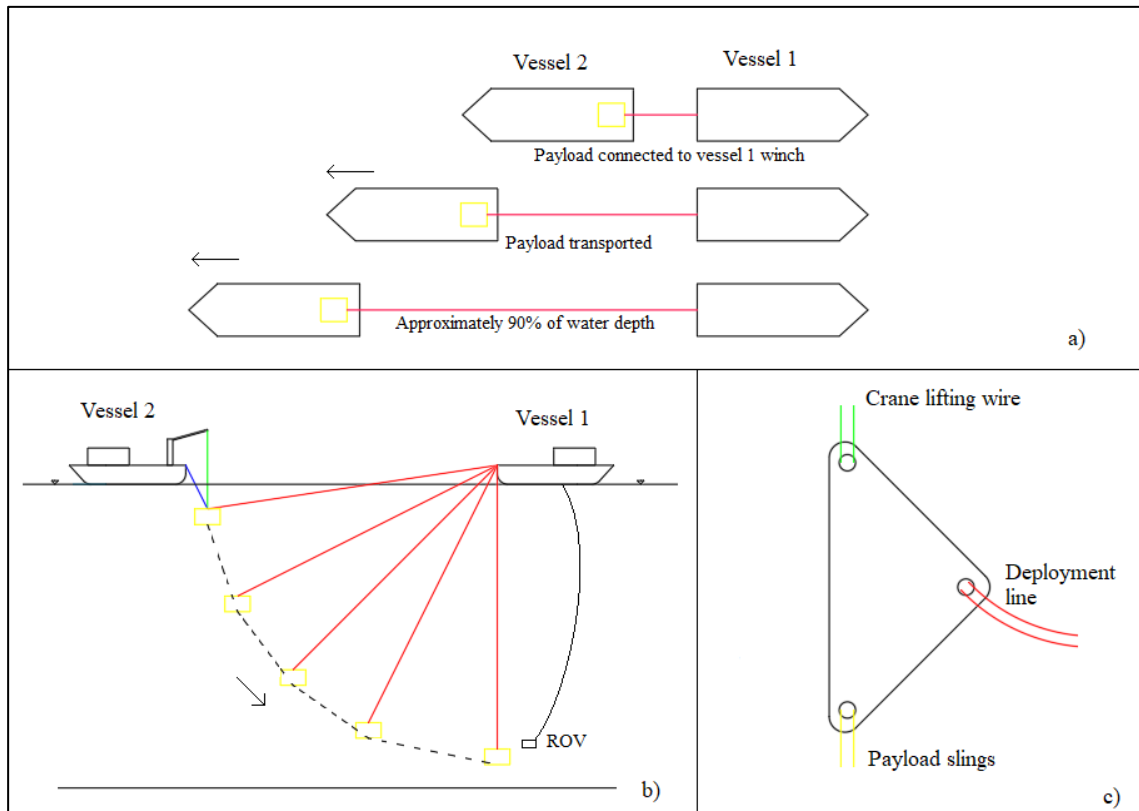


Figure 4-3: Pendulous Installation Method as described by Petrobras (Costa & de Lima, 2017).

- 4) The payload is over-boarded by the crane on vessel 2 and lowered through the splash zone to a depth of about 50 meters. Here it should not be affected by the wave dynamics.
- 5) The payload is released by a remotely operated release shackle, alternatively divers or ROV.
- 6) The payload goes into a free fall, following a pendulum trajectory towards the target site as illustrated in Figure 4-3 b).
- 7) The payload stops above the target site. The distance from the seabed will depend on the initial horizontal distance from the target site and the elongation of the deployment line.
- 8) The payload is lowered to the seabed, and active heave compensation is applied if necessary.
- 9) The payload is installed on the seabed as for conventional installation.

Wang et al. approach

The first steps of this method are similar to Petrobras' approach. Instead of releasing the payload into a free-fall, the launch vessel stays connected, and reverses back towards the target site while feeding out wire. The approach is illustrated in Figure 4-4.

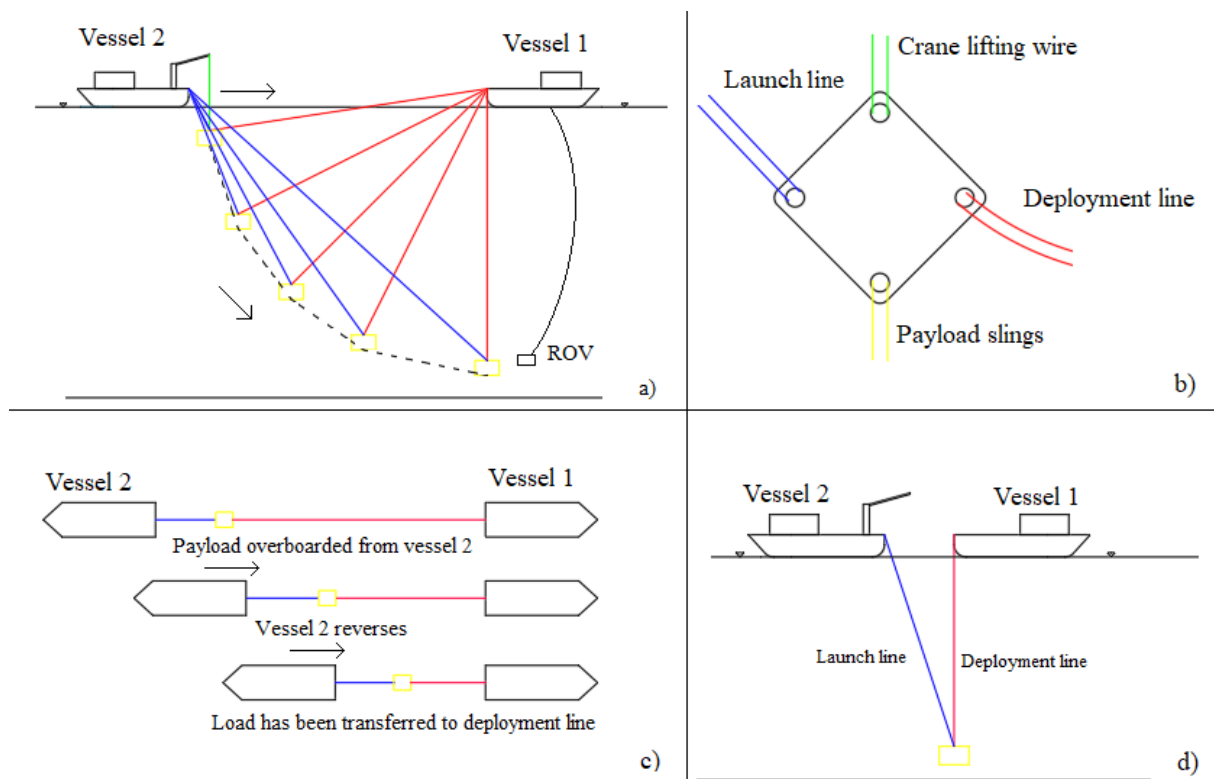


Figure 4-4: Pendulous installation method as described by Wang et al. (Wang, et al., 2013).

- 1) Initially the installation vessel (Vessel 1) and the launch vessel (Vessel 2) are both positioned above the target site. The payload is located on the deck of vessel 2. Vessel 1 deploys an ROV to assist the landing.
- 2) The payload is connected in a fibre rope (deployment line) to an A&R winch on vessel 1, using a quad-plate rigging arrangement as shown in Figure 4-4 b).
- 3) Vessel 2 transports the payload away from the target site, to a distance that corresponds to about 90 percent of the water depth at the target site. The deployment line is fed out freely and will thus have a final length corresponding to about 90 percent of the water depth.
- 4) The payload is connected to an A&R winch on the deck of vessel 2. The rope from this winch is designated as “launch line”. The connection is made through the quad-plate arrangement.
- 5) The payload is over-boarded by the crane on vessel 2 and lowered through the splash zone to a depth of about 50 meters. At 50 meters the load should be completely transferred from the crane wire to the launch line.
- 6) The payload is released by a remotely operated release shackle, alternatively divers or ROV. Vessel 2 starts reversing towards the target site (Figure 4-4 c), while also feeding out the launch line. The speed of the vessel and the winch must be coordinated.

- 7) The payload follows a pendulum trajectory towards the target site as shown in Figure 4-4 a), and the load is gradually transferred from launch line to deployment line.
- 8) The payload reaches the bottom of the trajectory (Figure 4-4 d), and so the load is completely transferred to the deployment line. The distance from the seabed will depend on the initial horizontal distance from the target site and the elongation of the deployment line.
- 9) Both winches are fed out to lower the payload to the seabed. Active heave compensation can be applied to the deployment line if necessary. The load remains on the deployment line.
- 10) The payload is installed on the seabed as for conventional installation.

(Wang, et al., 2013)

The latter approach is slower but allows for better control of the payload as well as manoeuvring.

4.4 Advantages and challenges

The PIM is not necessarily a very challenging operation to perform. The planning phase would be the most complex, as both detailed CFD-studies and testing of scale models should be included. This is to ensure the stability of the payload, which is crucial. Phase 1 and phase 3 are similar to conventional installations. In phase 2 the operation cannot be controlled by the crew.

In table 2 in *Installation of Manifolds- a success story* Petrobras compares different non-conventional installation techniques. They list advantages and disadvantages. Note that these are the specific advantages and disadvantages for Petrobras itself, and are therefore relative to their own resources. For the PIM:

Advantages:

- It does not require heave compensation systems;
- Immune to the resonance effect for great depths and large weights;
- Does not require large time operating window of critical resource (transportation vessel);

(Costa & de Lima, 2017, p. 17)

Other implicit advantages can be identified when considering the method:

Simplified operational procedure: The deployment line must be connected to the payload while the latter is located on another vessel. After this the payload need only to be lowered through the wave zone, before it is released. In the freefall phase, the payload is controlled only by gravity and the damping of the water. It is beyond the control of the crew. When it is suspended, there are other challenges related to the landing, but these are also present for conventional installation methods.

Does not require FRDS: Referencing chapter 2.2.1, special riggings are necessary when utilizing fibre ropes in conventional installation. But not when applying the PIM. The rope is fed out without

tension, and the increase in tension during lowering is gradual. The omission of the requirement for special riggings or special cranes can reduce the cost of the vessels involved.

Disadvantages:

- **(Translated from Portuguese)** Requires critical resource to place manifold in water.
- **(Translated from Portuguese)** Requires specific studies for design and verification of stability in the initial phase (free-fall).
- Requires use of materials of low availability in stock (polyester ropes and floats).

(Costa & de Lima, 2017, p. 17).

Other implicit disadvantages that can be identified from the procedure are:

Multiple vessels: The need for more than one vessel is a disadvantage. If the vessels involved are operated by the installer or has lower day-rates combined than a more advanced vessel, it would be economical. However, multiple vessels require coordination during the marine operation. Referencing the procedures from chapter 4.3, the vessels also need to interact. Especially the approach suggested by Wang et. al. is potentially a complex operation.

Complex planning: Characteristically, the planning phase is the most complex part of the PIM as the stability of the payload must be ensured. The planning phase involves detail engineering. The detailed engineering should include both numerical modelling and testing of scale models of the payload. The payload can also be designed particularly for being installed with the PIM. Ribeiro, Segura and Ferreira presented this topic at the 2006 OMAE conference, where they suggested the following (Ribeiro, Segura, & Ferreira, 2006):

- Hydrodynamic-adapted geometry, e.g. vertical or near vertical panels around equipment.
- Open holes in the mud mat.
- Dead weight at the manifold mud mat.

Lowering cannot be aborted when initiated

When released, the payload cannot be stopped (for the Petrobras approach). If the operation for any reason must be aborted, the payload must be allowed to reach the end of its trajectory and then be hoisted back to the surface. In the base case, the installation vessel is not equipped with a crane and one is therefore dependent on a separate vessel to retrieve it from the water. Referencing the introduction to chapter 2, an operation is not considered to be over until the handled object is in a *safe* position. When suspended from the installation vessel it should not be considered in a safe condition. The operation is thus not over until the object is either installed, or sea fastened on a vessel.

4.5 Risk Analysis

The PIM is not a standard operation and even if it has been qualified for use by Petrobras there are new elements of risk when applying this method. Lack of available data and the simplified model used in this thesis did not provide sufficient basis for a quantitative risk analysis. Since a detailed procedure is not established, a procedure HAZOP is not applicable either. However, it is possible to perform a standard risk analysis by applying the methods suggested in chapter 2.4, and make comparisons. In this sub-chapter a hazard identification is performed by using the HAZOP and HAZID methods presented in chapter 2.4.3. The results are presented in tables and used to do cause & consequence analyses as described in chapter 2.4.4. This way a risk picture was established. Risk analysing can in principle be done as detailed as one wishes, so some constraint was necessary.

4.5.1 Hazard identification

Using guidewords suggested by DNV (see chapter 2.4.3 in this thesis) (Det Norske Veritas, 2003), one can determine undesired events by identifying deviations from normal conditions. In this sub-chapter the guidewords are applied to the Petrobras Procedure in chapter 4.3. The results of the HAZOP are listed in the tables in the following sub-chapters and presented in HAZID work sheets.

4.5.1.1 *Phase 1:*

Phase 1 is considered as the lift-off from deck and submerging of the payload down to release depth. This is identical to conventional lowering. Note that the preparation is not included, that is the positioning of the launch vessel.

Deviations from normal conditions for phase 1 is listed in Table 4-1, while Table 4-2 is a HAZID work sheet for phase 1.

Table 4-1: EPH for phase 1.

Guideword	Deviation	Cause	Consequence
More	Higher wire tension than predicted.	Larger dynamic loading than predicted or unaccounted for load components.	Smaller safety factor than planned for, in worst case rupture of the cable.
More	Larger pendulum motions than planned for.	Higher sea states than planned for, Mathieu instability or poor crane handling.	Reduced safety of deck personnel, chance of collision with deck equipment.
More	Larger vertical oscillations than planned for.	Higher sea states than planned for, or additional swell waves.	Increased chance of re-hitting the deck.
More	Higher loads in splash zone than predicted.	Higher sea states than planned for.	Increased forces on system while crossing splash zone.

Table 4-2: HAZID work sheet for undesired events in phase 1

Activity	Undesired event	Description of consequences	Existing risk reducing measures (probability and/or consequence)	Actions/measures to reduce/eliminate risk	Comments (Concerned parameter)
Lift-off	Higher wire tension than predicted	Smaller safety factor or in worst case rupture of cable.	Documentation of payload components' weight and crane capacity. Computer models of payload.	Perform on-site simulation of lifting operation to predict dynamic responses based on real-time data.	Risk is to assets (payload and vessel), and deck personnel if cable ruptures and tension is released.
Lift-off	Larger vertical motions than predicted.	Increased chance of re-hit of payload to deck.	Calculate max safe hoisting speed.	Use computer simulations on-site and real-time to determine sufficient hoist speed.	Risk to assets (vessel, payload or deck equipment).
In air	Higher wire tension than predicted	Worst case is rupture of cable dropped object.	Documentation of payload components' weight and crane capacity. Computer models of payload.	Perform on-site simulation of lifting operation to predict dynamic responses based on real-time data.	Risk to assets (vessel, payload, deck equipment) and personnel.
In air	Larger horizontal (pendulum) motions than predicted.	Increased chance of collisions to deck equipment, personnel or vessel side.	Use deck winches to restrict horizontal movements.	Use computer simulations to predict amplitudes or natural frequencies.	Risk is to assets (vessel, payload, deck equipment) and deck personnel.
Submerging payload	Larger forces than expected.	Higher loads on lifting system and payload.	Calculation and simulation of forces during submerging.	Use computer simulations on-site to use real-time data. Use AHC.	Risk is to asset (payload).

4.5.1.2 Phase 2

Phase 2 is considered to start at the release of the payload and last until the end of the pendulum trajectory. Deviations from normal conditions for phase 2 is listed in Table 4-3, while Table 4-4 is a HAZID work sheet for phase 2.

This phase separates the PIM from conventional installation, and so if the risk pictures it to be adjusted it should be done after a study of this phase.

Pendulous Installation Method

Table 4-3: EPH for phase 2.

Guideword	Deviation	Cause	Consequence
No/Not	Remote release mechanism does not release payload.	Mechanism fails.	No release.
More	More vertical oscillations than planned for during release.	Higher sea states than planned for.	May interfere with release: If ROV or divers are deployed it can be harmful.
More	Higher wire tension than predicted.	Larger dynamic loading than predicted.	Smaller safety factor than planned for, in worst case rupture of the cable.
Less	Less payload stability than predicted.	Different hydrodynamic behaviour than expected.	Can cause line contact or entanglement.
As well as	Horizontal excursions during lowering.	Stronger current than planned for.	May increase lowering time or cause unanticipated hydrodynamic behaviour.
As well as	Vortex Induced Vibrations of deployment line.	Relative velocity of water around deployment line.	Causes instability of payload.

Table 4-4: HAZID work sheet for undesired events in phase 2

Activity	Undesired event	Description of consequences	Existing risk reducing measures (probability and/or consequence)	Actions/measures to reduce/eliminate risk	Comments (Concerned parameter)
Release	Release mechanism fails.	Installation not initiated.	ROV or divers ready as contingency.	Apply backup-mechanism.	Risk to asset (lost productivity).
Release	Large vertical motions.	Possible damage to ROV or injury of diver.	Application of AHC.	Design release by remotely controlled mechanism.	Risk to asset (ROV) or personnel.
Pendulum trajectory	Higher wire tension than planned for.	Smaller safety factor or in worst case rupture of cable.	Documentation of payload components' weight and crane capacity. Computer models of payload.	Perform on-site simulation of lowering to predict dynamic responses based on real-time data.	Risk to asset.
Pendulum trajectory	Less payload stability than predicted.	Payload can start uncontrolled rotations which can cause line contact or entanglement.	Buoyancy modules on deployment line. Increased mass of mud mat.	Add ballast tanks with pumps to rotate ballast. Remotely operated.	Risk to asset.
Pendulum trajectory	Horizontal excursions during lowering.	May increase lowering time. Exposes different geometry.	Model testing.	Detailed measurement of current by installation vessel ROV.	Risk to asset.
Pendulum trajectory	Vortex Induced Vibrations of deployment line.	Causes instability of payload (see "Less payload stability than predicted" above).	Model testing.	Calculate and identify excitation regions.	Risk to asset.

4.5.1.3 Phase 3

Phase 3 is considered to start as the pendulum trajectory ends and the payload is suspended from the installation vessel. It ends when the payload is placed on the seabed. Deviations from normal conditions for phase 3 is listed in Table 4-5, while Table 4-6 is a HAZID work sheet for phase 3.

Table 4-5: EPH for phase 3.

Guideword	Deviation	Cause	Consequence
More	Larger vertical oscillations than planned for.	Higher sea states than planned for.	Necessitates AHC. Can harm ROV if the ROV is connected.
More	Payload closer to seabed than intended.	More elongation of deployment rope than predicted.	Possible collision with seabed.
More	Larger horizontal oscillations than planned for.	Higher sea states than planned for.	Landing accuracy becomes more difficult.
More	Larger horizontal offset than planned for.	Stronger current than predicted.	Increased time spent on repositioning of vessel.

Table 4-6: HAZID work sheet for undesired events in phase 3

Activity	Undesired event	Description of consequences	Existing risk reducing measures (probability and/or consequence)	Actions/measures to reduce/eliminate risk	Comments (Concerned parameter)
Landing	Larger vertical oscillations than planned for.	Unsafe to land. Can harm ROV if ROV is connected.	AHC.	Study weather to make sure conditions remain within AHC capacity.	Risk to asset (lost productivity or ROV).
Landing	Payload close to seabed.	Vertical oscillations can cause collision with seabed.	Sufficient safety factor in initial length of rope.	Continuous tracking, enables control by winch.	Risk to asset (payload).
Landing	Larger horizontal oscillations than planned for.	Makes landing accuracy more difficult.	-	Perform on-site data simulations with real-time data to predict motions.	Risk to asset (lost productivity).
Landing	Larger horizontal offset than planned for.	Necessitates topside manoeuvring.	-	Do real-time current measurements to enable manoeuvring during lowering.	Risk to asset (lost productivity).

The events can also be presented in logical diagrams to illustrate the different events leading to a failure. These diagrams can for example be simple block diagrams or fault trees. Figure 4-5 shows a fault tree based on the event “Wire ruptures” and Figure 4-6 for “Payload not released”, both from phase 2. The figures are based on Table 4-4. Such diagrams can be made for all undesired events, but since that is a comprehensive task that is not the main focus of this thesis, only these two figures are included.

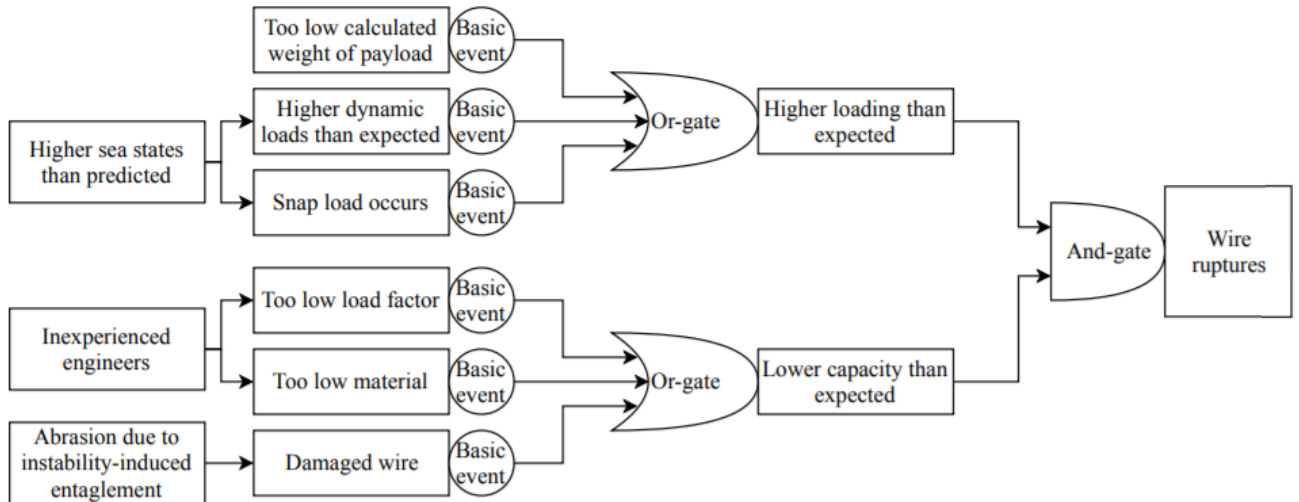


Figure 4-5: Fault tree for event "Wire ruptures"

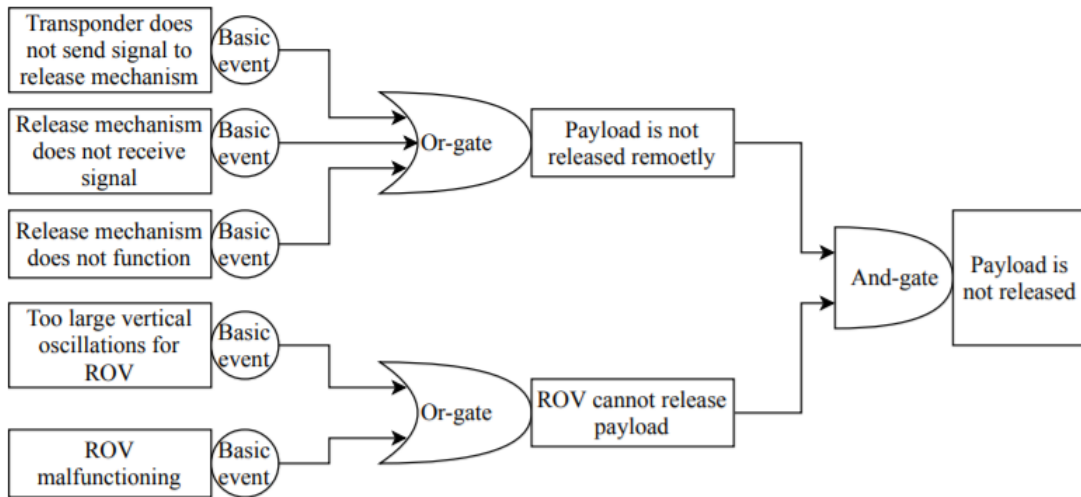


Figure 4-6: Fault tree for event "Payload is not released"

4.5.2 Cause and consequence analysis

Referencing chapter 2.4.4, it can be useful to study the condition, environment or situation leading to the cause of an undesired event. In the bow-tie diagram in Figure 2-14 this would be the sub-section to the left. By evaluating the causes, one can determine which barriers can be used to reduce the probability of the undesired event. For complicated systems a system HAZOP should be performed. Here in this thesis only one additional level in the bow-tie is studied as, as some restraint had to be shown. A complete study would require work beyond the scope of the risk analysis in this thesis.

In Table 4-7 the undesired events are listed from the EPHs in chapter 4.5.1. The cause of the event is described, and the condition leading to it. Note that in some cases more than one "cause" comes from the same condition. The barriers in this table are meant to reduce the probability of an undesired event occurring. Table 4-8 lists the same undesired events as Table 4-7, but with focus on the consequences. The barriers in this table are meant to reduce the consequences of an event that *has* occurred.

Table 4-7: Cause study

#	Undesired event	Cause	Condition leading to the cause	Barrier
1	Higher wire tension than predicted	Larger dynamic loading than predicted.	Insufficient case-specific studies.	Numerical simulations and model-testing.
2	Larger vertical motions than predicted	Swell waves present. Higher sea states than planned for.	Poor weather reports or poor study of weather reports.	Continuous study of weather supported by meteorologist.
3	Larger pendulum motions than predicted.	Higher wave conditions than planned for or wind present.	See #2	In-air: Use winches to restrict motion.
4	Remote release mechanism does not release payload.	Mechanism fails. Can be signals, mechanical or electronics.	Insufficient protection during transport or storage, or lack of quality control.	Standards for how equipment is to be transported or stored.
5	Less payload stability than predicted.	Different hydrodynamic behaviour than expected.	Insufficient studies prior to operation.	Add buoyancy elements or “parachute” to increase stability.
6	Larger horizontal offset than planned for	Stronger current than predicted.	Insufficient study of currents.	Real-time measurements to enable topside manoeuvres.

Table 4-8: Consequence study

#	Undesired event	Consequence of occurrence	Barrier
1	Higher wire tension than predicted	Rupture	Protecting padding below payload to reduce damage.
2	Larger vertical motions than predicted	In-air: Re-hits deck. Landing: Unsafe landing. Can harm ROV if ROV is connected.	In air: see #1. Landing: AHC.
3	Larger pendulum motions than predicted.	In air: Collision Landing: Reduces accuracy during landing.	In air: Reduce number of crew on deck. Use winches to limit motion.
4	Remote release mechanism does not release payload.	Payload is not released.	Design-in of contingency mechanism.
5	Less payload stability than predicted.	Payload starts uncontrolled rotations which can cause line contact or entanglement. This causes abrasion of the rope.	Rope can be coated to prevent abrasion on the load bearing rope.
6	Larger horizontal offset than planned for	Time must be spent on topside manoeuvring.	Use overshoot method described in chapter 2.2.5.

4.5.3 Risk description

The main difference between the PIM and conventional installation is in phase 2. It can be argued that if the payload stability can be ensured, the risk should not be any higher than for conventional installation. Figure 4-7 is a risk matrix that illustrates the presumed risk of performing the PIM for the parameters listed in chapter 2.4.1. It should be noted that this is subjective, as well as dependent on multiple variables. The following are explanations for the decisions made for all four parameters.

Personnel (A2) = Acceptable

Personnel are only exposed during phase 1. All crew should be sufficiently qualified and informed of the procedures. Deck winches can be applied if large horizontal motions are expected, and the minimum required number of crew should be present on the deck. These barriers reduce the probability of an accident to remote (A). To reduce the consequences of an accident involving crewmembers, all should be equipped with recommended safety gear. That said, the handled objects are typically large and heavy, meaning an accident can cause major injury (2).

Environment (B4) = Acceptable

The environment is exposed in all phases, however the only undesired event that affects the environment is rupture of the deployment line in which case the payload is lost. The PIM only concerns the installation, and since the payload is not connected to the SPS there is no chance of spilling hydrocarbons. The only consequence to the environment is therefore littering of the seabed, and the equipment can also be retrieved (4). This is assuming the payload is not landed on/collides with production risers, export lines or other live operating equipment, as this could cause more severe consequences. The probability is set as unlikely (B), since the proper barriers should prevent loss of the payload.

Assets (B2) = Medium

The assets are exposed in all phases. The most severe consequence is loss of the payload. Assuming the cost of the payload to be between USD 1 million and USD 10 million (see risk matrix in Figure 2-15) the consequence of a lost payload is severe (2). Even though the probability is set to unlikely (B) (the undesired event is the same as for environment), the severe consequence puts the risk into the *medium risk* section. It is then important that the barriers listed in this chapter are implemented, as DNV recommends that the operation can only be executed after cost-efficient risk reducing measures are implemented (Det Norske Veritas, 2003).

If, however, the operation as a whole is considered, it is important to take into account the extra cost/reduced cost of applying the PIM compared to conventional installation. If the utilization of multiple vessels is more expensive than using a single vessel for conventional installation, the risk

becomes higher. If the operation requires that the single vessel is specialized to a degree which makes it more expensive to operate than the two required for the PIM, then the risk becomes lower.

Reputation (B2) = Medium

Difficult to determine, however it can be assumed that the worst consequence to the reputation is still the loss of a payload. This is still considered unlikely (B). If a contractor is responsible for the installation, it could be considered reckless to apply an unknown method, which would damage the reputation of the contractor extensively on a national level (2). If the operation is a prestigious one, it might even have an international impact.

On the other hand, should the operation be a success, it might have a positive consequence for the reputation, as the installing party might be considered visionary, inventive and skilled.

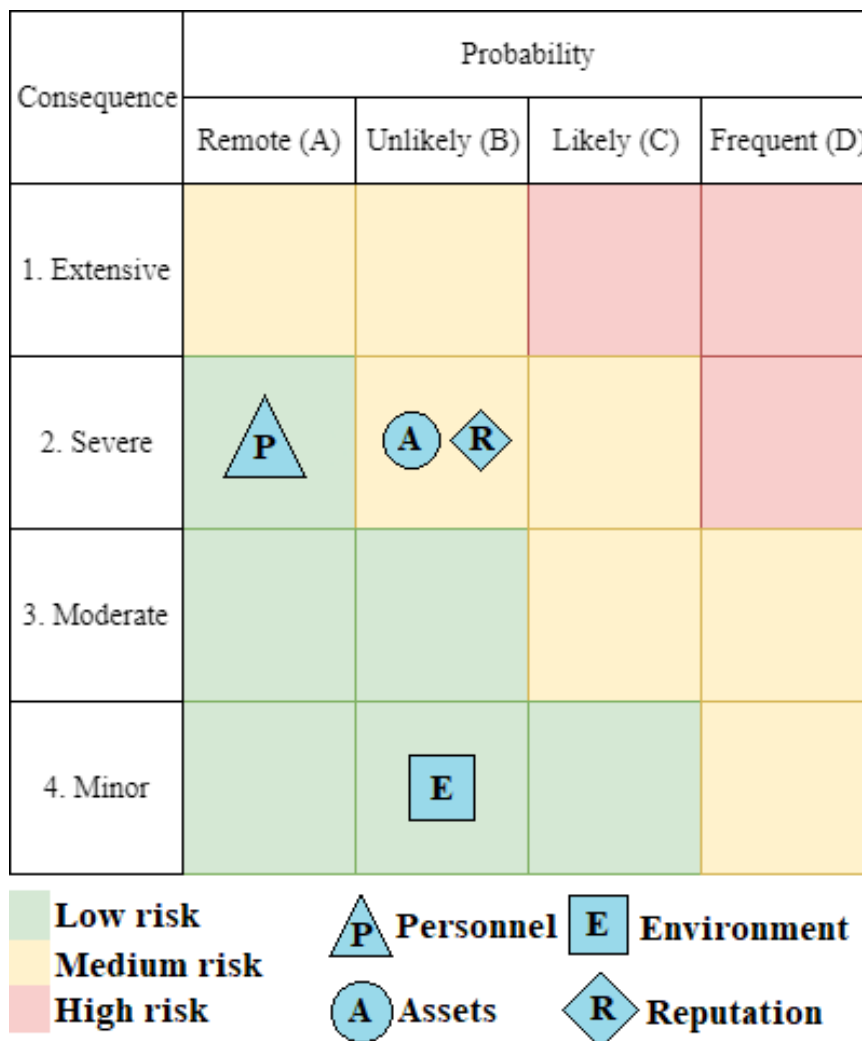


Figure 4-7: Risk matrix for PIM

Chapter 5

SIMO modelling and inputs

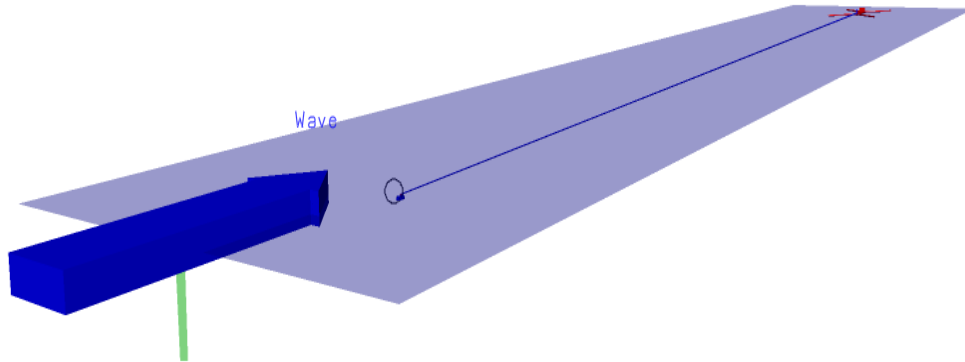


Figure 5-1: Modelling in SIMA

The simulations in this thesis are done using the DNV GL software SIMO in the SIMA platform, and the purpose of this chapter is to describe the models. The scope of this thesis was to do a sensitivity study, and the priority was thus to model different equipment types in different environments. A detailed study of each case is beyond the scope of this thesis. In addition to the free-fall phase, the landing process is also simulated to be able to evaluate the motions of the payload with respect to the required accuracy. It is noted that an obvious effect of the simplified models is that issues like stability and local forces were not studied. This can be done in detailed studies of specific cases. The lowering through the splash zone is the same as for conventional installation in shallow water and is therefore not included. This reduced the number of necessary simulations.

5.1 General

The models are designed for obtaining the following results, for different equipment types and environmental conditions:

- Lowering times
- Tension in deployment line
- Horizontal motions during landing
- Vertical oscillations during landing

The coordinate system is illustrated in Figure 5-2. In all models, the target site is at coordinates $X = 0$ and $Y = 0$, while Z depends on the water depth. For phase 2, the initial horizontal distance from payload to target site is the water depth minus 100 meters. The payload is located 50 meters under the

sea surface. For phase 3, the payload is located around 50 meters above the seabed, depending on the elongation of the deployment line.

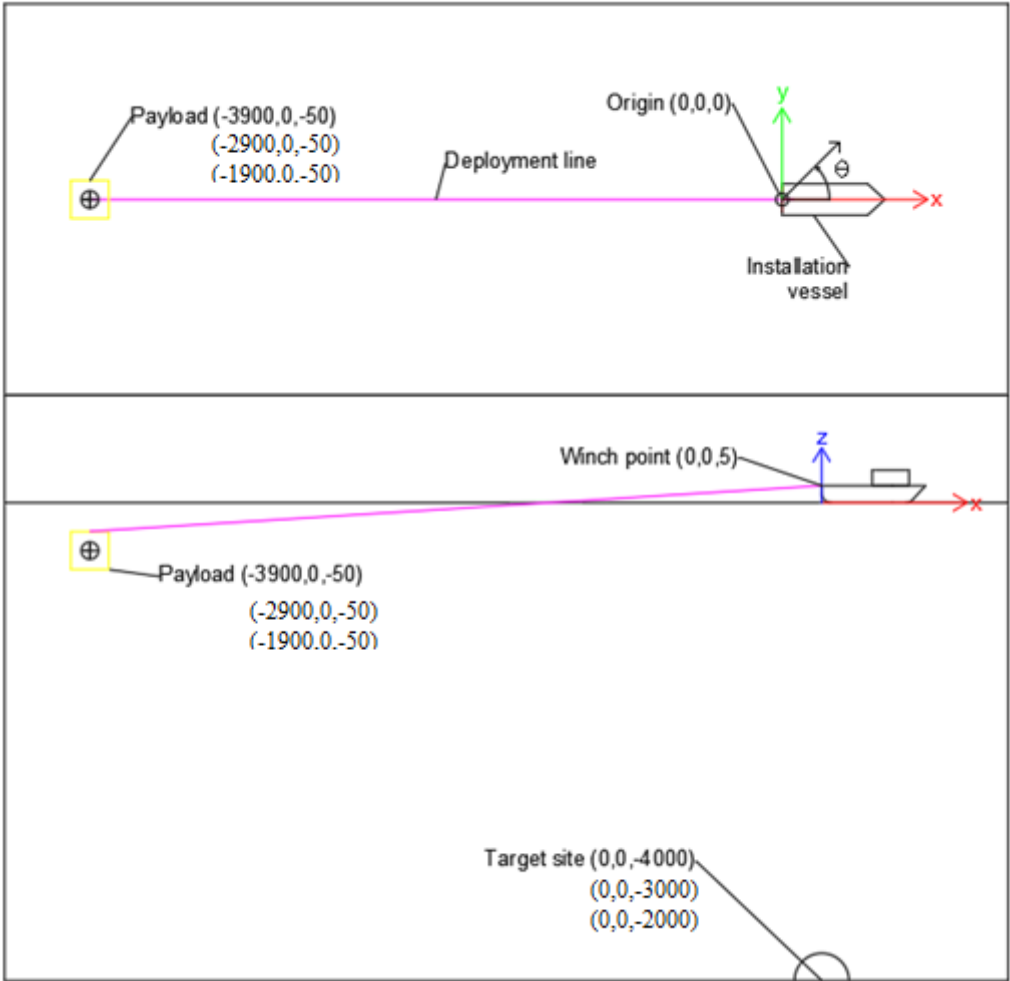


Figure 5-2: Coordinates of interest

5.2 Environment

It is noted that the study in this thesis considers the operations' sensitivity to different environmental conditions. To do a sensitivity study, different conditions sets were simulated. Waves and currents are modelled. Because the simulation starts with the payload already submerged, modelling wind conditions was not necessary. With respect to waves and current both, the ideal scenario would be for waves to generate as little motions as possible, with a weak current in line with the pendulum motion.

Waves

For a specific case, appropriate wave spectrums should be selected. The two-parameter JONSWAP wave spectrum was used in the model. As mentioned in chapter 3.1.1.3, this spectrum is better for modelling the energy of the highest waves. The variables in the simulations were significant wave height, wave peak period and average wave propagation direction. All used wave conditions are included in Appendix B). Significant wave heights of 3 meters is the harshest condition simulated.

This is usually not acceptable conditions for installation of heavy objects but is included to model extreme cases.

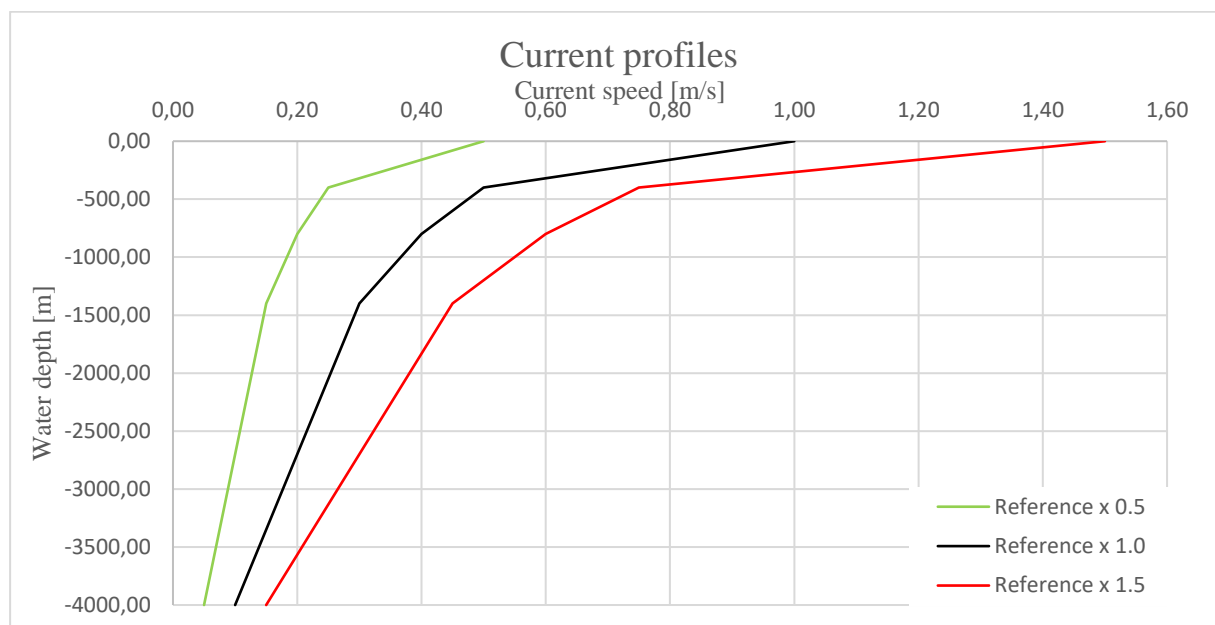


Figure 5-3: Current profiles

Current

Without measurements, current profiles are difficult to model accurately. It was therefore decided to design three currents of the same shape, only scaled with respect to each other. The shapes of the profiles are adapted from measurements made offshore Brazil, retrieved from *Deepwater current profile data sources for riser engineering offshore Brazil* (Jeans, et al., 2012). Currents may not always be unidirectional, however modelling such currents without measurements would be very random. A model with unidirectional currents gives a conservatively estimated horizontal offsets and loads. Figure 5-3 shows a plot of the current profiles used for these simulations, with a direction of 0 degrees, with reference to the coordinate system in Figure 5-2.

5.3 Equipment

Subsea hardware varies in shapes and sizes. To be able to do a sensitivity study, four models of different equipment types were designed for this thesis. As the purpose was studying the sensitivity to equipment types the models are simplified, as detailed analysis of specific designs is beyond the scope of this thesis. Figure 5-4 shows screenshots from the DNV GL software GeniE, showing the simplified models designed for this thesis. a) is a 280T-manifold, b) is a 150T-manifold, c) is an XT, d) is the tubing head spool (THS). The payloads are modelled in SIMO using slender elements. The properties are listed in Appendix B). The basic dimensions of the equipment are listed in Table 5-1.

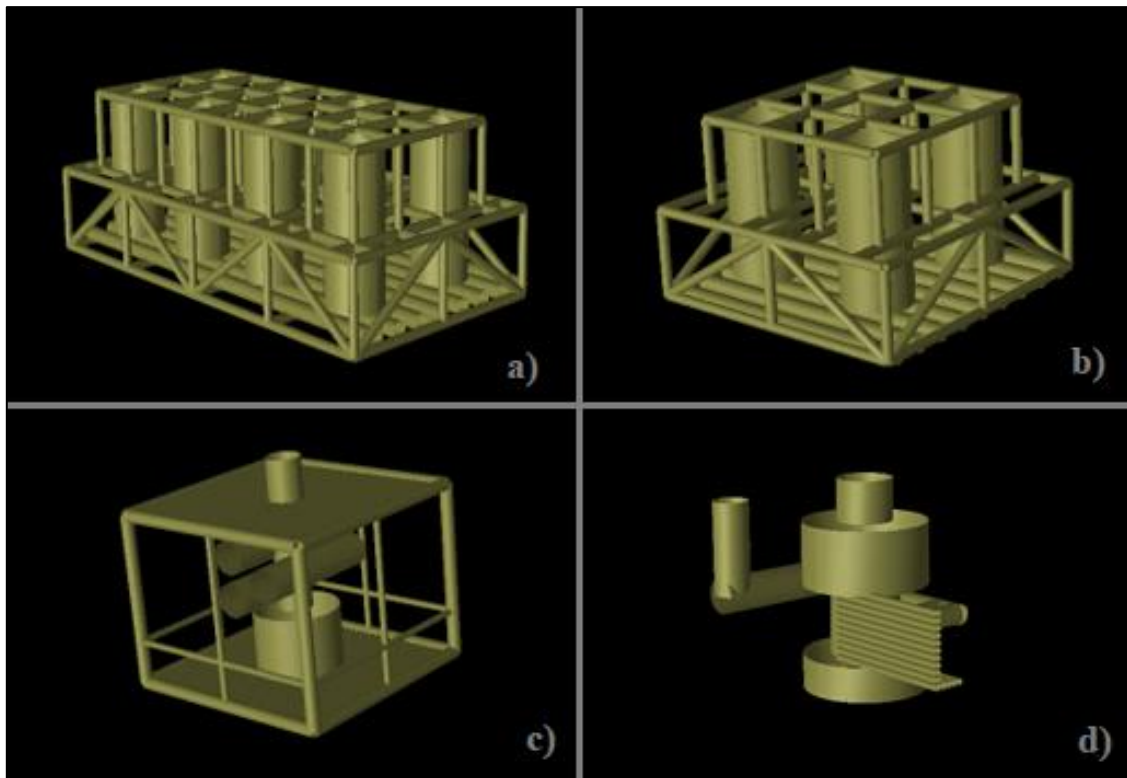


Figure 5-4: Equipment models from GeniE.

Table 5-1: Payload dimensions

Payload	Mass [kg]	Volume [m^3]	Length [m]	Width [m]	Height [m]
280T-manifold	$2.7968 * 10^5$	176.19	16	8	5
150T-manifold	$1.4715 * 10^5$	89.14	8	8	5
XT	50850	17.23	5	5	5
THS	24980	5.86	4	5	3

The 280T-manifold is modelled based on the dummy-manifold that was installed on the Roncador-field during Petrobras' test of the PIM. Weight distribution is loosely based on description from Ribeiro, Ferreira, Segura in *Subsea Manifold Design for Pendulous Installation Method in Ultra Deep water* (Ribeiro, Segura, & Ferreira, 2006). The 150T-manifold has the same properties but is reduced in size. The XT and the tubing head spool are based on information provided for this thesis.

5.4 Rigging

The rigging is modelled as “couplings” in SIMO, as it is what couples the dynamics of the payload and the vessel. In the model used for this thesis the rigging is the deployment line. Note that slings and the hook are not modelled. In *SIMO modelling tutorial*, this approximation is noted to be applied when the object is in deep water, below the wave zone, and individual sling forces are not in focus (SIMO

Project team, n.a.). The description fits the purpose of this thesis. For a real operation there would also be buoyancy elements placed above the hook, and this cannot be modelled in SIMO.

Two different coupling-types were used for the model in this thesis, as described in the *SIMO modelling tutorial* (SIMO Project team, n.a.): Simple wire coupling and Lift line coupling. The latter is more accurate but can only be used for a vertical lift line. Both are modelled with the same axial stiffness, and the more detailed input for the lift line coupling is listed in Table 5-2.

Simple wire coupling

Simplified zero-compression wire model without mass and drag. This was used for the freefall phase, since the more advanced *lift line coupling* requires the line to be vertical. The coupling is assumed to be a straight line, and since it is without mass and unaffected by drag it is a weakness in the model. It does, however, model the coupling of the payload and the vessel, as well as the tension in the line.

Table 5-2: Lift line coupling properties

Parameter	Value
Number of elements	3940
Diameter	0.155 m
Area	0.02 m ²
E-Module	132 GPa
Length	3980 m
Unit weight in air	14 kg/m
Ratio of weight in water to weight in air	0.0 (Neutral)
Transverse Drag coefficient	2.0
Longitudinal drag coefficient	0.01
Flexibility	$1.37 * 10^{-7}$
Damping (2% of EA)	49814664 Ns

Lift line coupling

According to the manual, this is the deepwater alternative to the simple wire coupling because it registers more forces on it. For a lift through the wave zone the drag on the line may not be necessary to model, but in deep water it is. The model is considered to be quite accurate for payload offset and static and dynamic forces at the end points. It includes mass, buoyancy, drag and inertia forces. It is modelled with a nominal young's modulus, diameter, drag coefficient and unit length. The length must be constant to model the forces properly. The current forces are calculated along a straight line, as is the buoyancy and mass. Offset is calculated by the software using the drag force from water particle velocity on the line. Transition of horizontal motion from the surface vessel motions is modified, as it is overestimated by the straight line-approximation (SIMO Project team, n.a.).

The mechanical properties of the rope that are listed in Table 5-2 are retrieved from a Dyneema fact sheet retrieved online (EuroFibres, n.a.). While relevant for the topic, detailed study of the fibre rope is beyond the scope of this thesis. Only one type was selected. An excerpt from the sheet is included in Appendix A). Otherwise the rope is modelled after numbers used by Wang et al. (Wang, et al., 2013).

The deployment line is connected to the vessel at the aft, as illustrated in Figure 5-5. The winch could of course be located at other parts of the vessel, but for AHTSs the main winch is located here. The main difference is that the model might be more sensitive to pitch than roll.

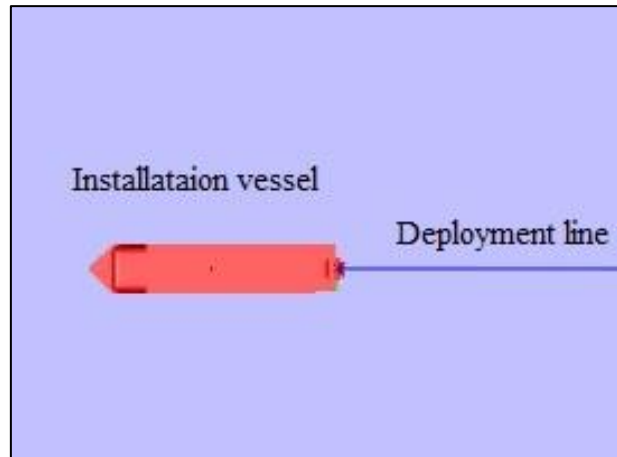


Figure 5-5: Deployment line and vessel

5.5 Vessel

The hydrodynamic data for the vessel used in the simulations was provided for this thesis. The original vessel is anonymous, but the data was obtained using the Wamit software. The vessel is 137.7 meters long, 27 meters wide and has a draught of 6.4 meters in the scenario simulated. It has an accumulated mass of 16 900 tons, and in all figures where it is visible it is represented by a crude model made for illustration. Selected transfer functions for the vessel is included in Appendix B).

5.6 Verification of models

The models established for this thesis are simplified. As a result, they cannot be assumed to be realistic in all aspects. It is however possible to verify that they are somewhat accurate for the values studied in this thesis. For phase 2 (freefall), a way of achieving this would be to compare the *shape* of the plots of tension and velocity obtained in this thesis, with the corresponding plots presented by Petrobras. For comparison, an early simulation of the 280T-manifold was used, since the model is based on the dummy manifold from the Petrobras presentation. In this sub-chapter, all references to “the presentation” is referencing *Numerical Analyses and Sensitivity Studies for Development of the Pendulous Method* (Roveri & Vardaro, 2006).

Comparison of tension with Petrobras

Figure 5-6 shows an excerpt from slide 16 in the presentation. The plots are of the tension in the cable from a numerical analysis and from measurements during their 1:1 scale model test. When comparing to Figure 5-7, which is from a simulation in this thesis, the general shape of the curves is similar.

The tension increases quickly before flattening as the payload trajectory flattens out. The SIMO results in Figure 5-7 also show the peak before the gradual tension that can be seen from the model test measurements. This is not seen in the Petrobras numerical analysis. It is however more dominant in the SIMO results. This is likely to be caused by the snap-load occurring because the line does not have buoyancy elements modelled. The tension-axis of the Petrobras numerical model shows other values than the SIMO results. However, even though the total mass is approximately the same, it is possible that the volume of the body is larger in the SIMO-model. The model design is based on pictures and therefore not necessarily completely accurate. The buoyancy is therefore different.

The rounder curves in Figure 5-6 compared to Figure 5-7 can be a result of the buoyancy elements installed on the lifting line. The initial tension is zero from SIMO and around 250 kilonewtons in the slide. This can be due to applied tension from the winch. The gradually increasing tension is also intuitively logical, since the payload trajectory flattens out and the vertical drag force is then reduced, while the vertical load component increases. More of the load is then taken by the deployment line.

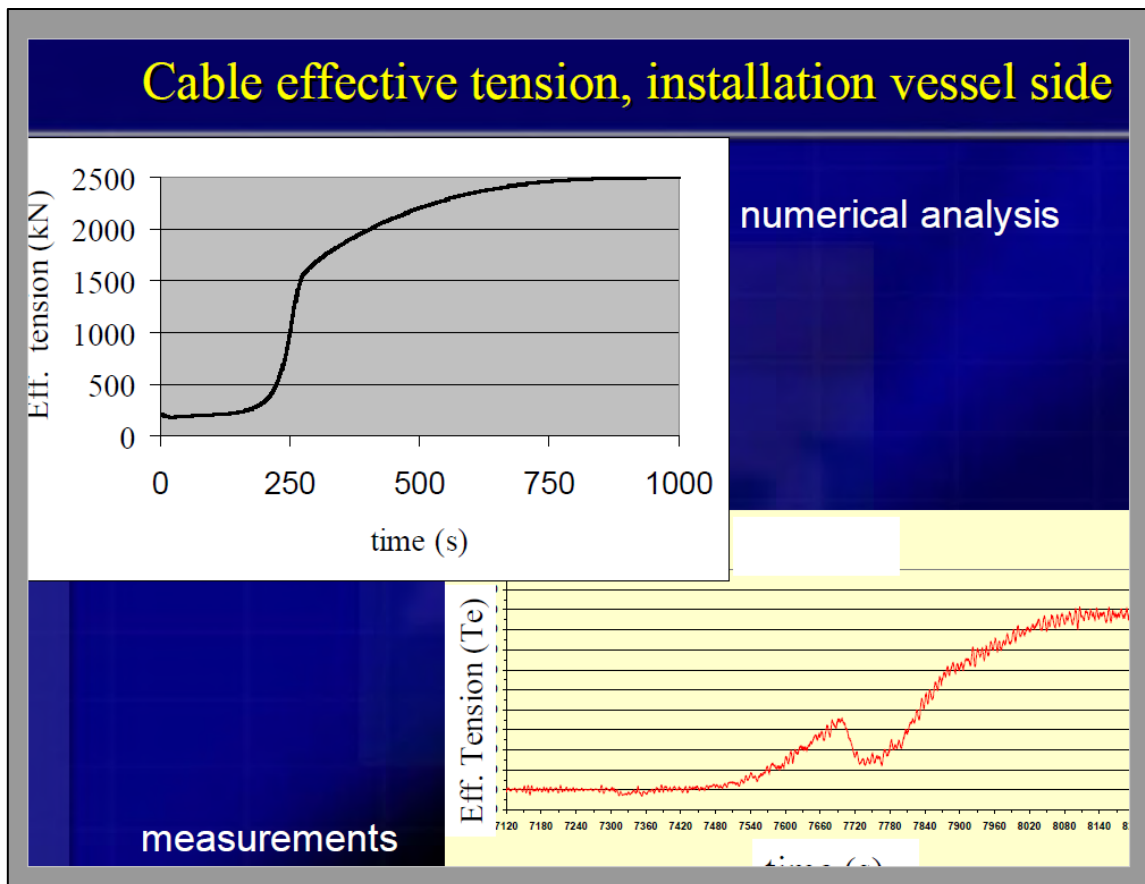


Figure 5-6: Tension obtained from numerical analysis and measurements by Petrobras (Roveri & Vardaro, 2006).

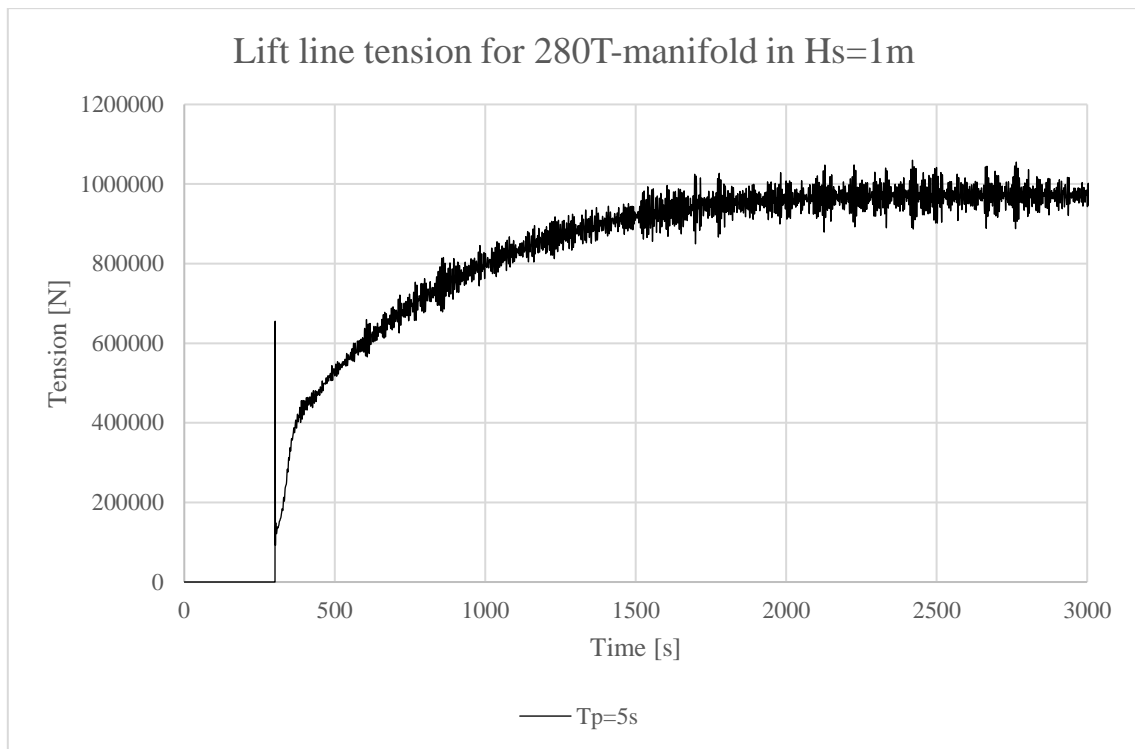


Figure 5-7: Tension obtained in SIMO simulations for this thesis

Comparison of vertical velocity with Petrobras

Figure 5-8 shows an excerpt from slide 17 in the presentation. The velocity is plotted from values from a numerical simulation and from measurements taken during the 1:1 scale model test. When compared to Figure 5-9 (obtained in SIMO), the shape from Petrobras' numerical simulation has a similar if not identical profile: A sudden drop at time zero, then increasing before flattening out. The measurements from the scale model are more unstable, but also here is there a sudden drop before the velocity is trending upward towards zero. For all three plots the vertical velocity is reduced to zero as the trajectory flattens out and becomes horizontal.

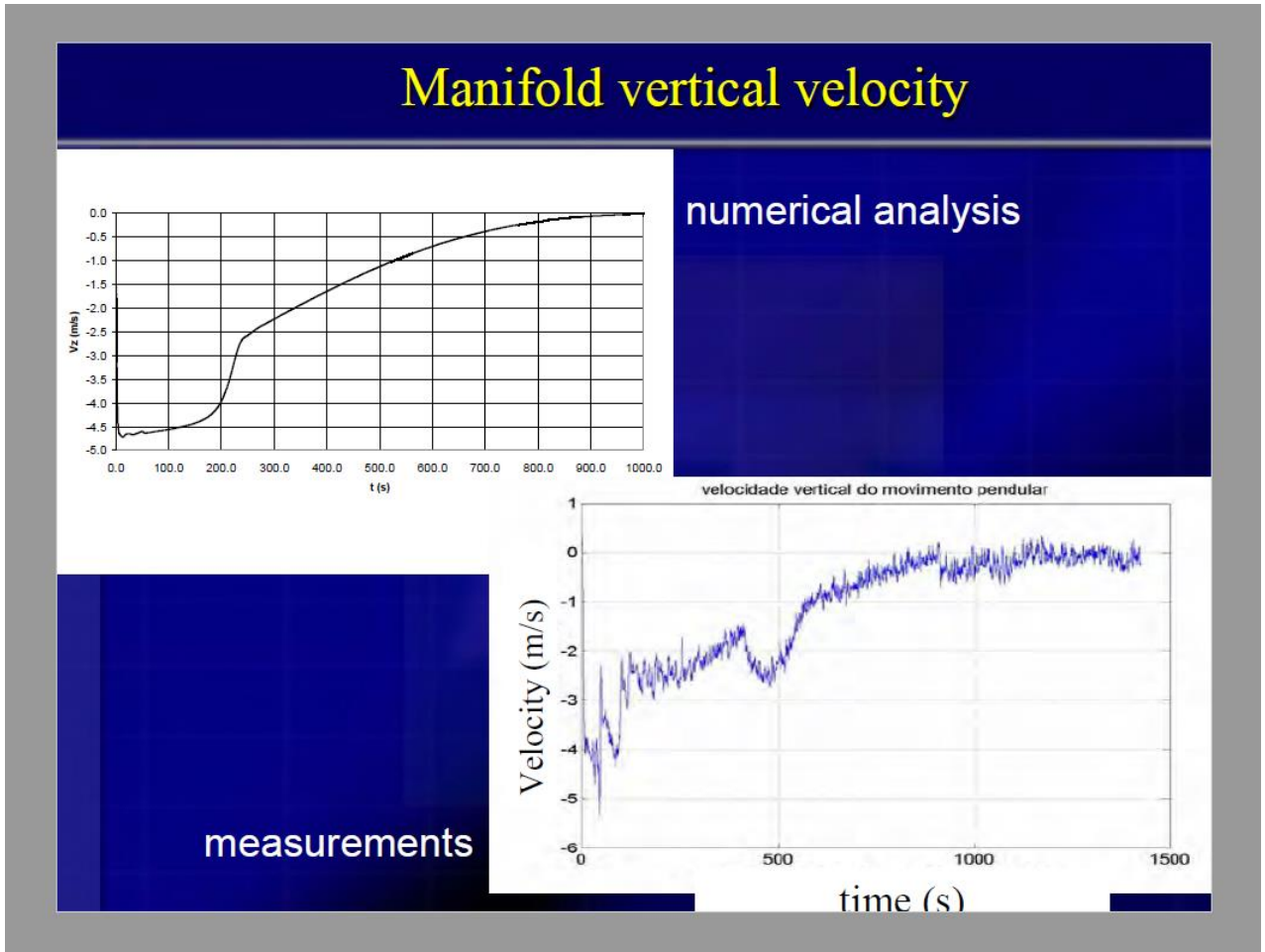


Figure 5-8: Velocity obtained from numerical analysis and measurements by Petrobras (Roveri & Vardaro, 2006)

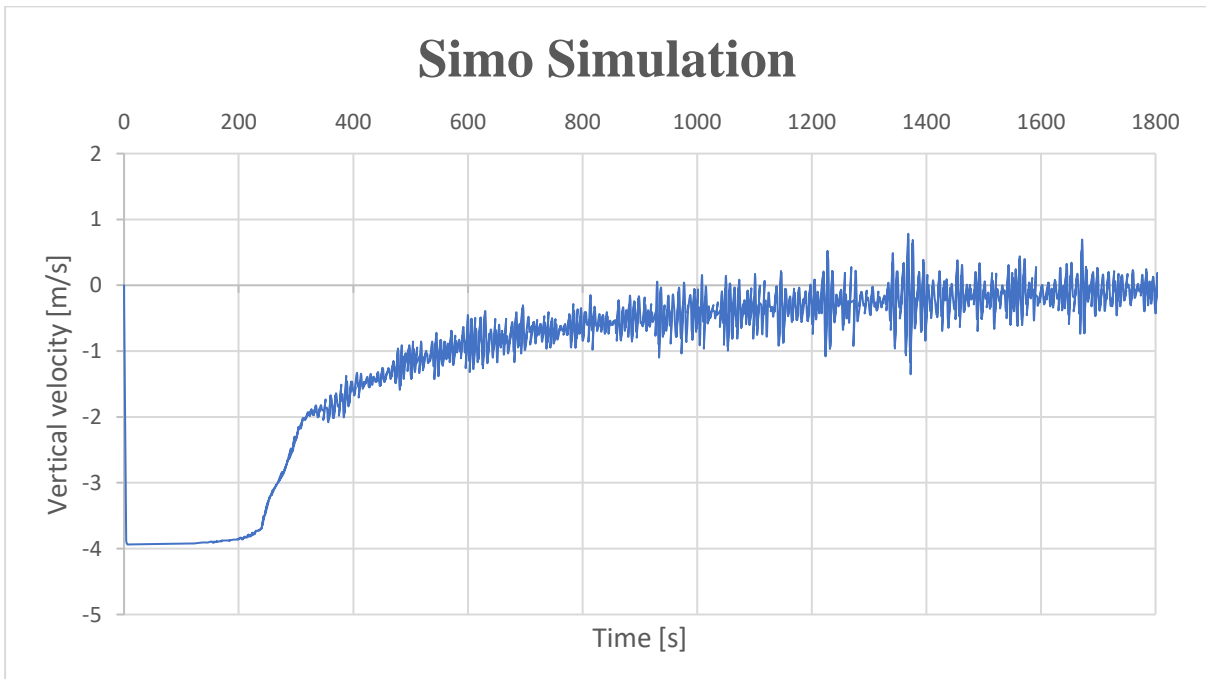


Figure 5-9: Velocity from SIMO simulations for this thesis

Weight and buoyancy

From the Archimedes principle, the tension in the deployment line for the suspended payload should equal to the weight minus the buoyancy. In Table 5-3 the theoretical tension and the results from SIMO are compared. The tension from SIMO is obtained by averaging the wire tension from the simulations when the payloads are suspended. The difference is negligible and is likely due to the difficulty in determining exactly when the payload becomes fully suspended from the wire.

Table 5-3: Theoretical and numerical tension in deployment line.

Payload	Weight [N]	Buoyancy force [N]	Theoretical tension [N]	Tension in SIMO [N]	Difference [N]	Rel. diff. [0.1%]
280T-manifold	2.74E+06	1771634	9.72E+05	9.73E+05	-9.74E+02	-1.00
150T-manifold	1.44E+06	896325	5.47E+05	5.47E+05	2.17E+02	0.40
XT	4.99E+05	173252	3.26E+05	3.26E+05	-4.13E+02	-1.27
THS	2.45E+05	58924	1.86E+05	1.86E+05	1.30E+02	0.70

Based on the results presented in this sub-chapter, the models are deemed sufficient for obtaining results for the values sought in this thesis.

5.7 Simulations

The potential number of simulations is unlimited. To restrict this number, not all cases initially intended were simulated. It was decided to begin the simulation with the payload submerged to the release depth. This way the lifting through the splash zone (phase 1) is omitted, as it is not different from shallow water lifting operations. 32 wave conditions and 3 current profiles (see Figure 5-3) were modelled, and water depths were 2,000m, 3,000m and 4,000m. Appendix B) contains lists of the different cases with respect to phase, equipment and environmental conditions. The following cases were simulated:

Phase 2:

- **All equipment types** simulated for WD=2,000m, 3,000m and 4,000m. Wave conditions were Hs=2m, Tp=8s, wave direction 0 degrees. Current from direction 0 degrees had reference profile (See Figure 5-3). The purpose was to study lowering times and tensions.
- **280T-manifold and XT** simulated for WD=4,000m. Wave conditions were variables (See Appendix B)). The purpose was to study sensitivity to wave conditions.

- **280T-manifold** simulated for WD= 4,000m. Wave conditions were $H_s=2m$, $T_p=8s$, wave direction 0 degrees. Current profile 2 (see Figure 5-3) from 90 degrees, 180 degrees, and no current at all was simulated. The purpose was to study sensitivity to current.

Phase 3:

- **280T-manifold** simulated for WD=3,000m, 4,000m. Wave conditions were variables (see Appendix B)). The purpose was to study sensitivity to wave conditions.
- **280T-manifold** simulated for WD=4,000m. Wave conditions were $H_s=2m$, $T_p=8s$, wave direction 0 degrees. Current profiles 1,2 and 3 (see Figure 5-3) were used. The purpose was to study sensitivity to currents.

5.8 Sources of errors

As the models established for this thesis are simplified, there are aspects of the model that require more advanced methods to be studied accurately.

Payload hydrodynamics: The payloads in these models are constructed from slender elements, and all members are thus subjected to the slender element approximation. For a case-specific study CFD analyses should be performed for detailed models to be able to predict the behaviour of the submerged payload.

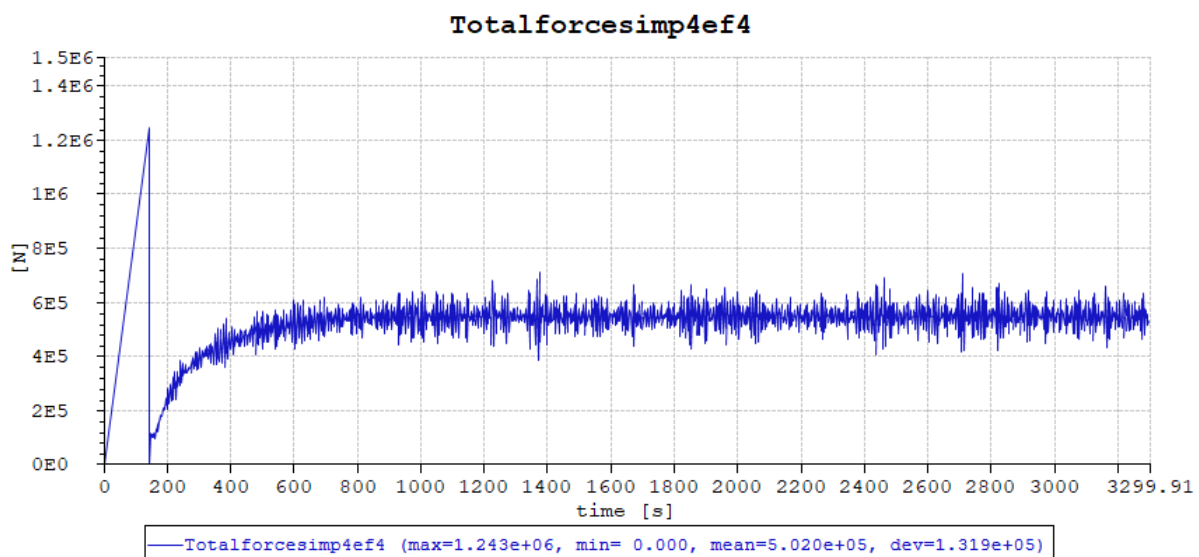


Figure 5-10: Spike in tension due to simple wire coupling.

Simple wire coupling: The simple wire coupling used in the phase 2 simulations is not affected by hydrodynamic forces. The drag force or VIV could affect the behaviour of the lift line and thus payload trajectory. The simple wire coupling is also assumed to be straight, and so does not bend. This

causes a spike in the wire tension when the wire tenses, as the tension is sudden rather than gradual. This is the result of a snap load. This is illustrated in Figure 5-10, which shows the result from an early simulation.

The software also skips some datapoints when zero measurements are made. In the example from Figure 5-10 it measures at time equal to 0 and then at time equal to more than 150 seconds. This gives the false impression that the tension is increasing gradually towards the snap load, which is not true. To compensate for this, in the results these spikes are removed from the figures as they are not realistic.

No buoyancy elements: Another drawback of the simple wire coupling is that it cannot be divided into different cross-sections. Therefore, the buoyancy elements fitted to the deployment line are not modelled. The purpose of these elements is to create a “wave”, as shown in Figure 5-11, that partly absorbs the spike in tension mentioned above. Moreover, the wave would absorb some of the winch point motion, reducing the amplitude of the oscillating tension. This is the concept of the “lazy-wave riser design”, described by Felista, Gudmestad, Karunakaran and Lars Olav Martinsen in *Review of Steel Lazy Wave Riser concepts for North Sea* (Felisita, Gudmestad, Karunakaran, & Martinsen, 2015). The buoyancy elements also contribute to the stability of the payload, as they create an upwards force through the slings and hook.

Unidirectional currents: While using a static, unidirectional current profile makes the calculation of loads and horizontal offset conservative, it does not allow for inclusion of effects caused by a varying current with changing directions.

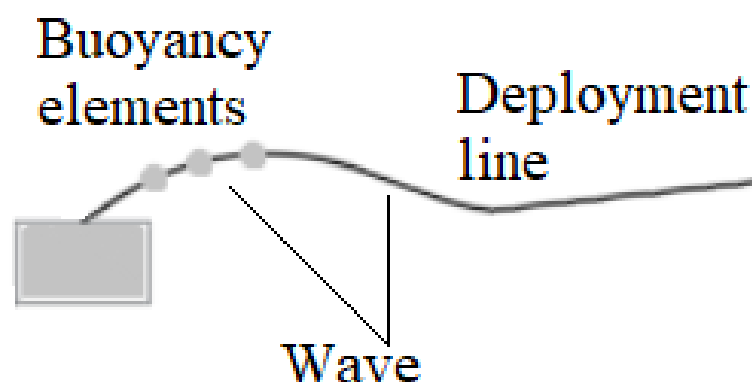


Figure 5-11: “Wave” on deployment line

Chapter 6

Results and discussions

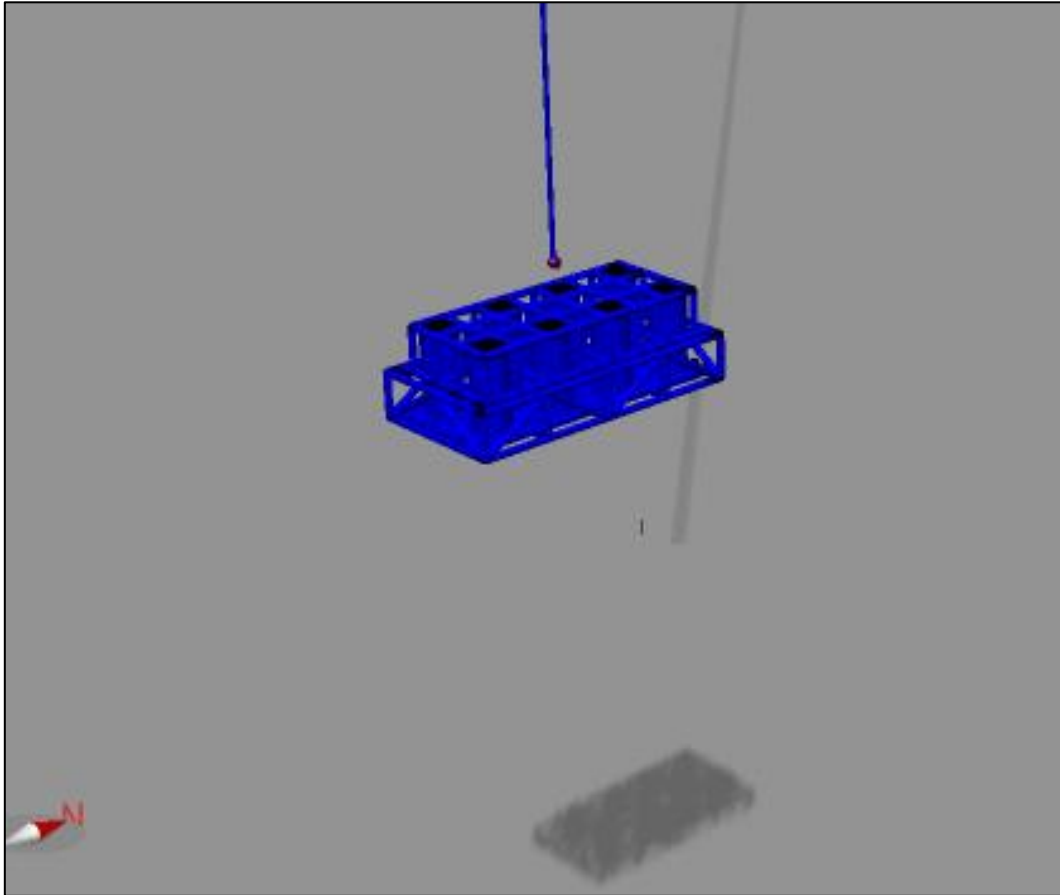


Figure 6-1: Screenshot from SIMO, landing of 280T

This chapter contains the results from the SIMO simulations. As it is also interesting to study the landing of payloads in 4,000 meters water depth, results from both from freefall phase (phase 2) and from the landing phase (phase 3) are included. The results are used to support the discussion of the PIM in relation to the challenges listed in chapter 2.2. These were the issues of lifting capacity, resonant behaviour, time spent on the lowering, horizontal offset and the landing. The results can mainly be used when considering lifting capacity, time consumption, horizontal offset and landing accuracy. Also included in this chapter is a discussion of the risk picture presented in chapter 4.5. The discussion regarding the economics of applying the PIM is limited, due to the limited knowledge of the topic. However, it is still relevant to discuss it as it is important for determining pros and cons of the method.

6.1 Lifting capacity

This chapter contains the discussion of the issue with lifting capacity. It is supported by the results obtained from the numerical simulations, where the tension in the lift line is studied. The purpose of this chapter is to discuss application of the PIM with regards to the lift line, contra conventional installation. The only acceptance criterium is that the tension cannot exceed the MBL of the lift line. HMPE rope has a very high MBL, such as the one suggested by Alan Wang et al, with an MBL of 1,200 tons which is almost 11.8 meganewtons. Given that the highest static load in this thesis is 973 kilonewtons (280T-manifold suspended), it is unlikely that the tension would exceed the criterium.

6.1.1 Issue with fibre rope

Referencing chapter 2.2.1, the issue with self-weight of steel wires in ultradeep water is overcome by switching from steel wires to fibre ropes. These are light, and some are weight neutral in water. The issue, however, is that their properties make it necessary to apply FRDSs to handle them and avoid heat generation and abrasion.

By applying the PIM, the rope is already reeled out to almost its full length without tension, and so there is no need to handle the interaction between the rope and the reeling system. Thus, one can avoid the issue with energy dissipation due to contact without using an FRDS. Since there is no contact there is no surface abrasion either. When not run through an FRDS, the rope is not subjected to excessive bending: This is because it is not bent repeatedly in multiple sheaves. Both energy dissipation methods mentioned in chapter 2.2.1 are thus avoided, even when using a conventional A&R winch. Another positive effect is that AHC can be applied without special treatment of the fibre rope. This is because it is possible to attach a length of steel wire to the upper end of the rope and use this in the AHC.

As Petrobras concluded in *The Need for the Pendulous Installation Method*, the PIM can therefore be said to allow for use of fibre ropes without any special rigging (FRDS) installed on the installation vessel (Cerqueira, Roveri, Peclat, & Labanca, 2006). It should also be less detrimental to the rope than an FRDS as there is less bending and abrasion. This should extend the working life of the rope.

6.1.2 Lift line tension during phase 2

The lift line tension is another point of interest. The tension during phase 2 should not be higher than when the payload is suspended, to prove that the PIM does not cause higher lift line tension than conventional installation.

6.1.2.1 Gradual increase in tension

Characteristically for the PIM the tension in the lift line will increase gradually. It starts at zero as the payload is released from the launch vessel, and then increases as the payload follows the pendulum trajectory. The lift line is therefore not fully loaded until it is vertical. The tension is plotted as a function of water depth in Figure 6-2. Notice the spike in tension prior to the gradual increase. This is

likely to be the result of a snap load that occurs since there are no curving of the lift line, and no buoyancy elements modelled.

The explanation for the gradual increase of tension is the increase in the vertical load component, and the drag force acting against the vertical translation of the payload. The drag force is acting opposite to the gravity, thus relieving the lift line of some of the tension. The drag force is a function of the payload's vertical velocity, which is also plotted in Figure 6-2, as a function of water depth. As the vertical velocity decreases, the wire tension increases. In the figure, it can be seen that the lift line tension and the vertical velocity are inversely proportional to each other. The velocity is reduced as the payload trajectory flattens out towards the end of the pendulum, and the lift line becomes vertical. The static tension reaches its maximum as the mean vertical velocity is zero. This is when the payload is suspended from the manifold, and the only vertical velocity is the vertical oscillations.

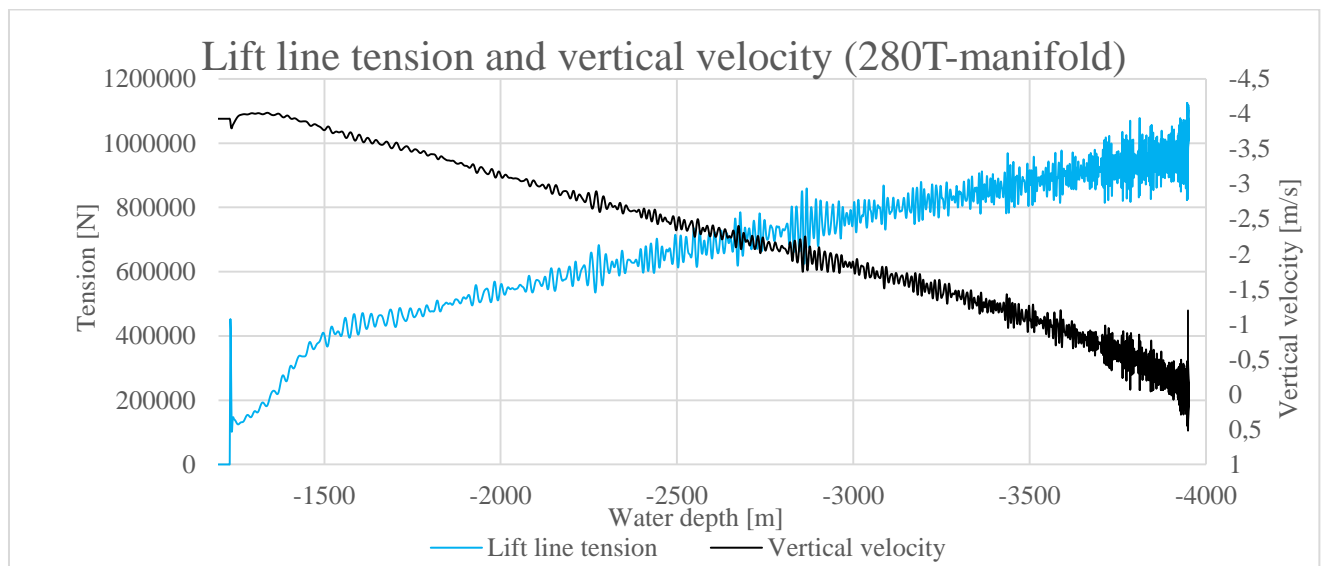


Figure 6-2: Lift line tension and vertical velocity of payload for 280T-manifold.

It can also be seen from Figure 6-2 that the *dynamic* component of the tension is increasing with water depth, as the oscillation amplitudes become larger. The increase is uneven, but the trend is that the tension amplitudes become larger as the pendulum trajectory reaches its end. This is logical, given that the static load increases. This gives a higher total load even if the dynamic amplification remains the same.

The tension plot in Figure 6-2 shows that the highest tension occurs as the payload is at its greatest water depth. This is true both for the mean (static) and maximum tension. This implies that there is not a higher lift line tension during phase 2 than for phase 3, and the PIM therefore should not cause higher tension in the lift line than conventional installation.

In Figure 6-3 the lift line tension for all equipment after they are released is plotted as a function of time in 4,000 meters water depth. In the figure one sees that the highest tensions occur after the curves

have reached the highlighted static loads. This is when the payloads are at 4,000 meters. The explanation is the same: the static load is at its maximum. Therefore, the dynamic loads become higher. The lift line tension is not higher during phase 2 than phase 3.

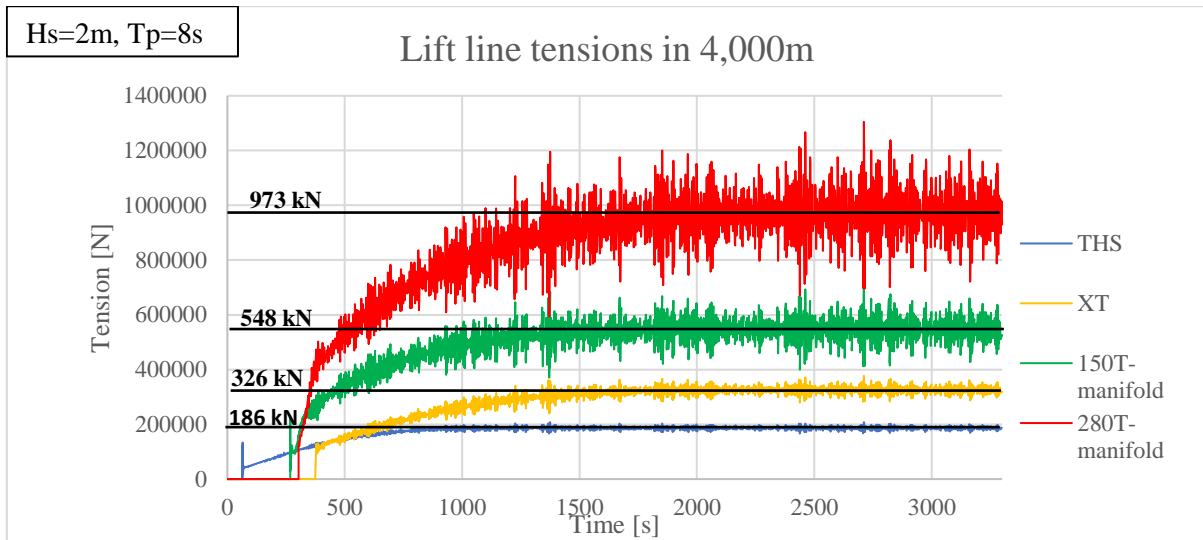


Figure 6-3: Gradual increase in tension for all equipment types

6.1.2.2 Sensitivity to water depth

It is also interesting to see how application of the PIM is affected by the water depth. Simulations were done for all the equipment types to see the effect. The gradual increase of tension discussed in sub-chapter 6.1.2.1 is the same for all water depths. This can be seen in Figure 6-4, where the tension is plotted as function of time during the decent. The shape of the curves is the same for all three water depths, and they also have more excited regions in the same intervals. Figure 6-5 plots the same scenarios as Figure 6-4, with expanded axes. Here it can be seen that for all water depths the tension increases until it reaches the highlighted static load. This is when the lift line becomes almost vertical.

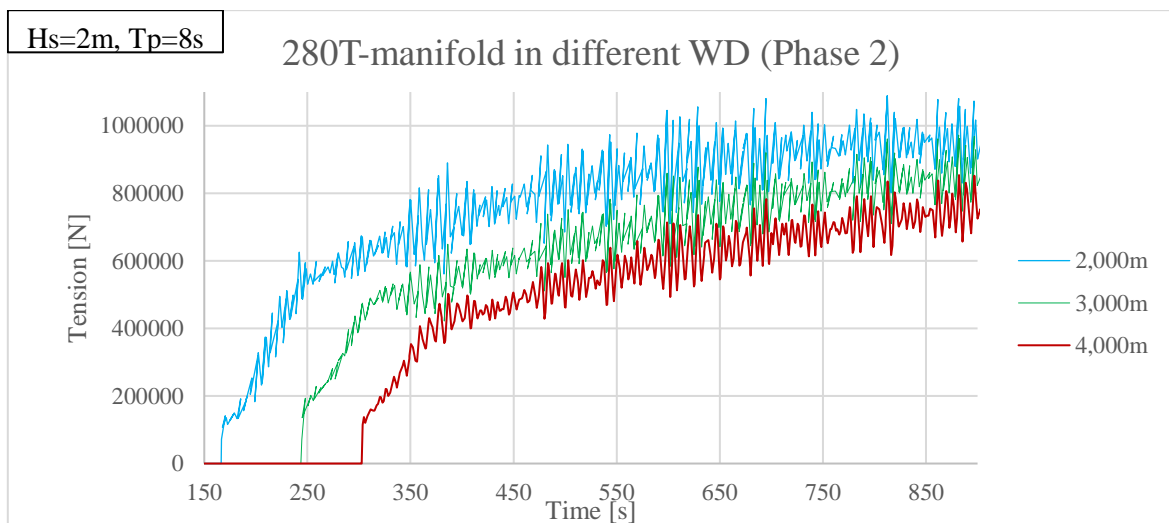


Figure 6-4: Gradual increase of tensions in Phase 2 in different water depths

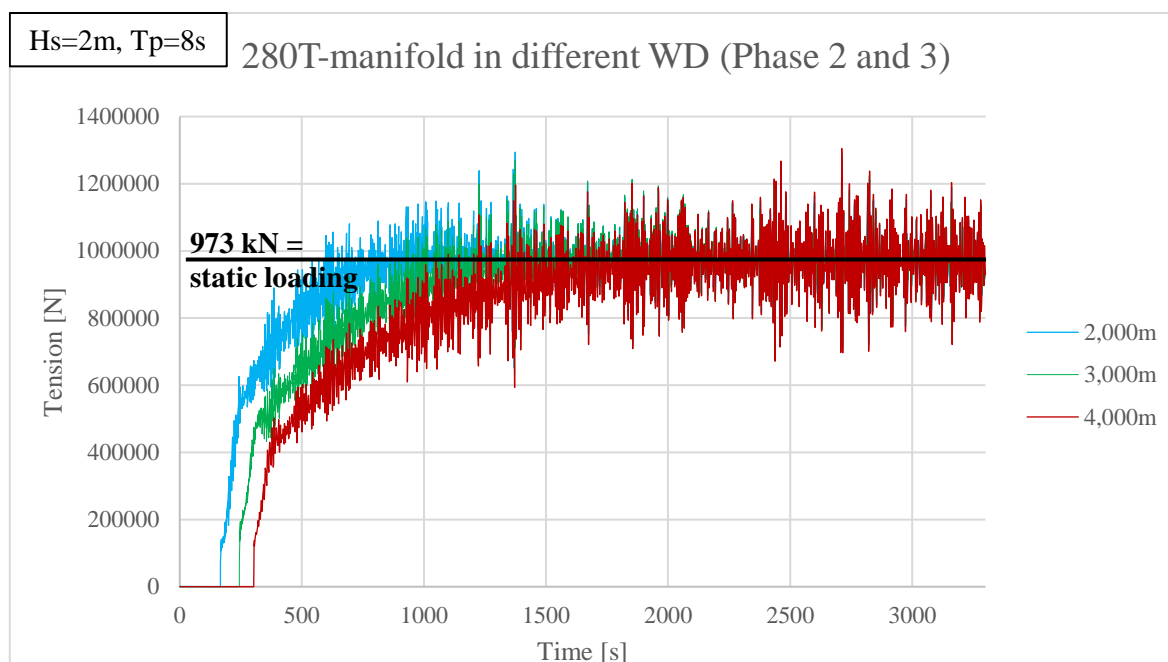


Figure 6-5: Tension in different water depths

The reason why the tension remains the same for all water depths is that the deployment line is modelled as an HMPE fibre rope which is weight neutral in water. This leaves only the weight of the payload as the static load component. In Table 6-1 the maximum and mean values for lift line tension are listed. The results are retrieved while the payloads are suspended. With the application of fibre ropes, the lift line tension should therefore not be an issue even in ultradeep waters. It is noted that the increased length of the lifting wire will increase the natural period of the system, so the dynamic loading will be dependent on different wave periods for different water depths. The method does however not appear to be sensitive to water depth for the scenarios modelled here. Only one wave scenario is modelled, but the different lengths and weights modelled will give a variety of different natural periods. Sensitivity to different wave conditions are elaborated in chapter 6.1.2.3.

Table 6-1: Lift line tension for different water depths ($H_s = 2\text{m}$, $T_p = 8\text{s}$)

	THS		XT		150T-manifold		280T-manifold	
	Max [N]	Mean [N]	Max [N]	Mean [N]	Max [N]	Mean [N]	Max [N]	Mean [N]
2,000 meters	$2.06 \cdot 10^5$	$1.86 \cdot 10^5$	$3.75 \cdot 10^5$	$3.26 \cdot 10^5$	$7.10 \cdot 10^5$	$5.48 \cdot 10^5$	$1.29 \cdot 10^6$	$9.73 \cdot 10^5$
3,000 meters	$2.09 \cdot 10^5$	$1.86 \cdot 10^5$	$3.74 \cdot 10^5$	$3.26 \cdot 10^5$	$7.05 \cdot 10^5$	$5.48 \cdot 10^5$	$1.29 \cdot 10^6$	$9.73 \cdot 10^5$
4,000 meters	$2.07 \cdot 10^5$	$1.86 \cdot 10^5$	$3.77 \cdot 10^5$	$3.26 \cdot 10^5$	$7.10 \cdot 10^5$	$5.47 \cdot 10^5$	$1.24 \cdot 10^6$	$9.73 \cdot 10^5$

6.1.2.3 Sensitivity to wave conditions

To study the method’s sensitivity to the wave conditions, simulations were done for different values of T_p and H_s . Regarding H_s , higher values were expected to give higher tensions as increased wave height is related to higher energy in the waves, as described in chapter 3.1. The purpose of studying different peak periods is to study whether any periods in particular give higher dynamic loading than others, as this can be a result of resonant behaviour. This can be noticed if any of the cases have an obviously higher tension than others. As discussed in chapter 2.2.3, typical values for T_p can range between 5 and 12 seconds, and this is the range of different peak periods simulated in this thesis.

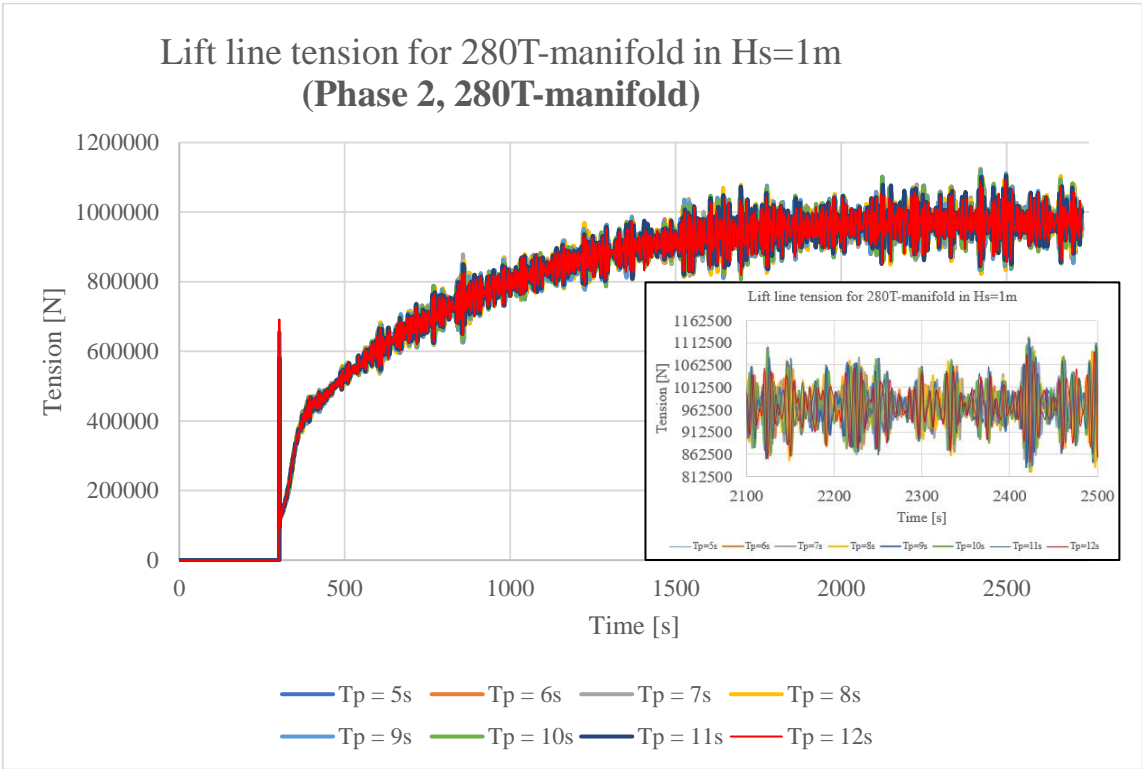


Figure 6-6: Tension for different wave peak periods

In Figure 6-6 the tension during phase 2 is plotted for all T_p , with $H_s = 1$ meter. The payload is the 280T manifold. The recessed picture shows a shorter time interval, and it can be seen that there is an obvious overlap, and it is difficult to pick out trends. The mean values are very similar.

In Figure 6-7 the maximum tensions for all H_s and T_p are plotted, from the same data as Figure 6-6. The highest maximum tension occurs for a peak period of 8 seconds, while the lowest occurs for 5 seconds. As expected the highest tensions comes from the highest significant wave heights, but it is worth noticing that the highest maximum tension occurs at $T_p=8$ seconds for all values of H_s .

In Table 6-2, the highest and lowest maximum tensions are listed, with its corresponding peak periods. It is confirmed that the trend is that the difference becomes larger for increasing H_s , and that the highest tension occurs at $T_p=8s$ for all H_s . It is not random, and the peak period has a significant

impact. For $H_s=3\text{m}$ the difference between highest and lowest is almost 184 kilonewtons, which is close to 20% of the static line tension of the suspended payload (972 kN). Table 6-3 shows the corresponding data for the XT. Here it can be seen that the differences are smaller, due to the lower mass of the payload. The highest tensions here occur at $T_p=9\text{s}$ and $T_p=8\text{s}$, and the lowest are still at $T_p=5\text{s}$. The dynamic properties of the system are changed due to the changed mass of the payload.

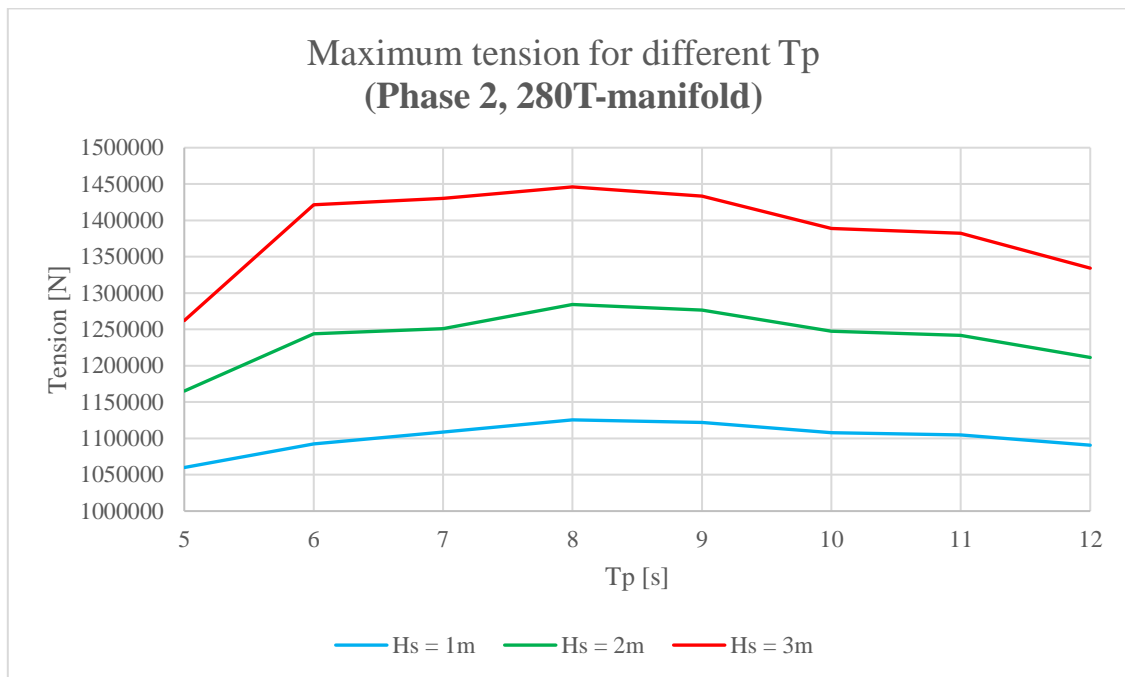


Figure 6-7: Maximum tension for different T_p (280T-manifold)

Table 6-2: Highest and lowest maximum tensions for different wave conditions (Phase 2, 280T-manifold).

Significant wave height	Highest <u>maximum</u> tension		Lowest <u>maximum</u> tension		Difference [kN]	Relative difference
	T_p	Tension [kN]	T_p	Tension [kN]		
Hs = 1m	8 s	1125.5	5 s	1059.9	65.6	5.8%
Hs = 2m	8 s	1284.3	5 s	1165.1	119.1	9.3%
Hs = 3m	8 s	1446.1	5 s	1262.1	183.9	12.7%

Table 6-3: Highest and lowest maximum tensions for different wave conditions (Phase 2, XT).

Significant wave height	Highest <u>maximum</u> tension		Lowest <u>maximum</u> tension		Difference [kN]	Relative difference
	T_p	Tension [kN]	T_p	Tension [kN]		
Hs = 1m	9 s	351.1	5 s	339.8	11.3	3.2%
Hs = 2m	9 s	376.7	5 s	357.5	19.1	5.1%
Hs = 3m	8 s	403.1	5 s	373.6	29.5	7.3%

Figure 6-8 plots the maximum tensions for the different H_s and T_p for the XT. Compared to Figure 6-7 it has the same shape, except for the peak at $T_p=11s$ which is unexpected. Intuitively it was expected that the curve would have only one peak. Further studies should be done to see if this is a statistical abnormality, though it is present at both $H_s=2m$ and $3m$. In Figure 6-7 there is also a noticeable change in the gradient between the same periods. It becomes more distinct for higher H_s . The change in vessel response to different waves is not linear, so this may be a cause.

However, the values are still very similar. Peaks for $H_s=1m$ and $H_s=2m$ are as mentioned at 9 seconds, and at 8 seconds for $H_s=3m$. Apart from the peak at 11 seconds the trend is, as for the 280T-manifold, that the medium long waves result in the highest tensions.

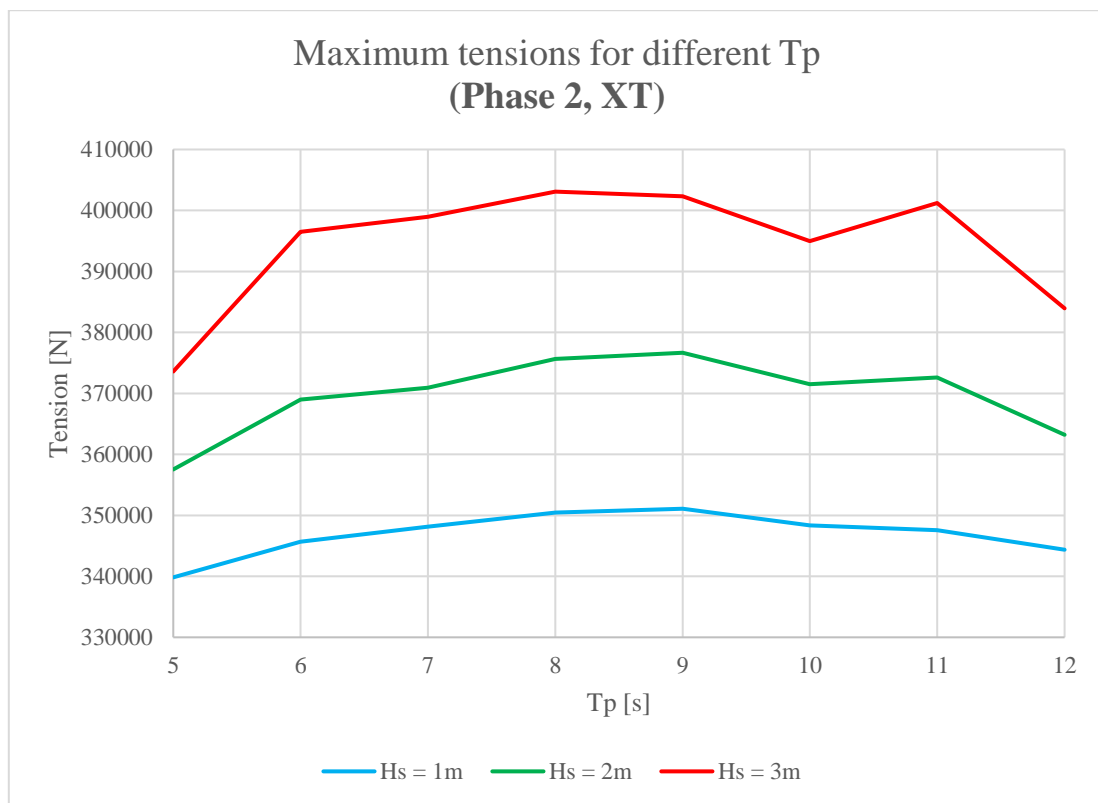


Figure 6-8: Maximum tension for different T_p (XT)

6.1.2.4 Sensitivity to wave direction

While attempts should be made to have the pendulum trajectory as parallel as possible to the current (or strongest expected current direction), waves may make this impractical. The approach angle of the waves affects the responses of the vessel, and therefore also the winch point motion. This causes different responses of the payload, and therefore this should be studied. Figure 6-9 illustrates the wave directions simulated in this thesis. In Figure 6-10 the maximum and mean lift line tensions are plotted for different wave directions. The payload is the 280T-manifold.

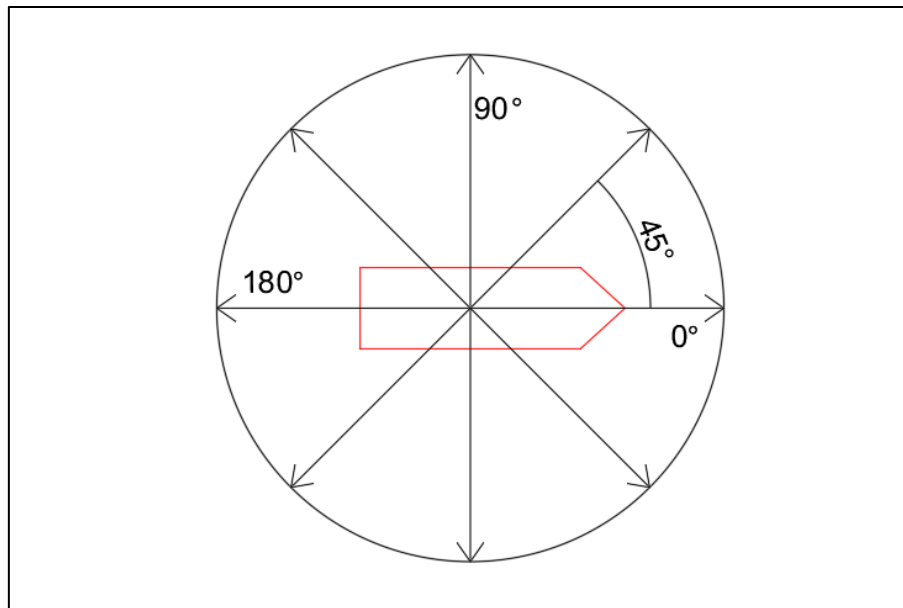


Figure 6-9: Wave directions

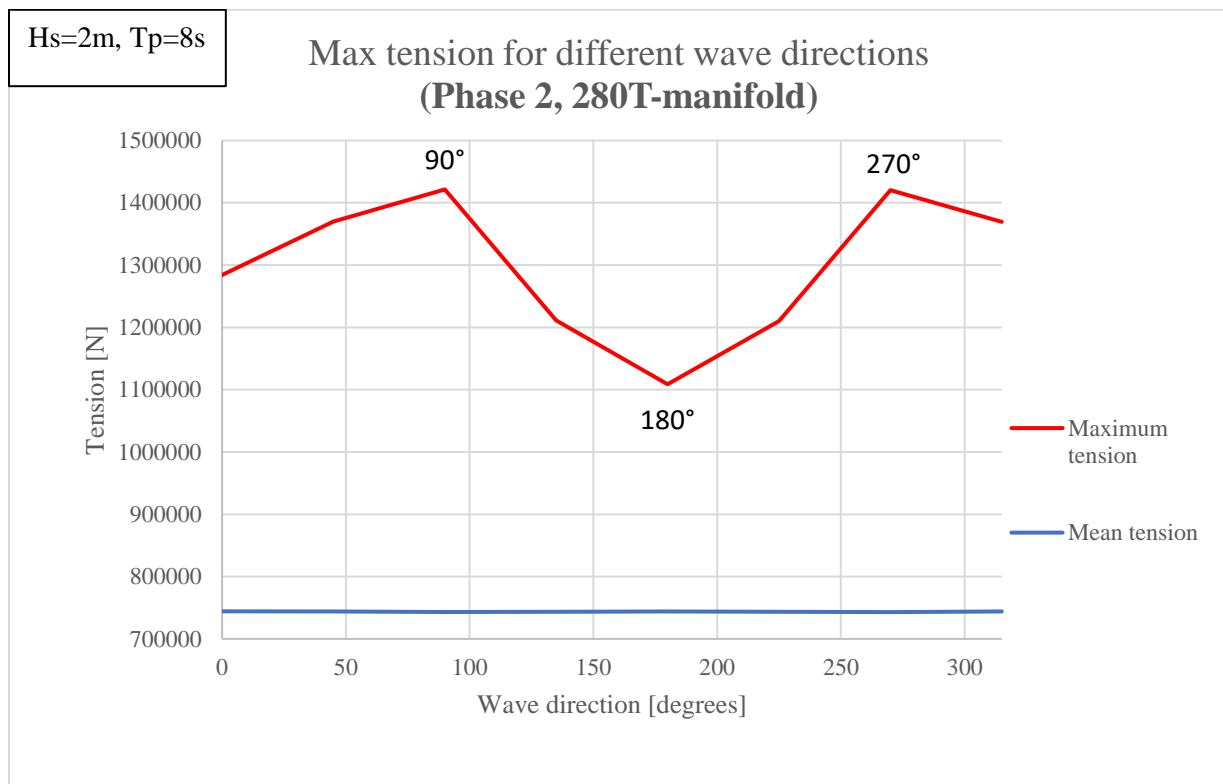


Figure 6-10: Max lift line tensions in different wave directions.

Immediately the flat plot of the mean tension is obvious. This is expected, as the mean tension should not be affected by the vessel response. However, for the maximum tension there are clear differences. The figure is more or less symmetric (360 degrees is not plotted), which is logical. The largest values are for 90 and 270 degrees, and the smallest for 180. When looking at Figure 6-9 and Figure 6-10 together, 90 and 270 degrees are waves in the transverse direction relative to the vessel. This is the

least favourable direction with regards to vessel responses. For 180 degrees the waves come directly towards the bow of the vessel, which is the most favourable.

In Table 6-4 the maximum tensions for all tested wave directions are listed. It is clear that the angles where the vessel is approaching the waves are the most favourable. In Table 6-2 it was shown that the largest difference in tension for different T_p was a 183.9 kilonewtons increase from $T_p=5s$ to $T_p=8s$ (In $H_s = 3m$). By having the vessel facing the waves with the bow rather than the aft, the tension can be reduced by 175.5 kilonewtons. This shows the importance of positioning the vessel optimally.

Table 6-4: Max tensions for different wave directions (Phase 2, 280T-manifold).

Wave direction	Maximum tension [kN]	Deviation from tension at 0 degrees [kN]
0°	1284.3	0
45°	1370.0	85.7
90°	1421.5	137.2
135°	1211.0	-73.3
180°	1108.7	-175.5
225°	1210.3	-74.0
270°	1420.2	136.0
315°	1369.4	85.2

6.1.3 Lift line tension during phase 3

Phase 3 is the same as the landing phase for conventional installation. As the results presented in chapter 6.1.2 shows, the highest tensions in the lift line occur in this phase, when the payload is suspended. The changes in the tension is due to the dynamic loading, causing the tension to oscillate around the mean value. In Figure 6-11 the lift line tension for the 280T-manifold is plotted as a function of time. The tension values oscillate around the static load of 972 kilonewtons.

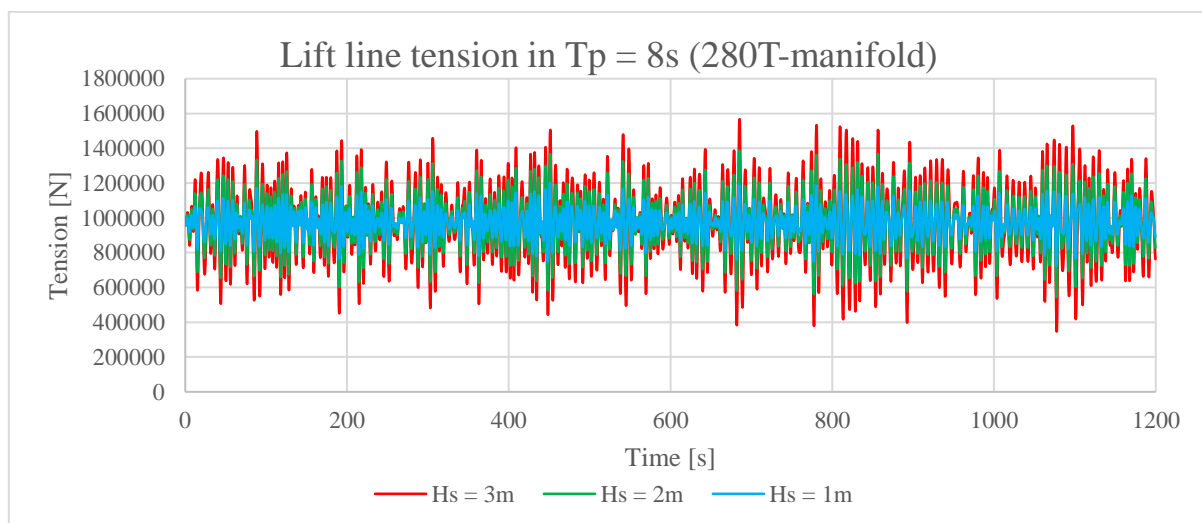


Figure 6-11: Lift line tension in $T_p=8s$ for 280T-manifold

In Figure 6-12 the highest and lowest tensions for different values of H_s are plotted as a function of the peak period. The main contributor to increased dynamic loading is as expected the significant wave height as can also be seen in Figure 6-11. As was also the case for phase 2 in chapter 6.1.2.3, the peak period makes a difference as well. In chapter 6.1.2.3 the medium long waves ($T_p=8$ and 9s) caused the highest tensions, but here it is the shorter waves. Again, the difference becomes larger for the higher waves. The figure is also almost symmetric, and it can be seen that for $H_s=3\text{m}$ and $T_p=6\text{s}$, the minimum tension is less than 300 kilonewtons. This is almost a 70% reduction in tension. It is important to study these scenarios properly, to avoid a situation where the tension is reduced to zero. This causes snap loads, which can lead to high tensions in the lift line.

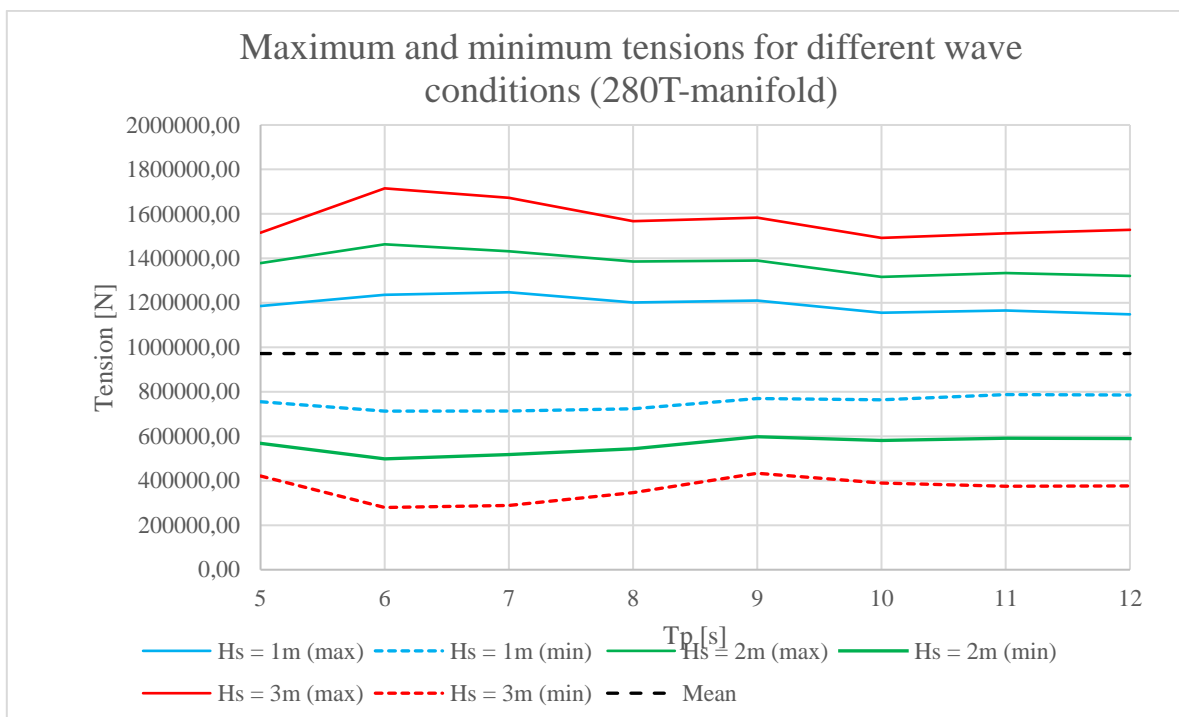


Figure 6-12: Maximum and minimum tensions for different wave conditions (280T-manifold)

In Table 6-5 the values used to plot Figure 6-12 are listed. The highest and lowest values are listed in bold. As the figure illustrates, it is the shorter waves that causes the largest oscillations in the tension, and for the highest waves the dynamic loading is very high. A loading of 1745 kilonewtons ($H_s=3\text{m}$, $T_p=6\text{s}$) gives a dynamic load/static load ratio of 1.76 (DAF). The standard deviation follows the same pattern, and so the trend can be expected to continue for a longer interval as well. In Table 6-6 the DAFs from all the simulated weather conditions for the 280T-manifold are listed.

HMPE ropes can have a very high tensile strength, and the high dynamic loading may not be an issue if the rigging is designed for such high loads. The large amplitudes in the tension does however indicate large amplitudes of the vertical motion, which is another issue that should be addressed. This is more related to the landing, however, and is discussed in chapter 6.5. It should also be noted that AHC can be used to reduce or remove the oscillations, depending on the capacity of the AHC.

Results and discussions

Table 6-5: Maximum and minimum tensions for different wave conditions (280T-manifold).

Tp	Hs = 1m			Hs = 2m			Hs = 3m		
	Max tension [kN]	Min tension [kN]	Standard deviation [kN]	Max tension [kN]	Min tension [kN]	Standard deviation [kN]	Max tension [kN]	Min tension [kN]	Standard deviation [kN]
5	1186.42	755.99	85.01	1378.43	568.91	173.31	1514.99	421.93	236.39
6	1236.55	713.24	90.54	1463.41	498.47	167.28	1714.99	279.85	246.13
7	1247.69	714.39	86.99	1432.59	518.51	159.76	1672.44	289.30	233.66
8	1201.45	723.69	80.81	1386.27	543.97	151.15	1566.88	346.68	215.52
9	1209.64	769.19	73.68	1389.98	598.03	140.15	1582.68	433.72	204.45
10	1156.09	764.38	67.03	1316.77	580.83	129.22	1492.15	389.68	190.68
11	1165.09	787.59	61.62	1334.38	591.13	119.84	1512.57	376.02	178.21
12	1148.42	785.70	56.55	1320.86	589.94	110.74	1528.16	376.59	165.66

Table 6-6: Dynamic amplification factors for 280T-manifold in different conditions.

Tp [s]	Hs=1m	Hs=2m	Hs=3m
5	1.22	1.42	1.56
6	1.27	1.51	1.76
7	1.28	1.47	1.72
8	1.24	1.43	1.61
9	1.24	1.43	1.63
10	1.19	1.35	1.53
11	1.20	1.37	1.56
12	1.18	1.36	1.57

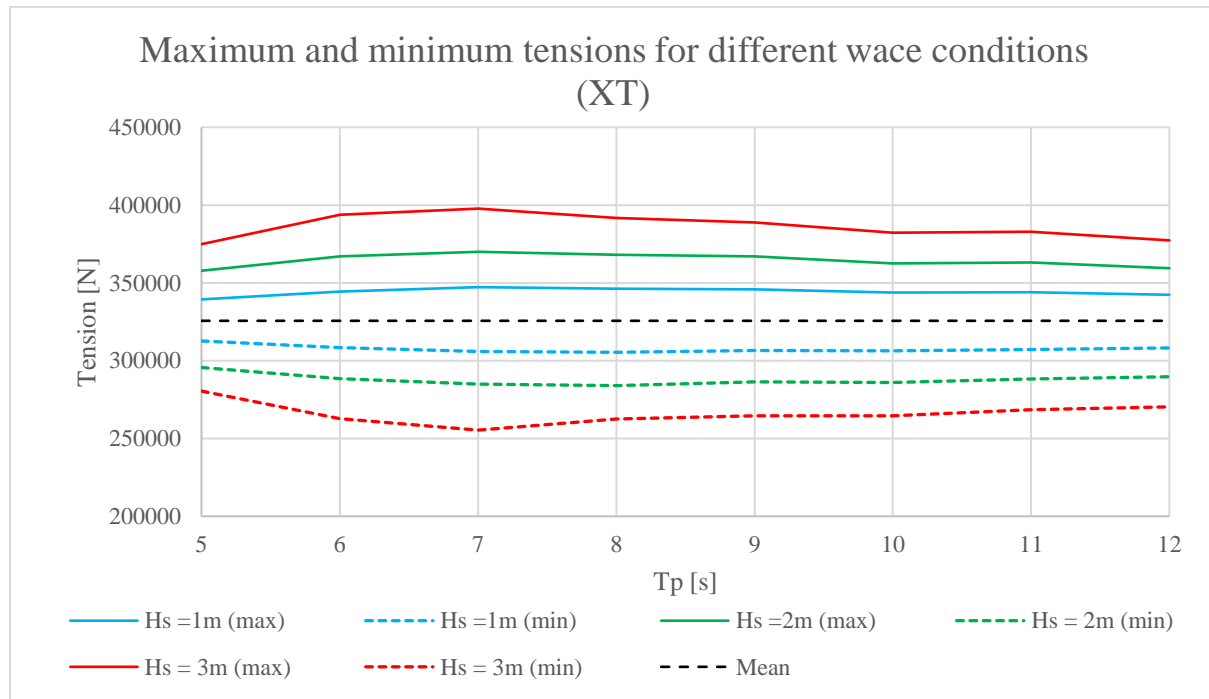


Figure 6-13: Maximum and minimum tensions for different wave conditions (XT)

Figure 6-13 and Table 6-7 plots and lists the maximum and minimum tensions in different wave conditions for the XT. Compared to the corresponding values for the 280T-manifold the highest values occur for longer waves, but the highest values are still skewed towards the shorter waves. For the XT the highest maximum occurs for $T_p=7s$, and for the manifold at 6 seconds. For the XT, the difference in max tension at 6 and 7 seconds is only 4 kilonewtons.

Table 6-7: Maximum and minimum tensions for different wave conditions (XT)

Tp	Hs = 1m		Hs = 2m		Hs = 3m	
	Max tension [kN]	Min tension [kN]	Max tension [kN]	Min tension [kN]	Max tension [kN]	Min tension [kN]
5	339.40	312.67	357.79	295.59	374.87	280.46
6	344.39	308.34	367.05	288.35	393.76	262.81
7	347.26	306.02	369.97	284.94	397.72	255.39
8	346.18	305.39	368.09	283.97	391.78	262.53
9	345.85	306.63	366.94	286.33	388.90	264.64
10	343.85	306.34	362.59	286.01	382.34	264.65
11	344.01	307.27	363.09	288.16	382.88	268.47
12	342.27	308.13	359.46	289.75	377.37	270.36

6.1.4 Findings on lift line tension

Phase 2 versus phase 3: The results presented in chapter 6.1 show that the tension is not higher during the freefall phase than for when the payload is suspended. It is important to note that the phase 2 results should be conservative, given that buoyancy elements on the deployment line would create a “wave” on the line that would absorb some of the motions generated by the winch point motion.

Water depth: The results show no added issues with tension when the water depth is increased. This is also as expected, given that the deployment line is weight neutral in water. The static load is therefore the same for all cases, and the dynamic loads does not seem to be very sensitive to the increased water depth. Different water depths and payload masses will however change the dynamic properties of the system. But conventional installation systems will have an increasing natural period with water depth, unlike the PIM which only has one for each scenario.

Gradual increase in tension: All results show that, as expected, the tension increases gradually during the lowering. This corresponds well with the calculated vertical velocity, since this directly affects the vertical drag force. The drag force works against gravity, reducing the tension in the line. When the motion becomes increasingly horizontal, the vertical drag force is reduced and the tension increases. The vertical component of the weight is also increased as the trajectory flattens out.

Wave conditions: As expected the main reason for increased tension is the significant wave height. What can be taken away from the results is that the wave peak periods of 8 and 9 seconds gave the highest tensions in phase 2. These are the two median wave lengths tested in this thesis. The shorter

waves gave the lowest tension during phase 2, but in phase 3 the highest tension came at $T_p=6s$. As described in 6.1.2.3, the relative difference between highest and lowest maximum was almost 13% for the 280T-manifold. Wave directions also have significant impacts, but this is as anticipated given the expected vessel responses.

Accept criteria

The highest lift line tension recorded in the simulations for this thesis comes from phase 3, for a significant wave height of 3 meters and peak period of 6 seconds. The tension in that case was 1715 kilonewtons for the 280T-manifold. This equates to almost 175 tons, which is less than the payload weight in air. It is less than the minimum break load for the HMPE rope suggested by Alan Wang et al., which was 1,200 tons (Wang, et al., 2013). Also with a safety factor of 1.5 as recommended for such lift cases by DNV in *Standard 2.22 – Lifting appliances* (Det Norske Veritas, 2011) this is within the accept criteria ($1,200 * 10^3 kg * \frac{9.81m}{s^2} = 11,722 * 10^3 N > 1.5 * 1715 * 10^3 N = 2,572 * 10^3 N$).

6.2 Resonance

Referencing chapter 2.2.3, resonance or the possibility of resonant behaviour necessitates careful handling of a submerged payload. When lowering a suspended payload, the natural period of the system increases gradually. The system then has more chances of resonating with high-energy waves. When installing in water depths of 4,000 meters the possibility of hitting a critical period is significant due to the large interval of natural periods the system will have.

By using the PIM, the rope is already reeled out to almost its full length when it is suspended. The natural period of the system then remains constant during the lowering. Figure 6-14 illustrates the example used in chapter 2.2.3 where the natural periods increase as the length of the wire increases. In Figure 6-14 a constant value is added to represent the natural period for axial motion while using the PIM. This reduces the chance of the system coming into resonance, as it will not resonate with waves shorter than its own natural frequency.

When avoiding axial resonance, AHC is not necessary during the pendulum lowering. This is another way of avoiding excessive bending, as a rope is bent repeatedly in an active heave compensator. AHC may still be necessary during the landing. However, as mentioned it is possible to attach a short length of steel wire at the end of the deployment line. Steel has a lower sensitivity to high temperatures and abrasion. The steel length can then be used in the AHC instead of the fibre rope. The rope is then not affected, and it will maintain its properties. It can also prolong the safe working life of the rope. This may also in some cases allow for portable AHC systems instead of specialized cranes.

Hence it can be argued that applying the PIM is beneficial both because it reduces the probability of resonance being an issue, and it reduces the wear and tear of the fibre rope.

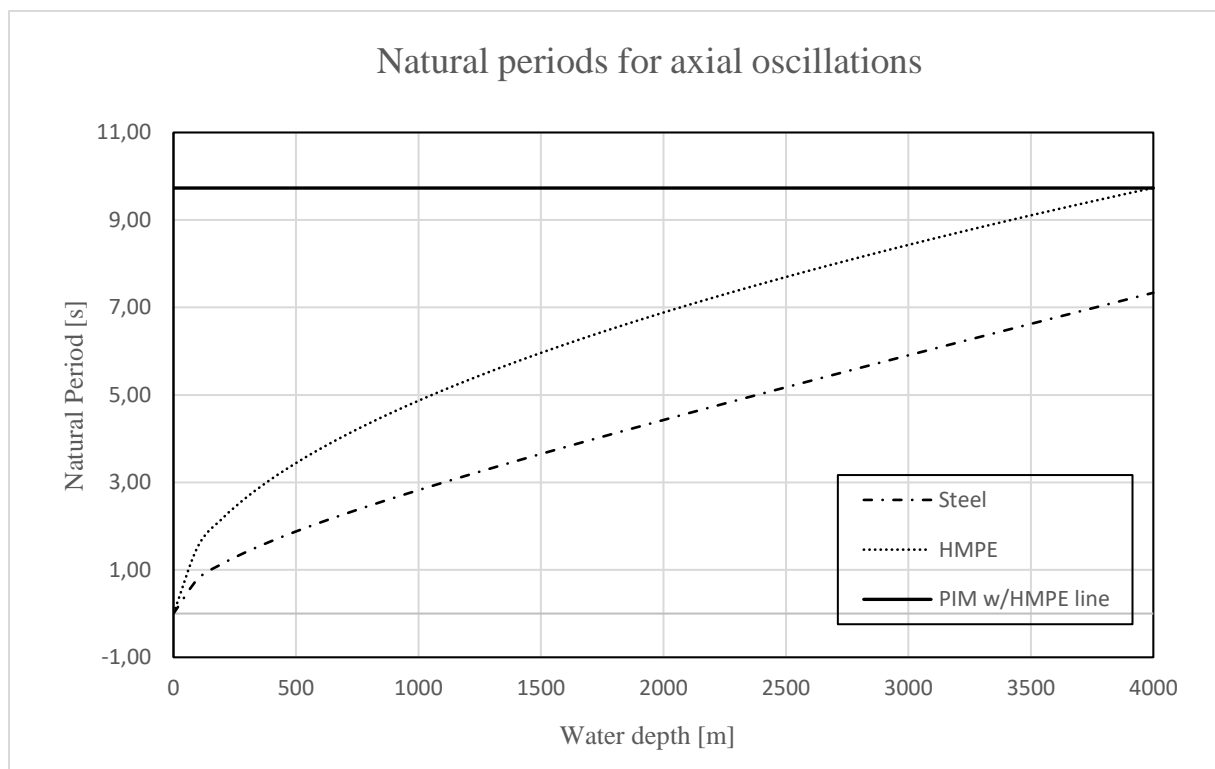


Figure 6-14: Natural periods for different systems

It is noted that application of the PIM does not eliminate the possibility of resonance. The probability is reduced because the natural period of the system will not *change* during the operation, which is the case for vertical lowering. Vertical installation therefore has more possibilities of hitting a critical period.

As for the simulations done in this thesis, the results presented in chapter 6.1.2 show no sign of true resonance or resonant behaviour during phase 2. The medium length waves cause a noticeable higher maximum tension (see Figure 6-7 and Figure 6-8), meaning that some wave periods are more optimal than others. But there is no sign of uncontrolled, increasing oscillations in the tension as is the case for true resonance.

Figure 6-15 contains two plots of the tension for the 280T-manifold. To the left the H_s is a variable, and to the right the T_p is the variable. For true resonance the tension amplitudes would increase continuously, which does not happen. The figure shows that the system is much more sensitive to significant wave height than to the peak period.

The increase seen here is due to the gradually increased static load. Because of the limiting effect of the damping in the water, it could be considered resonant behaviour if the amplitudes rose rapidly and remained on a constant high level. Recalling Figure 3-4 which described the DAF for different degrees

of damping, a sufficiently damped system will not have uncontrolled dynamic amplification. But the spikes that are noticed are single occurrences, and after these the tension becomes lower again.

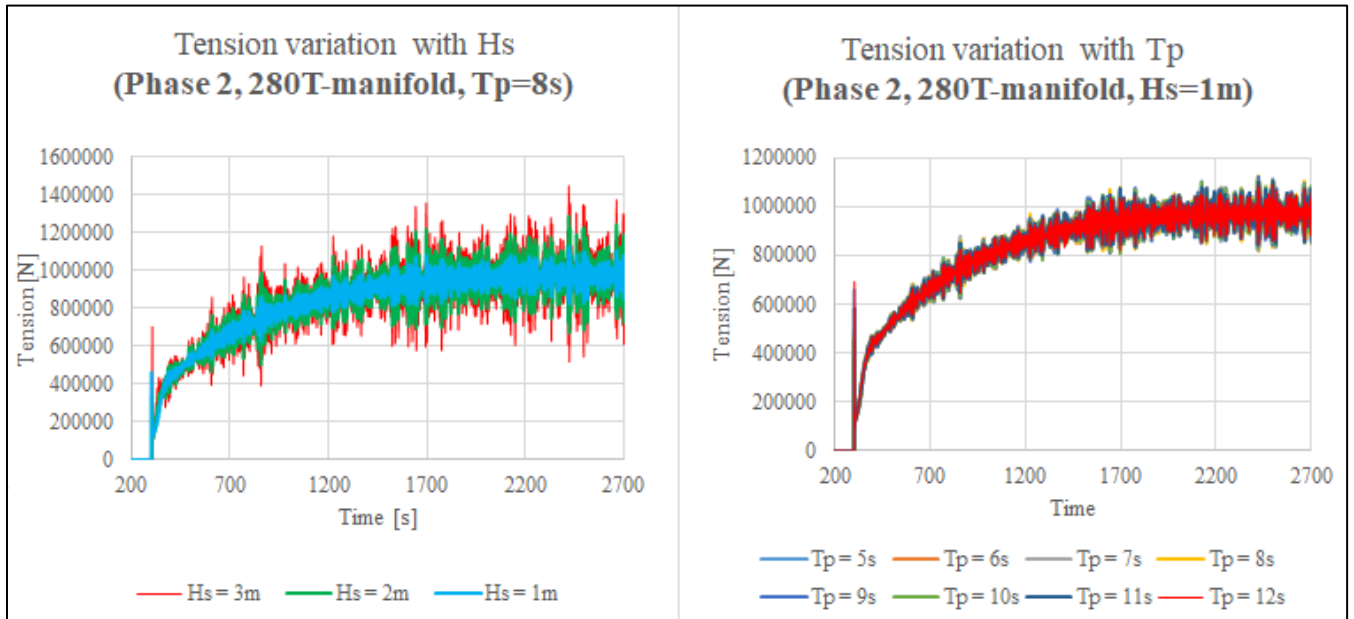


Figure 6-15: Tension variation with Hs and Tp

6.3 Time consumption

The reduced lowering time is a presumed advantage of applying the PIM. Less time spent on lowering the payload will decrease the unproductive time. Also, while the launch vessel transports the payload away, the installation vessel can deploy the ROV. The ROV lowering is done vertically, but by performing the two tasks simultaneously the ROV can reach the seabed and be prepared when the payload arrives.

The accept criteria is that the PIM should move the different payloads from the initial position to the seabed in less time than the references, which are hoist speeds of 40m/min and 60m/min. The possible hoist speed will depend on the size, shape and weight of the payload. 40m/min is a reasonable suggestion, and 60m/min would be a reference for a more ideal scenario.

In Figure 6-16 the vertical position of the 280T-manifold during phase 2 is plotted as a function of time, for different water depths. The curves have the expected profile, when considering the pendulum trajectory: a straight curve that flattens out as the motion becomes increasingly horizontal. As the payload comes towards the end of its trajectory the vertical velocity is almost zero. Figure 6-17 shows plots of the vertical velocity, corresponding to the position plots in Figure 6-16. As can be seen, the velocity is negative (downwards), and remains relatively constant until the gradual increase when the pendulum becomes increasingly horizontal.

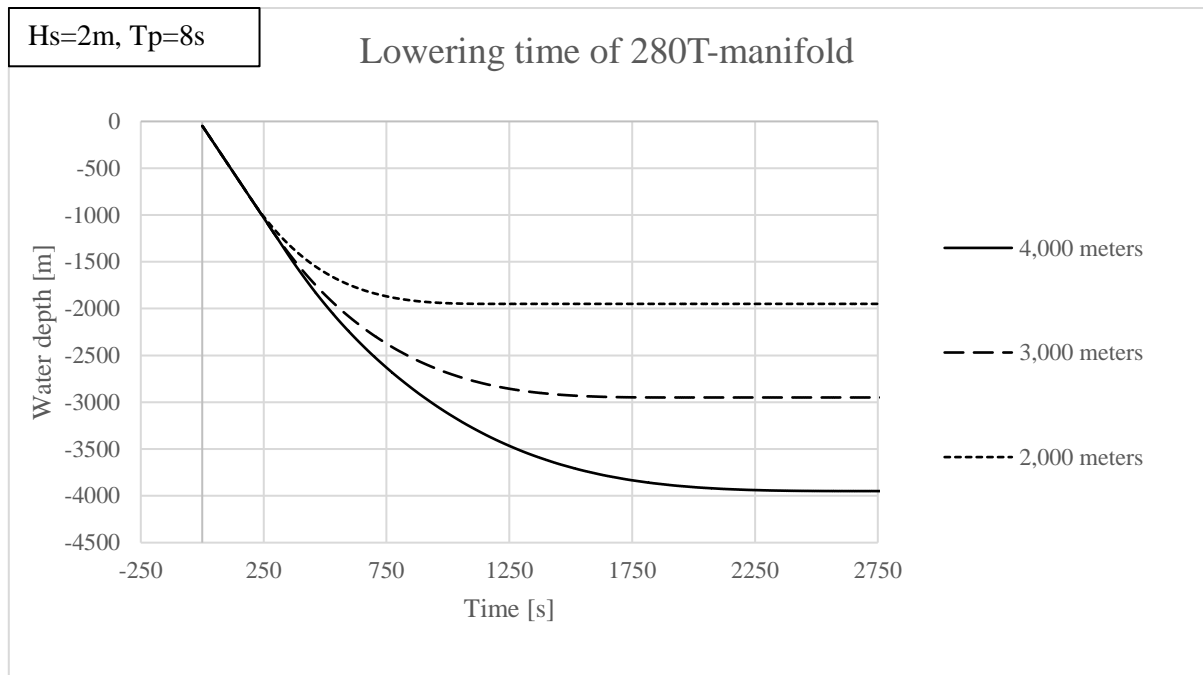


Figure 6-16: Lowering times for the PIM at increasing water depth.

Depending on what vertical lowering speed is used as a reference, the results from simulations done for this thesis shows that the lowering time can be significantly smaller when applying the PIM. Figure 6-18 is a plot of the vertical position of the different payloads as a function of time, from -50 meters to the end of the trajectory. It shows clearly that all payload types have a reduced lowering time relative to the references.

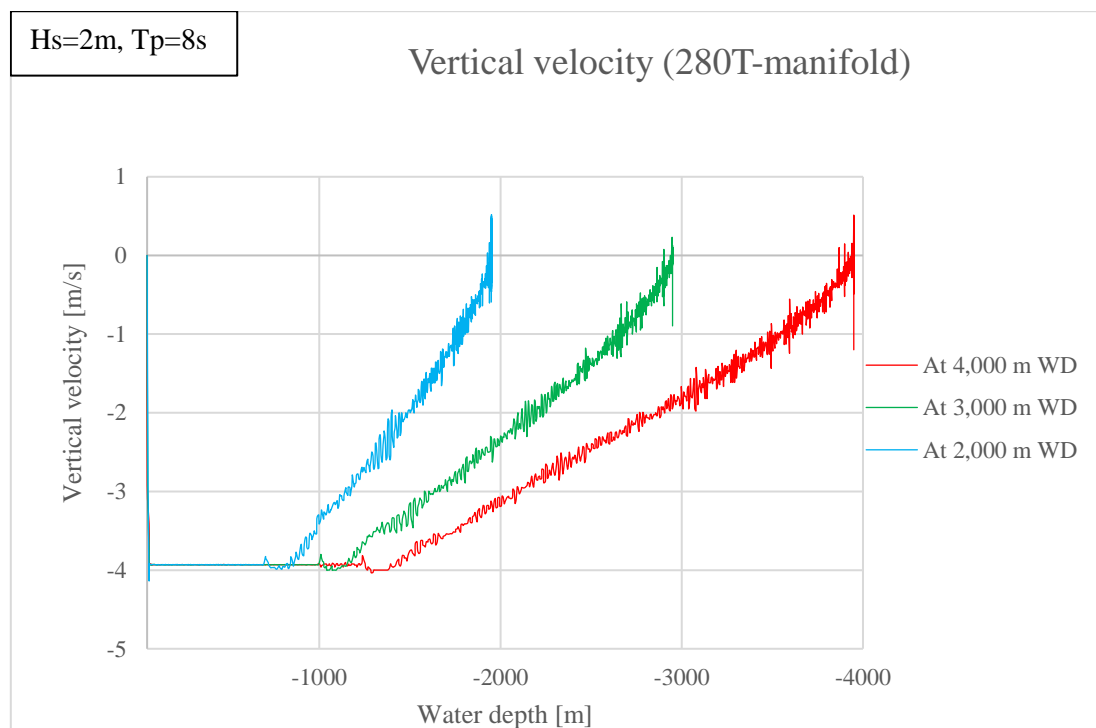


Figure 6-17: Vertical velocity of 280T-manifold

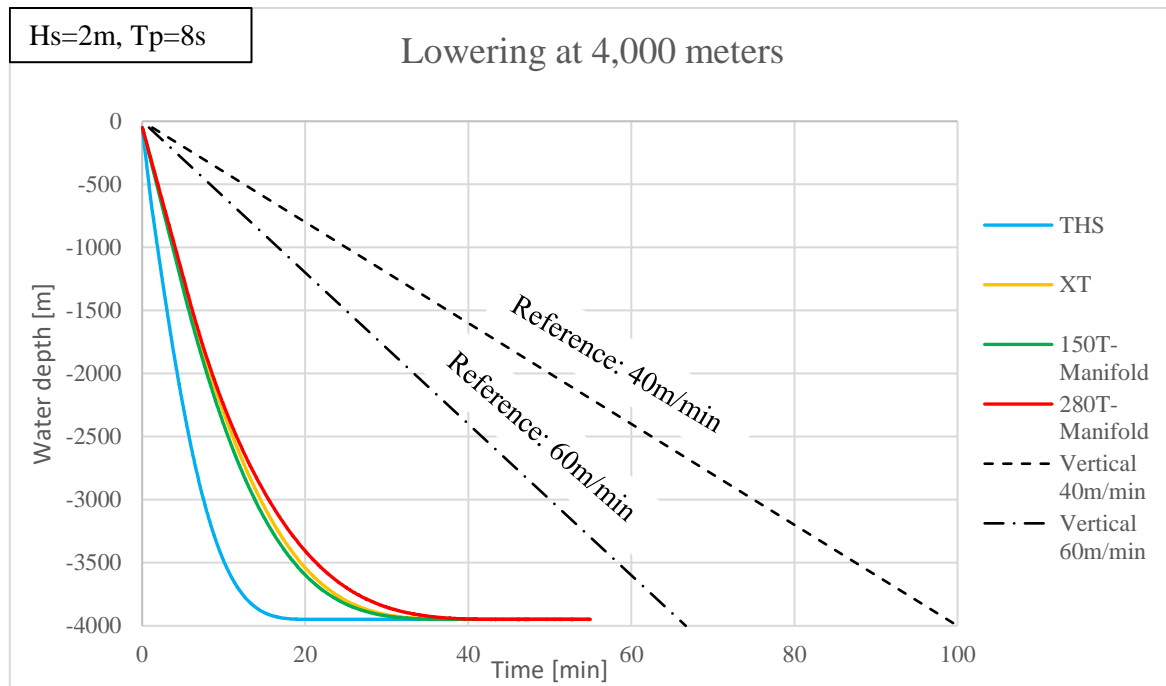


Figure 6-18: Vertical position of payload as a function of time

The total lowering times from 50 meters depth are listed in Table 6-8. The time noted is the time the payload reached the target x-coordinate for the first time. The table also includes the times for 2,000 meters and 3,000 meters. Looking at the numbers in the table, even for the higher hoisting speed the lowering time for the 280T-manifold is 30% shorter for the PIM.

Table 6-8: Lowering time of PIM in different water depths

Equipment type	Time until 2,000 meters [min]	Time until 3,000 meters [min]	Time until 4,000 meters [min]:
Vertical, 60m/min (From 50 meters depth)	31.7	48.3	65.0
Vertical, 40m/min (From 50 meters depth)	47.5	72.5	97.5
280T-manifold	20.0	32.2	45.8
150T-manifold	17.7	28.0	39.0
XT	17.9	28.7	40.2
THS	9.7	15.2	20.9

In the model used for this chapter, it must be noted that the payload is lowered in line with the current. This was decided as it would be the most optimal with regards to the lowering time. For the sake of comparison, simulations were also done for the 280T-manifold where it is lowered in no current at all,

and towards the current. Figure 6-19 shows how the current direction makes a small impact. However, it is very important to note that this model used the simple wire coupling, and the drag force on the lifting line is therefore not included. More detailed studies must be done for this topic.

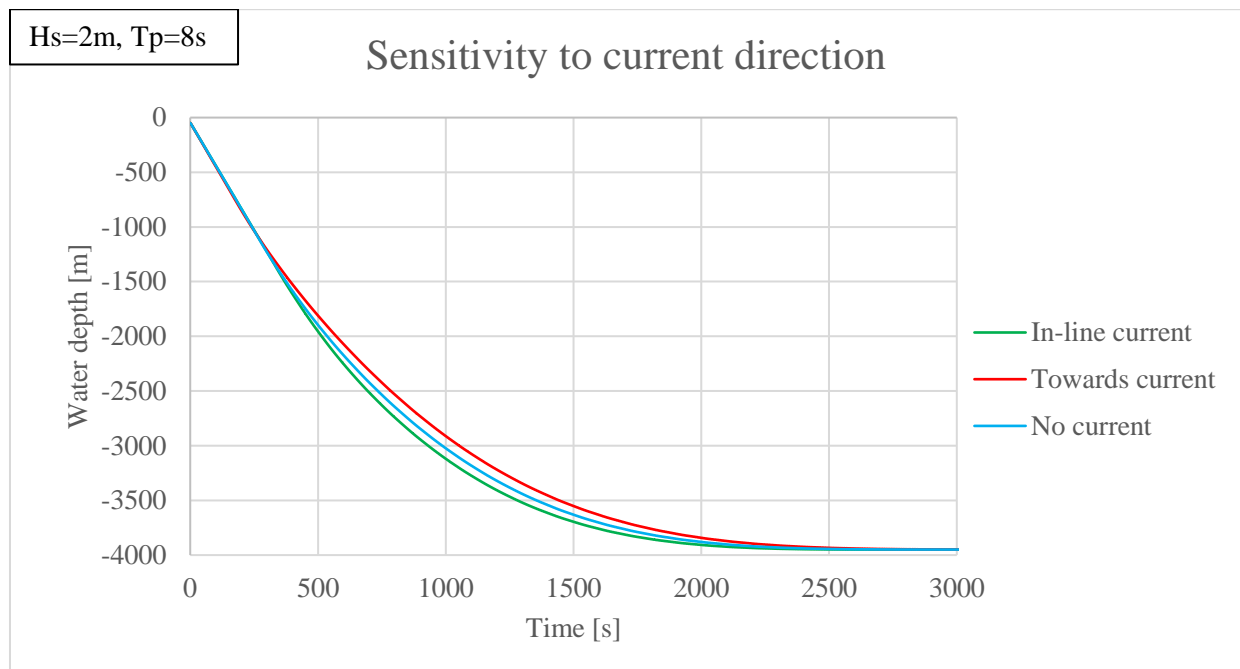


Figure 6-19: Lowering time sensitivity to current direction.

Findings on time consumption:

While the results for lowering times appear very promising with regards to the PIM, it is worth noting that the model is simplified. The drag force on the deployment line is excluded, and the payload models are made as approximations. Additional buoyancy elements for stability are not included either. It may also be unfair to begin the simulation at 50 meters water depth, as this excludes the transportation of the payload away from the target site.

The PIM still appears to allow for moving the payload down to extreme water depths at a higher speed than conventional installation. This would reduce the time spent on underwater activities. When less time is spent on the lowering, more time can be spent on the landing without increasing the length of the operation. This can be of importance when determining required weather-windows. A smaller weather window may thus be acceptable when applying the PIM. Further studies should be done to gain more accurate results.

Accept criteria:

Based on the simulations the PIM is significantly faster than conventional installation. The slowest object to the bottom is the 280T-manifold in 4,000 meters, but it is almost 52 minutes less time spent than for the main reference of 40m/min. While a more advanced model should be built to more accurately simulate phase 2, the difference is significant enough to be interesting for further studies.

6.4 Horizontal offset

The horizontal motion is a low-frequency response, meaning it is slow moving. A mean horizontal offset can be solved by repositioning the vessel topside, and the payload will follow. With reference to chapter 2.2.5, it can however cause delays, as one waits for the payload to resettle to its new mean position. Ideally the conditions have been measured prior to installation, so one can be able to predict with high accuracy where the vessel must be positioned to locate the payload above the target site.

6.4.1 Source of error

For the results regarding horizontal offset, two sources of error should be mentioned. First, in this thesis the current is modelled as constant and unidirectional. Therefore, the offset can be expected to be smaller in practice. If the current is not unidirectional the drag force will act in more than one direction. The results in this regard should therefore be conservative.

The other source of error is related to the model. For all results, the offset has a small, gradual increase. This is believed to be due to the low frequency drift of the vessel. This is an issue that would require further investigation. In Figure 6-20 the x-coordinate of the vessel model's centre is plotted as a function of time. For this short window the trend line shows that the vessel is drifting slowly in line with the current. Since the drift is linear, however, the results can be corrected by subtracting the value for the function for the trend line at the data points. Figure 6-21 illustrates how the correction is done.

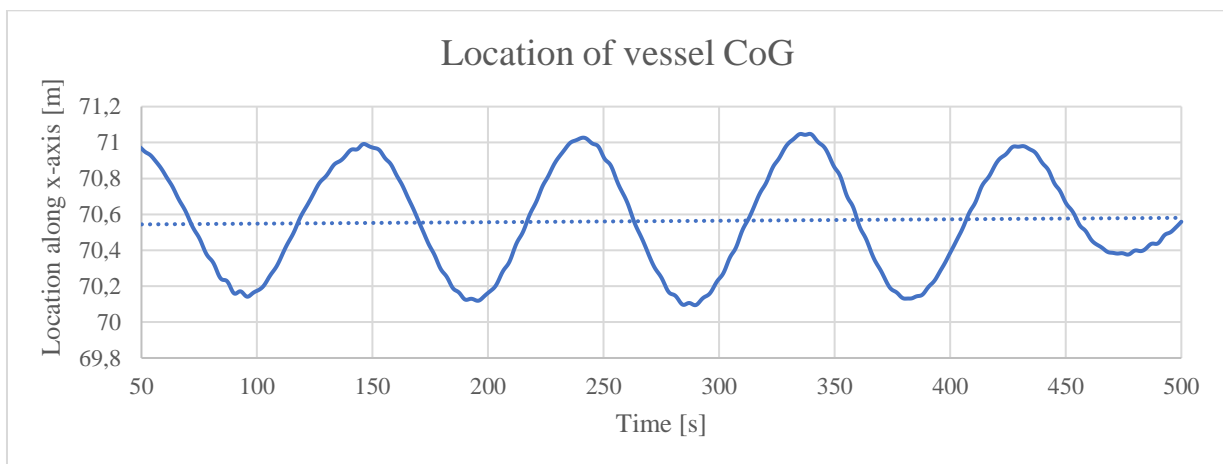


Figure 6-20: Slow drift of vessel

In theory the PIM is well suited for compensation for horizontal offset: the payload will follow the trajectory until it is suspended from the vessel. In Figure 6-22 the horizontal motion of three equipment types are plotted as a function of time. All travel along the pendulum trajectory and settle around zero (target site) after the pendulum is completed. If the conditions are mapped prior to the lowering, the vessel can be positioned such that at the end of the pendulum trajectory the payload will offset to the target site. Figure 6-22 is plotted from data obtained for a model using the simple wire coupling, meaning that the drag force on the lift line is not included.

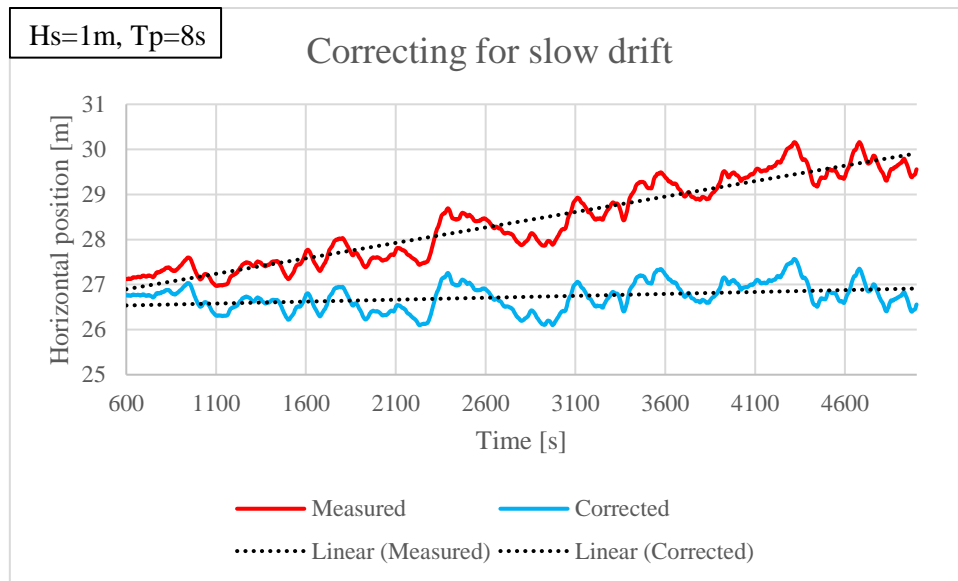


Figure 6-21: Correcting for slow drift

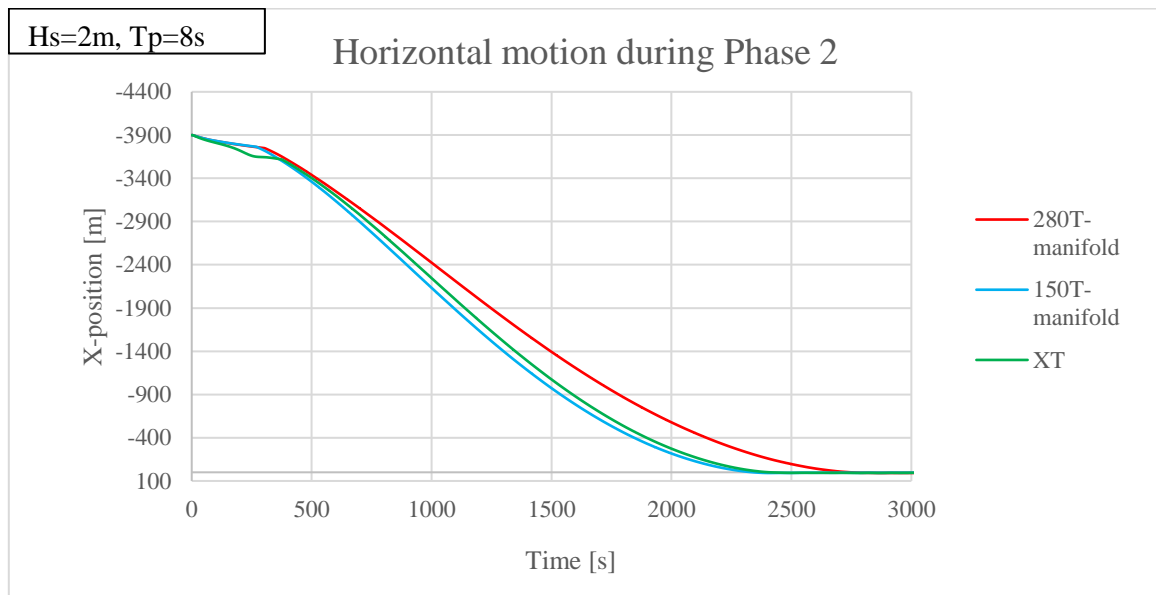


Figure 6-22: Horizontal motion during phase 2

6.4.2 Sensitivity to current

In practice the offset is of course dependent on environmental conditions. The most significant impact on the offset was expected to be the current, as it exerts a drag force both on the payload and the lift line. In Figure 6-23 the horizontal position of the 280T-manifold is plotted for the three different current profiles illustrated in chapter Figure 5-3. They are also turned 180 degrees, and there is a plot where there is no current at all. It is obvious that the current makes a large impact on the horizontal offset of the payload. The offset for the strongest current is around 60 meters, which is twice the offset of the medium current. Recall that in the model, the strongest current is modelled by a 50% increase of

the medium profile at all levels. The importance of the current to determine the offset is well exemplified by noticing the plot in Figure 6-23 where the current is removed from the model.

In Table 6-9 the mean and largest (absolute) offset are listed for the different current conditions. As can also be seen from Figure 6-23 the values are almost symmetrical around zero. The offsets are skewed slightly in the positive direction however. This is likely to be the result of the waves, which in this model has a propagation direction of 0°. With reference to chapter 3.1.1.1 the water particle velocity from the waves will contribute to the drag force on the lift line. When looking at the offset for no current in Table 6-9, the mean offset is slightly positive.

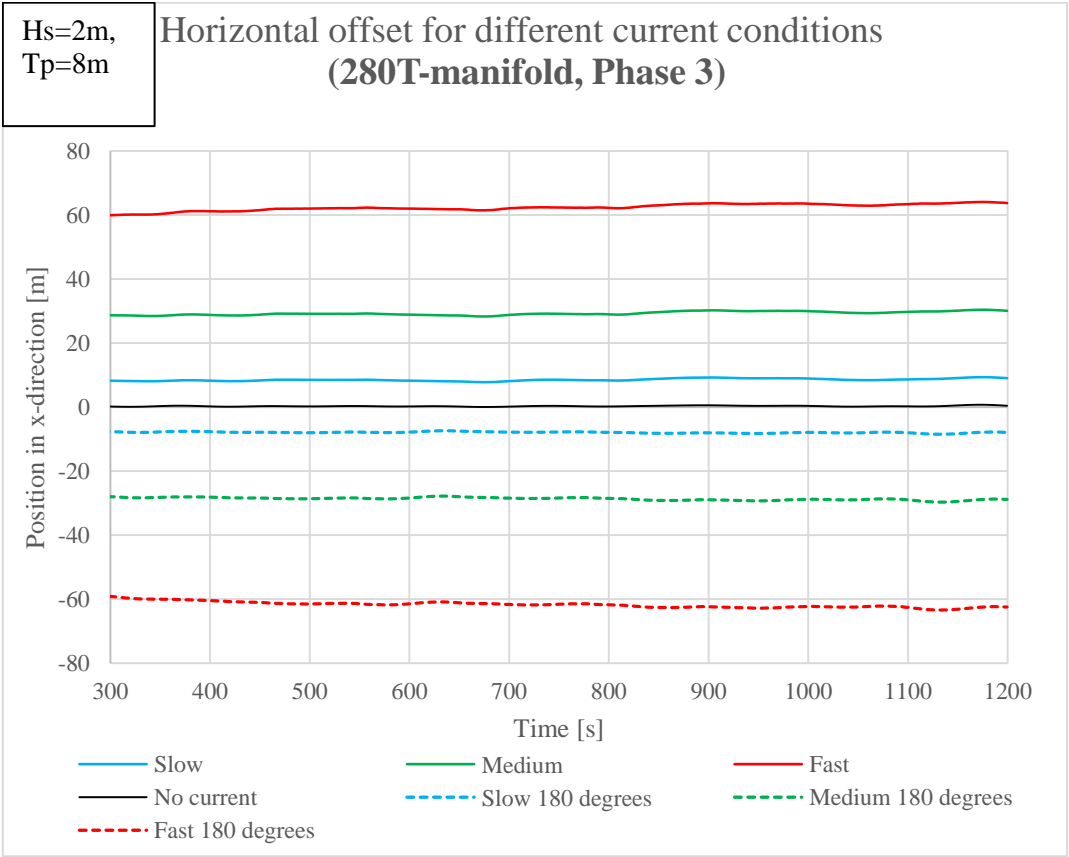


Figure 6-23: Horizontal offset for different current conditions.

Table 6-9: Offsets due to current

Offset	Slow	Medium	Fast	No current	Slow (180°)	Medium (180°)	Fast (180°)
Largest offset [m]	9.4	30.4	64.1	0.8	-8.5	-29.7	-63.4
Mean offset [m]	8.1	27.3	57.0	0.3	-7.5	-26.6	-56.4

6.4.3 Sensitivity to waves

In Figure 6-24 the horizontal offset of the 280T-payload is plotted as a function of time, for different values of wave peak period. The result is unexpected, as the offset increases noticeably with longer periods.

It is important to note that these simulations are done for the exact same model, and that only the peak period of the waves is changed from dataset to dataset. Since the only variable is the T_p , this is assumed to be the cause and is therefore investigated. Each set of data viewed separately are not unreasonable given the presence of a current. Note that the results for $T_p=8$ in Figure 6-24 have a similar offset as the medium current in Figure 6-23. These have the same current and the same period.

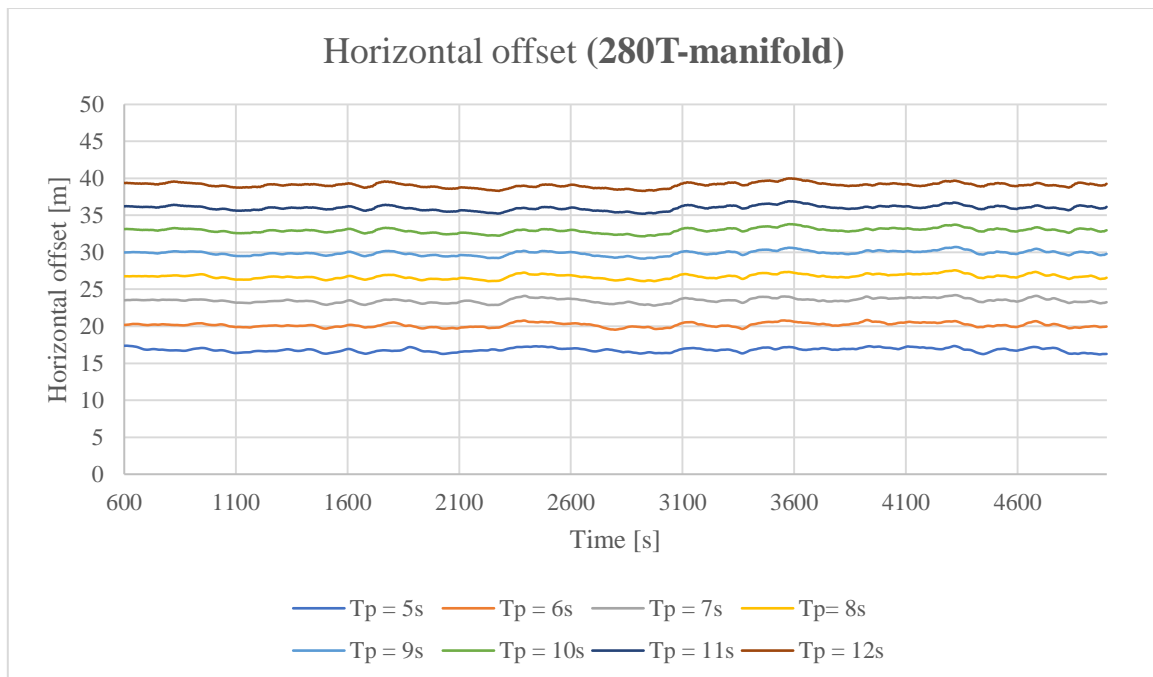


Figure 6-24: Horizontal offset of 280T-manifold for different T_p

The only large contributor to offset was expected to be the current, which is why this result was unexpected. The water particle velocity from the current should create a drag force on the lift line, causing the offset. The wave conditions also cause water particle velocity; however, this was expected to only affect the section closest to the surface and therefore not have a large effect on the offset.

By also plotting the offset for different significant wave heights, one can see that there is further indication that it is the wave conditions that cause the difference in offset. Figure 6-25 shows this, as the offset is plotted for different values of H_s .

In the figure it can be seen that the offset increases with higher significant wave heights. The shapes of the curves are the same, with larger oscillation amplitudes for the higher H_s . The large difference in offset when the peak period is the variable should be investigated further.

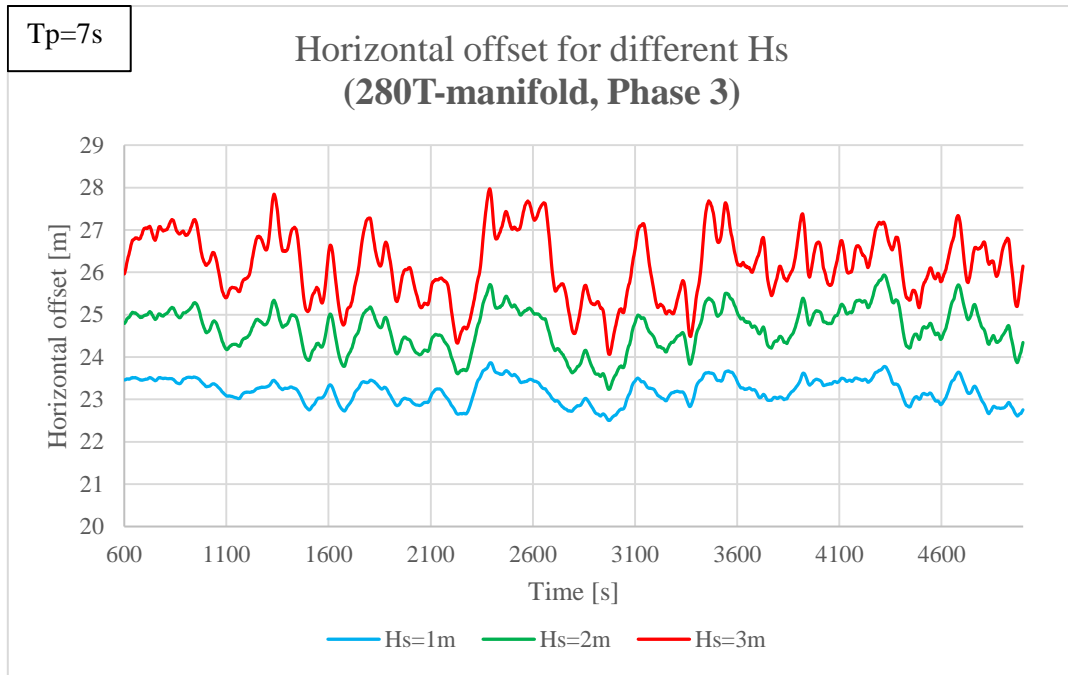


Figure 6-25: Horizontal offset of 280T-manifold for different Hs

However, a possible explanation in favour of these results can be found in the theory. In chapter 3.1.1.1 linear wave theory is explained. Equation (5) and (7) are horizontal water particle velocity and the dispersion relation respectively (both equations use the deep water-approximation):

$$(5) u_{deep} = \frac{\xi_0 k g}{\omega} e^{kz} \sin(\omega t - kx),$$

$$(7) L = 1,56T^2$$

(Gudmestad, Marine Technology and Operations Theory and Practice, 2015).

Remembering that $k = \frac{2\pi}{L} \rightarrow k = \frac{2\pi}{1,56T^2}$ and that $\omega = \frac{2\pi}{T}$, equation 5 can be written as:

$$u_{deep} = \frac{\xi_0 g}{1.56T} e^{\left(\frac{2\pi}{1.56T^2}\right) * z}$$

Since z (vertical position) is negative, the exponent determines how fast the decay of the water particle velocity is for water depth. This means that the shorter waves (shorter Tp) has a higher velocity close to the surface, but that the longer waves cause a slower decay of the velocity. Therefore, for the longer wave periods the wave velocity the velocity from the waves affect the lift line for a longer section.

The formula could explain both Figure 6-24 and Figure 6-25, as the velocity profile is dependent both on the wave amplitude and the wave period. That said, it is uncertain whether or not the effect should be as prominent as it appears from these results. As mentioned, this should therefore be investigated further.

6.4.4 Findings

Because the results are not as expected, more research should be done on how the wave peak period affects the horizontal offset. While it is possible that the effect can be explained by wave theory, the study is not sufficient to draw a conclusion. Currents on the other hand, can be said to have a large impact on the offset as was expected. The most effective measure against uncertainty for the offset would likely be to track the horizontal position of the payload by use of acoustic positioning during the lowering, and then manoeuvre topside as needed. Optimally this could be done real-time to save time. If conditions can be sufficiently mapped prior to the operation, it should be possible to create a model that can predict the offset with satisfactory accuracy.

Accept criteria:

The PIM has no effect on the horizontal offset. It should not be a critical problem if it can be predicted. Even if it is not predicted accurately, a mean offset can be compensated for by topside motions. It will require more time, however.

6.4.5 Remarks

In this sub-chapter it can be interesting to reference the alternative procedure described in chapter 4.3. The method proposed by Wang et. al. includes a separate rope (launch line) connected to the launch vessel. The launch line remains connected to the payload rigging when the payload is suspended, and it could therefore be possible to manoeuvre the payload by repositioning the launch vessel. This may be a measure to compensate for a horizontal offset without manoeuvring the installation vessel.

6.5 Landing and accuracy

In this chapter the horizontal and vertical oscillations of the suspended payload are of interest. The mean horizontal offset is ignored, because when the payload has settled at its offset it oscillates around this position.

In the model used to obtain the results for these chapters, both the wave propagation direction and the current direction is zero degrees. This means all movements in the y-direction can be neglected. If the directions had been changed, the angle of the motions would be skewed, but should not be larger than the results in this chapter.

To compensate for the slow drift mentioned in chapter 6.4.1, the linear increase is removed from the results as was done for the offset. Here the values are also adjusted so they show oscillations around the mean offset. This is done to make it easier to compare the different results, as it omits the difference in horizontal offset due to variations of the T_p . It is done as is shown in Figure 6-26. It can be done because the increase is linear, as shown in Figure 6-26 a). When the gradual increase of the mean value is removed, the plot becomes Figure 6-26 b). The constant mean can be subtracted from b)

to arrive at c). In Figure 6-26 c) the oscillations around the local origin is plotted. This allows for study of the horizontal oscillations and compare the results for different peak periods.

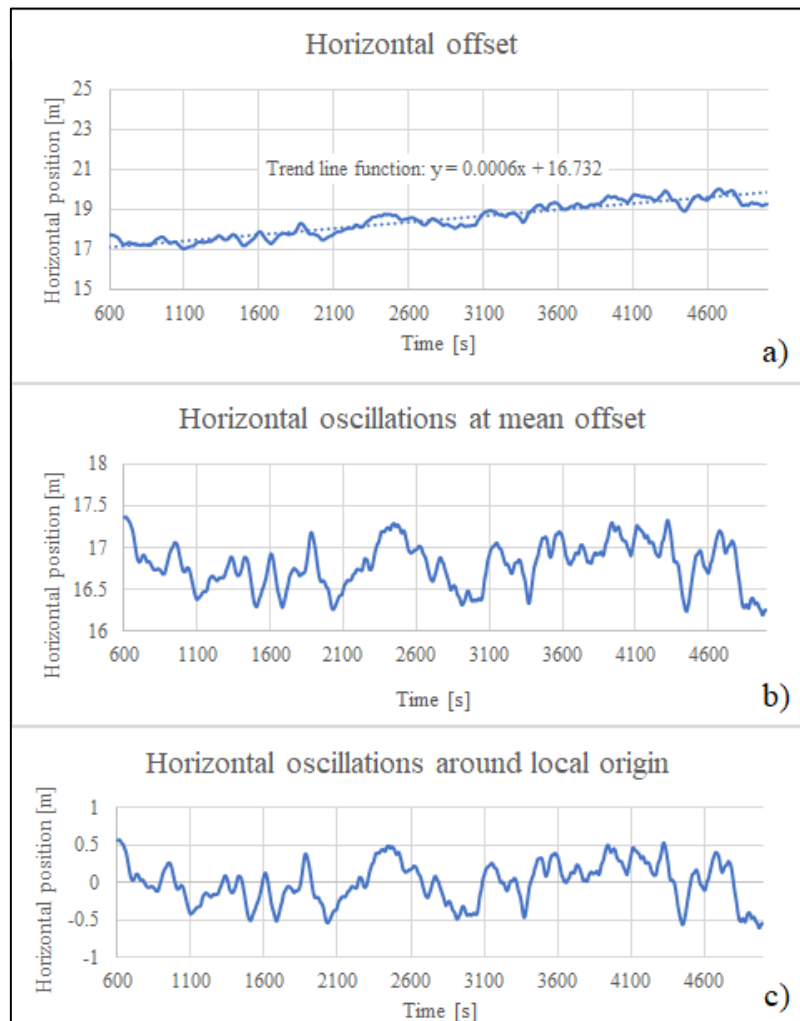


Figure 6-26: Adjusting for mean horizontal offset

The horizontal and vertical oscillations are dynamic responses, unlike the mean offset which is a static response due to constant forces. The oscillations are caused by the vessel's responses to the waves.

6.5.1 Landing accuracy

The study of the horizontal oscillations is of interest because of the landing accuracy. If the payload has too large horizontal motions during the landing it can be difficult to position it at the desired location.

The acceptance criteria for positioning will be different for different types of equipment but positioning within a margin of error of five by five meters (5 meters peak-to-peak) should be sufficient for the types of equipment to be lowered with the PIM.

In Figure 6-27 the horizontal position of the suspended 280T-manifold is plotted as a function of time. The oscillations appear random and may be considered a stochastic process. The amplitudes are

however very small, as the largest offset are around 60 centimetres. The conditions can be considered benign at $H_s=1\text{m}$ and $T_p=5\text{s}$. It is also important to note the large timespan in which the motions are occurring, which for the figure below is 4400 seconds or 73 minutes. The horizontal oscillations are low-frequency motions. This is confirmed by plotting the horizontal velocity of the payload, as shown in Figure 6-28. As can be seen from the figure the velocity does not exceed 4 centimetres per second.

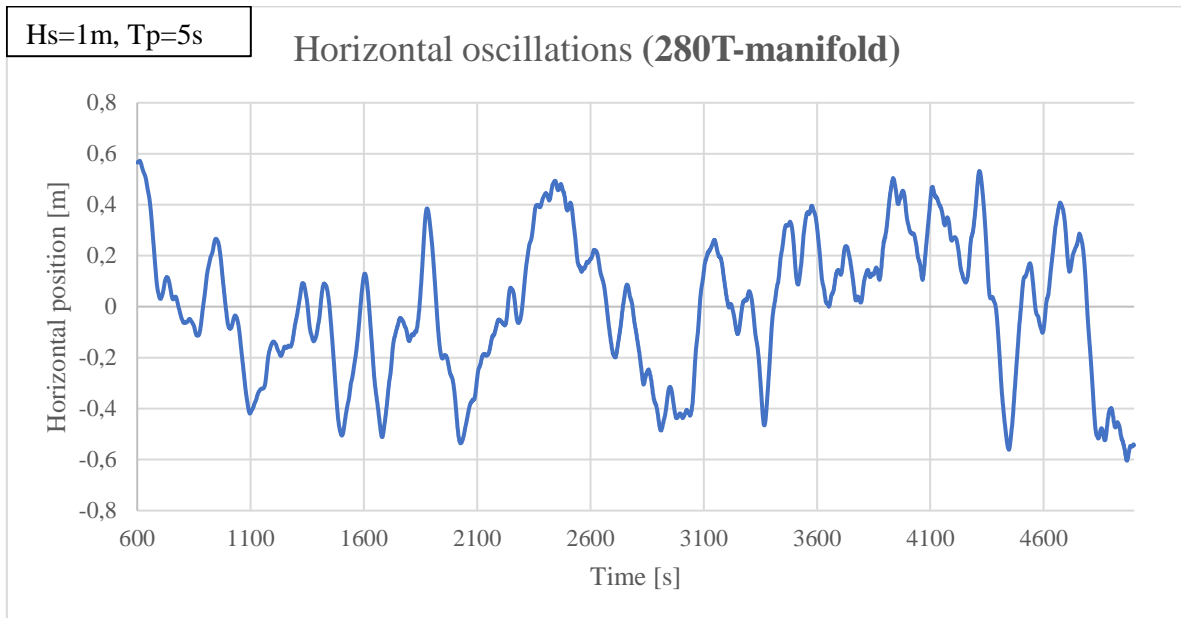


Figure 6-27: Horizontal oscillations of suspended 280T-manifold

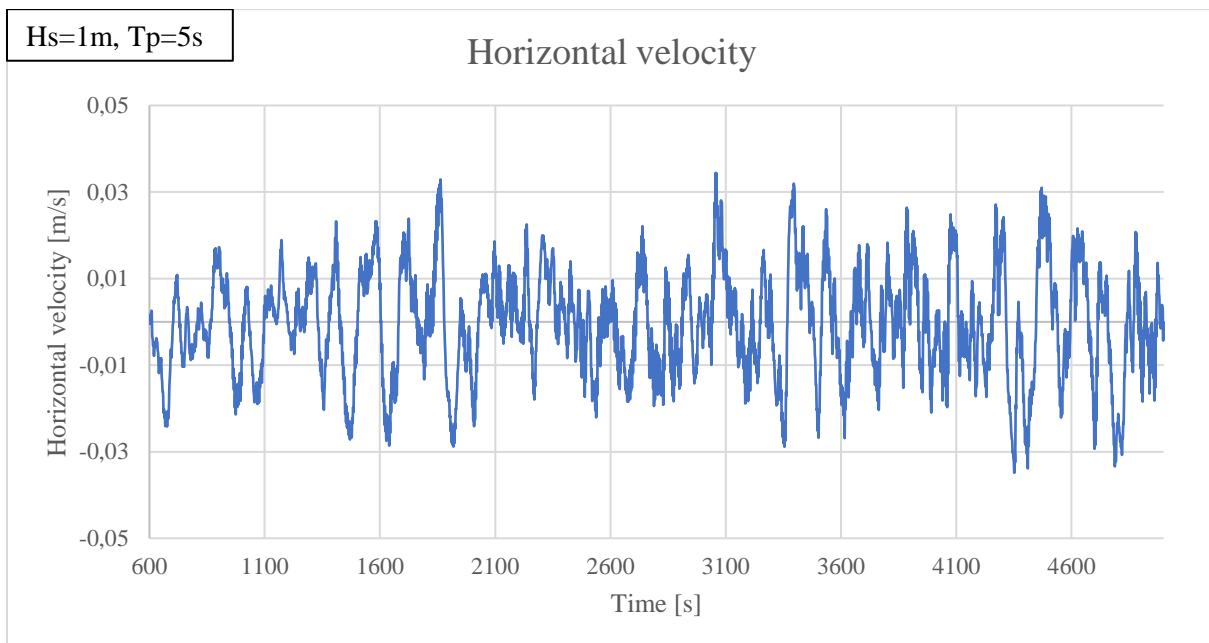


Figure 6-28: Horizontal velocity of suspended 280T-manifold

The motions were expected to increase with higher sea states, as the topside responses become larger. In Figure 6-29 the largest and smallest horizontal-motion amplitudes are plotted for the different significant wave heights and peak periods. It can be seen that the largest amplitudes occur for $H_s=3$

meters for all periods. In Table 6-10 the values used to plot Figure 6-29 are listed, with the highest values for each case in bold. The largest values occur for the longest period ($T_p=11s$) for all simulated cases. However, in the positive x-direction $T_p=5s$ gives a larger response than $T_p=9s$ both for $H_s=2m$ and $3m$, so there seem to be an element of randomness in the responses.

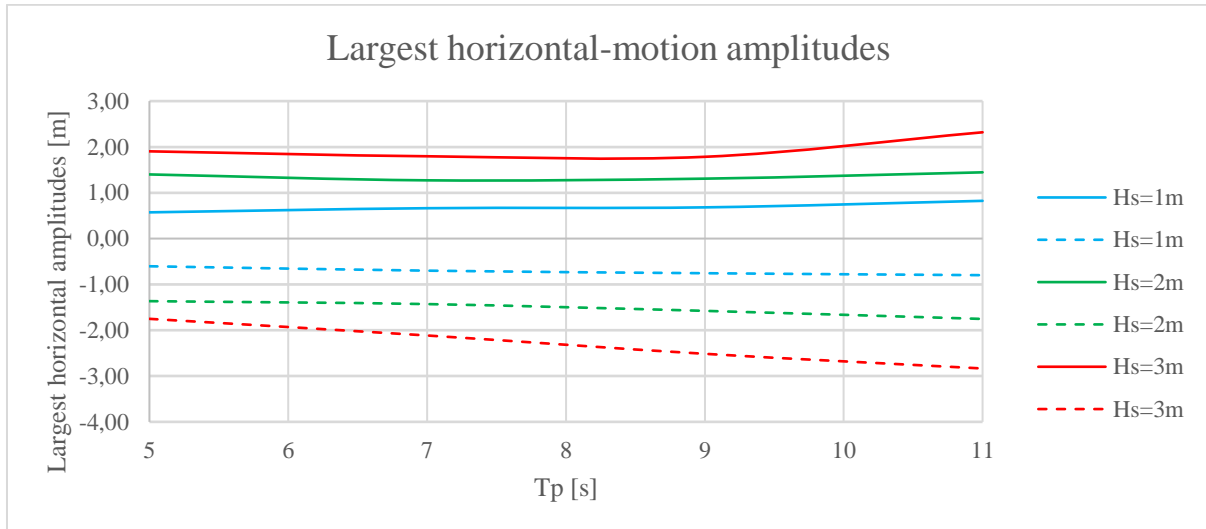


Figure 6-29: Largest horizontal-motion amplitudes

Note that in Table 6-10 the standard deviation follows the same pattern as the amplitudes. This is logic as with the larger amplitudes the payload is further away from its origin for longer periods of time.

Table 6-10: Largest horizontal-motion amplitudes

T_p [s]	Hs=1m			Hs=2m			Hs=3m		
	Max [m]	Min [m]	StdDev [m]	Max [m]	Min [m]	StdDev [m]	Max [m]	Min [m]	StdDev [m]
5	0.57	-0.60	0.28	1.40	-1.37	0.60	1.90	-1.75	0.78
7	0.66	-0.70	0.29	1.27	-1.43	0.51	1.80	-2.12	0.79
9	0.68	-0.76	0.30	1.31	-1.58	0.57	1.78	-2.51	0.85
11	0.82	-0.80	0.32	1.45	-1.75	0.65	2.32	-2.84	1.00

In Figure 6-30 the horizontal oscillations of the 280T-manifold are plotted in a peak period of 11 seconds for all three H_s . It can be seen that the plots have the same shape, but the oscillations are amplified by the harsher sea states. The highest peak-to-peak difference occurs in this simulation and is 5.16 meters. The payload moves between the two extremes (2.32m and -2.84m) in almost 20 minutes, however ($t=1782s$ and $t=2973s$), which reveals a very slow motion. Neither is this a direct translation. The largest direct translation is 4.36m. The velocity of the payload is plotted for different H_s in Figure 6-31, and while it is clear that the higher sea states cause higher velocity, the motion is still very slow.

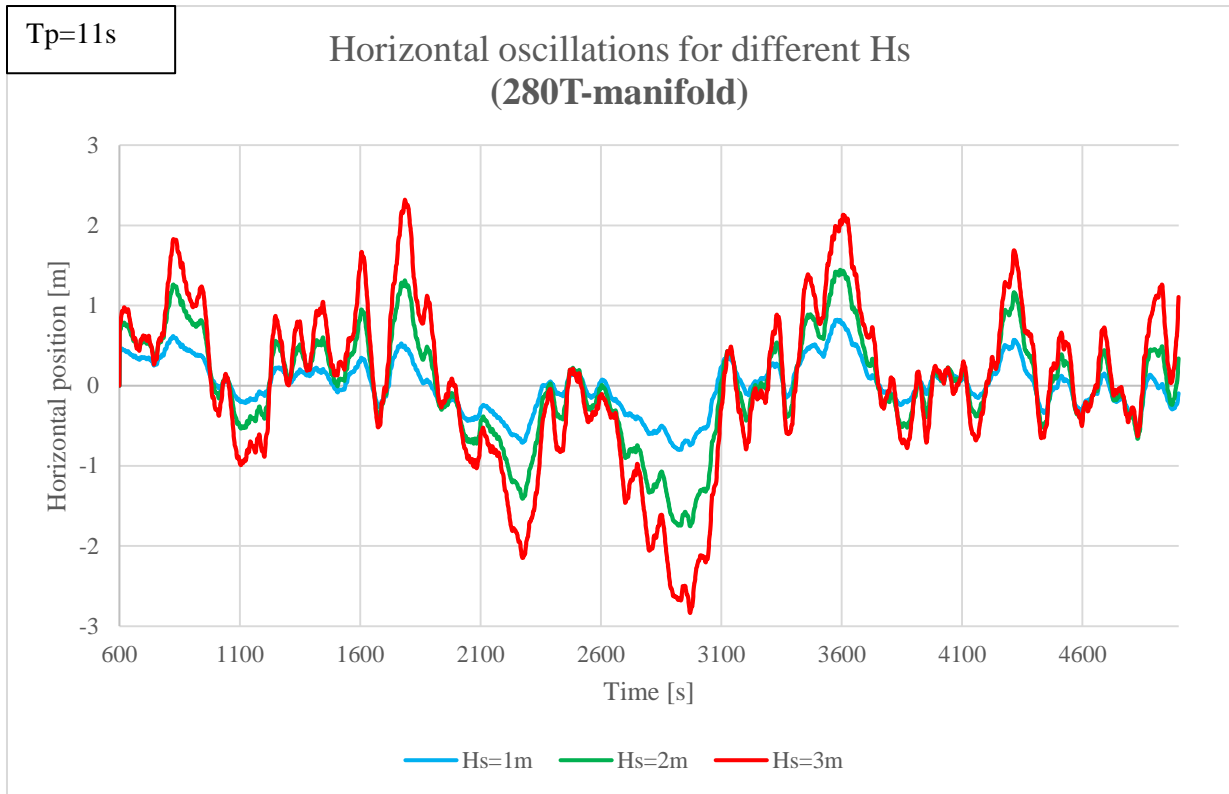


Figure 6-30: Horizontal oscillations for different Hs (280T-manifold)

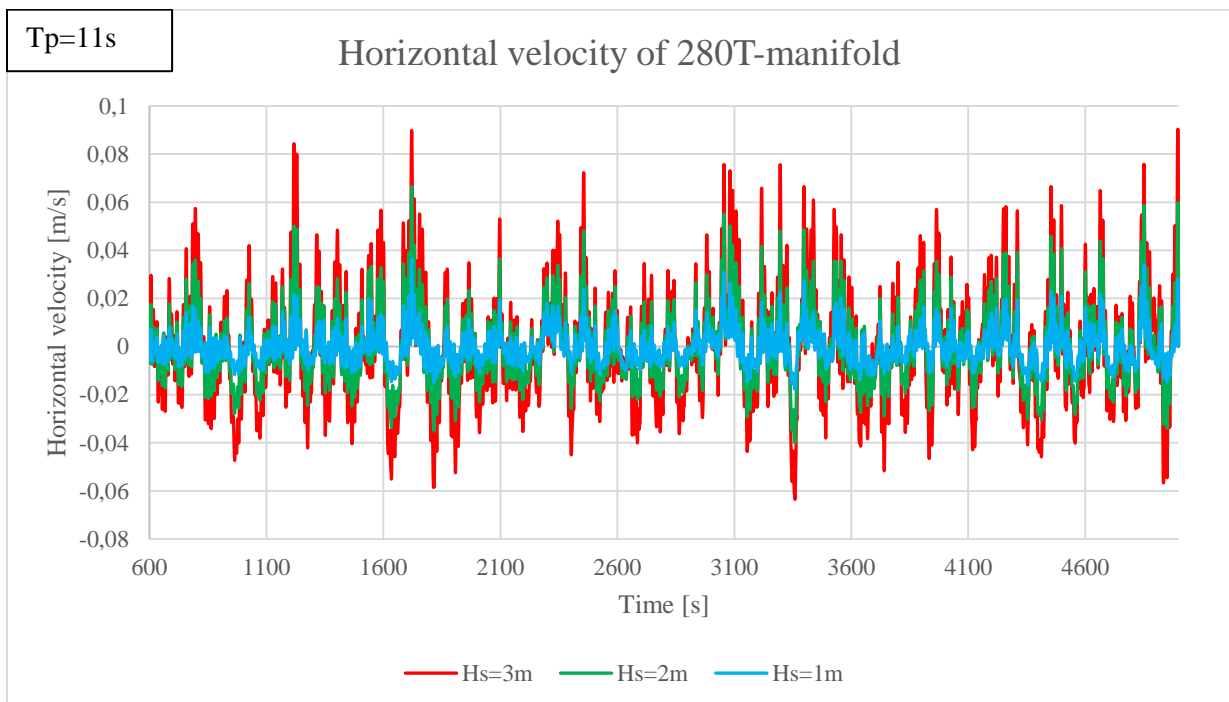


Figure 6-31: Horizontal velocity of 280T-manifold for different Hs.

Table 6-11 lists the highest absolute value of the horizontal velocity for the different sea states. As can be seen, the fastest the payload moves is 9 centimetres per second. The highest values are listed in bold.

Table 6-11: Horizontal velocity of 280T-manifold in different sea states.

Tp	Hs=1m	Hs=2m	Hs=3m
[s]	Velocity [m/s]	Velocity [m/s]	Velocity [m/s]
5	-0.017	0.031	-0.065
7	0.024	0.037	0.067
9	0.024	0.040	-0.065
11	0.036	0.066	0.090

6.5.2 Vertical oscillations

If the vertical oscillations are too large it may be difficult to land the payload without damaging it or the soil. Connection or orientation by ROV can also be difficult if the vertical oscillations are excessive. Accept criteria should be that the oscillations are within the range of the AHC to reduce the motions, both with respect to oscillation amplitudes and to acceleration. While capacities vary, based on specification sheets (see Figure A-2 and Figure A-3) a peak-to-peak amplitude of 3 meters and an acceleration of 7 m/s² is selected in this thesis.

In Figure 6-32 the vertical position of the 280T-manifold is plotted as a function of time, for all peak periods. It is not immediately clear from the figure, but the trend is that the longer Tp gives larger oscillations. The largest peaks-to-peak difference for all Tp are around t=1715 seconds and t=4850 seconds. By plotting them side by side it can be seen that the former has the largest difference (Figure 6-33). Studying the datasets, it can be seen that this is the case for all conditions apart from Tp=5 and Tp=6. The deviation ranges between 1 and 11 centimetres, and these conditions also give the smallest responses. The study is therefore limited to the interval 1700-1750 seconds to make the figures clearer.

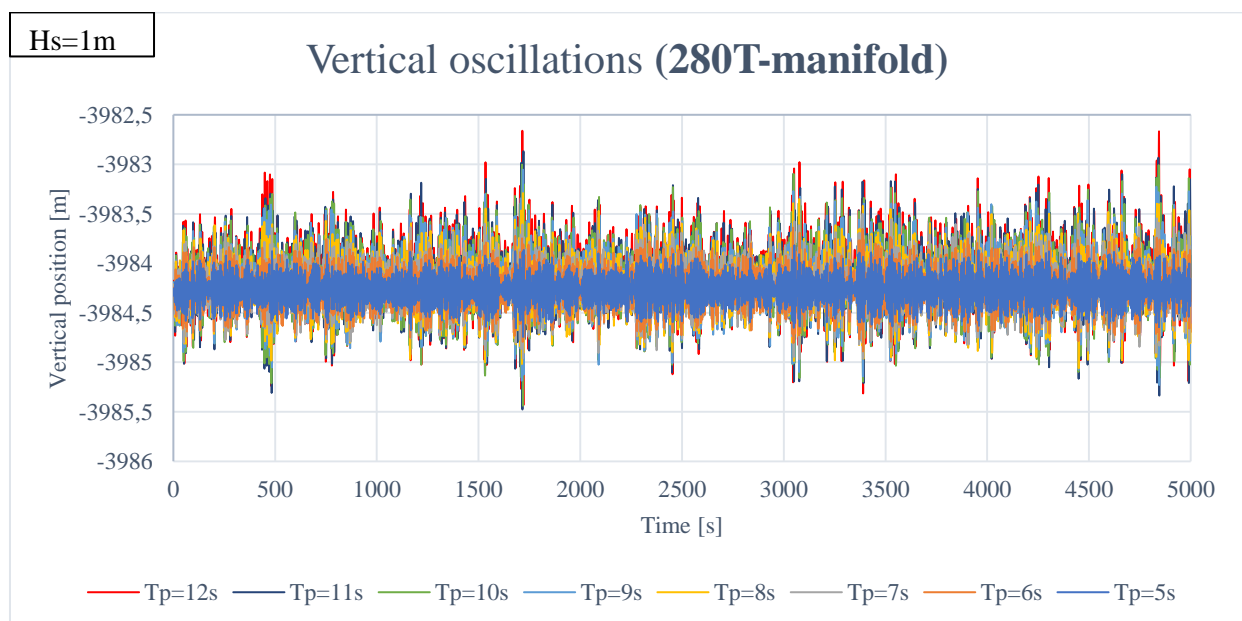


Figure 6-32: Vertical oscillations of 280T-manifold in Hs=1m

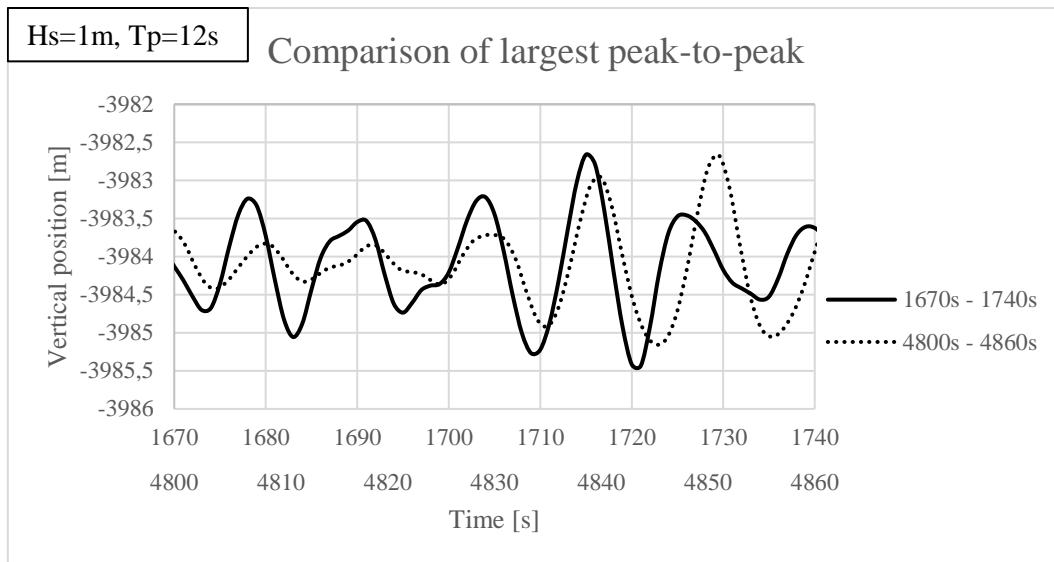


Figure 6-33: Locating the biggest peak-to-peak difference.

In Figure 6-34 the vertical oscillations around the largest amplitudes are plotted for the five longest peak periods. It can be seen that the largest peak-to-peak difference comes for the longest periods. In Table 6-12 the largest peaks and differences are listed, confirming that the largest differences come for the longest period. In the table it is also seen that the period can also cause large peak-to-peak differences. The difference for $H_s=1\text{m}$, $T_p=12\text{s}$ is larger than for $H_s=2\text{m}$, $T_p=5,6$ and 7 seconds. This implies that both the peak period and the significant wave height can have a large impact on the oscillation amplitudes. Only for $H_s=3\text{m}$, and peak periods between 9 and 12 seconds does the peak-to-peak difference exceed 6 meters, which was the accept criteria for vertical oscillations.

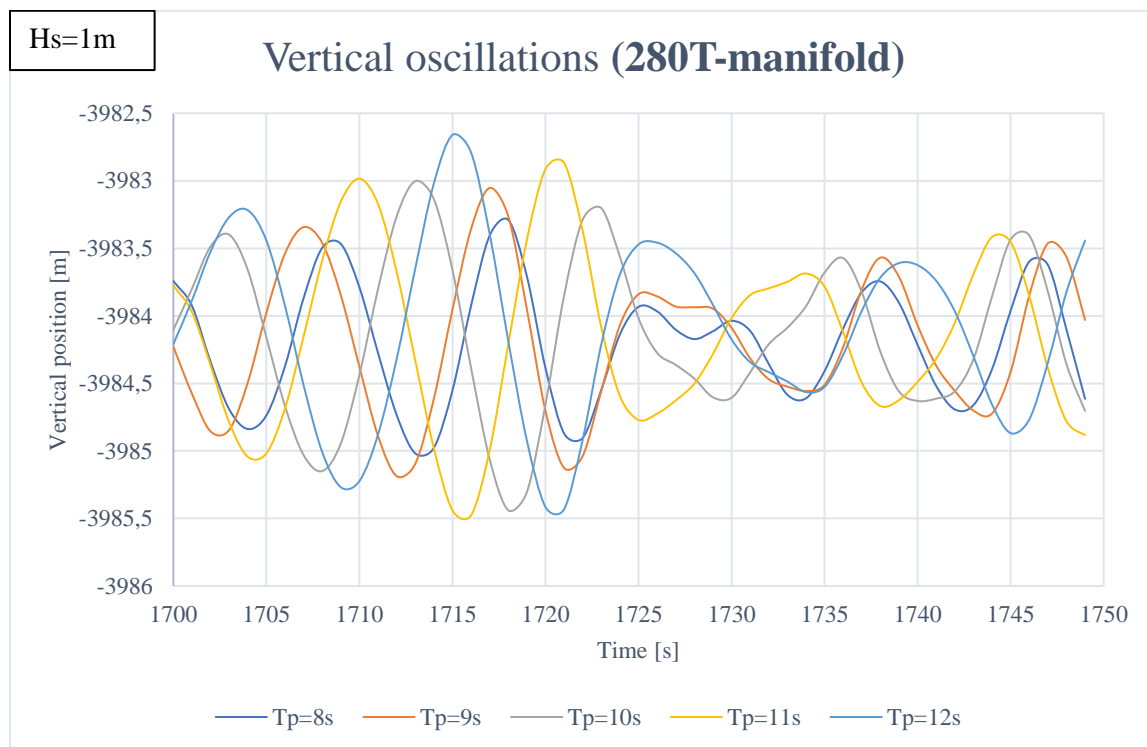


Figure 6-34: Vertical oscillations for different T_p (280T-manifold)

Table 6-12: Vertical oscillations for 280T-manifold in all conditions

Tp	Hs=1m			Hs=2m			Hs=3m		
	[s]	Max[m]	Min [m]	Diff. [m]	Max[m]	Min [m]	Diff. [m]	Max[m]	Min [m]
5	-3983.86	-3984.74	0.88	-3983.54	-3985.03	1.48	-3983.30	-3985.30	1.99
6	-3983.72	-3984.79	1.07	-3983.25	-3985.29	2.04	-3982.80	-3985.81	3.01
7	-3983.60	-3984.96	1.36	-3982.95	-3985.56	2.60	-3982.30	-3986.18	3.88
8	-3983.29	-3985.02	1.73	-3982.38	-3985.79	3.41	-3981.53	-3986.54	5.01
9	-3983.05	-3985.19	2.13	-3981.95	-3986.11	4.17	-3980.92	-3986.99	6.07
10	-3983.00	-3985.44	2.44	-3981.85	-3986.61	4.76	-3980.74	-3987.68	6.94
11	-3982.87	-3985.48	2.61	-3981.54	-3986.81	5.27	-3980.24	-3988.12	7.87
12	-3982.66	-3985.43	2.77	-3981.25	-3986.75	5.51	-3979.90	-3988.04	8.14

In Table 6-13 the highest absolute values for the velocity and acceleration are listed for all conditions. Again, it can be seen that the fastest velocity for a low Hs-values is faster than the slowest velocity for a high Hs-value (Hs=1m, Tp=12s gives a higher velocity than Hs=2m, Tp=7s). While this can be an area to investigate further, none of the accelerations are close to exceeding the accept criteria.

Table 6-13: Maximum vertical velocity and acceleration of 280T-manifold

Tp [s]	Hs=1m		Hs=2m		Hs=3m	
	Vel. [m/s]	Acc. [m/s ²]	Vel. [m/s]	Acc. [m/s ²]	Vel. [m/s]	Acc. [m/s ²]
5	-0.40	-1.17	-0.66	-1.23	-0.90	-1.26
6	-0.45	-1.08	-0.81	-1.00	1.13	-0.95
7	0.55	-1.35	1.00	-1.53	1.46	-1.72
8	-0.58	-0.89	-1.15	-0.84	-1.65	-1.22
9	-0.72	-1.00	-1.36	-0.92	-1.91	-1.26
10	0.73	-0.92	1.37	0.87	1.99	1.29
11	0.78	-1.02	1.50	-0.92	2.17	-1.38
12	-0.76	-1.37	-1.49	-1.59	-2.17	-1.81

6.5.3 Findings

Acceptance criteria for accuracy:

The horizontal oscillations are as mentioned low frequency motions. The largest interval measured exceeds the criteria for accuracy, which was of 5 meters horizontal peak-to-peak difference. However, this is not a direct translation i.e. not part of the same oscillation. It also covers a time span of nearly 20 minutes. The criteria should therefore not be considered exceeded.

Acceptance criteria for landing:

The vertical oscillations are more than an order of magnitude faster than the horizontal oscillations. Landing the payload with the velocities measured here could damage it or the landing site. However, the results indicate that only four of the 32 wave conditions cause the maximum peak-to-peak motion

of the vertical oscillations to exceed the criteria (6 meters peak-to-peak). All others are smaller. There does not seem to be any problems with exceeding the criteria set for the acceleration either (7 m/s^2).

6.5.4 Remarks

Even in relatively harsh conditions the landing and landing accuracy seem to be mostly within acceptable limits based on the results. The winch is in this simulation mounted at the aft of the vessel, and the wave induced motions on this location will be smaller than for a crane tip. It is then possible that the motions of the payload are smaller than they would have been from a crane. Without results for such a case for comparison no conclusion can be drawn, however it may be interesting to study. If it was the case, this would be another advantage of the PIM. Since conventional installations are usually done by crane vessels, lowering with a deck-mounted winch can be a topic to study for conventional installation as well. Again, one will require two vessels as the payload will have to be submerged.

6.6 Risk

Only phase 2 separates the PIM from conventional installation. Since there is inadequate experience with the method, the probability of undesirable events can be said to increase. The issue is the limited (or lack of) understanding of the hydrodynamic behaviour of the payload in freefall. The threat is undesired rotational motions. Numerical simulations can assist predictions, however only 1:1 scale model testing can present reliable results. Add to this an element of randomness and it becomes difficult to be certain of the behaviour of the payload.

1:1 scale model testing is a comprehensive operation with significant costs. It is therefore impractical to repeat this to gain sufficient data on potential deviations. But if the test can be used to discover inaccuracies in the data models, the models can be adjusted. If the models can be made sufficiently reliable it will become possible to more accurately predict the hydrodynamic behaviour by for example Monte Carlo simulations. Addition of buoyancy elements on the deployment line and increased weight in the bottom of the payload is a measure to inhibit rotational motions, as is addition of “parachutes”, ballast tanks or similar equipment. Hence, if the stability of the payload can be assured, the PIM should not be considered to have a higher probability of failure than conventional installation.

The risk should be considered with regards to the parameters discussed in chapter 2.4:

Personnel: Only in phase 1 are personnel exposed (unless divers are used to release the payload). Therefore, using the PIM does not increase risk to personnel relative to conventional installation.

Environment: Failure during lowering of equipment has a very limited impact on the environment, since the equipment is not live. If the stability of the payload is ensured by the mentioned risk reducing measures, the risk is unchanged.

Assets and/or lost production: If the stability of the payload is ensured as mentioned above, the probability of failure is not higher for the PIM. However, if applying the PIM enables use of less technologically advanced vessels with lower day rates, then the reduced cost will reduce the effort of the installation in terms of cost. The lowering time may also be reduced. The risk could then then be considered smaller for the PIM, as the consequence to assets is lower.

Reputation: The consequence of a failure may be a damaged reputation, as it could be considered reckless to apply a method where there is little experience. On the other hand, a success may lead to positive consequences for the reputation, as it could be considered innovative and proactive to apply new methods.

6.7 Economics

It is difficult to do a proper discussion of the economic impact of applying the PIM, without doing an extensive market study of vessel day-rate and mobilisation costs. It is also not certain how much resources it will take if for example 1:1 scale model-testing is to be performed, and the method is likely to result in more engineering hours prior to the operation. A detailed study of this is beyond the scope of this thesis. Therefore, this discussion is hypothetical rather than fact based.

The question to be answered is mainly that of vessel costs. While the engineering phase should be longer due to lack of experience with the method, the potential impact of reduced vessel costs is likely to dwarf the cost of engineering hours. With reference to Figure 2-16: Deepwater subsea CAPEX, the design and project management is estimated to be 6% of the CAPEX, while installation is 33%.

And so, the answer to the question of vessel costs depend on the mobilisation cost and day-rates: If the PIM allows for use of for example a crane barge, an AHTS and an RSV, will the total cost of these be smaller than operating an HLV or an advanced OCV with the necessary, advanced FRDS or fibre rope cranes?

With reference to the prices listed in Table 2-4 in chapter 2.5 it is very possible that it is: 50,000\$ in day rates for an AHTS little compared to 430,000\$ for a semi-submersible lifting vessel. More likely the price of an advanced OCV would be smaller than for the semi-submersible, but as mentioned no conclusion can be drawn without a proper study.

Chapter 7

Conclusion

The purpose of this thesis was to evaluate the use of the pendulous installation method in water depths beyond what has been done today. In this thesis the depth of 4,000 meters was considered. The PIM has already been applied in a real installation scenario, and the feasibility has thus been proven. Therefore, the focus of this thesis was to study the effect of using this method instead of a conventional installation method in the said water depth. It should be noted that new crane technologies are being developed, and new fibre rope/steel wire-hybrids came on the market while the thesis was written. Nevertheless, there are certain aspects of the PIM that can be very beneficial when operating in ultradeep water. In short it can be concluded that the PIM is still relevant because it allows for use of vessels with less advanced equipment. But detailed and case-specific studies should always be done to determine whether it is suited for the specific operation. This chapter contains the conclusion of the thesis, as well as potential future work on the topic.

7.1 Conclusion

As mentioned, new technology has been introduced since the beginning of this thesis, allowing for application of conventional installation methods even in ultradeep waters beyond 3,000 meters. This has been made possible by improving the fibre rope deployment technology, and it is becoming possible to use subsea cranes to land increasingly heavy equipment in these water depths. Applying subsea cranes provides all the advantages of a rotating crane when it comes to manoeuvring the suspended payload. These special cranes are new and advanced, and not yet available in large numbers. Such specialized equipment will also potentially increase the cost of utilizing the vessel.

This is where the PIM may become relevant: it allows for lowering of heavy equipment to the seabed without any special rigging or specialized vessels. The PIM requires utilization of more than one vessel. However, the requirements of these are lower than for one vessel in conventional operations. It can in practice be done by a crane barge, a ROV support vessel and an anchor handling vessel. Therefore, it is possible that applying this method can reduce the cost of installation, if the alternatives are advanced, low-availability high-cost vessels. A proper study of the economics was not made in this thesis; There may also not be a universally true answer for the economical question, as it needs to be assessed from operation to operation.

One disadvantage of the PIM is the lack of experience with the method. Any application of the PIM would require comprehensive studies, preferably including model testing. In a scenario, however, where the PIM became a familiar method, it would be interesting to see if it could compete with conventional methods. The main issue to overcome is the stability of the payload during its descent. Several different measures have been suggested to improve this aspect of the operation. If these are

Conclusion

implemented properly, the overall risk in the operation should not be any higher than for conventional installation.

When it comes to the performance of the PIM, it appears to not be very sensitive to water depth. Because of the application of low density fibre ropes, the lift line tension is not higher in 4,000 meters than in 2,000 meters. Application of fibre ropes in conventional installation requires specialized fibre rope deployment systems, and this is not the case for the PIM. Therefore, no special rigging is required, and so the operation can be carried out by smaller vessels.

Conventional installation also appears to be slower when compared to the PIM. The descent of the payload is dictated by gravity, and the vertical velocity becomes higher than the hoist speed of a crane. It is noted that the model used in this thesis is a simplified one. But given the large time difference in favour of the PIM, it is at least an aspect of the method that can be worth studying further. The reduced time means that more time can be spent on positioning and landing the payload, without adding to the total time spent on the operation.

Furthermore, the results regarding the tension in the liftwire during the pendulum lowering did not exceed the highest value for the suspended payload in any of the simulated conditions. The increase of the tension is gradual when applying the PIM, and the highest values occurred as the payload was suspended from the vessel after reaching its target depth. The results for dynamic loading in the thesis might even be considered conservative, given the simplifications made to the model: If buoyancy elements are added to the deployment line as has been described, it is possible that much of the dynamic loading would be absorbed by the buoyancy-induced “wave” on the deployment line just above the payload. This is after all the case for the “steel lazy-wave riser”-configuration.

For conventional installation the full static load is held throughout the lowering. Since the lifting system will have a gradual increase in natural period during the descent, there is a higher possibility that the system will resonate with ocean waves at some water depths. The probability for resonance is reduced when applying the PIM, because the deployment line is at its full length from the start. It will therefore have a constant natural period.

The challenges in 4,000 meters water depth when it comes to the landing makes no difference whether the lowering is done conventionally or by use of the PIM. The motions in deep water are highly dependent on the environmental conditions, especially the significant wave height and currents. Simulations of different wave peak periods shows that this also impacts the payload motions, sometimes to a large degree, but less so than the significant wave height. A notable exception was the results for mean horizontal offset, where the wave peak period had a larger impact than expected. The current did however have a larger effect. An effective measure against a horizontal offset may be the alternative approach to the PIM, where both vessels stay connected to the payload during the lowering.

While slower, it grants the ability to manoeuvre the suspended payload by repositioning the second vessel.

The results obtained in this thesis indicates that for all but the very harsh wave conditions, the vertical and horizontal oscillations of the suspended payload are not unacceptably large. When considering the capabilities of active heave compensation systems, vertical oscillations can in many cases be negated. The horizontal oscillations can have large amplitudes, but they have a very low frequency that would allow for acceptable precision for landing of heavy equipment. For smaller equipment and high requirements to accuracy, more studies should be done.

As a conclusion, it can be said that based on the studies in this thesis the PIM is an exciting option to conventional installation in 4,000 meters water depth. The performance seems, for aspects such as the lowering velocity and the lower technological requirements for the installation vessels, to be better suited for ultradeep water than conventional installation. It may be more demanding in the planning phase but can simplify and increase the speed of the operations offshore. And hours onshore are less costly than offshore. All operations are of course different, and a general recommendation may not be possible to give even with improved modelling and in-depth studies. It is however possible that the pendulous installation method will become an interesting alternative to consider when the industry starts operating in water depths of 4,000 meters.

7.2 Future work

This thesis has been a general study of the pendulous installation method, and there are several options for further work that can be done on the topic.

Improved model:

By using a simplified model in this thesis, many aspects of the PIM could not be studied. The model can be improved, for example in the following ways:

- A point of interest that can be elaborated on is the responses of the deployment line, such as how it curves during the lowering or whether vortex-induced vibrations cause instability. By using a model that allows for different types of cross sections, buoyancy elements can also be added to the deployment line, and the results be more accurate. This can be achieved by using the DNV GL software RIFLEX combined with SIMO. This allows for a more detailed study of the deployment line.
- Second, the equipment models used in this thesis are simplified by using the slender element approximation. For accurate results, CFD analyses of the equipment should be performed to

Conclusion

establish more accurately the drag coefficients and added masses for each type of equipment.

It is also possible to use scale model testing to support the results of the CFD analyses.

Project study

This thesis gave a general overview, but the attempt was to put the emphasis on the technical aspects of the method. In a more project-centred study, evaluation of project costs, mobilisation time, comparisons of different methods and more can be considered. This will provide a more thorough picture when it comes to whether the PIM is beneficial to perform from an organisational point of view.

Case-specific study

The fact that this thesis attempted to provide a sensitivity study limited the modelling in terms of detail. This led to simplification of the equipment models, assumptions of environmental conditions and hypothetical scenarios for the suggestions regarding risk and economics. It would be interesting to see a case-specific study, where the PIM was considered as a potential alternative. This would require more information of cost, procedures and equipment, as well as environmental conditions and vessel availability.

References

- Aker Solutions. (n.a.). *What we deliver*. Retrieved March 20, 2018, from Aker Solutions: <https://akersolutions.com/what-we-do/products-and-services/tie-in-systems/>
- Aven, T. (2015). *Risk Analysis*. Singapore: Markono Print Media Pte Ltd.
- Bai, Y., & Bai, Q. (2012). *Subsea Engineering Handbook*. Oxford: Elsevier.
- Cerqueira, M., Roveri, F., Peclat, L. E., & Labanca, E. L. (2006). The Need for the Pendulous Installation Method. Hamburg: International Conference on Offshore Mechanics and Arctic Engineering.
- Costa, L. T., & de Lima, U. A. (2017). Installation of Manifolds- A Success Story. *OTC-27967-MS*. Rio de Janeiro: Offshore Technology Conference.
- Crout, R. (2008, September). Oil and Gas Platform Ocean Current Profile Data. National Oceanic and Atmospheric Administration.
- de Boer, T. B., Braadbaart, J., & Nieuwenkamp, J. O. (2013). SPE 166562. *Deep Sea Installation with Fibre Rope Technology - a New Concept in Winches for the Best Performance and Durability of Rope*. Aberdeen: Society of Petroleum Engineers.
- de Vries, J., van Drunen, J., van Dijk, R., & Zoontjes, R. (2011, May). OTC 21291. *Offshore Monitoring Campaign on Installation of Suction Piles in Deep Water Fields*. Houston: Offshore Technology Conference.
- Det Norske Veritas. (2003, January). DNV-RP-H101 Risk Management in marine- and subsea operations. Det Norske Veritas.
- Det Norske Veritas. (2009, April). Recommended Practice DNV-RP-H103 Modelling and Analysis of Marine Operations. Høvik, Norway: Det Norske Veritas.
- Det Norske Veritas. (2011, October). DNV-OS-H101 Marine Operations, General.
- Det Norske Veritas. (2011, October). Standard for Certification No. 2.22 - Lifting Appliances. Det Norske Veritas.
- Det Norske Veritas. (2014, April). DNV OS-H205 Lifting operations. Det Norske Veritas.
- Det Norske Veritas. (2014, April). DNV-RP-C205 Environmental Conditions and Environmental Loads. Det Norske Veritas.
- D'Souza, R. (2015, September 9). *Future deepwater developments bring challenges, opportunities*. Retrieved from Offshore: <http://www.offshore-mag.com/articles/print/volume-75/issue-9/deepwater-update/future-deepwater-developments-bring-challenges-opportunities.html>
- EIA. (2016, October 26). *Offshore oil production in deepwater and ultra-deepwater is increasing*. Retrieved September 16, 2017, from U.S. Energy Information Administration: <https://www.eia.gov/todayinenergy/detail.php?id=28552>
- EuroFibres. (n.a.). *Dyneema Fact Sheets*. Retrieved March 2018, from Issuu: <https://issuu.com/eurofibres/docs/name8f0d44>
- Felisita, A., Gudmestad, O. T., Karunakaran, D., & Martinsen, L. O. (2015). *Review of Steel Lazy Wave Riser Concepts for North Sea*. St. John's: International Conference on Ocean, Offshore and Arctic Engineering.

References

- Gudmestad, O. T. (2015). *Marine Technology and Operations Theory and Practice*. Southampton: WIT Press.
- Gudmestad, O. T., & Sarkar, A. (2010). OMAE2010-20489. *Splash zone analysis of subsea structures*. Shanghai: International Conference on Ocean, Offshore and Arctic Engineering.
- Heerema. (n.a.). *Thialf*. Retrieved February 15, 2017, from Heerema Marine Contractors: <https://hmc.heerema.com/fleet/thialf/>
- International Marine Contractors Association. (2013, May). Guidelines for installing ROV Systems on Vessels or Platforms. International Marine Contractors Association. Retrieved March 20, 2018, from http://www.oceanologyinternational.com/_novadocuments/412909?v=636459019564600000
- Jeans, G., Harrington-Missin, L., Herry, C., Prevosto, M., Maisondieu, C., & Lima, J. (2012, July). Deepwater Current Profile Data Sources for Riser Engineering Offshore Brazil. Rio de Janeiro: International Conference on Ocean, Offshore and Arctic Engineering.
- Jeong, C. K., Zhang, W., & Spreeken, A. (2013). Float-over Feasibility in Brazilian Sea Water. *OTC 24304*. Rio De Janeiro: Offshore Technology Conference.
- Kuppens, M. L., da Silva, J. L., Contarini, M. d., & Pinto, F. J. (2006). Roncador Field Subsea Manifold: a Risk Analysis Approach to Verify the New Installation Procedure. Hamburg: International Conference on Offshore Mechanics and Arctic Engineering.
- Li, L. (2017). Crane operations 2: Subsea lifting.
- Lian, W., & Sortland, B. (1996). *Manoeuvring of Bodies Suspended at Extreme Water Depths*. Los Angeles: International Society of Offshore and Polar Engineers.
- Liu Yong-Le, N. (2016, December 2). Cost efficient deep-water lowering with HMPE rope. Asia: Dyneema. Retrieved from Subsea UK.
- Lohr, C., & Smith, K. (2010). *Perdido Development Project - Spar & Moorings*. Houston: Offshore Technology Conference.
- Lohr, C., & Smith, K. (2010). *Perdido Development Project - Spar & Moorings*. Houston: Offshore Technology Conference.
- MacGregor. (2017). *AHC Cranes*. Retrieved May 29, 2018, from MacGregor: <https://www.macgregor.com/Products-solutions/products/offshore-and-subsea-load-handling/ahc-cranes/>
- Marintek. (2003, April 1). Deep-Water Marine Operations. *Review*. Sintef.
- Maritimt Magasin. (2016, September 20). *Normand Maximus*. Retrieved February 15, 2018, from Maritimt Magasin: <http://maritimt.com/nb/batomtaler/normand-maximus-092016>
- Maurício, J., Lima, T., Kuppens, M. L., da Silveira, P., & Stock, P. K. (2008). Development of Subsea Facilities in the Roncador Field (P-52). *OTC 19274* (p. 18). Houston: Petrobras.
- National Instruments. (2012, August). *Differences between Frequency Domain and Time Domain*. Retrieved from National Instruments: http://zone.ni.com/reference/en-XX/help/370051V-01/cvi/libref/analysisconcepts/differences_between_frequency_domain_and_time_domain/
- Oceaneering. (n.a.). *ROV Systems*. Retrieved March 20 2018, from Oceaneering: <https://www.oceaneering.com/rov-services/rov-systems/>

-
- Offshore Support Journal. (2018, Januar 3). *Manufacturers bringing advantages of fibre rope cranes to the market*. Retrieved March 1, 2018, from Offshore Support Journal: http://www.osjonline.com/news/view,manufacturers-bringing-advantages-of-fibre-rope-cranes-to-market_50330.htm
- OG21. (2015, April 24). OG21 TTA4 REPORT Subsea cost reduction. *Subsea cost reduction*. Norges teknologistrategi for petroleumssektoren.
- Orcina. (n.d.). *Vessel Theory: RAO and Phases*. Retrieved November 15, 2017, from Orcina: <https://www.orcina.com/SoftwareProducts/OrcaFlex/Documentation/Help/Content/html/VesselTheory,RAOsandPhases.htm>
- Orcina. (n.d.). *Vessel Theory: RAO and Phases*. Retrieved November 15, 2017, from Orcina: <https://www.orcina.com/SoftwareProducts/OrcaFlex/Documentation/Help/Content/html/VesselTheory,RAOsandPhases.htm>
- Prasanna, D. (2014, May 8). *The Ship's motion at sea*. Retrieved June 4, 2018, from Hubpages: <https://hubpages.com/travel/theshipmotionsatsea>
- Rexroth. (n.a.). *150 TON ACTIVE HEAVE COMPENSATION ABOARD DIVING SUPPORT VESSEL*. Retrieved June 6, 2018, from Bosch Group: https://dc-corp.resource.bosch.com/media/general_use/industries_2/machinery_applications_and_engineering/offshore/downloads/Heave_Compensation_Success_Story_SBM.pdf
- Rexroth. (n.d.). 150 Ton active heave compensation system aboard diving support vessel. Rexroth. Retrieved October 30, 2017, from https://dc-corp.resource.bosch.com/media/general_use/industries_2/machinery_applications_and_engineering/offshore/downloads/Heave_Compensation_Success_Story_SBM.pdf
- Ribeiro, M. L., Segura, M. V., & Ferreira, J. A. (2006). *Subsea Manifold Design For Pendulous Installation Method in Ultra Deep Water*. Hamburg: International Conference on Offshore Mechanics and Arctic Engineering.
- Roll Royce. (n.a.). *Subsea cranes*. Retrieved June 6, 2018, from Rolls Royce: https://www.rolls-royce.com/~media/Files/R/Rolls-Royce/documents/marine-product-finder/factsheets-cranes/17Cranes_2p-100817-1.pdf
- Roveri, F. E., & Vardaro, E. (2006). *Numerical Analyses and Sensitivity Studies for Development of the Pendulous Method*. Hamburg: International Conference for Offshore Mechanics and Arctic Engineering.
- SIMO Project team. (n.a.). *SIMO Modelling Tutorial*. SIMO Project team.
- Solstad Farstad ASA. (2017). *Normand Maximus*. Retrieved March 12, 2018, from Solstad Farstad: <https://www.solstadfarstad.com/fleet/ocvcsv-vessels/normand-maximus>
- Sonardyne Inc. (2016, September). *Ranger 2 USBL Underwater Tracking and Positioning*. Sonardyne Inc.
- Stock, P. F., Ferreira, J. A., da Silva, J. L., & Machado, R. D. (2006). *Pendulous Installation Method Report of the Full Scale Offshore Test*. Hamburg: International Conference of Offshore Mechanics and Arctic Engineering.
- Subsea World News. (2014, October 28). *Aker Wayfarer to Get Rolls-Royce Handling System*. Retrieved March 1, 2018, from Subsea World News: <https://subseaworldnews.com/2014/10/28/aker-wayfarer-to-get-rolls-royce-handling-system/>
-

References

- Sundberg, J. D. (2018, April 4). Offshoreskiprate har doblet seg på én dag - tidoblet på to uker. E24. Retrieved April 4, 2018, from <https://e24.no/boers-og-finans/dof/offshoreskiprate-har-doblet-seg-paa-en-dag-tidoblet-paa-to-uker/24301748>
- The Sea Musketeers. (2016, April 23). *Aliens of the deep*. Retrieved March 14, 2018, from The Sea Musketeers: <https://www.seamusketeeer.com/single-post/2016/04/23/Aliens-of-the-deep-microbes-flourish-beneath-the-ocean-floor>
- Torben, S. R., Ingeberg, P., Bunes, Ø., Bull, S., & Paterson, J. (2007). OTC 18932. *Fibre Rope Deployment System For Ultradeepwater Installations*. Houston: Offshore Technology Conference.
- Torben, S., & Ingeberg, P. (2011, May). Field Pilot of Subsea Equipment Installation in Deep Water using Fibre Rope in Two-fall Arrangement. Houston, Texas, USA: Ofshore Technology Conference.
- Vladtime. (2015). Retrieved March 14, 2018, from Vladtime: <http://www.vladtime.ru/nauka/458323-uchenye-vody-okeanov-stremitelno-zaselyayut-tainstvennye-formy-zhizni.html>
- Wang, A. M., Zhu, S., Zhu, X., Xu, J., He, M., & Zhang, C. (2013). *Pendulous Installation Method and its Installation Analysis for a Deepwater Manifold*. Anchorage: International Society of Offshore and Polar Engineers.
- Wang, A., Yang, Y., Zhu, S., Li, H., Xu, J., & He, M. (2012, June). Latest Progress in Deepwater Installation Technologies. Tanggu, Tianjin, China: International Society of Offshore and Polar Engineers.

Appendix

Appendix A) Specification sheets



Fact sheet

Ultra High Molecular Weight Polyethylene fiber from DSM Dyneema

UHMWPE fiber combines excellent mechanical properties with low density, resulting in high performance-on-weight basis.

The UHMWPE fiber from DSM Dyneema is a gel-spun, multi-filament fiber produced from ultra high molecular weight polyethylene, with main characteristics: high strength, low weight, low elongation at break, and resistance to most chemicals. To stimulate developments, this sheet provides an overview of properties measured on UHMWPE fibers from DSM Dyneema. The disclosed data is not valid for any other source of UHMWPE fibers.

Fiber range.

UHMWPE fibers from DSM Dyneema are produced in three strength ranges and several linear densities with a characteristic very low filament diameter. The tensile properties are correlated with the fiber linear density. Detailed information per fiber type is available on request, as Product Data Sheets, Product Specification Sheets, Material Safety Data Sheets and Fact Sheets.

UHMWPE Fiber type	Tensile strength			Tensile modulus			Elongation to break %
	N/tex	g/den	GPa	N/tex	g/den	GPa	
SK78 SK75	3.4 – 4.0	38 – 45	3.3 – 3.9	112 – 137	1267 – 1552	109 – 132	3-4
SK65 SK62 SK60	2.5 – 3.4	28 – 38	2.4 – 3.3	67 – 102	759 – 1158	65 – 100	
SK25	2.2	25	2.2	54	608	52	

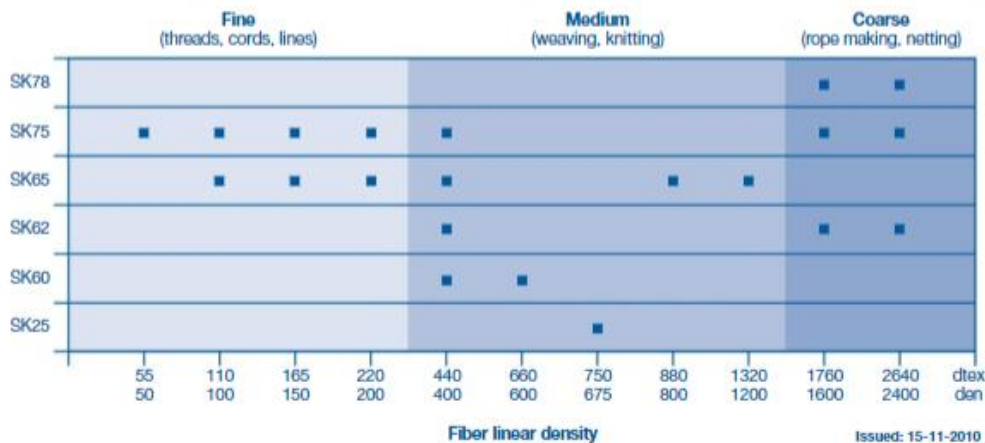


Figure A-1: Dyneema fibre rope specification excerpt (EuroFibres, n.a.)

Specification sheets

SWL	50t
Operating depth	3000 m
Min outreach	3 m
Max outreach	20 m
AHC capacity (Peak to peak)	6 m at 8 s (50t, all depths)
Heavy lift capacity (double fall)	100t at 1500 m
Tugger winch capacity	3t
Slewing	360 degrees continuous
Peak power consumption	950 kW
Certification	DNVGL, others upon request

Approximate values, provided for information only. Specifications may vary for given applications.

Figure A-2: Rolls Royce subsea crane specification excerpt (Roll Royce, n.a.)

150 TON ACTIVE HEAVE COMPENSATION SYSTEM ABOARD DIVING SUPPORT VESSEL

SBM uses special vessels to position valuable and sensitive equipment on the seabed at depths down to 3,000 metres. The use of a 150 ton active heave compensation system from Bosch Rexroth enables SBM to carry out this work in a most reliable, efficient and safe manner.

To perform work at depths greater than 3,000 m below sea level, the ships used by SBM are equipped with many advanced systems and technologies. One of these is the active heave compensation system. This system, which compensates for heave caused by ocean swell, allows sensitive equipment or other loads to be placed on the seabed – gently, and under full control. At the same time, it protects the hoisting cable from potential breakage due to internal resonance caused by wave movement.

Linear heave compensation

SBM's active heave compensation system operates continuously based on measurements made by the Motion Reference Unit, or MRU. These measurements describe the vertical movements of the

ship, and thereby the motion that needs to be compensated for. An advanced and extremely fast controller processes this data and uses this to govern the hydraulic system which controls the hydraulic cylinder. The cylinder is extended or retracted to shorten or lengthen the cable which is reeled over the cylinder, such that the load is suspended motionless in relation to the seabed.

Combined hydraulics and air

Mounted below deck, the system can achieve a compensating capacity of at least 90%. What makes this solution unusual is the specially-designed compensation cylinder, which combines both a pneumatic and hydraulic cylinder. The pneumatic compartment bears and compensates for the static load, while the

Tough application

Active heave compensation for vessel movements of ± 3 m.

Ingenious solution

The development, assembly, testing and commissioning of an active heave compensation system that uses hydraulics to compensate for dynamic aspects and air to compensate for the static load.



Exactly

Based on MRU measurements, the system achieves a compensating capacity of no less than 90% of the load movement at the overboard point.

The Drive & Control Company



hydraulic compartment provides the forces to compensate for friction losses, inertia and other dynamic effects. Thanks to this unique combination, the required hydraulic capacity is only a fraction of the theoretical peak capacity that would be required from the winch if there were no heave compensation installed. This has resulted in considerable energy savings.

To ensure reliable operation under harsh conditions at sea, the hydraulic

From design to commissioning

Bosch Rexroth developed the entire system for SBM, also providing the required system components, which were virtually all manufactured in-house. These include the drive section including the hydraulic power unit and the hydraulic cylinder, the air supply unit, plus the control section with software, control cabinets and operator panels. Bosch Rexroth also performed the commissioning. The

Solved with

- ▶ Accumulator for energy storage and recovery.
- ▶ Wave amplitude: ± 3 m.
- ▶ Mean wave periodicity: 10 s.
- ▶ Depth: 3,000 m.
- ▶ Lorem Maximum acceleration: 7m/s².

Figure A-3: Rexroth AHC specs excerpt (Rexroth, n.a)

TRACK EVERYTHING, IN ANY DEPTH, FROM ANY VESSEL.

TRACK A TOWFISH, POSITION AN ROV, DP YOUR VESSEL, SEARCH THE SEABED OR NAVIGATE AN AUV. WHEN YOU NEED TO INVEST IN ULTRA-SHORT BASELINE (USBL) ACOUSTIC TECHNOLOGY TO SUPPORT YOUR UNDERWATER OPERATIONS, RANGER 2 HAS THE PERFORMANCE YOU NEED, AT THE INVESTMENT LEVEL YOU CAN AFFORD TO GET THE PROJECT COMPLETED FASTER AND MORE EFFICIENTLY THAN ANY OTHER SYSTEM ON THE MARKET.

ENGINEERED LIKE NO OTHER

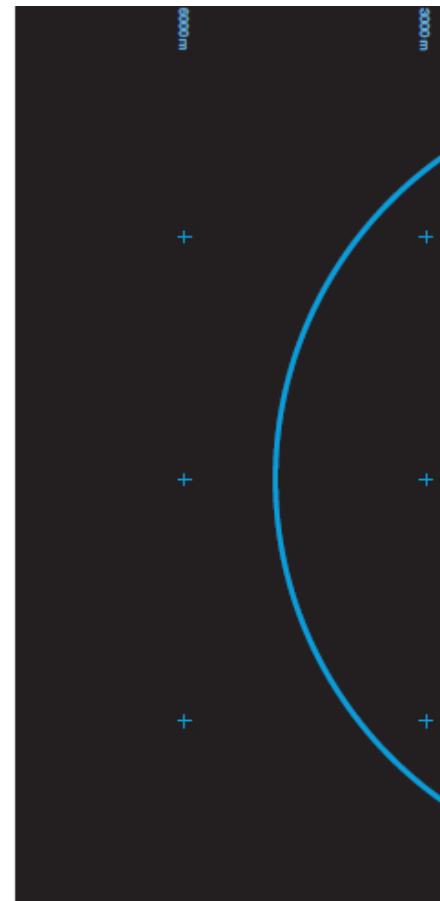
All USBL systems calculate position by measuring the range and bearing from a vessel-mounted transceiver to an acoustic transponder fitted to a moving target or placed on the seabed. But not all USBL systems do it with the accuracy and precision offered by Ranger 2.

We've taken everything that made our original Ranger system so effective and advanced it to the next level. That next level is our award-winning 6G (sixth generation) acoustic hardware platform and Sonardyne Wideband®2 digital signal architecture which work seamlessly together to deliver the best possible USBL positioning performance and operator experience.

Vessel and vehicle hardware is easy to install and configure. It can track your equipment to beyond 7,000 metres and update its position every second. It's engineered for shallow water, deep water, high elevation and multi-user operating scenarios. And if your vessel's fitted with a DP system – regardless of what make it is – Ranger 2 can interface with it.

THE ONLY USBL YOU'LL NEED

Every survey, ocean science, DP and seismic exploration project is different; different water depths, different vessels and different targets to position. But that shouldn't mean you need a different USBL system for each one.



WHY IT'S GOOD FOR YOUR OPERATIONS

- Simple, intuitive software
- Tracks an unlimited number of targets; ROVs, towfish, AUVs...
- Operating range beyond 7,000 metres
- Better than 0.1% system accuracy when optimised
- Up to 1 second position updates
- Compatible with all makes of DP system
- Automated setup reduces vessel delays
- Application packs available bringing extra features specific to your operations
- User training available worldwide
- Multi-user capable
- Track record of success on all types of vessel

Figure A-4: Sonardyne acoustic tracking (Sonardyne Inc, 2016).

Appendix B) Simulation inputs

B.1 Simulation cases

Table B-1: Simulation current cases phase 3

Phase 3		280T-manifold		
Current profile:	Hs [m]	Tp [s]	Direction [°]	
Slow current profile	2	8	0	
Medium current profile	2	8	0	
Fast current profile	2	8	0	

Table B-2: Simulation equipment types phase 2

Phase 2			
Equipment type	Hs [m]	Tp [s]	Direction [°]
THS	2	8	0
XT	2	8	0
150T-manifold	2	8	0
280T-manifold	2	8	0

Table B-3: Simulation current direction phase 2

Phase 2		280T-manifold		
Current direction [°]	Hs [m]	Tp [s]	Direction [°]	
0	2	8	0	
90	2	8	0	
180	2	8	0	

Simulation inputs

Table B-4: Simulation wave cases phase 2

Phase 2		280 T Manifold			XT		
Condition	Hs [m]	Tp [s]	Direction [°]	Hs [m]	Tp [s]	Direction [°]	
1	1.00	5.00	0.00	1.00	5.00	0.00	
2	1.00	6.00	0.00	1.00	6.00	0.00	
3	1.00	7.00	0.00	1.00	7.00	0.00	
4	1.00	8.00	0.00	1.00	8.00	0.00	
5	1.00	9.00	0.00	1.00	9.00	0.00	
6	1.00	10.00	0.00	1.00	10.00	0.00	
7	1.00	11.00	0.00	1.00	11.00	0.00	
8	1.00	12.00	0.00	1.00	12.00	0.00	
9	2.00	5.00	0.00	2.00	5.00	0.00	
10	2.00	6.00	0.00	2.00	6.00	0.00	
11	2.00	7.00	0.00	2.00	7.00	0.00	
12	2.00	8.00	0.00	2.00	8.00	0.00	
13	2.00	9.00	0.00	2.00	9.00	0.00	
14	2.00	10.00	0.00	2.00	10.00	0.00	
15	2.00	11.00	0.00	2.00	11.00	0.00	
16	2.00	12.00	0.00	2.00	12.00	0.00	
17	3.00	5.00	0.00	3.00	5.00	0.00	
18	3.00	6.00	0.00	3.00	6.00	0.00	
19	3.00	7.00	0.00	3.00	7.00	0.00	
20	3.00	8.00	0.00	3.00	8.00	0.00	
21	3.00	9.00	0.00	3.00	9.00	0.00	
22	3.00	10.00	0.00	3.00	10.00	0.00	
23	3.00	11.00	0.00	3.00	11.00	0.00	
24	3.00	12.00	0.00	3.00	12.00	0.00	
25	2.00	8.00	0.00	2.00	8.00	0.00	
26	2.00	8.00	45.00	2.00	8.00	45.00	
27	2.00	8.00	90.00	2.00	8.00	90.00	
28	2.00	8.00	135.00	2.00	8.00	135.00	
29	2.00	8.00	180.00	2.00	8.00	180.00	
30	2.00	8.00	225.00	2.00	8.00	225.00	
31	2.00	8.00	270.00	2.00	8.00	270.00	
32	2.00	8.00	315.00	2.00	8.00	315.00	

Table B-5: Simulation wave cases phase 3

Phase 3		280 T Manifold			XT		
Condition	Hs [m]	Tp [s]	Direction [°]	Hs [m]	Tp [s]	Direction [°]	
1	1.00	5.00	0.00	1.00	5.00	0.00	
2	1.00	6.00	0.00	1.00	6.00	0.00	
3	1.00	7.00	0.00	1.00	7.00	0.00	
4	1.00	8.00	0.00	1.00	8.00	0.00	
5	1.00	9.00	0.00	1.00	9.00	0.00	
6	1.00	10.00	0.00	1.00	10.00	0.00	
7	1.00	11.00	0.00	1.00	11.00	0.00	
8	1.00	12.00	0.00	1.00	12.00	0.00	
9	2.00	5.00	0.00	2.00	5.00	0.00	
10	2.00	6.00	0.00	2.00	6.00	0.00	
11	2.00	7.00	0.00	2.00	7.00	0.00	
12	2.00	8.00	0.00	2.00	8.00	0.00	
13	2.00	9.00	0.00	2.00	9.00	0.00	
14	2.00	10.00	0.00	2.00	10.00	0.00	
15	2.00	11.00	0.00	2.00	11.00	0.00	
16	2.00	12.00	0.00	2.00	12.00	0.00	
17	3.00	5.00	0.00	3.00	5.00	0.00	
18	3.00	6.00	0.00	3.00	6.00	0.00	
19	3.00	7.00	0.00	3.00	7.00	0.00	
20	3.00	8.00	0.00	3.00	8.00	0.00	
21	3.00	9.00	0.00	3.00	9.00	0.00	
22	3.00	10.00	0.00	3.00	10.00	0.00	
23	3.00	11.00	0.00	3.00	11.00	0.00	
24	3.00	12.00	0.00	3.00	12.00	0.00	
25	2.00	8.00	0.00	2.00	8.00	0.00	
26	2.00	8.00	45.00	2.00	8.00	45.00	
27	2.00	8.00	90.00	2.00	8.00	90.00	
28	2.00	8.00	135.00	2.00	8.00	135.00	
29	2.00	8.00	180.00	2.00	8.00	180.00	
30	2.00	8.00	225.00	2.00	8.00	225.00	
31	2.00	8.00	270.00	2.00	8.00	270.00	
32	2.00	8.00	315.00	2.00	8.00	315.00	

B.2 Vessel RAO

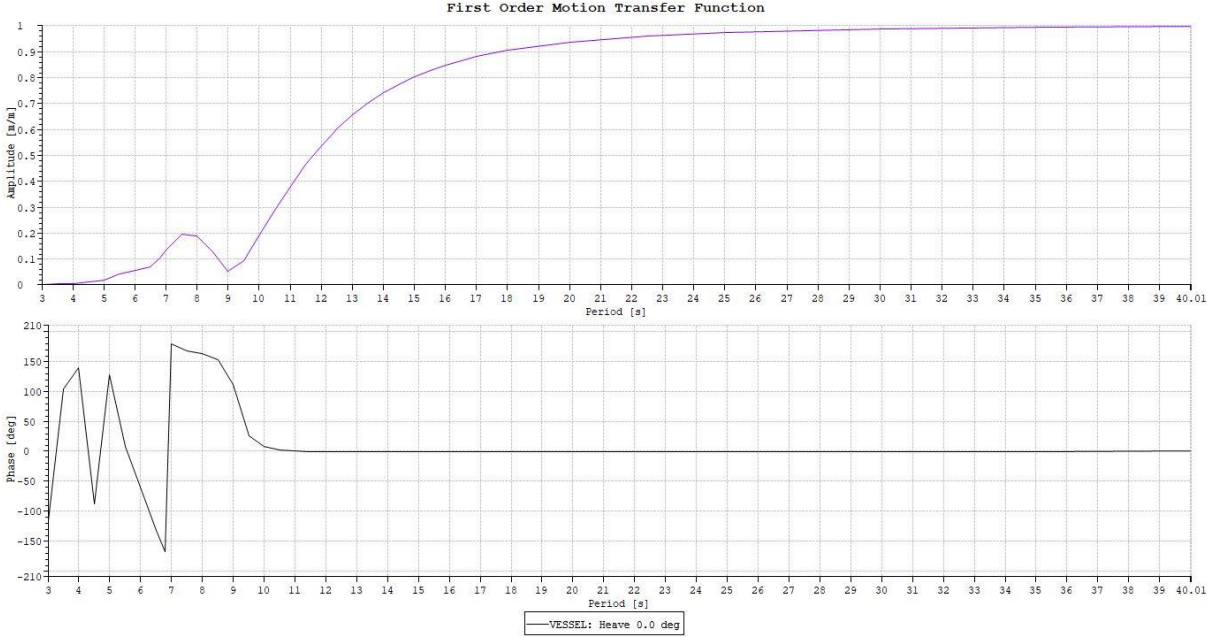


Figure B-1: Heave 0.0 degrees

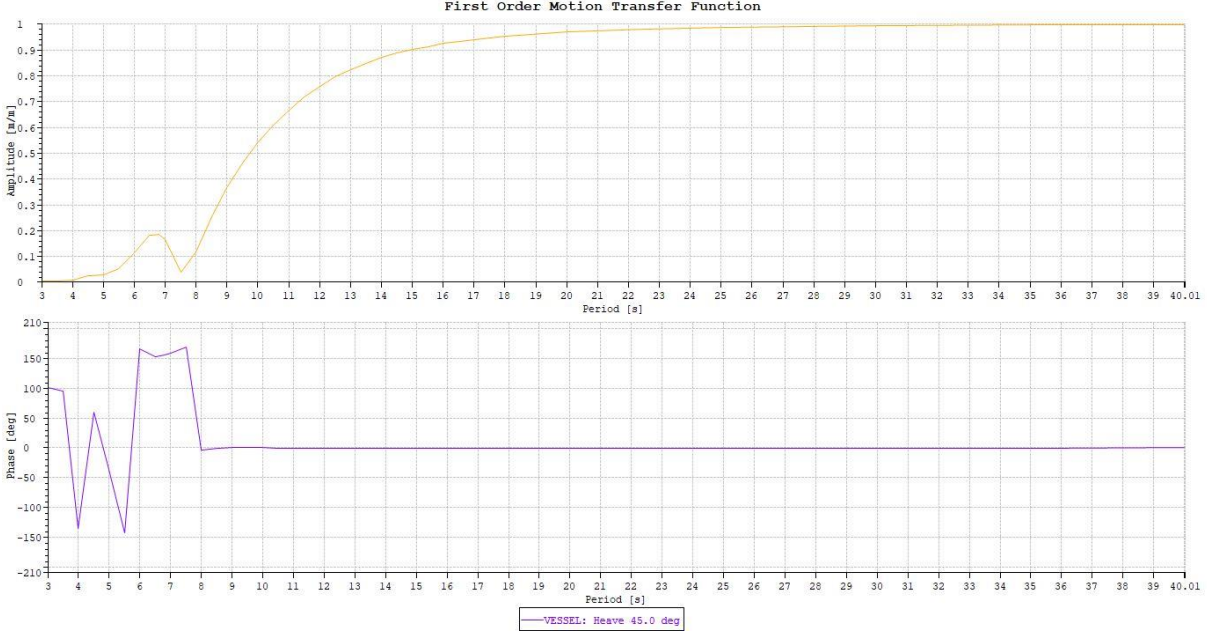


Figure B-2: Heave 45 degrees

First Order Motion Transfer Function on VESSEL in Test

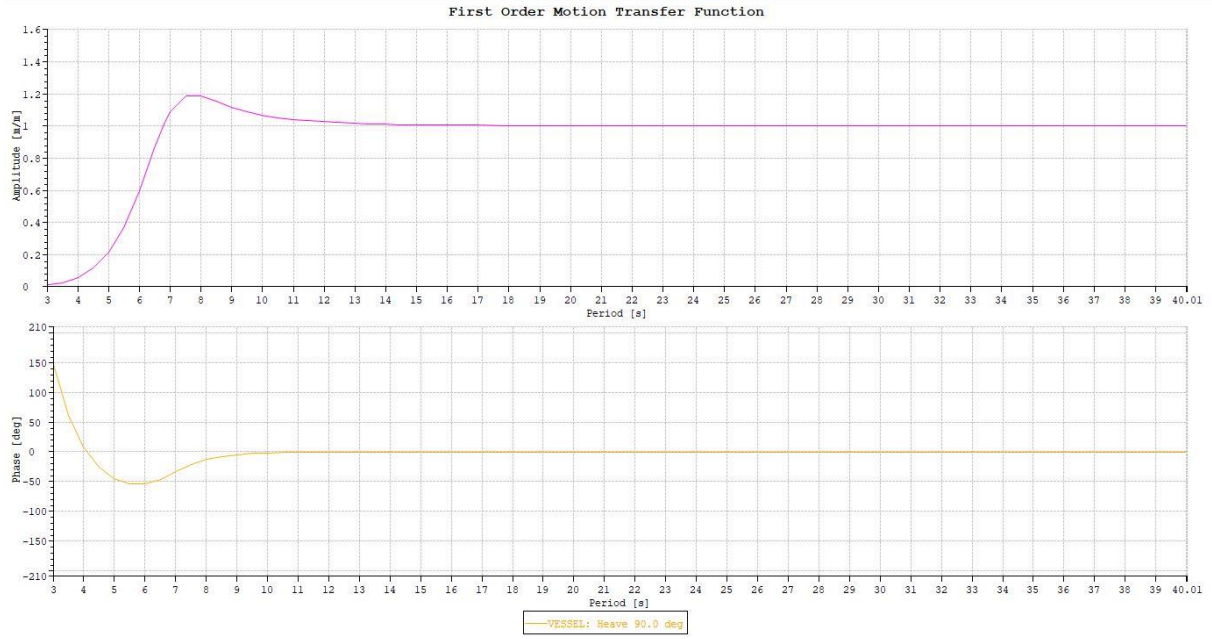


Figure B-3: Heave 90 degrees

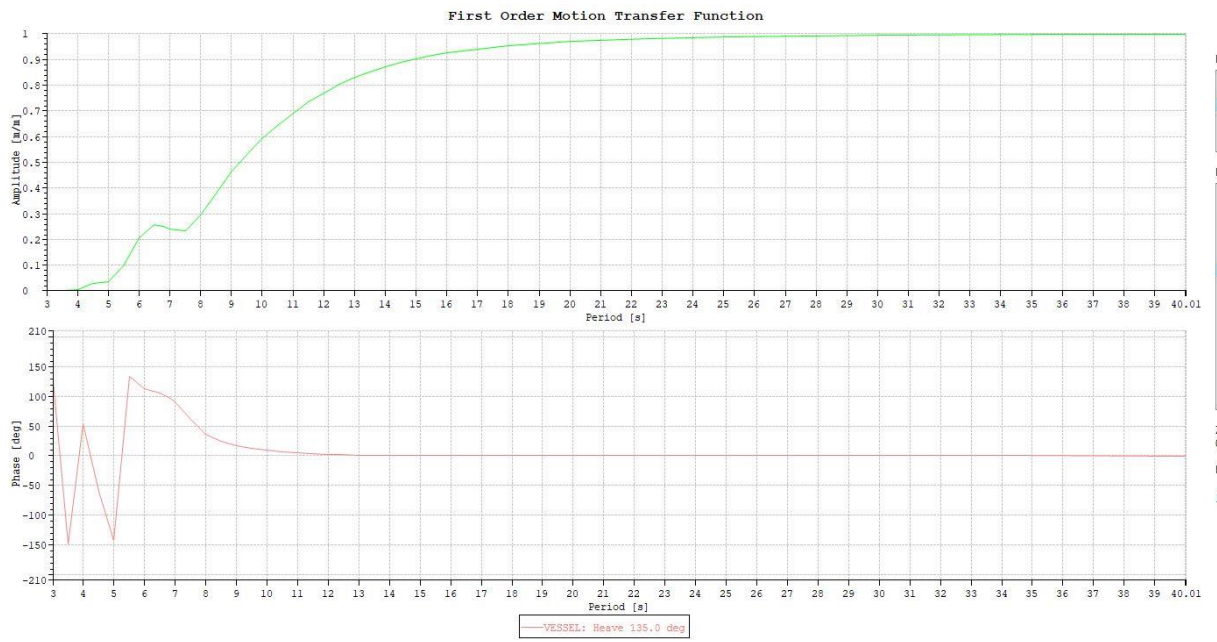


Figure B-4: Heave 135 degrees

Simulation inputs

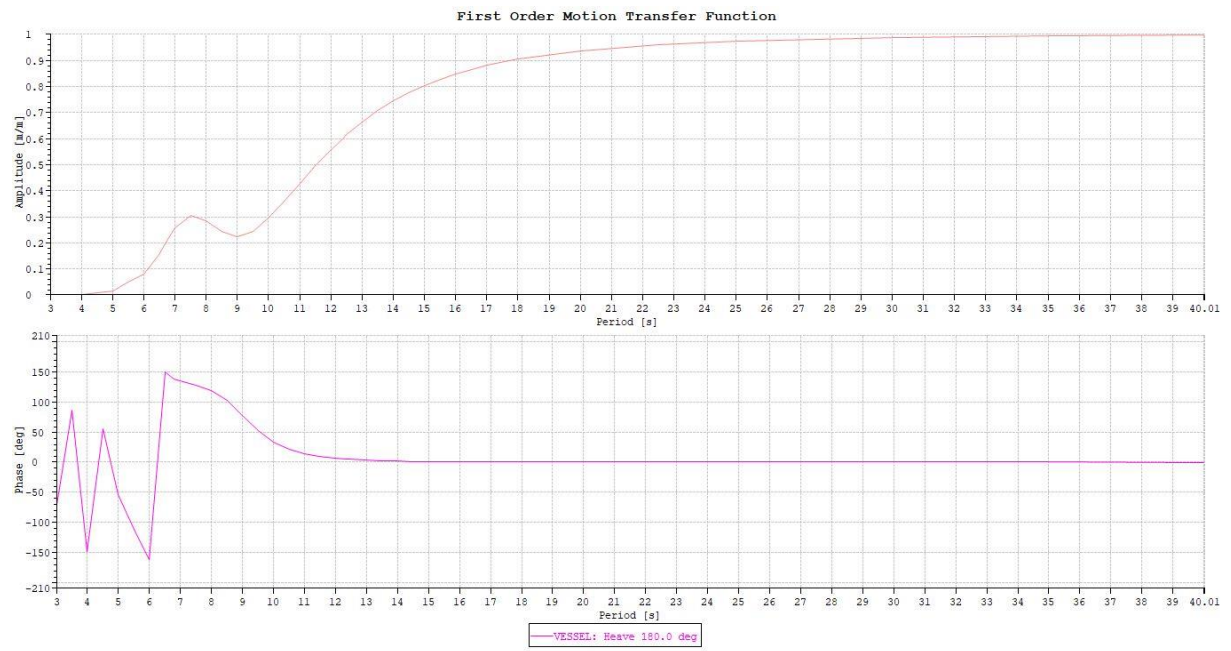


Figure B-5: Heave 180 degrees

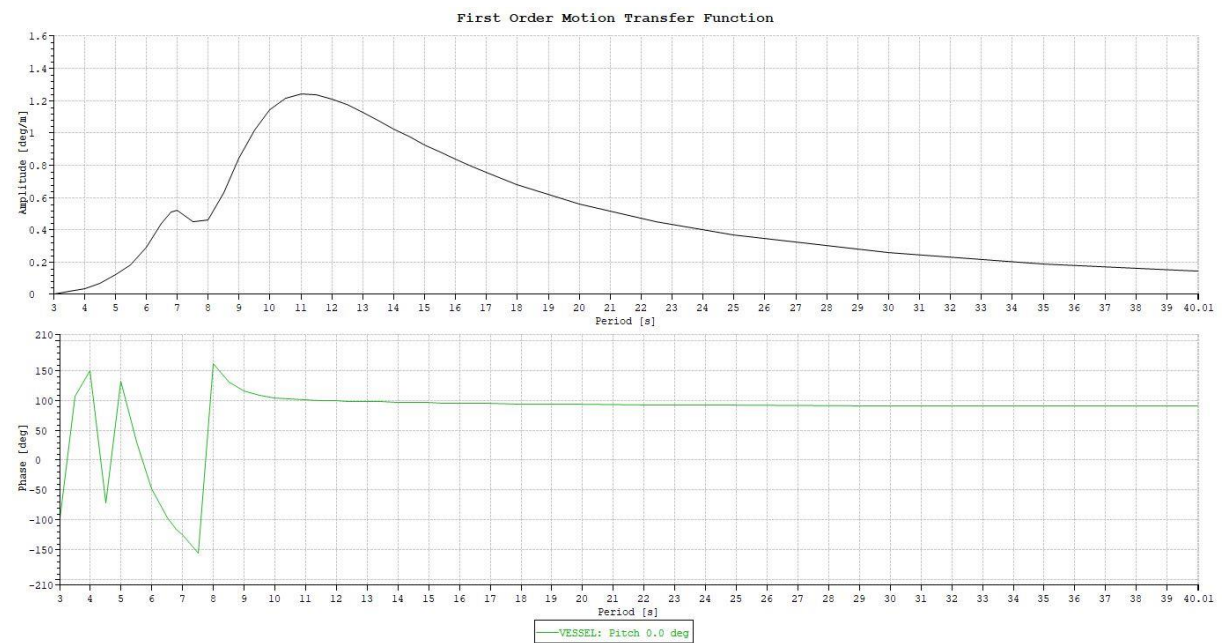


Figure B-6: Pitch 0 degrees

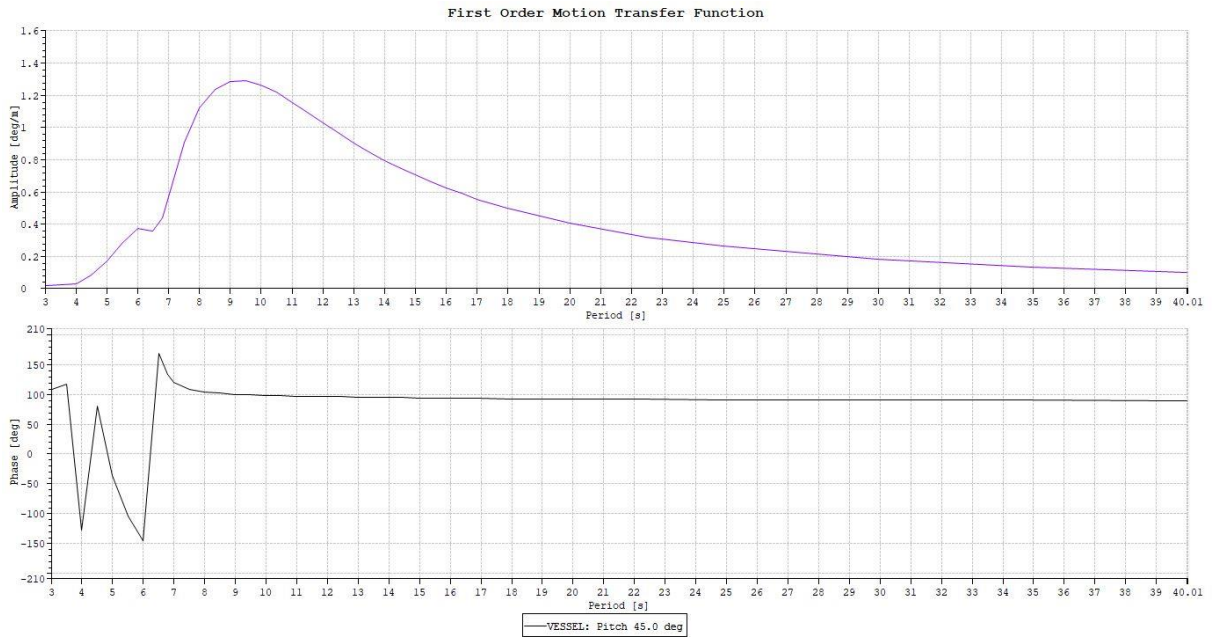


Figure B-7: Pitch 45 degrees

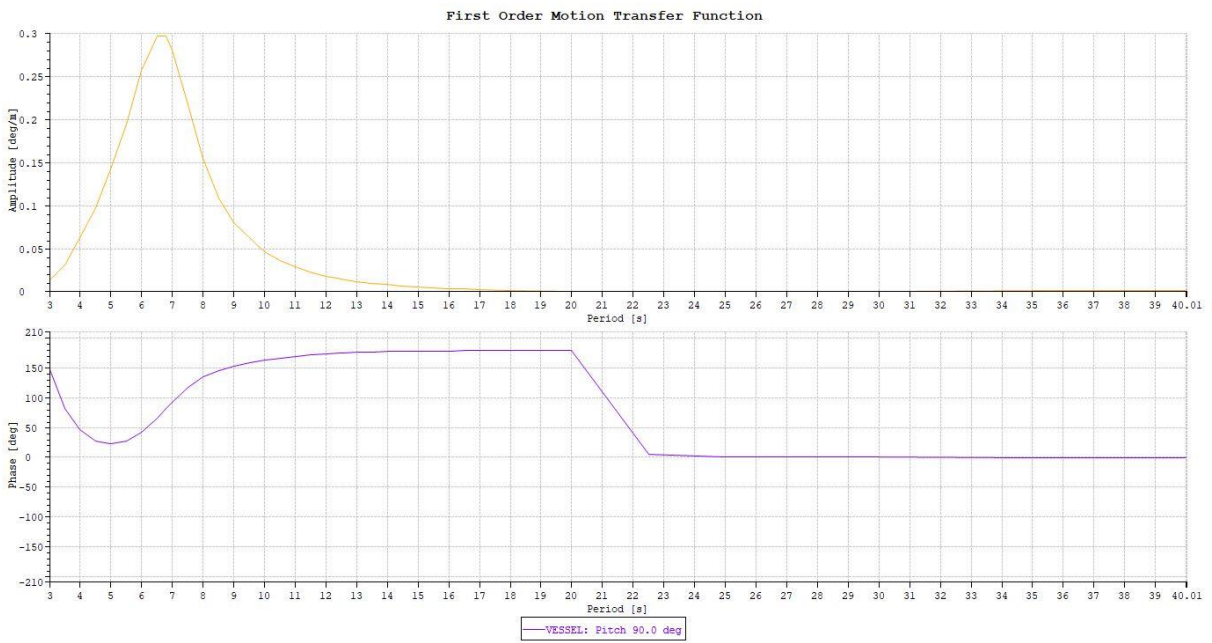


Figure B-8: Pitch 90 degrees

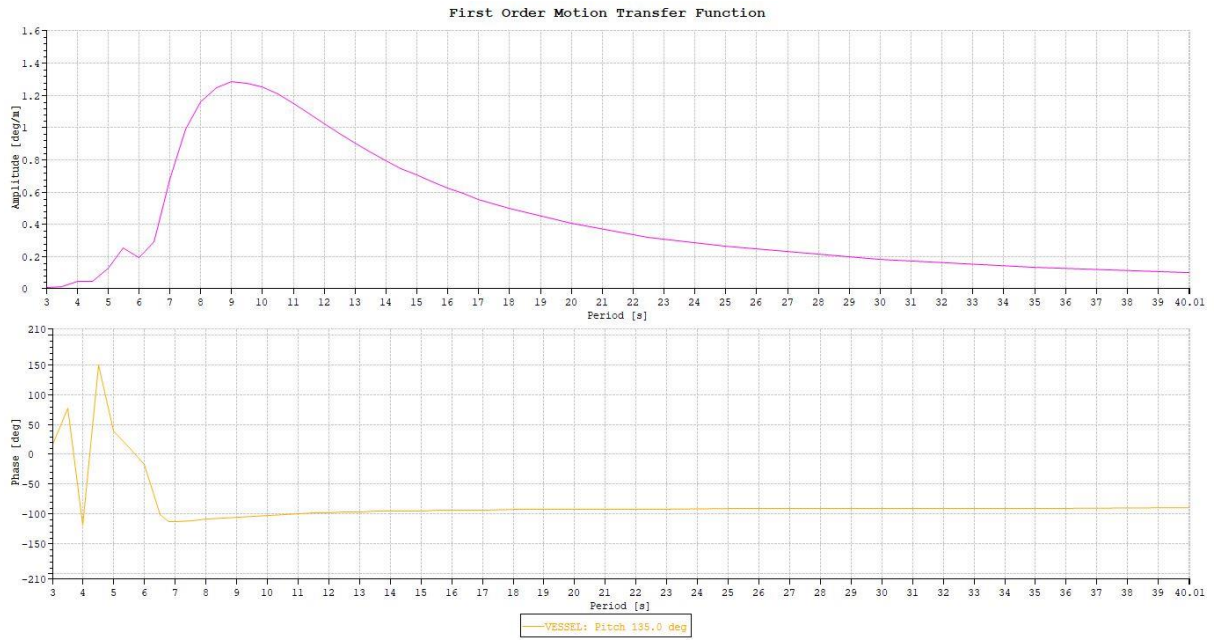


Figure B-9: Pitch 135 degrees

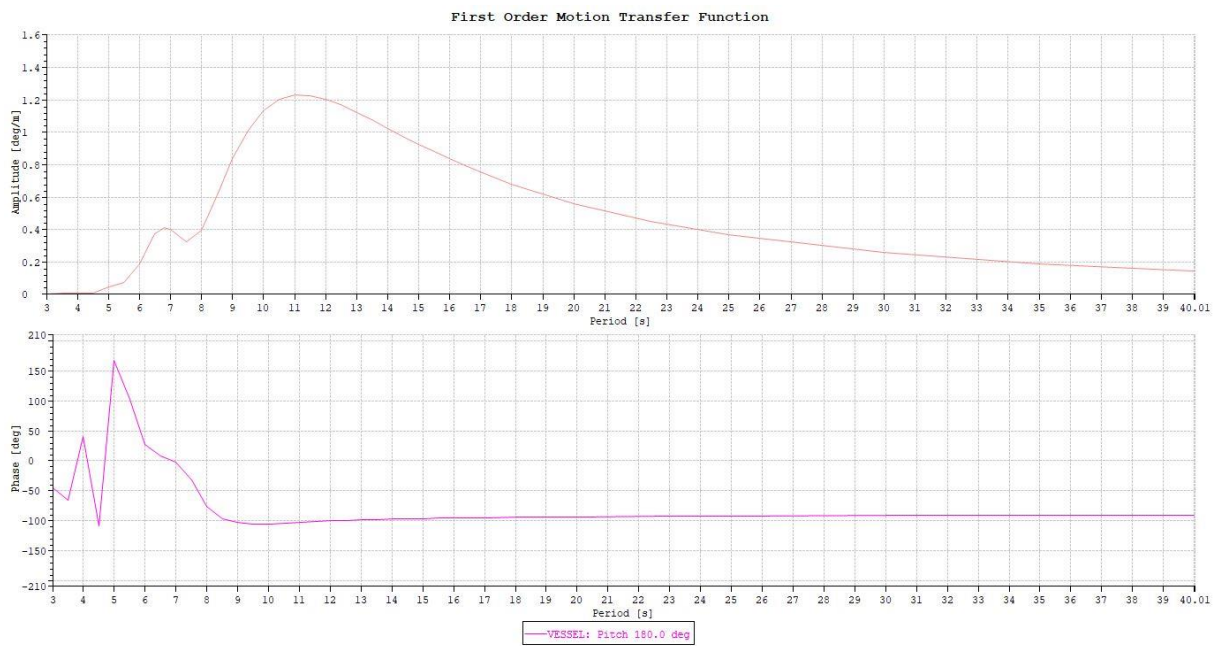


Figure B-10: Pitch 180 degrees

B.3 Payload properties

Table B-6: 280T-payload element properties

Name	Body	X-End1 [m]	Y-End1 [m]	Z-End1 [m]	X-End2 [m]	Y-End2 [m]	Z-End2 [m]	Specified Volume	Distributed Mass	Strips	xref	yref	zref	C2x	C2y	C2z	Amx	Amy	Amz
Bm1	Payload	-8	-4	0	-8	-4	2.5	0.07	230	10	0	0	0	0	99.94	99.94	0	72.45	72.45
Bm2	Payload	-4	-4	0	-4	-4	2.5	0.07	230	10	0	0	0	0	99.94	99.94	0	72.45	72.45
Bm3	Payload	0	-4	0	0	-4	2.5	0.07	230	10	0	0	0	0	99.94	99.94	0	72.45	72.45
Bm4	Payload	4	-4	0	4	-4	2.5	0.07	230	10	0	0	0	0	99.94	99.94	0	72.45	72.45
Bm5	Payload	8	-4	0	8	-4	2.5	0.07	230	10	0	0	0	0	99.94	99.94	0	72.45	72.45
Bm6	Payload	-8	0	0	-8	0	2.5	0.07	230	10	0	0	0	0	99.94	99.94	0	72.45	72.45
Bm7	Payload	-8	4	0	-8	4	2.5	0.07	230	10	0	0	0	0	99.94	99.94	0	72.45	72.45
Bm8	Payload	-4	0	0	-4	0	2.5	0.07	230	10	0	0	0	0	99.94	99.94	0	72.45	72.45
Bm9	Payload	-4	4	0	-4	4	2.5	0.07	230	10	0	0	0	0	99.94	99.94	0	72.45	72.45
Bm10	Payload	0	0	0	0	0	2.5	0.07	230	10	1	0	0	0	99.94	99.94	0	72.45	72.45
Bm11	Payload	0	4	0	0	4	2.5	0.07	230	10	0	0	0	0	99.94	99.94	0	72.45	72.45
Bm12	Payload	4	0	0	4	0	2.5	0.07	230	10	0	0	0	0	99.94	99.94	0	72.45	72.45
Bm13	Payload	4	4	0	4	4	2.5	0.07	230	10	0	0	0	0	99.94	99.94	0	72.45	72.45
Bm14	Payload	8	0	0	8	0	2.5	0.07	230	10	0	0	0	0	99.94	99.94	0	72.45	72.45
Bm15	Payload	8	4	0	8	4	2.5	0.07	230	10	0	0	0	0	99.94	99.94	0	72.45	72.45
Bm16	Payload	-8	-4	0	8	-4	0	0.07	230	10	0	0	0	0	99.94	99.94	0	72.45	72.45
Bm17	Payload	-8	0	0	8	0	0	0.07	230	10	1	1	0	0	99.94	99.94	0	72.45	72.45
Bm18	Payload	-8	4	0	8	4	0	0.07	230	10	0	0	0	0	99.94	99.94	0	72.45	72.45
Bm19	Payload	-8	4	0	-8	-4	0	0.07	230	10	0	0	0	0	99.94	99.94	0	72.45	72.45
Bm20	Payload	-4	4	0	-4	-4	0	0.07	230	10	0	0	0	0	99.94	99.94	0	72.45	72.45
Bm21	Payload	0	4	0	0	-4	0	0.07	230	10	1	0	0	0	99.94	99.94	0	72.45	72.45
Bm22	Payload	4	4	0	4	-4	0	0.07	230	10	0	0	0	0	99.94	99.94	0	72.45	72.45
Bm23	Payload	8	4	0	8	-4	0	0.07	230	10	0	0	0	0	99.94	99.94	0	72.45	72.45
Mudmat1	Payload	-8	0	0.25	8	0	0.25	0.2	900	10	0	0	0	0	166.56	166.56	0	201.26	201.26
Mudmat2	Payload	-8	1	0.25	8	1	0.25	0.2	900	10	0	0	0	0	166.56	166.56	0	201.26	201.26
Mudmat3	Payload	-8	2	0.25	8	2	0.25	0.2	900	10	0	0	0	0	166.56	166.56	0	201.26	201.26
Mudmat4	Payload	-8	3	0.25	8	3	0.25	0.2	900	10	0	0	0	0	166.56	166.56	0	201.26	201.26
Bm24	Payload	-8	4	0.25	8	4	0.25	0.07	230	10	0	0	0	0	99.94	99.94	0	72.45	72.45
Mudmat5	Payload	-8	-1	0.25	8	-1	0.25	0.2	900	10	0	0	0	0	166.56	166.56	0	201.26	201.26
Mudmat6	Payload	-8	-2	0.25	8	-2	0.25	0.2	900	10	0	0	0	0	166.56	166.56	0	201.26	201.26
Mudmat7	Payload	-8	-3	0.25	8	-3	0.25	0.2	900	10	0	0	0	0	166.56	166.56	0	201.26	201.26
Bm25	Payload	-8	4	2.5	-8	-4	2.5	0.07	230	10	0	0	0	0	99.94	99.94	0	72.45	72.45
Bm26	Payload	-4	4	2.5	-4	-4	2.5	0.07	230	10	0	0	0	0	99.94	99.94	0	72.45	72.45
Bm27	Payload	0	4	2.5	0	-4	2.5	0.07	230	10	0	0	0	0	99.94	99.94	0	72.45	72.45
Bm28	Payload	4	4	2.5	4	-4	2.5	0.07	230	10	0	0	0	0	99.94	99.94	0	72.45	72.45
Bm29	Payload	8	4	2.5	8	-4	2.5	0.07	230	10	0	0	0	0	99.94	99.94	0	72.45	72.45
Tree1	Payload	6	2	0.5	6	2	5	3.14	1250	10	0	0	0	0	1025	1025	0	3220.13	3220.13
Tree2	Payload	6	-2	0.5	6	-2	5	3.14	1250	10	0	0	0	0	1025	1025	0	3220.13	3220.13
Tree3	Payload	2	2	0.5	2	2	5	3.14	1250	10	0	0	0	0	1025	1025	0	3220.13	3220.13
Tree4	Payload	-2	2	0.5	-2	2	5	3.14	1250	10	0	0	0	0	1025	1025	0	3220.13	3220.13
Tree5	Payload	-6	2	0.5	-6	2	5	3.14	1250	10	0	0	0	0	1025	1025	0	3220.13	3220.13
Tree6	Payload	2	-2	0.5	2	-2	5	3.14	1250	10	0	0	0	0	1025	1025	0	3220.13	3220.13
Tree7	Payload	-2	-2	0.5	-2	-2	5	3.14	1250	10	0	0	0	0	1025	1025	0	3220.13	3220.13
Tree8	Payload	-6	-2	0.5	-6	-2	5	3.14	1250	10	0	0	0	0	1025	1025	0	3220.13	3220.13
Bm30	Payload	8	4	2.5	-8	4	2.5	0.07	230	10	0	0	0	0	99.94	99.94	0	72.45	72.45
Bm31	Payload	-8	-4	2.5	8	-4	2.5	0.07	230	10	0	0	0	0	99.94	99.94	0	72.45	72.45
Bm32	Payload	-7	4	2.5	-7	-4	2.5	0.07	230	10	0	0	0	0	99.94	99.94	0	72.45	72.45
Bm33	Payload	-5	4	2.5	-5	-4	2.5	0.07	230	10	0	0	0	0	99.94	99.94	0	72.45	72.45
Bm34	Payload	-3	4	2.5	-3	-4	2.5	0.07	230	10	0	0	0	0	99.94	99.94	0	72.45	72.45
Bm35	Payload	-1	4	2.5	-1	-4	2.5	0.07	230	10	0	0	0	0	99.94	99.94	0	72.45	72.45
Bm36	Payload	1	4	2.5	1	-4	2.5	0.07	230	10	0	0	0	0	99.94	99.94	0	72.45	72.45
Bm37	Payload	3	4	2.5	3	-4	2.5	0.07	230	10	0	0	0	0	99.94	99.94	0	72.45	72.45
Bm38	Payload	5	4	2.5	5	-4	2.5	0.07	230	10	0	0	0	0	99.94	99.94	0	72.45	72.45
Bm39	Payload	7	4	2.5	7	-4	2.5	0.07	230	10	0	0	0	0	99.94	99.94	0	72.45	72.45
Bm40	Payload	8	3	2.5	-8	3	2.5	0.07	230	10	0	0	0	0	99.94	99.94	0	72.45	72.45
Bm41	Payload	8	1	2.5	-8	1	2.5	0.07	230	10	0	0	0	0	99.94	99.94	0	72.45	72.45
Bm42	Payload	8	-1	2.5	-8	-1	2.5	0.07	230	10	0	0	0	0	99.94	99.94	0	72.45	72.45
Bm43	Payload	8	-3	2.5	-8	-3	2.5	0.07	230	10	0	0	0	0	99.94	99.94	0	72.45	72.45
Bm44	Payload	-7	-3	2.5	-7	-3	5	0.07	230	10	0	0	0	0	99.94	99.94	0	72.45	72.45
Bm45	Payload	-7	-1	2.5	-7	-1	5	0.07	230	10	0	0	0	0	99.94	99.94	0	72.45	72.45
Bm46	Payload	-7	1	2.5	-7	1	5	0.07	230	10	0	0	0	0	99.94	99.94	0	72.45	72.45
Bm47	Payload	-7	3	2.5	-7	3	5	0.07	230	10	0	0	0	0	99.94	99.94	0	72.45	72.45
Bm48	Payload	-5	-1	2.5	-5	-1	5	0.07	230	10	0	0	0	0	99.94	99.94	0	72.45	72.45
Bm49	Payload	-3	-1	2.5	-3	-1	5	0.07	230	10	0	0	0	0	99.94	99.94	0	72.45	72.45
Bm50	Payload	-1	-1	2.5	-1	-1	5	0.07	230	10	0	0	0	0	99.94	99.94	0	72.45	72.45
Bm51	Payload	1	-1	2.5	1	-1	5	0.07	230	10	0	0	0	0	99.94	99.94	0	72.45	72.45
Bm52	Payload	3	-1	2.5	3	-1	5	0.07	230	10	0	0	0	0	99.94	99.94	0	72.45	72.45
Bm53	Payload	5	-1	2.5	5	-1	5	0.07	230	10	0	0	0	0	99.94	99.94	0	72.45	72.45
Bm54	Payload	7	-1	2.5	7	-1	5	0.07	230	10	0	0	0	0	99.94	99.94	0	72.45	72.45
Bm55	Payload	-5	1	2.5	-5	1	5	0.07	230	10	0	0	0	0	99.94	99.94	0	72.45	72.45
Bm56	Payload	-3	1	2.5	-3	1	5	0.07	230	10	0	0	0	0	99.94	99.94	0	72.45	72.45
Bm57	Payload	-1	1	2.5	-1	1	5	0.07	230	10	0	0	0	0	99.94	99.94	0	72.45	72.45
Bm58	Payload	1	1	2.5	1	1	5	0.07	230	10	0	0	0	0	99.94	99.94	0	72.45	72.45
Bm59	Payload	3	1	2.5	3	1	5	0.07	230	10	0	0	0	0	99.94	99.94	0	72.45	72.45
Bm60	Payload	5	1	2.5	5	1	5	0.07	230	10	0	0	0	0	99.94	99.94	0	72.45	72.45

Simulation inputs

Bm61	Payload	7	1	2.5	7	1	5	0.07	230	10	0	0	0	0	99.94	99.94	0	72.45	72.45
Bm62	Payload	-5	3	2.5	-5	3	5	0.07	230	10	0	0	0	0	99.94	99.94	0	72.45	72.45
Bm63	Payload	-3	3	2.5	-3	3	5	0.07	230	10	0	0	0	0	99.94	99.94	0	72.45	72.45
Bm64	Payload	-1	3	2.5	-1	3	5	0.07	230	10	0	0	0	0	99.94	99.94	0	72.45	72.45
Bm65	Payload	1	3	2.5	1	3	5	0.07	230	10	0	0	0	0	99.94	99.94	0	72.45	72.45
Bm66	Payload	3	3	2.5	3	3	5	0.07	230	10	0	0	0	0	99.94	99.94	0	72.45	72.45
Bm67	Payload	5	3	2.5	5	3	5	0.07	230	10	0	0	0	0	99.94	99.94	0	72.45	72.45
Bm68	Payload	7	3	2.5	7	3	5	0.07	230	10	0	0	0	0	99.94	99.94	0	72.45	72.45
Bm69	Payload	-5	-3	2.5	-5	-3	5	0.07	230	10	0	0	0	0	99.94	99.94	0	72.45	72.45
Bm70	Payload	-3	-3	2.5	-3	-3	5	0.07	230	10	0	0	0	0	99.94	99.94	0	72.45	72.45
Bm71	Payload	-1	-3	2.5	-1	-3	5	0.07	230	10	0	0	0	0	99.94	99.94	0	72.45	72.45
Bm72	Payload	1	-3	2.5	1	-3	5	0.07	230	10	0	0	0	0	99.94	99.94	0	72.45	72.45
Bm73	Payload	3	-3	2.5	3	-3	5	0.07	230	10	0	0	0	0	99.94	99.94	0	72.45	72.45
Bm74	Payload	5	-3	2.5	5	-3	5	0.07	230	10	0	0	0	0	99.94	99.94	0	72.45	72.45
Bm75	Payload	7	-3	2.5	7	-3	5	0.07	230	10	0	0	0	0	99.94	99.94	0	72.45	72.45
Bm76	Payload	-7	-3	5	7	-3	5	0.07	230	10	0	0	0	0	99.94	99.94	0	72.45	72.45
Bm77	Payload	-7	-3	5	-7	3	5	0.07	230	10	0	0	0	0	99.94	99.94	0	72.45	72.45
Bm78	Payload	-7	3	5	7	3	5	0.07	230	10	0	0	0	0	99.94	99.94	0	72.45	72.45
Bm79	Payload	7	3	5	7	-3	5	0.07	230	10	0	0	0	0	99.94	99.94	0	72.45	72.45
Bm80	Payload	-5	-3	5	-5	3	5	0.07	230	10	0	0	0	0	99.94	99.94	0	72.45	72.45
Bm81	Payload	-3	-3	5	-3	3	5	0.07	230	10	0	0	0	0	99.94	99.94	0	72.45	72.45
Bm82	Payload	-1	-3	5	-1	3	5	0.07	230	10	0	0	0	0	99.94	99.94	0	72.45	72.45
Bm83	Payload	1	-3	5	1	3	5	0.07	230	10	0	0	0	0	99.94	99.94	0	72.45	72.45
Bm84	Payload	3	-3	5	3	3	5	0.07	230	10	0	0	0	0	99.94	99.94	0	72.45	72.45
Bm85	Payload	5	-3	5	5	3	5	0.07	230	10	0	0	0	0	99.94	99.94	0	72.45	72.45
Bm86	Payload	-7	1	5	7	1	5	0.07	230	10	0	0	0	0	99.94	99.94	0	72.45	72.45
Bm87	Payload	-7	-1	5	7	-1	5	0.07	230	10	0	0	0	0	99.94	99.94	0	72.45	72.45
Bm88	Payload	8	4	0	4	4	2.5	0.07	230	10	0	0	0	0	99.94	99.94	0	72.45	72.45
Bm89	Payload	4	4	2.5	0	4	0	0.07	230	10	0	0	0	0	99.94	99.94	0	72.45	72.45
Bm90	Payload	0	4	0	-4	4	2.5	0.07	230	10	0	0	0	0	99.94	99.94	0	72.45	72.45
Bm91	Payload	-4	4	2.5	-8	4	0	0.07	230	10	0	0	0	0	99.94	99.94	0	72.45	72.45
Bm92	Payload	8	-4	0	8	0	2.5	0.07	230	10	0	0	0	0	99.94	99.94	0	72.45	72.45
Bm93	Payload	8	0	2.5	8	4	0	0.07	230	10	0	0	0	0	99.94	99.94	0	72.45	72.45
Bm94	Payload	8	-4	0	4	-4	2.5	0.07	230	10	0	0	0	0	99.94	99.94	0	72.45	72.45
Bm95	Payload	4	-4	2.5	0	-4	0	0.07	230	10	0	0	0	0	99.94	99.94	0	72.45	72.45
Bm96	Payload	0	-4	0	-4	-4	2.5	0.07	230	10	0	0	0	0	99.94	99.94	0	72.45	72.45
Bm97	Payload	-4	-4	2.5	-8	-4	0	0.07	230	10	0	0	0	0	99.94	99.94	0	72.45	72.45
Bm98	Payload	-8	-4	0	-8	0	2.5	0.07	230	10	0	0	0	0	99.94	99.94	0	72.45	72.45
Bm99	Payload	-8	0	2.5	-8	4	0	0.07	230	10	0	0	0	0	99.94	99.94	0	72.45	72.45

Table B-7: 150T-manifold element properties

Name	Body	X-End1 [m]	Y-End1 [m]	Z-End1 [m]	X-End2 [m]	Y-End2 [m]	Z-End2 [m]	Specified Volume	Distributed Mass	Strips	xref	yref	zref	C2x	C2y	C2z	Amx	Amy	Amz
Bm1	Payload	-4	-4	0	-4	-4	2.5	0.07	230	10	0	0	0	0	99.94	99.94	0	72.45	72.45
Bm2	Payload	0	-4	0	0	-4	2.5	0.07	230	10	0	0	0	0	99.94	99.94	0	72.45	72.45
Bm3	Payload	4	-4	0	4	-4	2.5	0.07	230	10	0	0	0	0	99.94	99.94	0	72.45	72.45
Bm4	Payload	-4	0	0	-4	0	2.5	0.07	230	10	0	0	0	0	99.94	99.94	0	72.45	72.45
Bm5	Payload	-4	4	0	-4	4	2.5	0.07	230	10	0	0	0	0	99.94	99.94	0	72.45	72.45
Bm6	Payload	0	0	0	0	0	2.5	0.07	230	10	0	0	0	0	99.94	99.94	0	72.45	72.45
Bm7	Payload	0	4	0	0	4	2.5	0.07	230	10	0	0	0	0	99.94	99.94	0	72.45	72.45
Bm8	Payload	4	0	0	4	0	2.5	0.07	230	10	0	0	0	0	99.94	99.94	0	72.45	72.45
Bm9	Payload	4	4	0	4	4	2.5	0.07	230	10	0	0	0	0	99.94	99.94	0	72.45	72.45
Bm10	Payload	-4	4	0	-4	-4	0	0.07	230	10	0	0	0	0	99.94	99.94	0	72.45	72.45
Bm11	Payload	4	4	0	4	-4	0	0.07	230	10	0	0	0	0	99.94	99.94	0	72.45	72.45
Bm12	Payload	-4	4	2.5	-4	-4	2.5	0.07	230	10	0	0	0	0	99.94	99.94	0	72.45	72.45
Bm13	Payload	0	4	2.5	0	-4	2.5	0.07	230	10	0	0	0	0	99.94	99.94	0	72.45	72.45
Bm14	Payload	4	4	2.5	4	-4	2.5	0.07	230	10	0	0	0	0	99.94	99.94	0	72.45	72.45
Tree1	Payload	2	2	0.5	2	2	5	3.14	1250	10	0	0	0	0	1025	1025	0	3220.13	3220.13
Tree2	Payload	-2	2	0.5	-2	2	5	3.14	1250	10	0	0	0	0	1025	1025	0	3220.13	3220.13
Tree3	Payload	2	-2	0.5	2	-2	5	3.14	1250	10	0	0	0	0	1025	1025	0	3220.13	3220.13
Tree4	Payload	-2	-2	0.5	-2	-2	5	3.14	1250	10	0	0	0	0	1025	1025	0	3220.13	3220.13
Bm15	Payload	-3	4	2.5	-3	-4	2.5	0.07	230	10	0	0	0	0	99.94	99.94	0	72.45	72.45
Bm16	Payload	-1	4	2.5	-1	-4	2.5	0.07	230	10	0	0	0	0	99.94	99.94	0	72.45	72.45
Bm17	Payload	1	4	2.5	1	-4	2.5	0.07	230	10	0	0	0	0	99.94	99.94	0	72.45	72.45
Bm18	Payload	3	4	2.5	3	-4	2.5	0.07	230	10	0	0	0	0	99.94	99.94	0	72.45	72.45
Bm19	Payload	-3	-3	2.5	-3	-3	5	0.07	230	10	0	0	0	0	99.94	99.94	0	72.45	72.45
Bm20	Payload	-3	-1	2.5	-3	-1	5	0.07	230	10	0	0	0	0	99.94	99.94	0	72.45	72.45
Bm21	Payload	-3	1	2.5	-3	1	5	0.07	230	10	0	0	0	0	99.94	99.94	0	72.45	72.45
Bm22	Payload	-3	3	2.5	-3	3	5	0.07	230	10	0	0	0	0	99.94	99.94	0	72.45	72.45
Bm23	Payload	-1	-1	2.5	-1	-1	5	0.07	230	10	0	0	0	0	99.94	99.94	0	72.45	72.45
Bm24	Payload	1	-1	2.5	1	-1	5	0.07	230	10	0	0	0	0	99.94	99.94	0	72.45	72.45
Bm25	Payload	3	-1	2.5	3	-1	5	0.07	230	10	0	0	0	0	99.94	99.94	0	72.45	72.45
Bm26	Payload	-1	1	2.5	-1	1	5	0.07	230	10	0	0	0	0	99.94	99.94	0	72.45	72.45
Bm27	Payload	1	1	2.5	1	1	5	0.07	230	10	0	0	0	0	99.94	99.94	0	72.45	72.45
Bm28	Payload	3	1	2.5	3	1	5	0.07	230	10	0	0	0	0	99.94	99.94	0	72.45	72.45
Bm29	Payload	-1	3	2.5	-1	3	5	0.07	230	10	0	0	0	0	99.94	99.94	0	72.45	72.45
Bm30	Payload	1	3	2.5	1	3	5	0.07	230	10	0	0	0	0	99.94	99.94	0	72.45	72.45
Bm31	Payload	3	3	2.5	3	3	5	0.07	230	10	0	0	0	0	99.94	99.94	0	72.45	72.45
Bm32	Payload	-1	-3	2.5	-1	-3	5	0.07	230	10	0	0	0	0	99.94	99.94	0	72.45	72.45

Bm33	Payload	1	-3	2.5	1	-3	5	0.07	230	10	0	0	0	0	99.94	99.94	0	72.45	72.45
Bm34	Payload	3	-3	2.5	3	-3	5	0.07	230	10	0	0	0	0	99.94	99.94	0	72.45	72.45
Bm35	Payload	-3	-3	5	-3	3	5	0.07	230	10	0	0	0	0	99.94	99.94	0	72.45	72.45
Bm36	Payload	-1	-3	5	-1	3	5	0.07	230	10	0	0	0	0	99.94	99.94	0	72.45	72.45
Bm37	Payload	1	-3	5	1	3	5	0.07	230	10	0	0	0	0	99.94	99.94	0	72.45	72.45
Bm38	Payload	3	-3	5	3	3	5	0.07	230	10	0	0	0	0	99.94	99.94	0	72.45	72.45
Bm39	Payload	4	4	0	0	4	2.5	0.07	230	10	0	0	0	0	99.94	99.94	0	72.45	72.45
Bm40	Payload	0	4	2.5	-4	4	0	0.07	230	10	0	0	0	0	99.94	99.94	0	72.45	72.45
Bm41	Payload	4	-4	0	0	-4	2.5	0.07	230	10	0	0	0	0	99.94	99.94	0	72.45	72.45
Bm42	Payload	0	-4	2.5	-4	-4	0	0.07	230	10	0	0	0	0	99.94	99.94	0	72.45	72.45
Bm43	Payload	-4	-4	0	-4	0	2.5	0.07	230	10	0	0	0	0	99.94	99.94	0	72.45	72.45
Bm44	Payload	-4	0	2.5	-4	4	0	0.07	230	10	0	0	0	0	99.94	99.94	0	72.45	72.45
Bm45	Payload	-4	-4	0	4	-4	0	0.07	230	10	0	0	0	0	99.94	99.94	0	72.45	72.45
Bm46	Payload	-4	-4	2.5	4	-4	2.5	0.07	230	10	0	0	0	0	99.94	99.94	0	72.45	72.45
Bm47	Payload	-4	4	2.5	4	4	2.5	0.07	230	10	0	0	0	0	99.94	99.94	0	72.45	72.45
Bm48	Payload	-4	4	0	4	4	0	0.07	230	10	0	0	0	0	99.94	99.94	0	72.45	72.45
Bm49	Payload	-3	-3	5	3	-3	5	0.07	230	10	0	0	0	0	99.94	99.94	0	72.45	72.45
Bm50	Payload	-3	3	5	3	3	5	0.07	230	10	0	0	0	0	99.94	99.94	0	72.45	72.45
Bm51	Payload	3	-1	5	-3	-1	5	0.07	230	10	0	0	0	0	99.94	99.94	0	72.45	72.45
Bm52	Payload	-3	1	5	3	1	5	0.07	230	10	0	0	0	0	99.94	99.94	0	72.45	72.45
Bm53	Payload	4	0	2.5	-4	0	2.5	0.07	230	10	0	0	0	0	99.94	99.94	0	72.45	72.45
Bm54	Payload	4	-4	0	4	0	2.5	0.07	230	10	0	0	0	0	99.94	99.94	0	72.45	72.45
Bm55	Payload	4	0	2.5	4	4	0	0.07	230	10	0	0	0	0	99.94	99.94	0	72.45	72.45
Mudmat1	Payload	4	0	0	-4	0	0	0.2	900	10	0	0	0	0	166.56	166.56	0	201.26	201.26
Mudmat2	Payload	4	-0.9	0	-4	-0.9	0	0.2	900	10	0	0	0	0	166.56	166.56	0	201.26	201.26
Mudmat3	Payload	4	-1.8	0	-4	-1.8	0	0.2	900	10	0	0	0	0	166.56	166.56	0	201.26	201.26
Mudmat4	Payload	4	-2.7	0	-4	-2.7	0	0.2	900	10	0	0	0	0	166.56	166.56	0	201.26	201.26
Mudmat5	Payload	4	-3.6	0	-4	-3.6	0	0.2	900	10	0	0	0	0	166.56	166.56	0	201.26	201.26
Mudmat6	Payload	4	0.9	0	-4	0.9	0	0.2	900	10	0	0	0	0	166.56	166.56	0	201.26	201.26
Mudmat7	Payload	4	1.8	0	-4	1.8	0	0.2	900	10	0	0	0	0	166.56	166.56	0	201.26	201.26
Mudmat8	Payload	4	2.7	0	-4	2.7	0	0.2	900	10	0	0	0	0	166.56	166.56	0	201.26	201.26
Mudmat9	Payload	4	3.6	0	-4	3.6	0	0.2	900	10	0	0	0	0	166.56	166.56	0	201.26	201.26

Table B-8: XT element properties

Name	Body	X-End1 [m]	Y-End1 [m]	Z-End1 [m]	X-End2 [m]	Y-End2 [m]	Z-End2 [m]	Specified Volume	Distributed Mass	Strips	xref	yref	zref	C2x	C2y	C2z	Amx	Amy	Amz
Corner1	Payload	2.5	-2.5	4	2.5	-2.5	0	0.07	300	10	0	0	0	0	99.94	153.8	0	72.5	72.5
Corner2	Payload	2.5	2.5	0	2.5	2.5	4	0.07	300	10	0	0	0	0	99.94	153.8	0	72.5	72.5
Corner3	Payload	-2.5	2.5	4	-2.5	2.5	0	0.07	300	10	0	0	0	0	99.94	153.8	0	72.5	72.5
Corner4	Payload	-2.5	-2.5	0	-2.5	-2.5	4	0.07	300	10	0	0	0	0	99.94	153.8	0	72.5	72.5
Corner5	Payload	-2.5	2.5	0	2.5	2.5	0	0.07	300	10	0	0	0	0	99.94	153.8	0	72.5	72.5
Corner6	Payload	2.5	-2.5	0	-2.5	-2.5	0	0.07	300	10	0	0	0	0	99.94	153.8	0	72.5	72.5
Corner7	Payload	2.5	-2.5	0	2.5	2.5	0	0.07	300	10	0	0	0	0	99.94	153.8	0	72.5	72.5
Corner8	Payload	-2.5	2.5	0	-2.5	-2.5	0	0.07	300	10	0	0	0	0	99.94	153.8	0	72.5	72.5
Corner9	Payload	-2.5	2.5	4	-2.5	-2.5	4	0.07	300	10	0	0	0	0	99.94	153.8	0	72.5	72.5
Corner10	Payload	-2.5	-2.5	4	2.5	-2.5	4	0.07	300	10	0	0	0	0	99.94	153.8	0	72.5	72.5
Corner11	Payload	2.5	2.5	4	2.5	-2.5	4	0.07	300	10	0	0	0	0	99.94	153.8	0	72.5	72.5
Corner12	Payload	2.5	2.5	4	-2.5	2.5	4	0.07	300	10	0	0	0	0	99.94	153.8	0	72.5	72.5
Bore1	Payload	0	0	1.5	0	0	5	0.38	900	10	1	0	0	0	233.19	233.19	0	394.5	394.5
Bigbore1	Payload	0	0	1.5	0	0	-0.5	1.77	1200	10	1	0	0	0	499.69	499.69	0	1811.3	1811.3
Bm16	Payload	-2.5	2.35	0	2.5	2.35	0	0.0078	30	10	0	0	0	0	33.31	33.31	0	8	8
Bm17	Payload	-2.5	2.2	0	2.5	2.2	0	0.0078	30	10	0	0	0	0	33.31	33.31	0	8	8
Bm18	Payload	-2.5	2.05	0	2.5	2.05	0	0.0078	30	10	0	0	0	0	33.31	33.31	0	8	8
Bm19	Payload	-2.5	1.9	0	2.5	1.9	0	0.0078	30	10	0	0	0	0	33.31	33.31	0	8	8
Bm20	Payload	-2.5	1.75	0	2.5	1.75	0	0.0078	30	10	0	0	0	0	33.31	33.31	0	8	8
Bm21	Payload	-2.5	1.6	0	2.5	1.6	0	0.0078	30	10	0	0	0	0	33.31	33.31	0	8	8
Bm22	Payload	-2.5	1.45	0	2.5	1.45	0	0.0078	30	10	0	0	0	0	33.31	33.31	0	8	8
Bm23	Payload	-2.5	1.3	0	2.5	1.3	0	0.0078	30	10	0	0	0	0	33.31	33.31	0	8	8
Bm24	Payload	-2.5	1.15	0	2.5	1.15	0	0.0078	30	10	0	0	0	0	33.31	33.31	0	8	8
Bm25	Payload	-2.5	1	0	2.5	1	0	0.0078	30	10	0	0	0	0	33.31	33.31	0	8	8
Bm26	Payload	-2.5	0.85	0	2.5	0.85	0	0.0078	30	10	0	0	0	0	33.31	33.31	0	8	8
Bm27	Payload	-2.5	0.7	0	2.5	0.7	0	0.0078	30	10	0	0	0	0	33.31	33.31	0	8	8
Bm28	Payload	-2.5	0.55	0	2.5	0.55	0	0.0078	30	10	0	0	0	0	33.31	33.31	0	8	8
Bm29	Payload	-2.5	0.4	0	2.5	0.4	0	0.0078	30	10	0	0	0	0	33.31	33.31	0	8	8
Bm30	Payload	-2.5	0.25	0	2.5	0.25	0	0.0078	30	10	0	0	0	0	33.31	33.31	0	8	8
Bm31	Payload	-2.5	0.1	0	2.5	0.1	0	0.0078	30	10	0	0	0	0	33.31	33.31	0	8	8
Bm32	Payload	-2.5	-0.05	0	2.5	-0.05	0	0.0078	30	10	0	0	0	0	33.31	33.31	0	8	8
Bm33	Payload	-2.5	-0.2	0	2.5	-0.2	0	0.0078	30	10	0	0	0	0	33.31	33.31	0	8	8
Bm34	Payload	-2.5	-0.35	0	2.5	-0.35	0	0.0078	30	10	0	0	0	0	33.31	33.31	0	8	8
Bm35	Payload	-2.5	-0.5	0	2.5	-0.5	0	0.0078	30	10	0	0	0	0	33.31	33.31	0	8	8
Bm36	Payload	-2.5	-0.65	0	2.5	-0.65	0	0.0078	30	10	0	0	0	0	33.31	33.31	0	8	8
Bm37	Payload	-2.5	-0.8	0	2.5	-0.8	0	0.0078	30	10	0	0	0	0	33.31	33.31	0	8	8
Bm38	Payload	-2.5	-0.95	0	2.5	-0.95	0	0.0078	30	10	0	0	0	0	33.31	33.31	0	8	8
Bm39	Payload	-2.5	-1.1	0	2.5	-1.1	0	0.0078	30	10	0	0	0	0	33.31	33.31	0	8	8
Bm40	Payload	-2.5	-1.25	0	2.5	-1.25	0	0.0078	30	10	0	0	0	0	33.31	33.31	0	8	8
Bm41	Payload	-2.5	-1.4	0	2.5	-1.4	0	0.0078	30	10	0	0	0	0	33.31	33.31	0	8	8
Bm42	Payload	-2.5	-1.55	0	2.5	-1.55	0	0.0078	30	10	0	0	0	0	33.31	33.31	0	8	8
Bm43	Payload	-2.5	-1.7	0	2.5	-1.7	0	0.0078	30	10	0	0	0	0	33.31	33.31	0	8	8
Bm44	Payload	-2.5	-1.85	0	2.5	-1.85	0	0.0078	30	10	0	0	0	0	33.31	33.31	0	8	8

Simulation inputs

Bm45	Payload	-2.5	-2	0	2.5	-2	0	0.0078	30	10	0	0	0	0	33.31	33.31	0	8	8
Bm46	Payload	-2.5	-2.15	0	2.5	-2.15	0	0.0078	30	10	0	0	0	0	33.31	33.31	0	8	8
Bm47	Payload	-2.5	-2.3	0	2.5	-2.3	0	0.0078	30	10	0	0	0	0	33.31	33.31	0	8	8
Bm49	Payload	-2.5	2.35	4	2.5	2.35	4	0.0078	30	10	0	0	0	0	33.31	33.31	0	8	8
Bm50	Payload	-2.5	2.2	4	2.5	2.2	4	0.0078	30	10	0	0	0	0	33.31	33.31	0	8	8
Bm51	Payload	-2.5	2.05	4	2.5	2.05	4	0.0078	30	10	0	0	0	0	33.31	33.31	0	8	8
Bm52	Payload	-2.5	1.9	4	2.5	1.9	4	0.0078	30	10	0	0	0	0	33.31	33.31	0	8	8
Bm53	Payload	-2.5	1.75	4	2.5	1.75	4	0.0078	30	10	0	0	0	0	33.31	33.31	0	8	8
Bm54	Payload	-2.5	1.6	4	2.5	1.6	4	0.0078	30	10	0	0	0	0	33.31	33.31	0	8	8
Bm55	Payload	-2.5	1.45	4	2.5	1.45	4	0.0078	30	10	0	0	0	0	33.31	33.31	0	8	8
Bm56	Payload	-2.5	1.3	4	2.5	1.3	4	0.0078	30	10	0	0	0	0	33.31	33.31	0	8	8
Bm57	Payload	-2.5	1.15	4	2.5	1.15	4	0.0078	30	10	0	0	0	0	33.31	33.31	0	8	8
Bm58	Payload	-2.5	1	4	2.5	1	4	0.0078	30	10	0	0	0	0	33.31	33.31	0	8	8
Bm59	Payload	-2.5	0.85	4	2.5	0.85	4	0.0078	30	10	0	0	0	0	33.31	33.31	0	8	8
Bm60	Payload	-2.5	0.7	4	2.5	0.7	4	0.0078	30	10	0	0	0	0	33.31	33.31	0	8	8
Bm61	Payload	-2.5	0.55	4	2.5	0.55	4	0.0078	30	10	0	0	0	0	33.31	33.31	0	8	8
Bm62	Payload	-2.5	0.4	4	2.5	0.4	4	0.0078	30	10	0	0	0	0	33.31	33.31	0	8	8
Bm63	Payload	-2.5	0.25	4	2.5	0.25	4	0.0078	30	10	0	0	0	0	33.31	33.31	0	8	8
Bm64	Payload	-2.5	0.1	4	2.5	0.1	4	0.0078	30	10	0	0	0	0	33.31	33.31	0	8	8
Bm65	Payload	-2.5	-0.05	4	2.5	-0.05	4	0.0078	30	10	0	0	0	0	33.31	33.31	0	8	8
Bm66	Payload	-2.5	-0.2	4	2.5	-0.2	4	0.0078	30	10	0	0	0	0	33.31	33.31	0	8	8
Bm67	Payload	-2.5	-0.35	4	2.5	-0.35	4	0.0078	30	10	0	0	0	0	33.31	33.31	0	8	8
Bm68	Payload	-2.5	-0.5	4	2.5	-0.5	4	0.0078	30	10	0	0	0	0	33.31	33.31	0	8	8
Bm69	Payload	-2.5	-0.65	4	2.5	-0.65	4	0.0078	30	10	0	0	0	0	33.31	33.31	0	8	8
Bm70	Payload	-2.5	-0.8	4	2.5	-0.8	4	0.0078	30	10	0	0	0	0	33.31	33.31	0	8	8
Bm71	Payload	-2.5	-0.95	4	2.5	-0.95	4	0.0078	30	10	0	0	0	0	33.31	33.31	0	8	8
Bm72	Payload	-2.5	-1.1	4	2.5	-1.1	4	0.0078	30	10	0	0	0	0	33.31	33.31	0	8	8
Bm73	Payload	-2.5	-1.25	4	2.5	-1.25	4	0.0078	30	10	0	0	0	0	33.31	33.31	0	8	8
Bm74	Payload	-2.5	-1.4	4	2.5	-1.4	4	0.0078	30	10	0	0	0	0	33.31	33.31	0	8	8
Bm75	Payload	-2.5	-1.55	4	2.5	-1.55	4	0.0078	30	10	0	0	0	0	33.31	33.31	0	8	8
Bm76	Payload	-2.5	-1.7	4	2.5	-1.7	4	0.0078	30	10	0	0	0	0	33.31	33.31	0	8	8
Bm77	Payload	-2.5	-1.85	4	2.5	-1.85	4	0.0078	30	10	0	0	0	0	33.31	33.31	0	8	8
Bm78	Payload	-2.5	-2	4	2.5	-2	4	0.0078	30	10	0	0	0	0	33.31	33.31	0	8	8
Bm79	Payload	-2.5	-2.15	4	2.5	-2.15	4	0.0078	30	10	0	0	0	0	33.31	33.31	0	8	8
Bm80	Payload	-2.5	-2.3	4	2.5	-2.3	4	0.0078	30	10	0	0	0	0	33.31	33.31	0	8	8
Bore2	Payload	-1.5	0.5	2.5	1.5	0.5	2.5	0.38	900	10	0	0	0	0	233.19	233.19	0	8	8
Bore3	Payload	-1.5	-0.5	2	1.5	-0.5	2	0.38	900	10	0	0	0	0	233.19	233.19	0	8	8
Bore4	Payload	-1.5	-0.5	3	1.5	-0.5	3	0.38	900	10	0	0	0	0	233.19	233.19	0	8	8
Support1	Payload	2.5	0	0	2.5	0	4	0.07	300	10	0	0	0	0	99.94	99.94	0	72.5	72.5
Support2	Payload	0	2.5	4	0	2.5	0	0.07	300	10	0	0	0	0	99.94	99.94	0	72.5	72.5
Support3	Payload	0	-2.5	4	0	-2.5	0	0.07	300	10	0	0	0	0	99.94	99.94	0	72.5	72.5
Support4	Payload	-2.5	0	0	-2.5	0	4	0.07	300	10	0	0	0	0	99.94	99.94	0	72.5	72.5
Support5	Payload	-2.5	2.5	1	2.5	2.5	1	0.07	300	10	0	0	0	0	99.94	99.94	0	72.5	72.5
Support6	Payload	-2.5	-2.5	1	2.5	-2.5	1	0.07	300	10	0	0	0	0	99.94	99.94	0	72.5	72.5
Support7	Payload	2.5	-2.5	1	2.5	2.5	1	0.07	300	10	0	0	0	0	99.94	99.94	0	72.5	72.5
Support8	Payload	-2.5	-2.5	1	-2.5	2.5	1	0.07	300	10	0	0	0	0	99.94	99.94	0	72.5	72.5

Table B-9: THS element properties

Name	Body	X-End1 [m]	Y-End1 [m]	Z-End1 [m]	X-End2 [m]	Y-End2 [m]	Z-End2 [m]	Specified Volume	Distributed Mass	Strips	xref	yref	zref	C2x	C2y	C2z	Amx	Amy	Amz
Bigbore1	Payload	0	0	0	0	0	0.5	2.54	4600	10	1	0	0	0	922.5	922.5	0	2608.31	2608.31
Midbore1	Payload	0	0	1.5	0	0	0.5	0.79	3300	10	1	0	0	0	512.5	512.5	0	805.03	805.03
Bore1	Payload	0	0	3	0	0	2.4	0.5	2500	10	1	0	0	0	410	410	0	515.22	515.22
Bigbore2	Payload	0	0	1.5	0	0	2.4	2.54	4600	10	1	0	0	0	922.5	922.5	0	2608.31	2608.31
Bigpipe1	Payload	2	-0.7	1.5	-0.5	-0.7	1.5	0.196	800	10	0	0	0	0	256.25	256.25	0	201.26	201.26
Bigpipe2	Payload	1.8	-0.7	1.5	1.8	-0.7	2.8	0.196	800	10	0	0	0	0	256.25	256.25	0	201.26	201.26
Plates1	Payload	0.5	0	1.5	0.5	2	1.5	0.0078	300	10	0	0	0	0	33.31	33.31	0	8.05	8.05
Plates2	Payload	0.5	0	1.4	0.5	2	1.4	0.0078	300	10	0	0	0	0	33.31	33.31	0	8.05	8.05
Plates3	Payload	0.5	0	1.3	0.5	2	1.3	0.0078	300	10	0	0	0	0	33.31	33.31	0	8.05	8.05
Plates4	Payload	0.5	0	1.2	0.5	2	1.2	0.0078	300	10	0	0	0	0	33.31	33.31	0	8.05	8.05
Plates5	Payload	0.5	0	1.1	0.5	2	1.1	0.0078	300	10	0	0	0	0	33.31	33.31	0	8.05	8.05
Plates6	Payload	0.5	0	1	0.5	2	1	0.0078	300	10	0	0	0	0	33.31	33.31	0	8.05	8.05
Plates7	Payload	0.5	0	0.9	0.5	2	0.9	0.0078	300	10	0	0	0	0	33.31	33.31	0	8.05	8.05
Plates8	Payload	0.5	0	0.8	0.5	2	0.8	0.0078	300	10	0	0	0	0	33.31	33.31	0	8.05	8.05
Plates9	Payload	0.5	0	0.7	0.5	2	0.7	0.0078	300	10	0	0	0	0	33.31	33.31	0	8.05	8.05
Plates10	Payload	0.5	0	0.6	0.5	2	0.6	0.0078	300	10	0	0	0	0	33.31	33.31	0	8.05	8.05
Plates11	Payload	0.5	0	0.5	0.5	2	0.5	0.0078	300	10	0	0	0	0	33.31	33.31	0	8.05	8.05
Pipe1	Payload	0.5	1	1.2	-0.5	1	1.2	0.07	500	10	0	0	0	0	99.94	99.94	0	72.45	72.45
Pipe2	Payload	0.5	1.3	1.2	-0.5	1.3	1.2	0.07	500	10	0	0	0	0	99.94	99.94	0	72.45	72.45
Pipe3	Payload	-0.5	1.4	1.2	-0.5	0	1.2	0.07	500	10	0	0	0	0	99.94	99.94	0	72.45	72.45
Plates12	Payload	0.4	0	0.5	0.4	2	0.5	0.0078	300	10	0	0	0	0	33.31	33.31	0	8.05	8.05
Plates13	Payload	0.3	0	0.5	0.3	2	0.5	0.0078	300	10	0	0	0	0	33.31	33.31	0	8.05	8.05
Plates14	Payload	0.2	0	0.5	0.2	2	0.5	0.0078	300	10	0	0	0	0	33.31	33.31	0	8.05	8.05
Plates15	Payload	0.1	0	0.5	0.1	2	0.5	0.0078	300	10	0	0	0	0	33.31	33.31	0	8.05	8.05

d